

General Disclaimer

One or more of the Following Statements may affect this Document

- This document has been reproduced from the best copy furnished by the organizational source. It is being released in the interest of making available as much information as possible.
- This document may contain data, which exceeds the sheet parameters. It was furnished in this condition by the organizational source and is the best copy available.
- This document may contain tone-on-tone or color graphs, charts and/or pictures, which have been reproduced in black and white.
- This document is paginated as submitted by the original source.
- Portions of this document are not fully legible due to the historical nature of some of the material. However, it is the best reproduction available from the original submission.

USE OF MAGSAT ANOMALY DATA FOR CRUSTAL STRUCTURE AND MINERAL RESOURCES IN THE U.S. MIDCONTINENT

(E84-10112) USE OF MAGSAT ANOMALY DATA FOR
CRUSTAL STRUCTURE AND MINERAL RESOURCES IN
THE US MIDCONTINENT Final Project Report,
Dec. 1980 - Sep. 1983 (Iowa Univ.) 177 p
HC A09/MF A01

N84-23005

Unclas

CSCS 08G G3/43 00112

Robert S. Carmichael
Department of Geology
The University of Iowa
Iowa City, Iowa 52242

October 1983

Final Project Report for period Dec. 1980-Sept. 1983



Prepared for

GODDARD SPACE FLIGHT CENTER
Greenbelt, Maryland 20771

INGSEC 04/20/84
M-001

USE OF MAGSAT ANOMALY DATA FOR CRUSTAL STRUCTURE AND MINERAL RESOURCES
IN THE U.S. MIDCONTINENT

Robert S. Carmichael
Department of Geology
University of Iowa
Iowa City, Iowa 52242

October 1983

Final Project Report for period Dec. 1980 - Sept. 1983

ORIGINAL CONTAINS
COLOR ILLUSTRATIONS

Prepared for
GODDARD SPACE FLIGHT CENTER
Greenbelt, Maryland 20771

NASA

TECHNICAL REPORT STANDARD TITLE PAGE

1. Report No.	2. Government Accession No.	3. Recipient's Catalog No.	
4. Title and Subtitle USE OF MAGSAT ANOMALY DATA FOR CRUSTAL STRUCTURE AND MINERAL RESOURCES IN THE U.S. MIDCONTINENT		5. Report Date October 1983	6. Performing Organization Code
7. Author(s) Robert S. Carmichael		8. Performing Organization Report No.	
9. Performing Organization Name and Address Department of Geology University of Iowa Iowa City, Iowa 52242		10. Work Unit No.	11. Contract or Grant No. NAS 5-26425
12. Sponsoring Agency Name and Address Goddard Space Flight Center National Aeronautics and Space Administration Washington, D.C. 20546 Technical Monitor: Harold Oseroff		13. Type of Report and Period Covered Final Project Report Dec. 1980-Sept. 1983	
14. Sponsoring Agency Code		15. Supplementary Notes	
16. Abstract Magnetic field data acquired by NASA's Magsat satellite is used to construct a long-wavelength magnetic anomaly map for the U.S. mid-continent. This aids in interpretation of gross crustal geology (structure, lithologic composition, resource potential) of the region. Magnetic properties of minerals and rocks are investigated and assessed, to help in evaluation and modelling of crustal magnetization sources and depth to the Curie-temperature isotherm.			
17. Key Words (Selected by Author(s)) U. S. Midcontinent satellite magnetic anomaly magnetite crustal magnetization		18. Distribution Statement	
19. Security Classif. (of this report) Unclassified	20. Security Classif. (of this page) Unclassified	21. No. of Pages 176	22. Price*

*For sale by the Clearinghouse for Federal Scientific and Technical Information, Springfield, Virginia 22151.

PREFACE

The objective of the work was to investigate the use and applicability of satellite magnetic anomaly data, acquired by NASA's Magsat mission of 1979-80, in reconnaissance interpretation of crustal geologic character. This would include major structure, tectonic development and evolution, petrologic (rock) composition, and thermal conditions in the lithosphere. The Magsat data provides long-wavelength magnetic information with a coverage, accuracy, and resolution not previously available. As such, the satellite data and maps constitute an important new aid for interpreting the crust of the Earth.

The scope of the project has been to

i) process the satellite magnetic data to yield an anomaly map of the central U.S. This has involved data selection to obtain an optimum data set, and then analysis including reduction to a $1^{\circ} \times 1^{\circ}$ latitude/longitude grid at common altitude datum (400 km), wavelength filtering, and reduction-to-the-pole to aid interpretations.

ii) relate the magnetic anomaly map to prospective crustal sources, in terms of crustal thickness variation, depth to Curie-isotherm, and petrologic variation between different geologic provinces. This can be done in conjunction with correlative geological and geophysical information such as regional gravity, aeromagnetism, seismic refraction to define crustal thickness, and available geological/structural data.

iii) investigate the prospective relation between satellite magnetic anomaly mapping, deep-seated geologic conditions and properties, and reconnaissance exploration for and assessment of supplies of such resources as mineral deposit provinces, energy fuels (oil, gas) in basins, and geothermal energy.

iv) assemble and evaluate data on magnetic minerals (primarily titanomagnetite) whose presence and properties are the source of the magnetization of crustal bodies. This will help in modelling and interpreting magnetic anomalies as witnessed at satellite altitudes, in terms of crustal composition, thickness, structure, and thermal regime.

One may conclude, at this early stage of analysis and interpretation of Magsat satellite magnetic data, that the regional and global anomaly maps

provide useful long-wavelength information on gross features of the Earth's crust. The satellite anomalies reflect, primarily, broad and deep-seated mid- to lower-crustal properties and conditions (magnetic mineral content of rocks, metamorphic state of basement rocks, crustal thickness, geothermal gradient). As such, they portray major geologic structures and terranes, such as continental blocks sutured together, rather than the much shallower and more localized sources such as intrusions in the upper crust which yield intense but much shorter-wavelength anomalies on aeromagnetic or surface maps.

In the U.S. central Midcontinent, the magnetic anomaly map reflects major geologic terranes and deep crustal petrology. It does not, at least at this stage of the investigation, indicate a magnetic signature for the MGA (Midcontinent Geophysical/Gravity Anomaly), which is the gravity and aeromagnetic signature of the late-Precambrian-age CNARS (Central North American Rift System)--a major failed paleorift. This is for several reasons: the CNARS/MGA major portion which trends from Lake Superior down to central Kansas,

- i) is oriented along the north-south azimuth of the satellite orbit track, and is less likely to show an anomaly than an east-west trending structure or boundary.

- ii) the CNARS, although a long and deep structure, is relatively narrow (60-150 km) for the resolution of satellite magnetic surveying, unless it is very anomalously magnetic; which leads to the following,

- iii) although the CNARS/MGA major portion is an immense seam of volcanic (basaltic) extrusives and intrusives in the upper- to middle-crust, and could be expected to have a large induced magnetization (due to susceptibility contrast) and an even larger remanent magnetization, its magnetic anomaly signature is modest in intensity at aeromagnetic heights and not apparent at satellite elevations. From geophysical modelling, this is because there is the presence of both normally and reversely polarized remanence in the rock complex due to a geomagnetic field reversal in Keweenaw time. The resulting net magnetization is much less than it would be for, say, induced magnetization alone.

For modelling of deep crustal sources, considerable progress can be made with the operating assumptions that,

- i) the main magnetization derives from the lower crustal rocks, especially if having mafic composition and intermediate-grade metamorphism.

ii) the dominant mineral species of concern is magnetite, with a Curie temperature (and corresponding isotherm as a lower bound to magnetization) of 560-575°C.

iii) the magnetization is dominantly induced, such that the vector of magnetization is in the direction of the local geomagnetic field.

It is recommended that work continue on analysing the existing Magsat anomaly data, on both a global and regional scale. Development and application of an optimum data-processing scheme, as for example including reduction-to-the-pole to spatially relate anomalies to sources, and cross-correlation with other digital data sets such as gravity and lower-crustal thickness, will continue to improve the resolution and use of the satellite magnetic data. For example, we have begun two new efforts to refine terrestrial application of the Magsat data: application of the techniques used for our initial study, to interpreting the Indian subcontinent/Himalayan region; and study of satellite magnetics to help interpret recent volcanic/geothermal regions such as hot spots (mantle plumes) and incipient rifts. The concept of using reduced-to-the-pole continental anomaly patterns (as NASA workers are now doing) to try to reassemble Mesozoic Gondwanaland, or disassemble Precambrian plate collisions in cratonic regions, is an intriguing application that holds great interest for the geoscience community.

TABLE OF CONTENTS

	page
Preface	iii
Table of Contents	vi
List of Illustrations	vii
Introduction	
The Satellite mission	1
The data	5
This project	8
Activity schedule	14
Data processing	
Correction of data, calculation of scalar field, correlation of tracks and passes, smoothing, reduction to grid and datum level, plotting anomaly maps, wavelength filtering, reduction-to-the-pole	15
Interpretation of central Midcontinent region	
Geologic setting	45
Correlative geophysical and geologic data	58
Inversion of magnetic anomalies to crustal sources	67
Resolution of satellite magnetics	77
Analysis and interpretation of satellite anomalies in the study area	
General factors for magnetic interpretation of crustal character	78
Related interpretations	85
Interpretation of study area	88
Geophysical modelling of CNARS/Midcontinent Geophysical Anomaly -- magnetics and gravity	97
Resources potential	106
Magnetic properties for magnetic modelling	
Magnetic mineralogy	118
Magnetite/ulvospinel/ilmenite	
Depth to Curie-temperature isotherm	144
Summary	146
Bibliography of External references	150
Bibliography of Project-related references	154
Appendix A: abstracts of project-related publications	155

LIST OF ILLUSTRATIONS

	Page
1. Magsat satellite	2
2. Magsat orbit dimensions, for 1979-80 (from EOS Trans. A.G.U., v. 61, p. 545, July 1980)	3
3. Comparison of theoretical magnetic anomalies at different altitudes	6
4. Geomagnetic indices during Magsat mission (from Japanese team).	7
5. Magsat crustal magnetic anomaly map, of delta-X vector component (Langel et al, 1982b). Arbitrary zero level.	9
6. As Figure 5, delta-Y.	10
7. As Figure 5, delta-Z.	11
8. Magsat crustal magnetic anomaly map, of total-field (scalar) magnitude (Langel et al, 1982b). Arbitrary zero level.	12
9. Total-field profile on track over U.S. Midcontinent, for pass 85.	17
(a) H_T , calculated from original tape data, with spikes; anomaly magnitude (in 10^2 nT) vs. latitude	
(b) Magnetic anomaly profile, after spikes removed	
10. Magnetic "anomaly" fields, as measured for pass 85.	
(a) Vector component H_x	18
(b) Vector component H_y	19
(c) Vector component H_z	20
(d) Calculated scalar (total-field) magnitude, H_T	21
11. H_x component field data at different times over same track.	
(a) Pass 254	23
(b) Pass 531	24
12. H_y component field data at different times over same track.	
(a) Pass 254	25
(b) Pass 531	26
13. Running-average smoothing of H_T for pass 85.	28
14. Data prism for grid point.	27
15. Track (latitude and longitude) over U.S. midcontinent, for pass 85.	30
16. Orbit (radius vs. latitude) for pass 85, along common track of passes 85, 254, and 531. Mean altitude about 380 km.	31
17. Comparison of H_T for two passes over same track as pass 85, from north-central Mexico (left) up to past North Dakota (right). Note that ordinate scales are different.	32

18.	Magsat vector component anomaly maps for U.S. midcontinent. $1^{\circ} \times 1^{\circ}$ latitude/longitude grid, data weighted-averaged to altitude of 400 km. Albers projection, contour interval of 2 or 4 nT. (Black, 1981)	
(a)	Base map	34
(b)	delta-X component	35
(c)	delta-Y component	36
(d)	delta-Z component	37
19.	Magsat scalar (total-field) anomaly map, for U.S. midcontinent. $1^{\circ} \times 1^{\circ}$ latitude/longitude grid, data weighted-averaged to altitude of 400 km. Albers projection, contour interval of 2 nT. (Black, 1981)	38
20.	Scalar anomaly map of Fig. 19, with (400 km) high-pass wavelength filter applied.	39
21.	Scalar anomaly map, $1^{\circ} \times 1^{\circ}$ data at 400 km altitude, high-pass filtered and reduced to the magnetic pole. Contour interval 2 nT. (Black, 1981)	41
22.	Comparison of scalar magnetic anomaly maps for the study area.	42
(a)	from NASA's preliminary map (March 1981), data from below 400 km, on $2^{\circ} \times 2^{\circ}$ blocks	
(b)	our map of filtered, reduced-to-the-pole data (Figure 21)	
23.	Comparison of magnetic anomaly maps of the midcontinent. Scalar field, H_T . C.I. = 2 nT.	44
(a)	Anomaly map.	
(b)	Filtered anomaly map.	
24.	Some major tectonic and geophysical features of the U.S. midcontinent. Albers-projection base map.	46
25.	Geologic structures in the central midcontinent.	47
26.	Region of main arm of CNARS, as outlined by MGA (Midcontinent Geophysical Anomaly).	48
27.	Bouguer gravity anomaly, or MGA, of CNARS in central midcontinent (map excerpt from Woollard and Joesting, 1964).	52
28.	Aeromagnetic anomaly map of MGA and environs in central midcontinent (from USGS/SEG Composite Magnetic Anomaly Map of U.S., U.S.G.S. Map 954A, 1982)	53
29.	Schematic of development of MGA in southwest Iowa, 1100-1200 million years ago (Anderson, 1981). Granitic rock has x's, basalts have short dashes, sediments have dots.	56
30.	Geologic age provinces of Precambrian basement, U.S. midcontinent (after Van Schmus and Bickford, 1981).	59

	Page
31. Crustal thickness (as depth of Moho below sea-level) in central midcontinent. Contours in km. (excerpt from Allenby and Schnetzler, 1983)	60
32. Free-air gravity anomaly map. Data average on $1^{\circ} \times 1^{\circ}$, high-pass filtered for wavelengths greater than 8° , and with contour interval of 10 milligals (from Von Frese et al, 1982b).	62
33. Iseismal contours for earthquakes in SE Nebraska (1935, Mercalli intensity VI) and NE Oklahoma (1952, Mercalli intensity VII). (data from Docekal, 1970)	63
34. Paleogeographic reconstruction of North American craton in late Precambrian (Keweenawan) time, 1100 million years ago, during formation of CNARS structure. From paleo-magnetic data.	66
35. Crustal thickness (as depth of Moho below sea-level) for continental U.S. Contours in km. (Allenby and Schnetzler, 1983)	71
36. Thickness of the lower-crustal (mafic) layer, for continental U.S., in km. (Allenby and Schnetzler, 1983)	73
37. Equivalent-source dipole moment strength, for continental U.S. Derived from inversion of POGO satellite magnetic anomaly field. Dipoles are on a grid $150 \text{ km} \times 150 \text{ km}$; contour values in 10^{17} amp-m^2 (from Allenby and Schnetzler, 1983, as modified from Mayhew, 1982)	74
38. Rock magnetization in the interpreted lower-crustal layer, for continental U.S. (Schnetzler and Allenby, 1983). Shaded area has insufficient data control. Units are amps/m (10^3 emu/cm^3).	75
39. Comparison of Magsat reduced-to-the-pole scalar magnetic anomaly map (Fig. 21) with overlay transparency of tectonic structures (Fig. 24).	89
40. Two-dimensional magnetic and gravity modelling of Kentucky/Tennessee magnetic high. Profiles are west-east; solid lines are measured anomalies, dashed lines are modelled. Densities in gm/cm^3 , magnetization contrast is 4 amp/m (0.004 emu/cm^3). (Mayhew, Thomas, and Wasilewski, 1980)	91
41. Location of profiles for geophysical modelling of CNARS/MGA paleorift structure, in southwest Iowa. On Bouguer gravity anomaly map; C.I. = 5 milligals.	99
42. Gravity and magnetic modelling on profile F-F' across MGA structure (Anderson and Black, 1981).	100
43. Gravity and magnetic modelling on profile H-H' across MGA structure (Anderson and Black, 1981).	101
44. Gravity and magnetic modelling on profile E-E' across MGA structure (Anderson and Black, 1981).	102

	Page
45. Location of known metallic-mineral deposits and provinces in the central midcontinent, for copper ("C"), zinc ("Z"), and lead ("L"). Numbers are keyed to listing in text here. Scale: 5° of latitude is about 550 km. (adapted from Tooker et al, 1980)	112
46. Magnetization intensity in the lower-crustal mafic layer, for central midcontinent (excerpt from Fig. 38; Schnetzler and Allenby, 1983). Units are amp/m.	116
47. Magnetic mineral compositions in ternary diagram FeO-TiO ₂ -Fe ₂ O ₃ . Solid-solution series "I" is titanomagnetite, "II" is ilmenohematite. (from Carmichael, 1982)	119
48. Typical geothermal gradients in geologic areas, as a basis for calculating Curie-temperature isotherm depths. 1--low gradient (e.g. Sierra Nevada, southwest USA); 2--ancient shield; 3--oceanic crust; 4--high gradient (e.g. Basin and Range, western USA). A, B, and C are T _c -gradients for titanomagnetites. (Carmichael, 1977)	145

INTRODUCTION

The Satellite Mission

NASA's Magsat satellite was launched October 30 1979 from Vandenberg Air Force Base in California (Langel et al, 1982a; and see Figure 1). It was placed into a sun-synchronous orbit, that is, in the twilight plane (dusk meridian) to avoid the highly conductive (Sq) dayside current region with its associated transient magnetic field effects. The orbit inclination was 96.76° , initial apogee was 561 km, and initial perigee was 352 km. As the mission proceeded, the orbit decayed to a more circular one (see Figure 2), until after $6\frac{1}{2}$ months the apogee was under 400 km and the satellite came down on June 11 1980.

Magnetic field data were collected from early November 1979 until the following May. On one complete orbital track, correction of the data for altitude effects will vary from, say at the early stage of the mission, from about 550 km to 350 km and back to 550 km again. The satellite location was known to about 30-60 meters radially from the Earth, and to about 300 meters horizontally.

The satellite had its magnetometers on the end of a 6-meter boom, to diminish the effects of spacecraft fields. The measuring apparatus included a cesium-vapor magnetometer for absolute (scalar) field measurements, and a triaxial set of flux-gate magnetometers for directional (vector) field measurements. The scalar instrument operated sporadically but was used to help calibrate the vector instruments. The vector field components, for the "attitude-corrected" data, are accurate to better than 6 nanoteslas (nT)* and the total (vector sum) field is accurate to better than 2 nT.

The magnetic fields as measured by the satellite included contributions from the terrestrial core field (of magnitude up to about 50,000 nT), and geomagnetic transient fields from external ionosphere/magnetosphere current systems (of magnitudes up to 100's of nT), and magnetic anomaly fields from magnetization originating in the Earth's crust (of magnitudes ± 20 nT from an arbitrary zero level), at Magsat altitudes.

* nanoTesla in S.I. units; equivalent is gamma in cgs units

ORIGINAL PAGE IS
OF POOR QUALITY

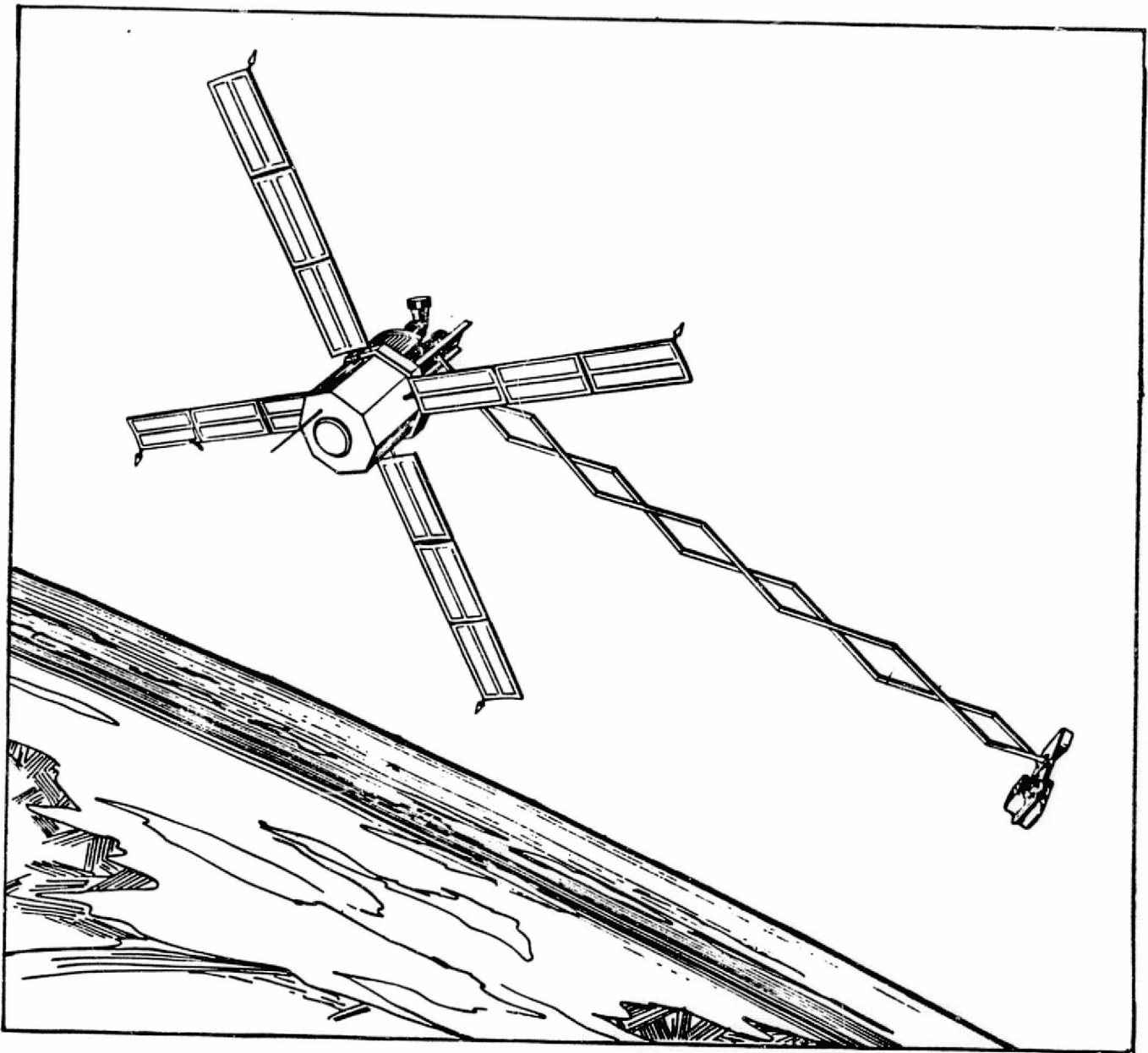


Figure 1: Artists Conception of Magsat

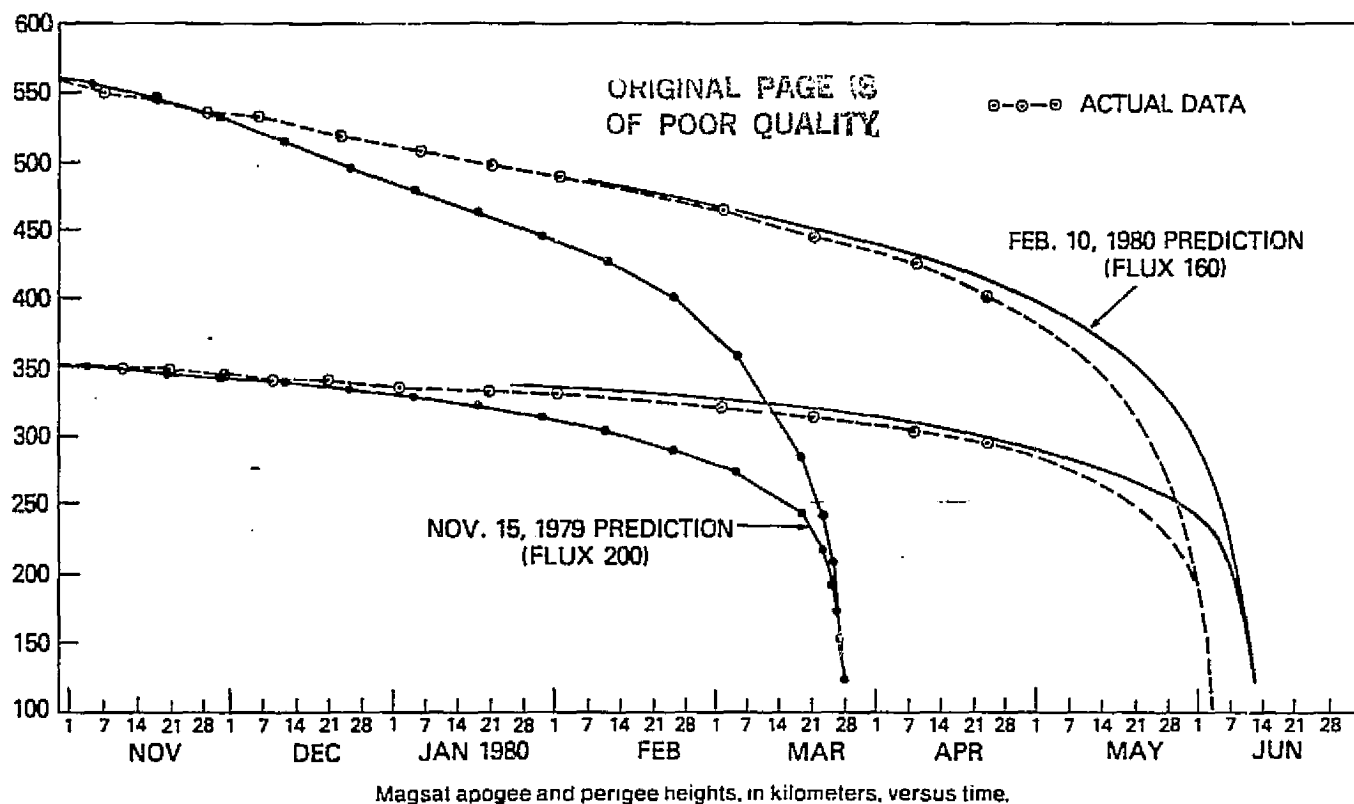


Figure 2. Magsat orbit dimensions, for 1979-80 (from EOS, v. 61, p. 545, July 1980)

Satellite	Inclination (deg)	Altitude Range (km)	Dates	Instrument	Approximate Accuracy (nT)	Coverage
Sputnik 3	65	440 - 600	5/58 - 6/58	Fluxgates	100	USSR
Vanguard 3	33	510 - 3750	9/59 - 12/59	Proton	10	Near ground station*
1963-38C	Polar	1100	9/63 - 1/74	Fluxgate (1-axis)	30 - 35	Near ground station
Cosmos 26	49	270 - 403	3/64	Proton	Unknown	Whole orbit
Cosmos 49	50	261 - 488	10/64 - 11/64	Proton	22	Whole orbit
1964-83C	90	1040 - 1089	12/64 - 6/65	Rubidium	22	Near ground station
OGO-2	87	413 - 1510	10/65 - 9/67	Rubidium	6	Whole orbit
OGO-4	86	412 - 908	7/67 - 1/69	Rubidium	6	Whole orbit
OGO-6	82	397 - 1098	6/69 - 7/71	Rubidium	6	Whole orbit
Cosmos 321	72	270 - 403	1/70 - 3/70	Cesium	Unknown	Whole orbit
Azur	103	384 - 3145	11/69 - 6/70	Fluxgate (2-axis)	Unknown	Near ground station
Triad	Polar	750 - 832	9/72 - present	Fluxgate	Unknown	Near ground station

*"Near ground station" indicates no on-board recorder. Data were acquired only when the spacecraft was in sight of a station equipped to receive telemetry.

Table 1. Satellites that have measured the near-earth geomagnetic field (from Langel, 1980).

One of the mission objectives, and our particular project interest, has been to map and analyse variations in the crustal-produced magnetic anomaly fields. This is to aid in assessing the utility of satellite magnetic data in interpreting crustal geological character and geophysical properties, such as major geologic structures, nature and evolution of continental tectonic regimes, crustal composition (rock type), prospective localization of economic resources (mineral deposit provinces, oil and gas basins, geothermal regions), and variations of crustal thickness.

Magsat was the first satellite to provide a global survey of vector magnetic fields and, because of its lower-altitude orbit, provides the most accurate and highest-resolution survey of the geomagnetic field and anomalies to date.

Other satellites have measured the near-earth's total (scalar) field, but to a lower accuracy. They are listed in Table 1 (Langel, 1979 and 1980). None of these missions were designed for solid-earth magnetic field studies. Only the POGO (Polar "Orbiting Geophysical Observatory") satellites of 1965-71 provided fairly accurate global surveys, and of the earth's total-field only. Those had satellite altitudes varying from 400 to 1500 km.

It was of considerable interest that even with the POGO data set, one could extract a component of field due to crustal magnetic sources. That is, one could begin to map crustal anomalies (Regan et al, 1975).

Table 2 lists a comparison of crustal anomaly mapping using the POGO data, and that from the more accurate, higher-resolution Magsat mission.

Table 2. Comparison of crustal magnetic anomaly mapping by satellite.

<u>POGO (1965-71)</u>	<u>MAGSAT (1979-80)</u>
- scalar field measurements	- both scalar and vector component field measurements
- most of the data from altitude above 500 km.	- data from about 300-500 km. altitude
- spatial resolution about 500 km	- spatial resolution about 200-250 km
- observed anomalies up to ± 10 nT	- observed anomalies up to ± 20 nT

An aspect of the vector component measurements is that they identify fields not parallel to the dominant main core field, so one has the prospect for interpreting the possible presence of remanent magnetization in large crustal sources. That is, one could separate the induced and any remanent component of magnetization. It would be very instructive to be able to identify and interpret the presence of crustal remanence from satellite data, if this proves to be possible (Galliher and Mayhew, 1982; Bhattacharyya, 1977).

Figure 3 shows how, in theory, the magnetic anomalies from two localized crustal sources should look at heights of 300, 450, and 600 km, assuming induced magnetization in a horizontal Earth's field. There should be a substantial increase in both anomaly amplitude and resolution, as one descends to the lower (satellite) altitude.

The Data

The satellite measured vector fields sixteen times a second and scalar fields (when operable) eight times a second. The data were pre-processed by NASA/Goddard Space Flight Center, and distributed on

CHRONFIN magnetic tapes - calibrated data in a North, East, and Z (downward) system

or

INV-B ("Investigator") magnetic tapes - data decimated to one sample each 5 seconds of time (i.e. one-fortieth of scalar data, one-eightieth of vector data); this corresponds to a point about every 36 km of orbit track.

The Investigator tapes are the preferred product for workers interested in assembling magnetic anomaly maps for regional crustal interpretation. Those tapes also include accessory information such as data/sample location in latitude, longitude, and radius, predicted geomagnetic field from a spherical harmonic core field model, local time, dip latitude, and an estimate of the external field. For the time-invariant crustal anomaly field, one would like data from magnetic "quiet" times, when there were low temporal magnetic variations. Parameters indicating this are the geomagnetic indices K_p and D_{st}^* , and Figure 4 shows how these varied over the 7-month lifetime of Magsat.

* e.g. D_{st} index measures temporal variation of magnetic fields produced by the equatorial ring currents (about 10^6 amperes, at about 5-8 earth radii and near the geomagnetic equator), relative to values on "quiet" days.

ORIGINAL PAGE IS
OF POOR QUALITY

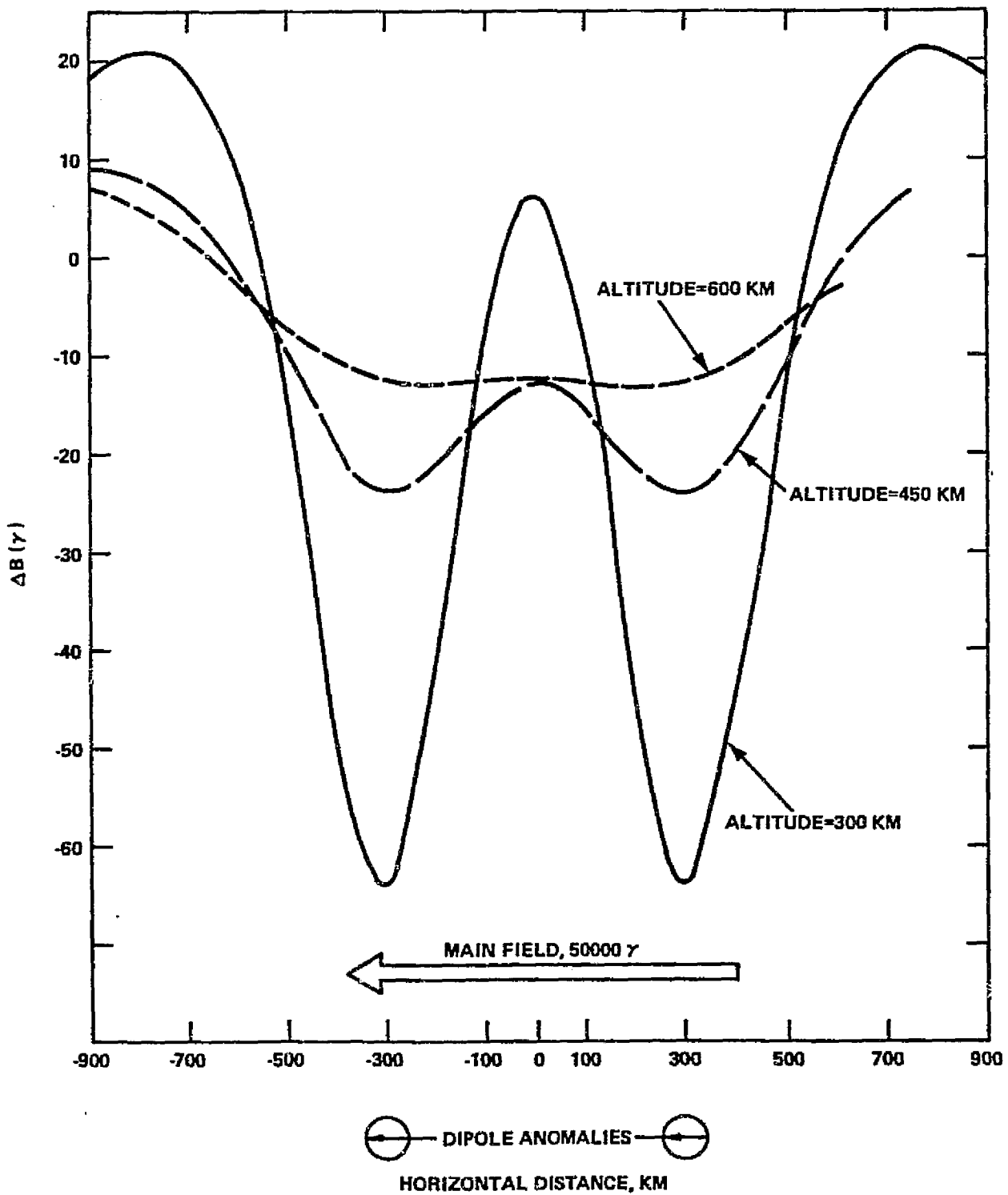


Figure 3. Comparison of theoretical magnetic anomalies
at different altitudes (from NASA).

ORIGINAL PAGE IS
OF POOR QUALITY

Days recommended by
Japanese Team

GEOMAGNETIC INDICES FOR MAGSAT MISSION
(DAILY AVERAGES)

▼ Very Quiet Days

▽ Quiet Days

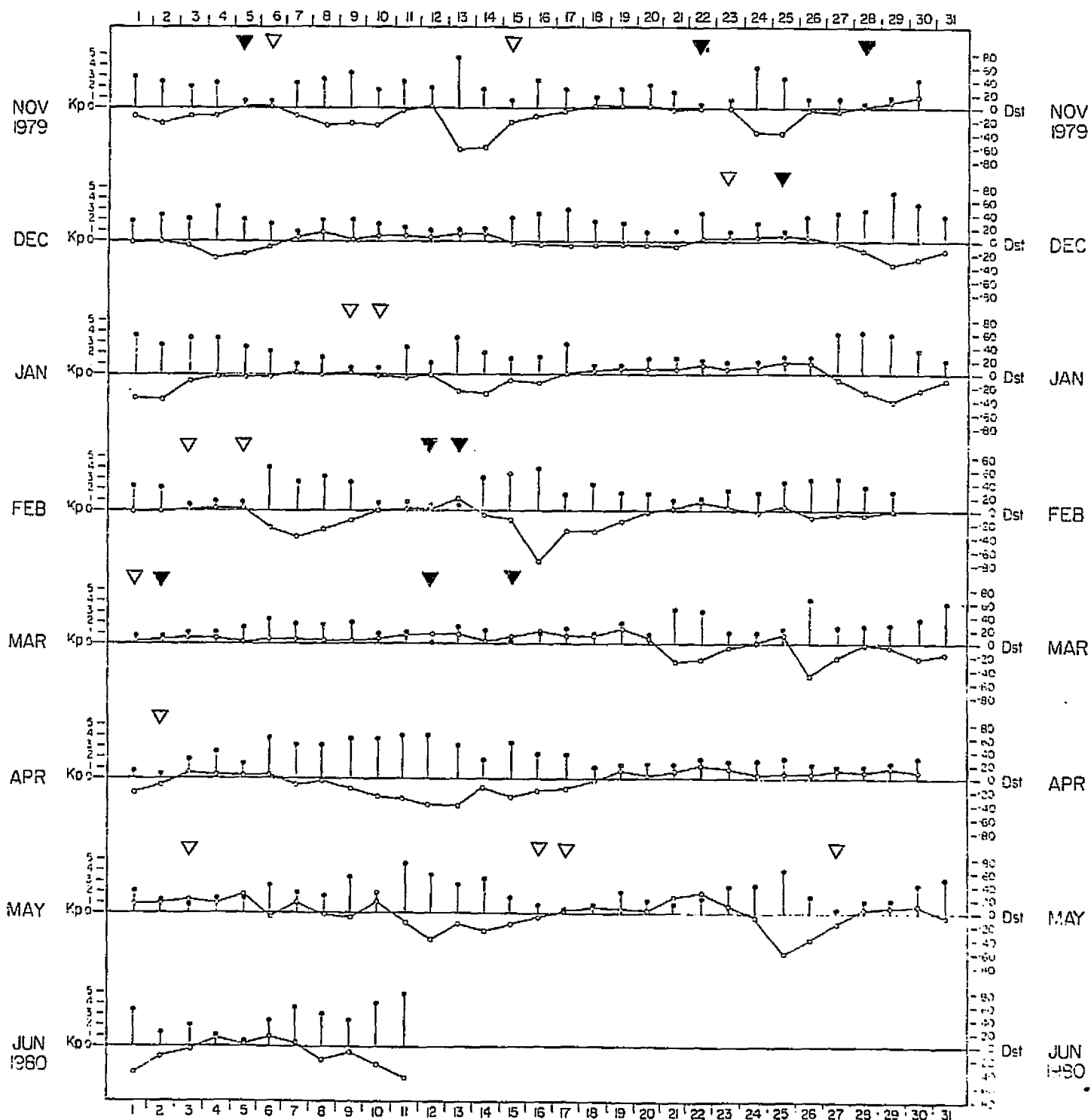


Figure 4. Geomagnetic indices during Magsat mission
(from Japanese project team)

On Figure 4 are indicated the best "quiet-time" days, as selected by the Japanese project team.

Another time-varying component contributing to measured magnetic fields could be that due to currents induced in the earth by the ionospheric currents. Lateral variations in electrical conductivity in the crust and upper mantle will give current distributions which could produce magnetic field patterns which might be fairly persistent in time. These are due to transient electromagnetic induction, and not true crustal magnetization. Their presence would be minimized by appropriate time-averaging and comparison of the data, particularly for magnetic "quiet-time" data being used.

The data were to be pre-processed by NASA at two levels of accuracy: "intermediate-attitude"-corrected, to 20 arc-minute accuracy, and "fine-attitude"-corrected, to 20 arc-second accuracy.

Spherical harmonic modelling of the magnetic field seen by Magsat, by Langel and others, yields a power spectrum of components that suggests that the internal core field has terms up to about order/degree 15, and that the crustal (anomaly) fields have terms from order/degree 13 and up. That is, the field originating from the crust dominates at order ("n") 15 and above. In processing Magsat data to get anomaly data, many workers typically thus take out a field model of order/degree 13.

After considerable data processing, NASA/Goddard provided global magnetic anomaly maps (Figures 5 to 8, Langel et al, 1982b). These were generally compiled from quiet-time data, and plotted on a global grid of $2^{\circ} \times 2^{\circ}$ latitude by longitude (i.e. about 220 x 220 km).

These maps were compiled as of November 1981. The zero levels are arbitrary, particularly for a given local geographic region, and in fact may vary in a relative way across the global map. The scalar anomaly map (Figure 8) is for $\pm 50^{\circ}$ latitude, has an average data altitude of 404 km, and has about 25 points per $2^{\circ} \times 2^{\circ}$ block used for the map assembly. For this map, the data range is from +18 nT to -22 nT. There is some apparent east-west banding, which can be non-crustal in origin. This could be introduced by,

- i) processing of data, e.g. by the along-track (north-south) filtering of data used to reduce the north-south striping originating from satellite passes having different altitudes and the resulting data having different arbitrary zero-levels

ORIGINAL PAGE
COLOR PHOTOGRAPH

MAGSAT ANOMALY MAP DELTA X CONTOURS

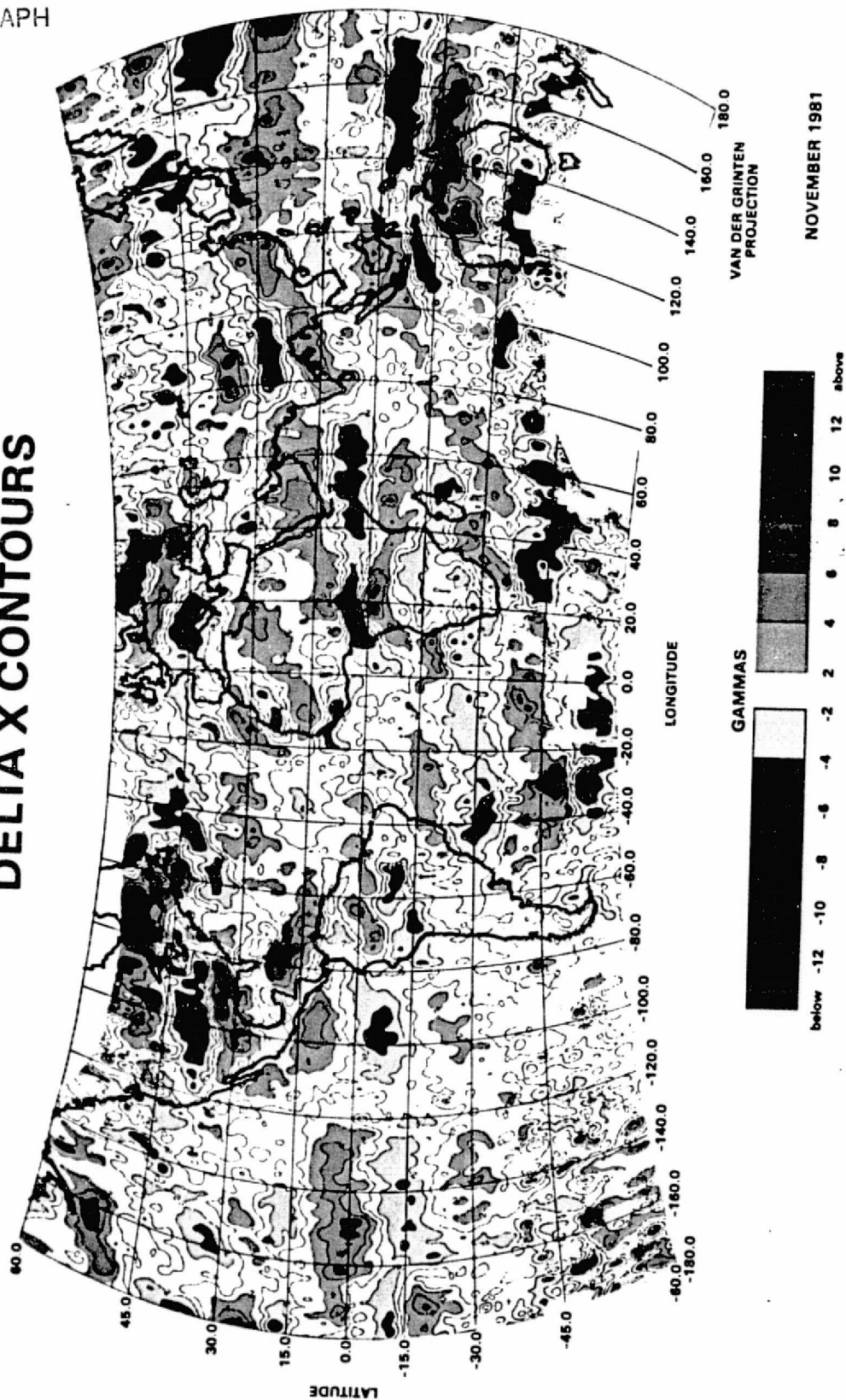


Figure 5. Magsat crustal magnetic anomaly map, of delta-X vector component (Langel et al, 1982b). Arbitrary zero level. Values are positive to the northward.

MAGSAT ANOMALY MAP DELTA Y CONTOURS

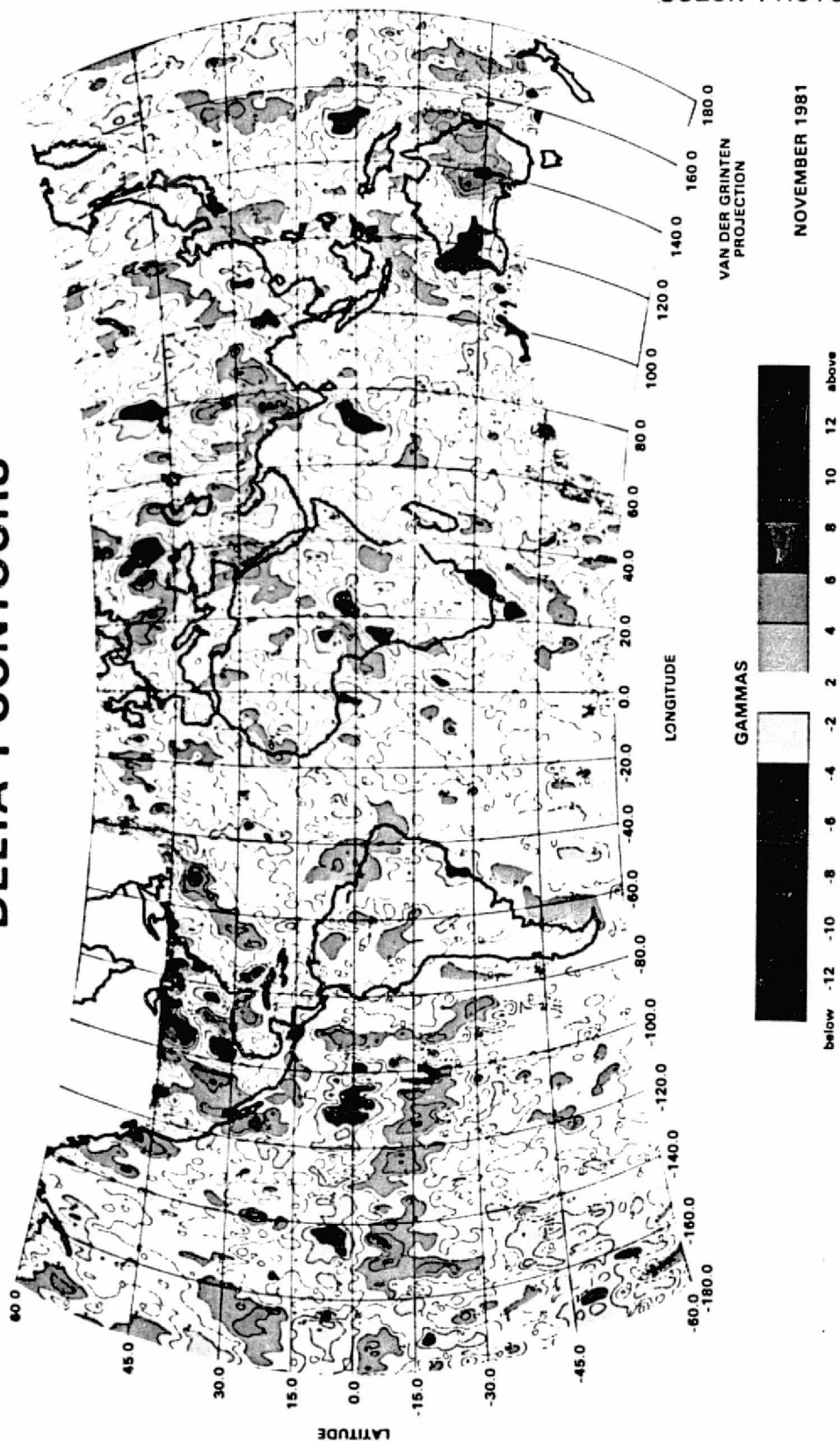


Figure 6. Magsat crustal magnetic anomaly map, of delta-Y vector component (Langel et al 1982b). Arbitrary zero level. Values are positive to the eastward.

ORIGINAL PAGE
COLOR PHOTOGRAPH

MAGSAT ANOMALY MAP DELTA Z CONTOURS

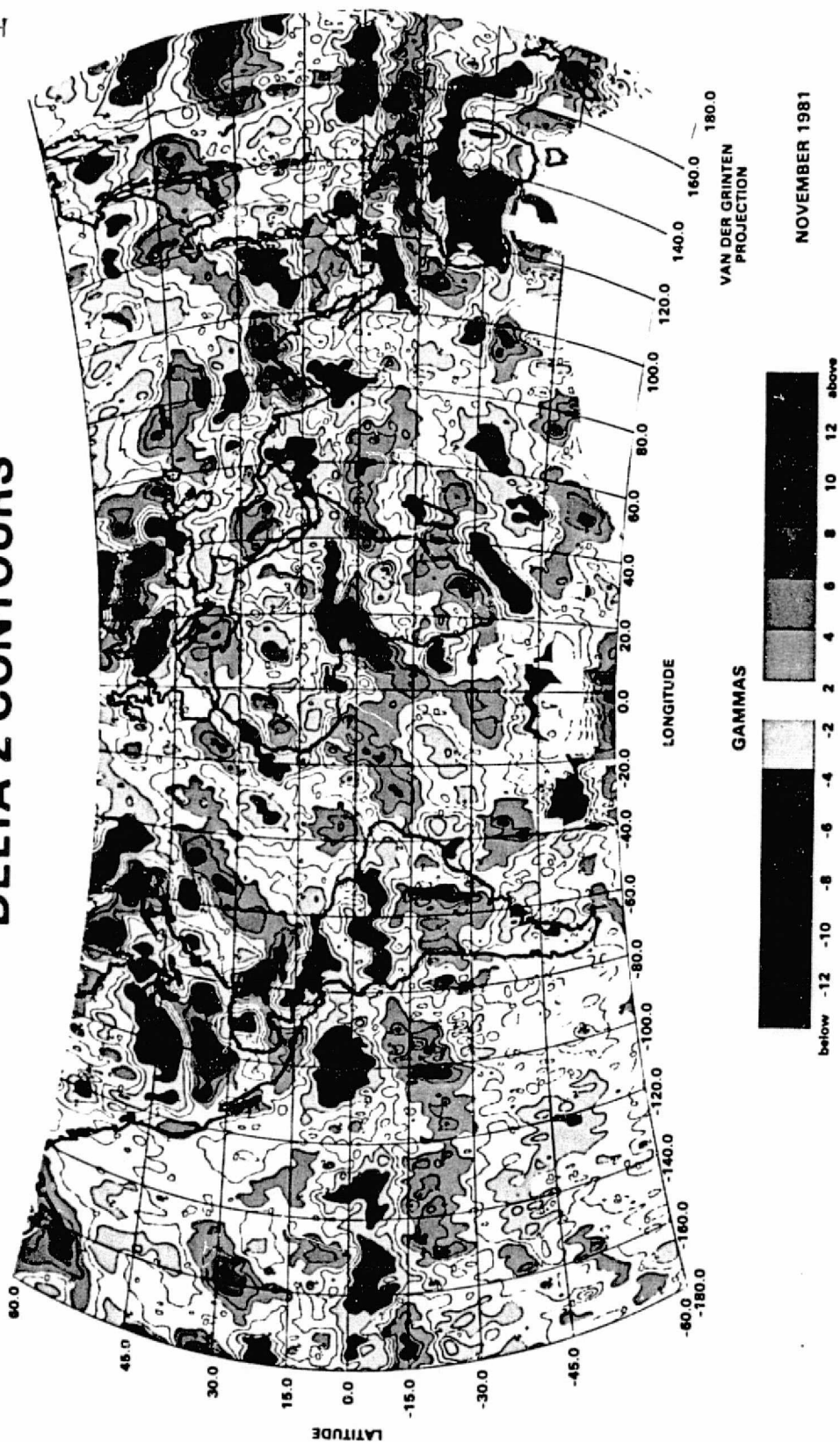


Figure 7. Magsat crustal magnetic anomaly map, of delta-Z vector component (Langel et al, 1982b). Arbitrary zero level.

**MAGSAT SCALAR ANOMALY MAP
RELATIVE TO MGST (4/81) MODEL**

AVERAGE ALTITUDE: 404 km AVERAGE PTS./2° x 2° BLOCK: 25

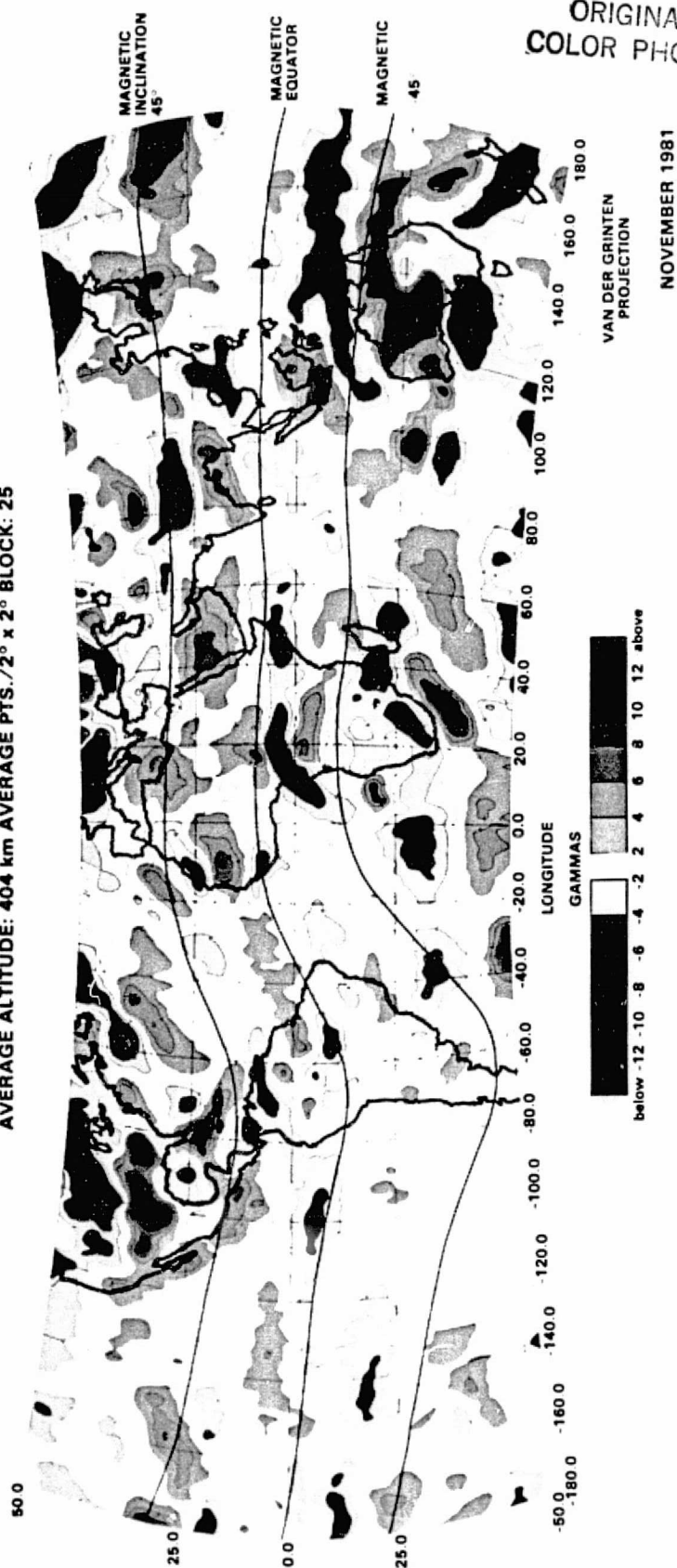


Figure 8. Magsat crustal magnetic anomaly map, of total-field (scalar) magnitude (Langel et al, 1982b). Arbitrary zero level.

- ii) the satellite tracks are north-south, which will tend to emphasize east-west features that are crossed in transit
- iii) incomplete removal of the field effects of the equatorial ring current, near the magnetic equator.

Thus east-west anomalies are emphasized* and the north-south anomalies are relatively suppressed. This has the effect of reducing the detectability of north-south crustal features.

The vector-component anomaly maps have field variations of up to ± 10 -15 nT. The magnitudes are,

<u>NASA anomaly map</u>	<u>field variations</u>
ΔX (positive northward)	+11 to -14 nT
ΔY (positive eastward)	+10 to -10
ΔZ (positive downward)	+15 to -14

For these maps, the latitude range given is $\pm 60^\circ$. There were about eight points per $2^\circ \times 2^\circ$ block, and there was an average altitude of about 430 km. In averaging the data, no adjustment was made for the different altitudes of the data, which varied from 340 to 552 km. It can be noted that the delta-X anomaly map has more apparent east-west anomalies* because of the along-track filtering in the north-south direction. The delta-Y map is noisier. This is presumably due to the influence of fields from ionospheric currents; for example, the equatorial ring current $\pm 15^\circ$ from the magnetic equator, and field-aligned sheet currents in the auroral zones (about 10 - 15° from the geomagnetic poles).

This Project

Our objective has been to use magnetic field data acquired by the Magsat satellite to construct a magnetic anomaly map of the U.S. central midcontinent. The data set will be the best that is practicable; for example, selected for reliability, and averaged on a $1^\circ \times 1^\circ$ latitude/longitude grid spacing rather than the customary $2^\circ \times 2^\circ$ spacing used for POGO studies and NASA's Magsat maps.

The magnetic anomaly map can then be used to help interpret (see p.13b, excerpt from Langel 1980) gross crustal character (geologic and tectonic terranes, crustal thickness and petrologic composition), and assessed as an aid in understanding the nature of the large-scale structural feature

* There can be an overlap of effects between east-west anomalies due to crustal sources being relatively emphasized, and apparent east-west anomalies being introduced as an artifact of the data processing

in the area--the Central North American Rift System (CNARS), especially the major portion of this which is expressed as the Midcontinent Geophysical/Gravity Anomaly (MGA).

The MGA/CNARS is a major crustal feature that extends over 1000 km from Lake Superior through Minnesota, Iowa, and to E.-central Kansas. It represents an extrusion and intrusion of mafic rocks in late-Precambrian time (Ke-

weenawan age, about 1100 million years ago), with crustal downwarping and then reactivation to form a central horst bounded by faults which have up to 10,000 meters of vertical displacement on them. The most prominent central portion of the MGA is in Iowa, where the central basaltic horst and flanking sedimentary troughs produce the most pronounced gravity anomaly in North America--over 160 milligals, in a lateral distance of less than 40 km. The MGA trend is the major part of the CNARS system, and represents a failed paleorift zone. Although the CNARS and its Precambrian basement rocks are buried over much of its extent in the central midcontinent, where the analogous and probably genetically-related terrain is exposed to the north end (northern Minnesota and Wisconsin) there are important economic mineral deposits--iron, zinc, lead, copper.

The regional, long-wavelength satellite magnetic data can be correlated with other geophysical and geologic data sets to help interpret the deeper and broader features and geologic setting. This thus adds new information for the geologic, tectonic, and structural framework of the region.

The data analysis techniques used should help in determining and refining optimum methods for processing the satellite magnetic data, for further application in interpreting magnetic anomalies for other geographic regions and geologic/crustal terranes.

Further on this project, an objective has been to compile and evaluate magnetic property data of crustal rocks of importance in modelling magnetic anomalies. This would include consideration of geothermal gradients and depth to the Curie-temperature (T_c) isotherm, at which magnetization is lost.

In addition to the continental-scale studies, several investigators will study more limited areas or particular tectonic features. Godivier (ORSTOM) will extend the work of Regan and Marsh²⁴ in the region around the Central African Republic where ORSTOM has a large amount of correlative data. Gasparini (Osservatorio Vesuviano) will investigate the Curie depth and volcanism in the Mediterranean area. Won (North Carolina State University) will study a combination of Magsat, aeromagnetic, and regional gravity data in the eastern Piedmont of the United States. Carmichael and associates (University of Iowa) will study the central midcontinent of the United States with particular attention to the known midcontinent geophysical anomaly.

(from Langel, 1980)

Activity Schedule

1980

- June 11 - Magsat satellite ends mission
- Dec. 3 - Project contract starts
- 3-6- Magsat meeting at Goddard Space Flight Center

1981

- Mar. 30 - we received sample data tape (limited profile data)
- July 10 - received first intermediate-attitude-corrected tape with profile data (for first 80 days of mission); i.e. first tape of our Investigator data set
- July 30-Aug. 14 - NASA Magsat meeting and IAGA Scientific Assembly, Edinburgh; and Internat. Conference on Tectonics, Oslo
- Aug. 19 - received second tape of Investigator data set
- Sept. 17-18 - Ann. Midwest Amer. Geophys. Un. meeting, Minneapolis
- Nov. 12 - received Investigator "final output" data tape, for quiet time data for period Jan. 19-May 19 1980

1982

- Oct. 17-21 - Ann. Soc. of Explor. Geophysicists meeting and Magsat session, Dallas
- Dec. - we requested a "no-cost" extension of contract, since Principal Investigator would be absent on a Leave assignment overseas for 5 months (as geoscientist on a college ship)

1983

- Jan.-May - P.I. on Leave overseas
- Sept. 3 - contract expires

DATA PROCESSING

In order to investigate the utility of satellite magnetic data for geologic interpretation, and resolution of causative crustal sources, we need an optimum data set. This would incorporate

- i) quiet-time data, from time intervals when the transient (external) field variations were a minimum
- ii) data "cleaned" of spurious information introduced in the data-acquisition or pre-processing operations, i.e. that is non-terrestrially based
- iii) comparison and correlation of data from spatially nearly-coincident orbit tracks, to best assure a reliable and consistent data set
- iv) data "reduced" to a common elevation and grid, so that data are equalized and distributed and maps can be contoured to reveal magnetic anomalies.

The objective is to remove contributions to the data set of time-varying fields (due to geomagnetic transients) and spatially-varying field values (due to differences in satellite altitude), and artifacts of the pre-processing of the raw data. This will yield the invariant field "morphology" which is due to crustal magnetization, and hence to the best resolution that can be achieved for the Magsat satellite orbital altitudes.

Correction of Data

The magnetic field profiles on individual orbital tracks^{*} have been examined to identify "bad" data points or profiles.^{**} The isolated spikes of the former can have magnitudes of tens of 1000's of nanoteslas. Data problems can include

- i) individual spikes of erroneous data
- ii) raised or lowered effective "zero level" of a profile, due to
 - hardware problems
 - pre-processing, before Investigator tape sets are produced
 - long-period (and hence long-wavelength) diurnal or geomagnetic-transient field effects on a particular orbit pass

* the "Investigator" tape data are decimated, so data points are about 36 km apart

** data processing here was performed on a Perkin-Elmer 3220 (Iowa Geological Survey) and IBM 370 (University of Iowa)

Changing the zero level of (part of) a profile, due to long-period field variations, would lead to striping of the anomaly map along the azimuth of the satellite tracks. This is roughly north-south. Such striping would obscure and confuse the identification and interpretation of crustal sources (structure, and features such as geologic province boundaries) that strike in a north-south direction.

Figure 9(a) shows an example of a pass (no. 85) over the U.S. mid-continent, from 25-50° N. latitude. The individual erroneous data spikes have magnitudes up to 57,000 nT, superimposed on the true anomalies with magnitudes of a couple of tens of nanoteslas. The true anomaly is thus rendered indistinguishable by comparison. When these spikes are removed, as seen in Figure 9(b), the proper anomaly field is revealed. It has a total amplitude here of about 24 nT*.

Calculation of scalar (total-field) anomaly data

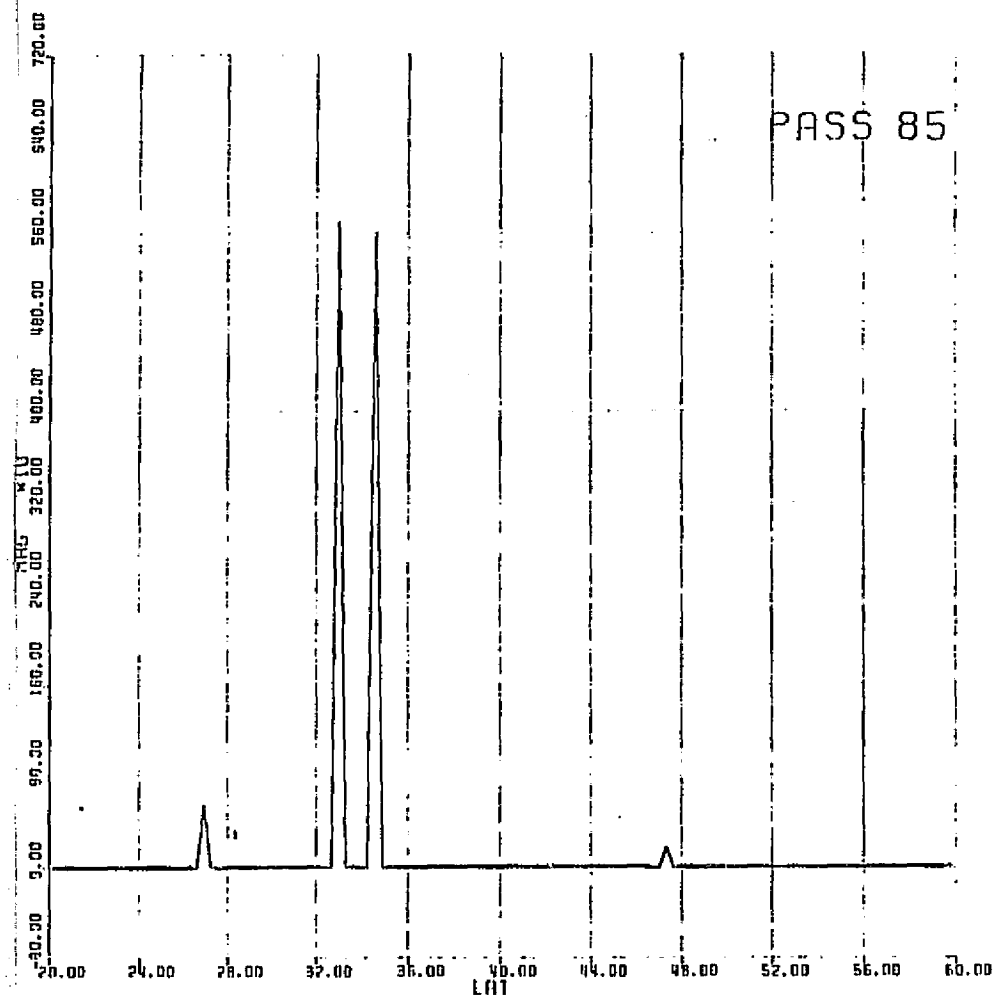
Since the total-field magnetometer did not perform continuous data gathering, the scalar magnetic field (H_T) magnitude can be calculated from the vector summation of the X (or H_x , for northward), Y (or H_y , for eastward), and Z (or H_z , for downward) component fields as measured by the vector magnetometers.

For example, Figure 10 shows the "raw" (NASA pre-processed) investigator data on pass 85, having a track profile over the U.S. midcontinent. Figure 10 (a), (b), and (c) show the H_x , H_y , and H_z components respectively of the "anomaly" field, with the calculated scalar total-field H_T being shown in Figure 10(d). At these relatively northerly magnetic latitudes, the H_z component and total-field H_T are similar; near the magnetic equator, the H_x component and H_T would be similar.

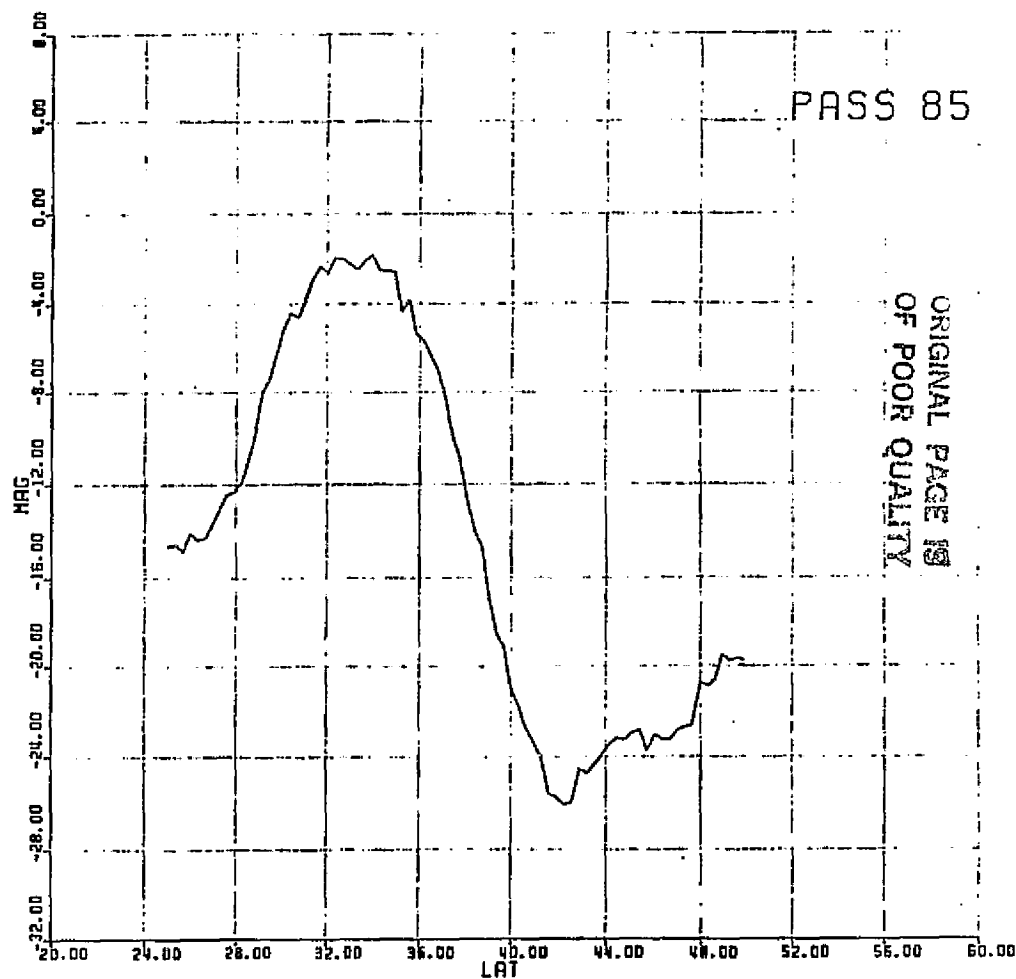
As is generally the case, at least at these magnetic mid-latitudes, the component-field profile data are "noisier" than the scalar magnitude profile.

* The zero-level datum on the data tape, and for contoured anomaly maps (for NASA's, and here) is arbitrary. In fact, because of processing corrections and techniques, the relative zero level can vary across a geographic region which is sufficiently large. In analyzing and interpreting profile or map anomalies, the extrema terms "high and low", "maximum and minimum", and "positive and negative" are fairly synonymous. A magnetic "negative" could be, with a lowered arbitrary zero level for the local region, actually be a relatively low-amplitude "positive".

Magnetic-field
Magnitude (in 10^2 nT)



(a) original tape magnetic data (H_T), with spikes;
"anomaly" magnitude vs. latitude



(b) magnetic anomaly profile, after spikes removed

Figure 9. Total-field profile on track over U.S. Midcontinent,
for pass 85

Field (nT)

ORIGINAL PAGE IS
OF POOR QUALITY

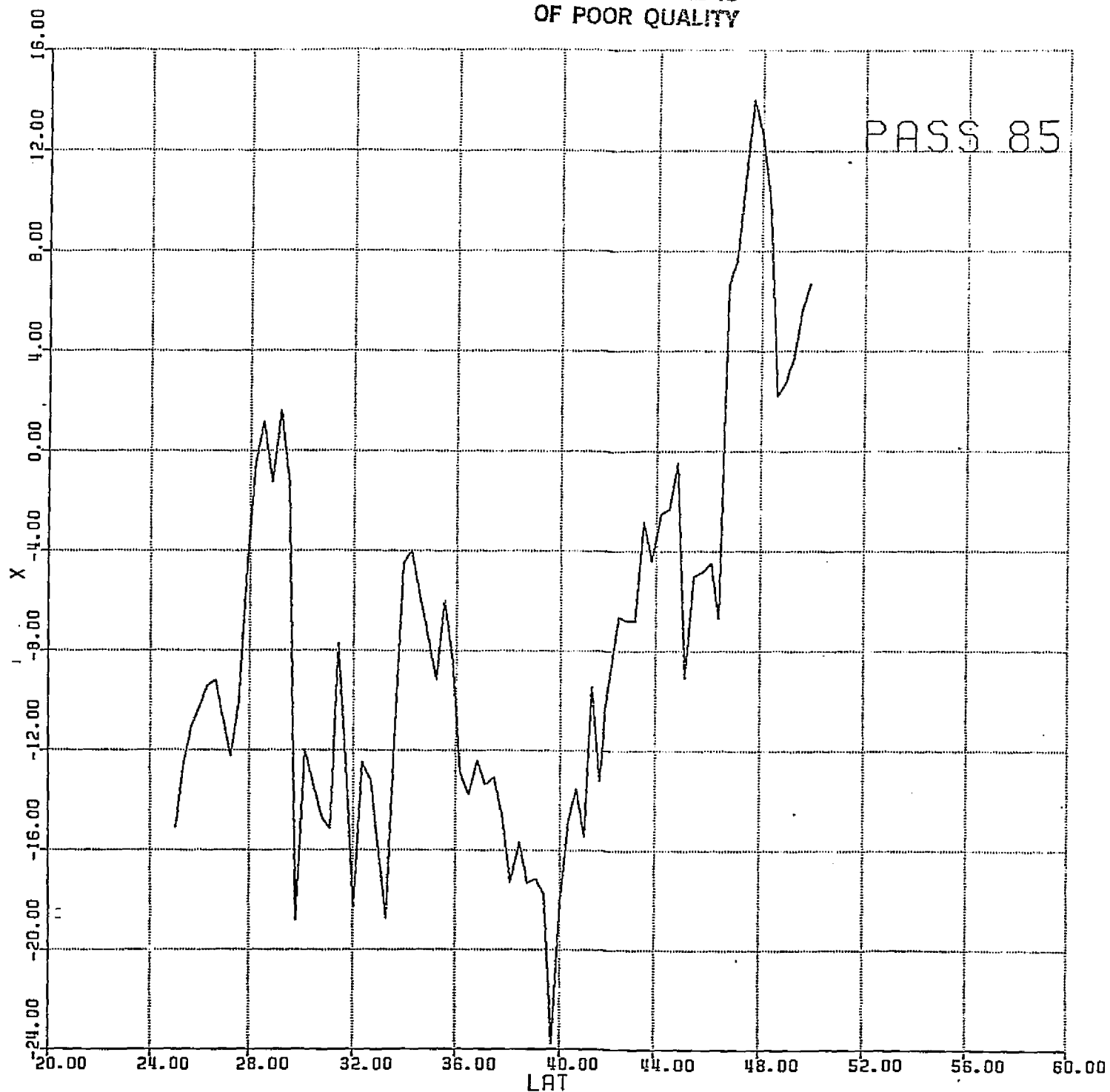


Figure 10. Magnetic "anomaly" fields, as measured for
pass 85. Field (nT) vs. latitude (degrees North).
(a) Vector component H_x .

Field (nT)

ORIGINAL PAGE IS
OF POOR QUALITY

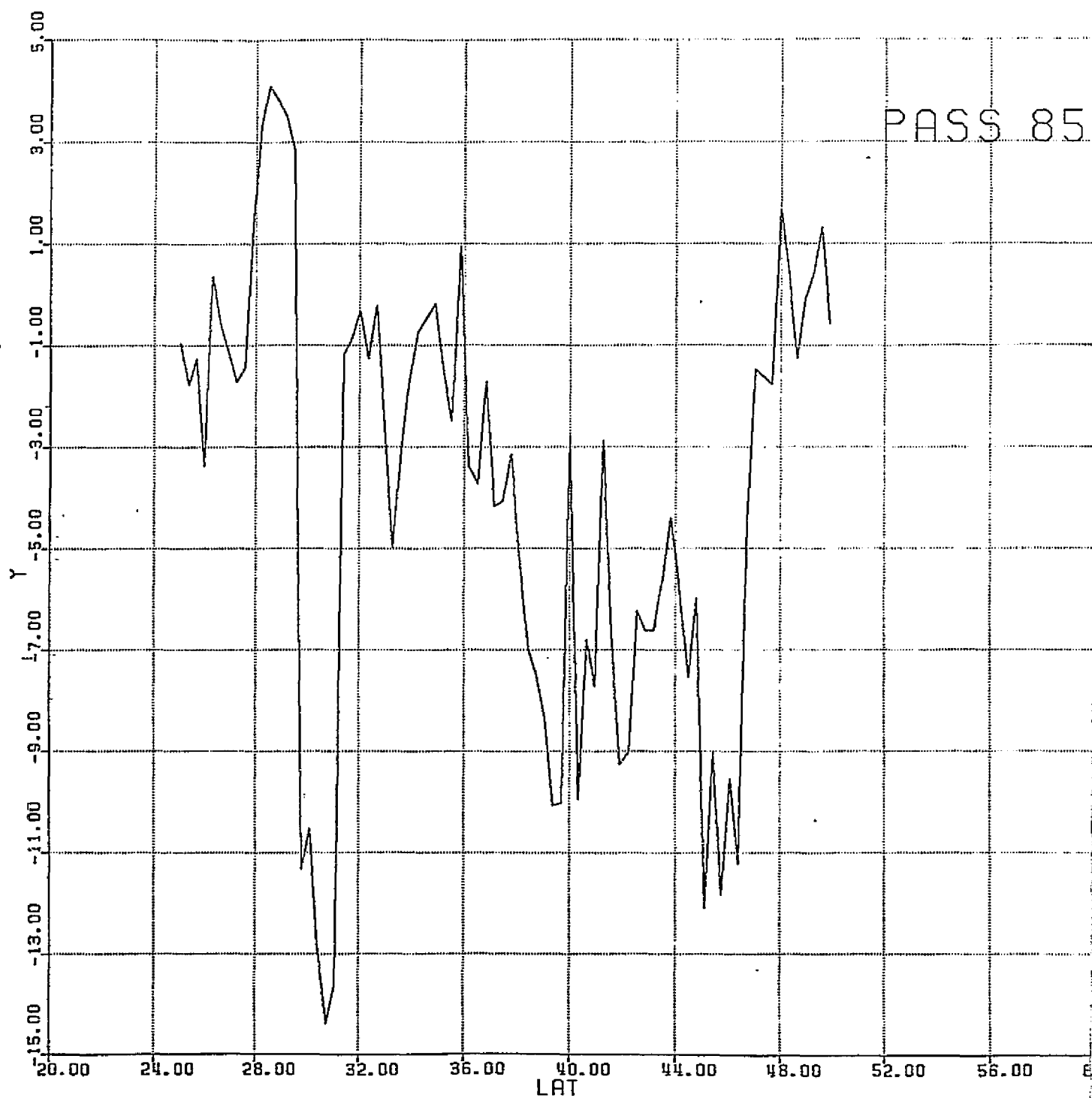


Figure 10 (continued)
(b) Vector component H_y

ORIGINAL PAGE IS
OF POOR QUALITY

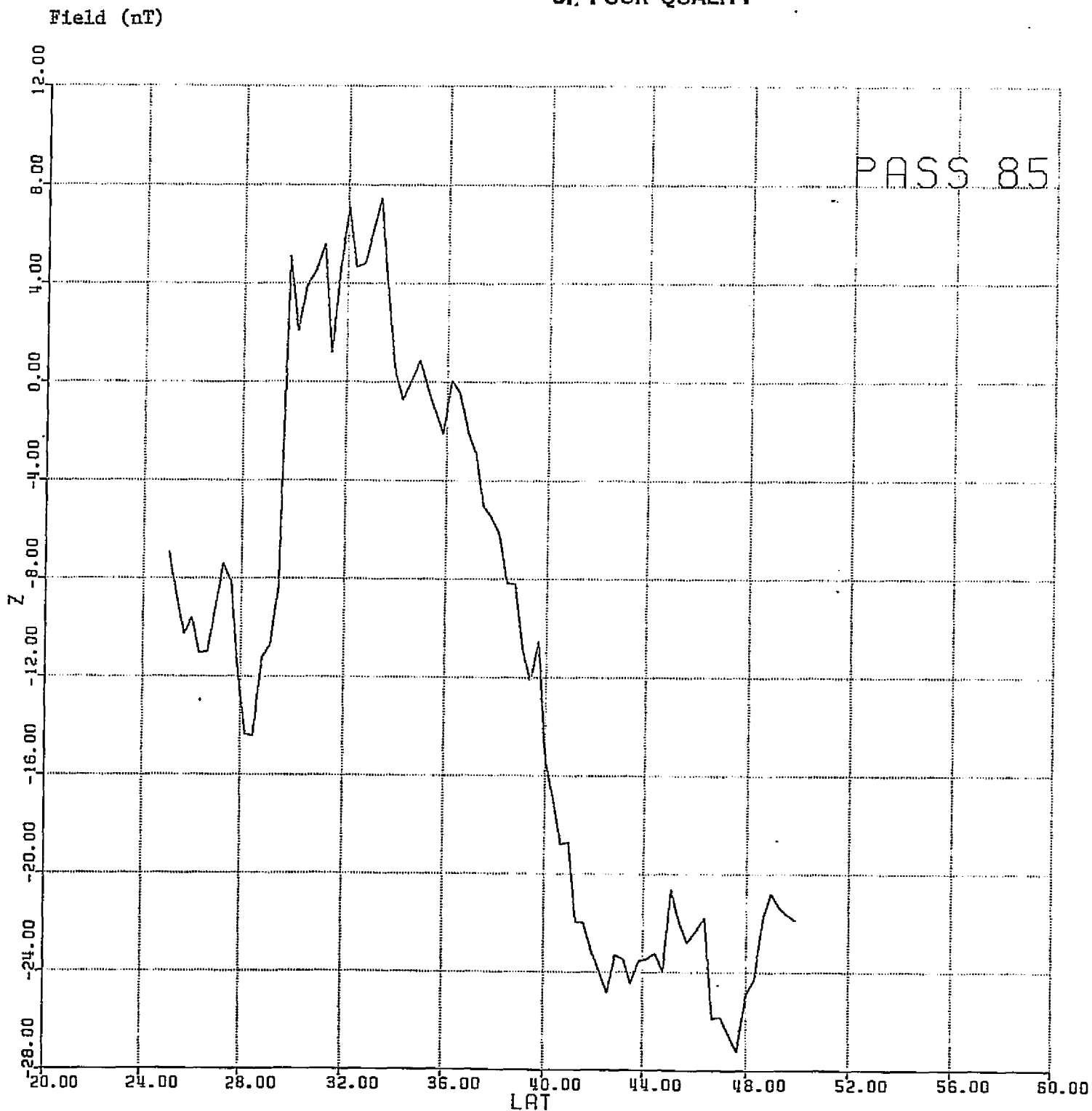


Figure 10 (continued)
(c) Vector component H_z

ORIGINAL PAGE IS
OF POOR QUALITY

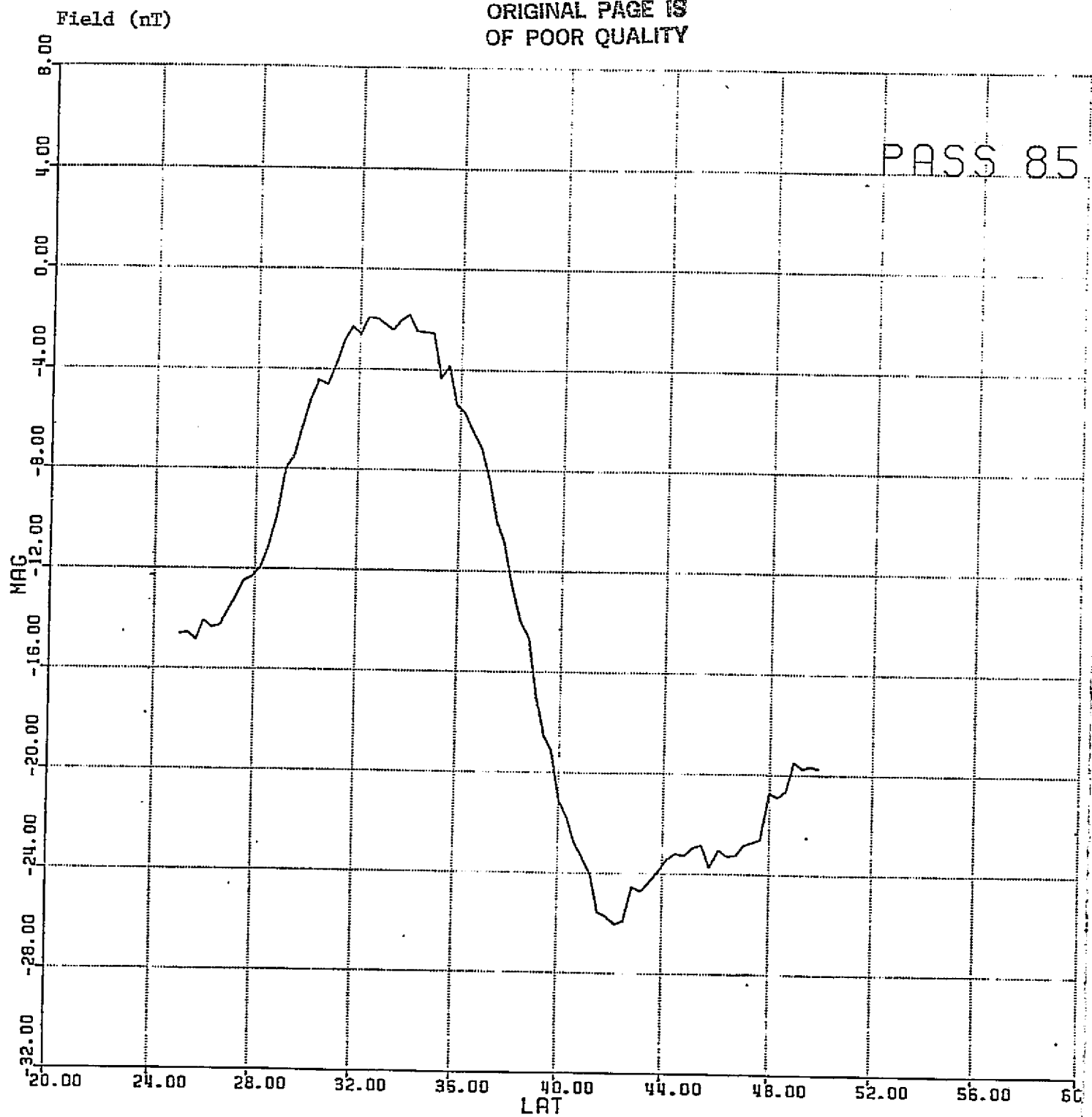


Figure 10 (continued)
(d) Calculated scalar (total-field) magnitude, H_T

The short-period "noise" variations, recorded as a function of time, are displayed as "short-wavelength" variations when plotted as a function of profile (track) distance. They have amplitudes of several nanoteslas. They are clearly temporal variations, since

- i) they are different for each pass over the same or near-neighbor tracks
- ii) they are too short to be produced at satellite elevation by true sources in the earth's crust.

These variations are thus not terrestrially-based, and need to be removed from the desired time-invariant crustal anomaly data set. This can be done by along-track filtering, or smoothing by a running average, of either the noisy component-field data or (preferably) of the calculated scalar magnitude data.

Correlation of tracks and passes

To develop an optimally reliable data set for the mapping of magnetic anomalies, we need to compare profile data for the same satellite track but at different times (i.e. different passes), for nearly-coincident tracks, and for tracks that cross. This comparison will allow recognition of time-varying magnetic-field effects that could masquerade as an "anomaly" on an individual profile. These will include the long-period field changes which would change the apparent "zero" base level for profiles which would contribute to striping in the north-south direction when profile data are averaged.

To illustrate the time-varying magnetic effects left in the "anomaly" profile data that are supplied, Figure 11 shows H_x component data for passes 254 (Figure 11(a)) and 531 (Figure 11(b)). These can be compared with Figure 10(a) for pass 85 over the same track. In terms of the geomagnetic-transients and base-level changes, the comparison shows,

pass	approx. relative "base level"	approx. short-period deviations from mean curve
85	- 6 nT	± 10 nT
254	0 (arbitrary reference)	+14 to -10
531	- 4	± 6

Similarly, Figure 12 shows H_y component data for passes 254 and 531, and can be compared to Figure 10(b) for pass 85.

Field (nT)

ORIGINAL PAGE IS
OF POOR QUALITY

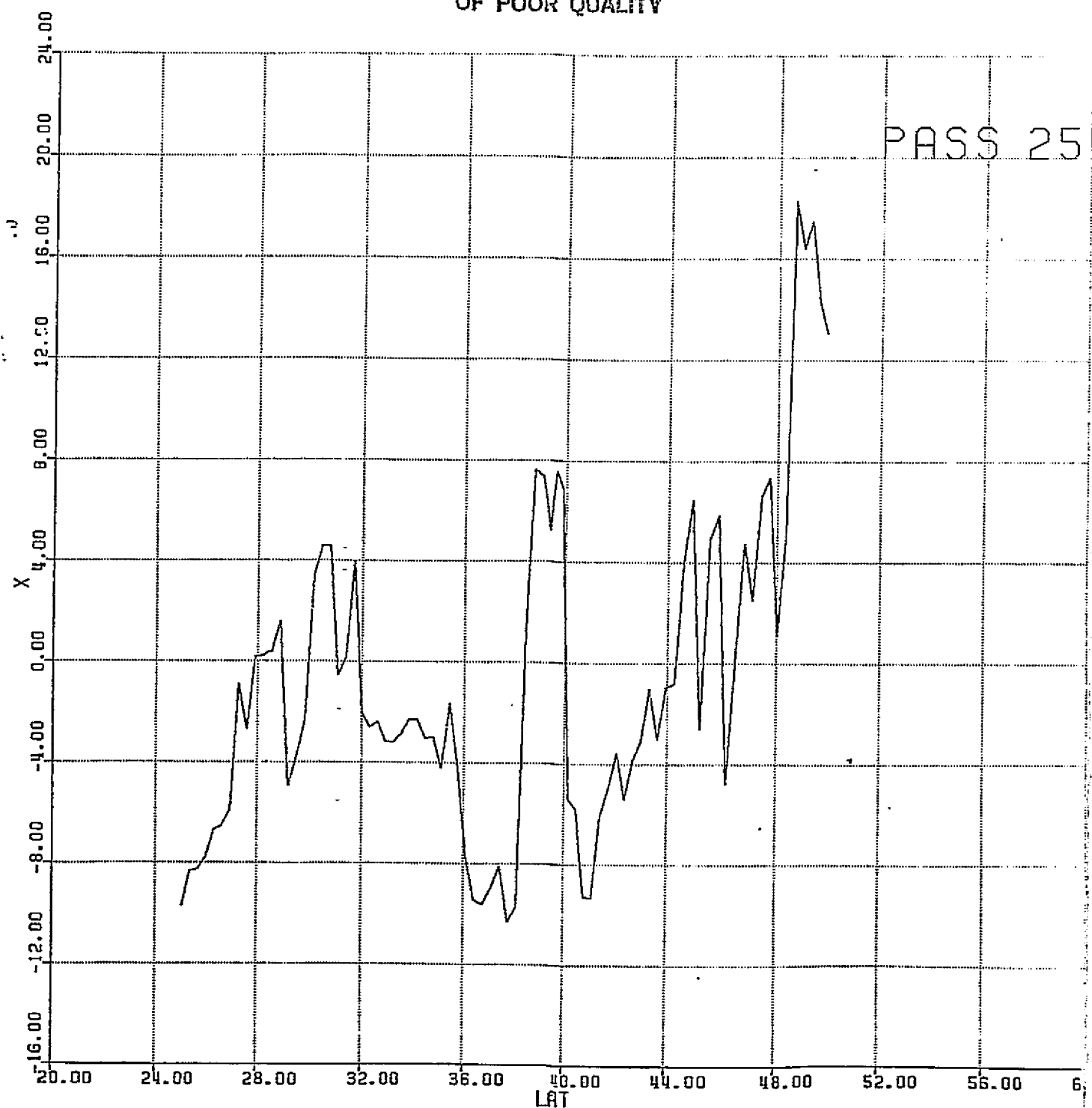


Figure 11. H_x component field data at different times over same track. Field (nT) vs. latitude (degrees North).
(a) Pass 254

Field (nT)

ORIGINAL PAGE IS
OF POOR QUALITY

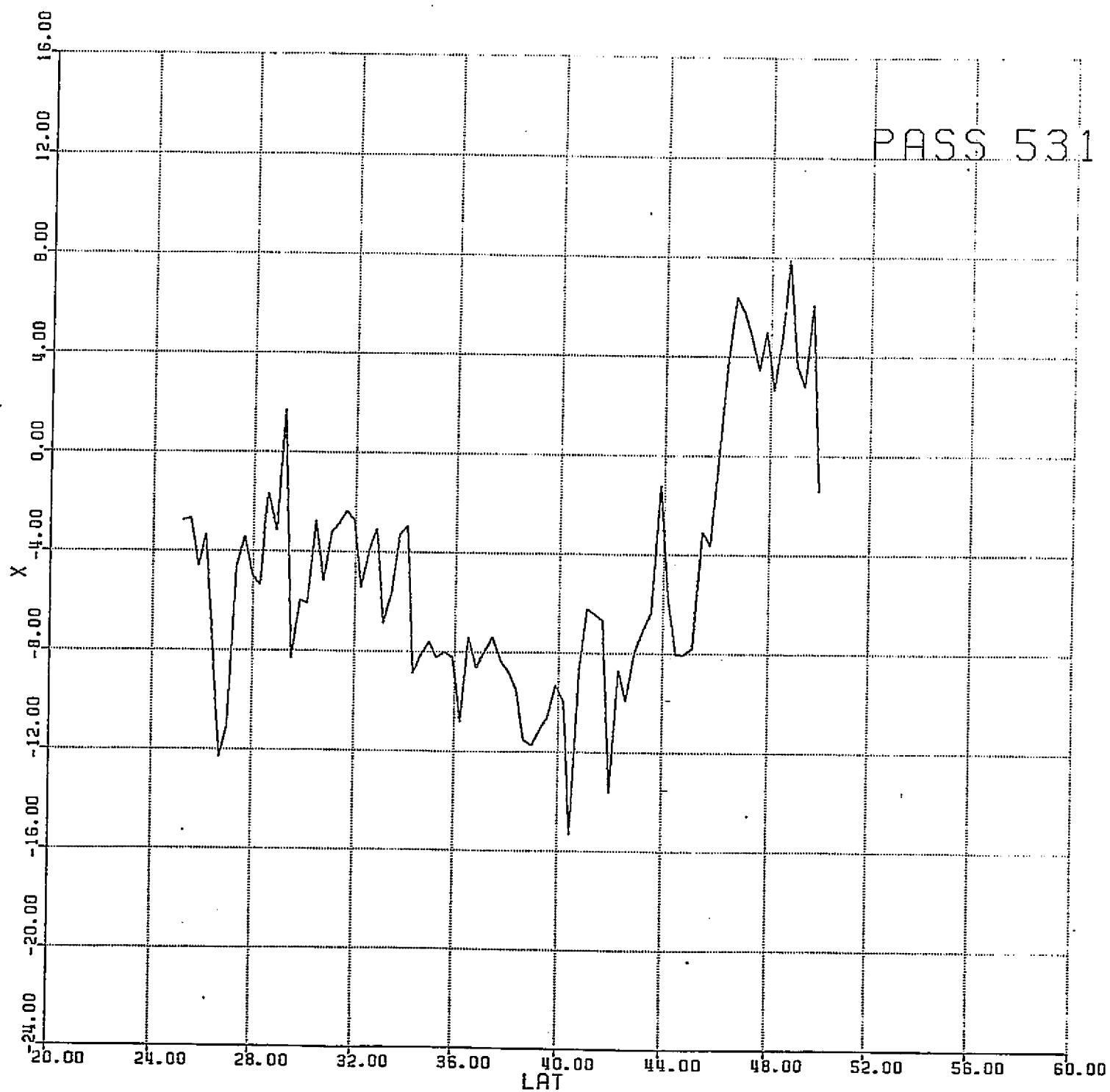


Figure 11 (continued)
(b) Pass 531

Field (nT)

ORIGINAL PAGE IS
OF POOR QUALITY

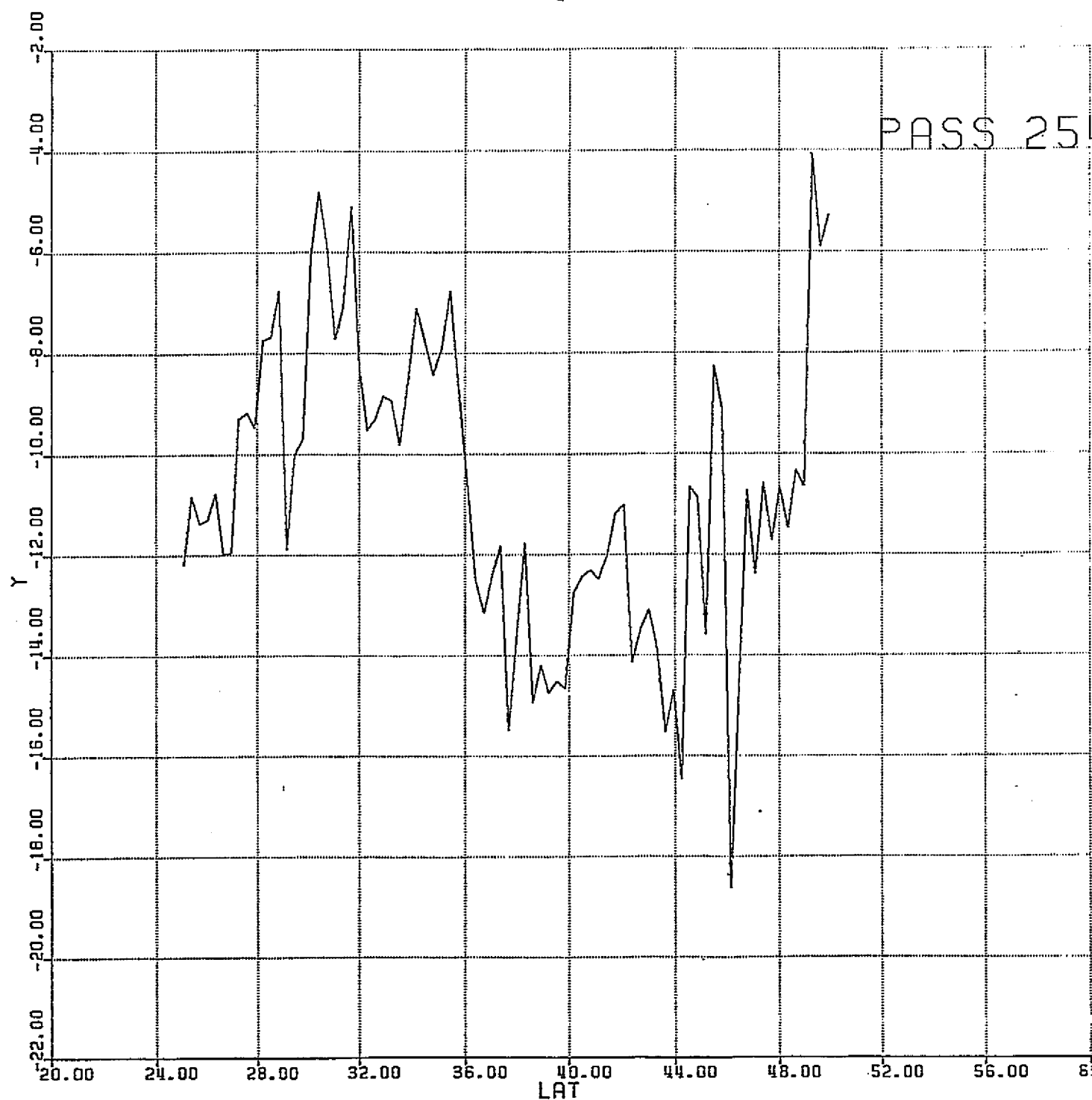


Figure 12. H_y component field data at different times over same track. Field (nT) vs. latitude (degrees North).

(a) Pass 254

ORIGINAL PAGE IS
OF POOR QUALITY

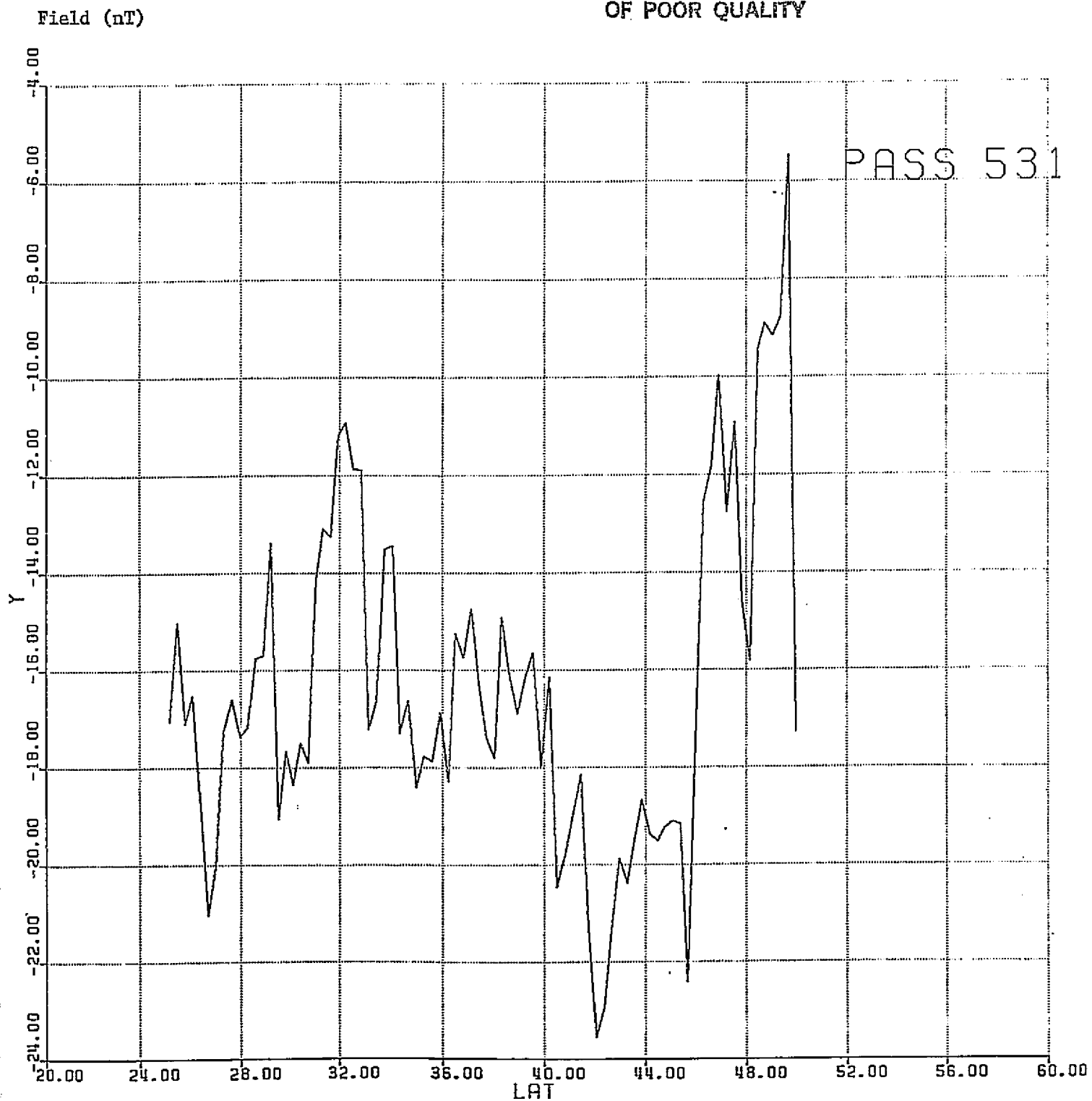


Figure 12 (continued)
(b) Pass 531

A comparison of H_y as recorded and pre-processed prior to distribution, for the three passes over the same track (see Figs. 10(b) and 12(a) and (b)), gives,

pass	approx. relative "base level"	approx. short-period deviations from mean curve
85	- 3 nT	+3 to -13 nT
254	-10	+3 to -6
531	-15	± 4

Smoothing of track (profile) data

Data along individual profiles can be statistically smoothed, to reduce the effect of geomagnetic transient disturbances. Figure 13 shows the effect of a running-average smoothing of the previous pass 85 (H_T scalar data, as seen in Figure 10(d)).

Reduction of data to grid and datum level

The satellite data are recorded in an uneven distribution in x (latitude), y (longitude), z (altitude), and time. To produce a regular grid of data suitable for contouring into an anomaly map, we establish a set of prisms (Figure 14) to include the selected satellite field values within the defined x, y, and z coordinates, for the whole time interval of the mission.

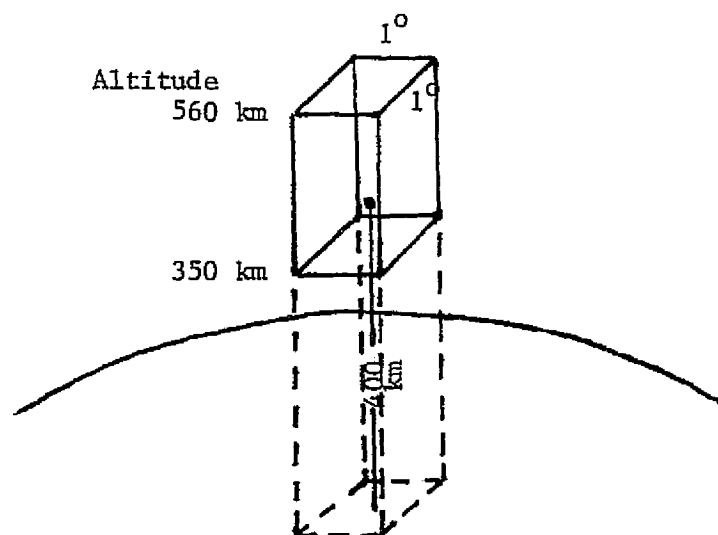


Figure 14. Data prism for grid point.

ORIGINAL PAGE IS
OF POOR QUALITY

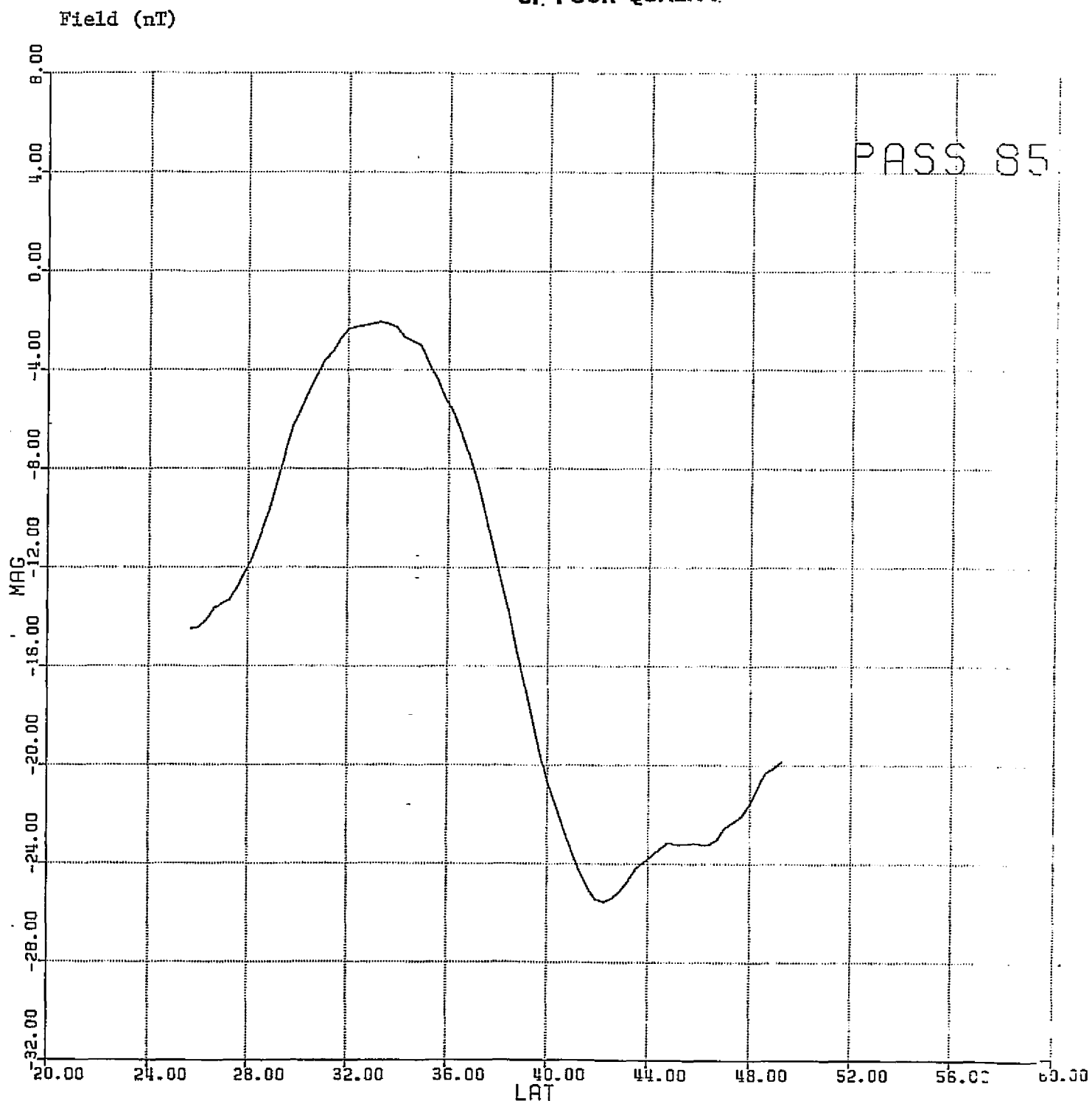


Figure 13. Running-average smoothing of scalar H_T field,
for pass 85. Field (nT) vs. latitude (degrees North).

As seen in Figure 14, each data prism is $1^{\circ} \times 1^{\circ}$ in latitude/longitude (i.e. about 110 km x 110 km), and varies in height from 350 up to 560 km*. The data will be interpolated and weighted-averaged vertically to a common datum altitude of 400 km, and laterally to the center of the prism, to form the net average data value (point) for that prism.

The variation in measured anomaly field values, and the averaging that will have to be done to produce a net data point, is illustrated by a track over the central midcontinent that has the three nearly-coincident passes 85, 254, and 531. This satellite track is shown in Figure 15 (for pass 85), and the corresponding orbit (height) is shown in Figure 16. Again, the latitude ranges from 25°N . (north-central Mexico) to 50°N . (north of North Dakota). The radius for this varies from about 6765 to 6735 km; subtracting a mean Earth's radius of 6371 km, the altitude varies from 394 down to 364 km. Comparison of the scalar (H_T) field for passes 254 and 531 is shown in Figure 17. This can be compared to Figure 9(b) for pass 85.

On this track, the large positive magnetic high is located over North Texas/Oklahoma. The anomaly amplitude (maximum relief) varies with the altitude of the satellite on a particular pass. This is summarized below,

pass	anomaly amplitude	mean altitude of pass
85	24 nT	380 km
254	20	430
531	15	520

The anomaly amplitude falls off with increased altitude, as expected.

Plotting magnetic field anomaly maps

The processed selected data can now be gridded, plotted, and contoured to display the magnetic anomaly field. In the maps to follow, the grid is $1^{\circ} \times 1^{\circ}$ in latitude/longitude, the data are interpolated to a 400 km altitude datum, and the map projection is Albers equal-area. The actual area of processed data is about 50% larger than the study area shown here, to include a beltway surrounding the data area and thus diminish "edge effects" in the subsequent data processing to follow.

* Recall that on one-half a satellite orbit, the altitude can vary as much as (e.g. near the start of the mission) from about 550 km down to about 350 km.

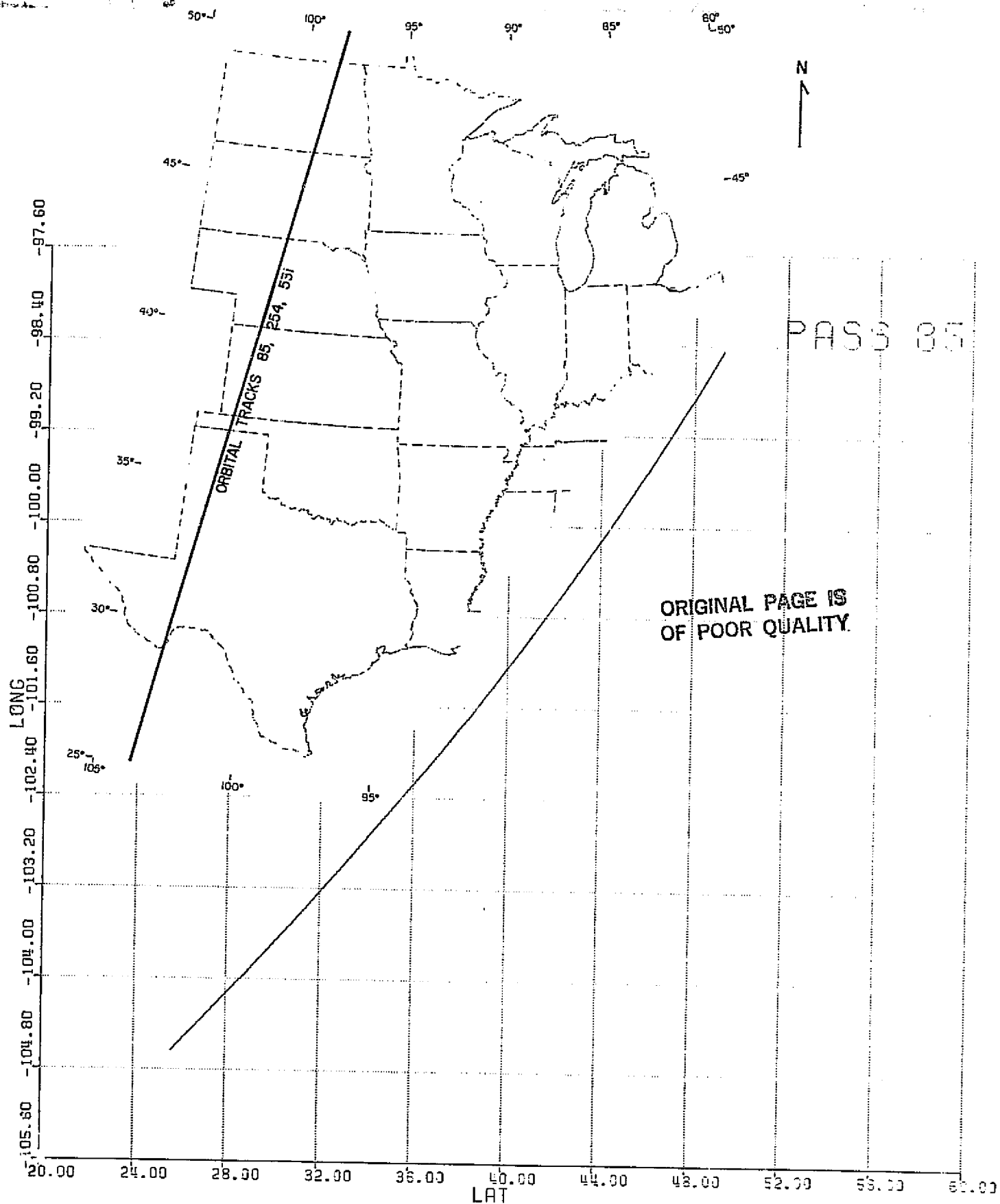


Figure 15. Track path (longitude vs. latitude) over U. S. midcontinent, for pass 85. Same track as for passes 254 and 531.

ORIGINAL PAGE IS
OF POOR QUALITY

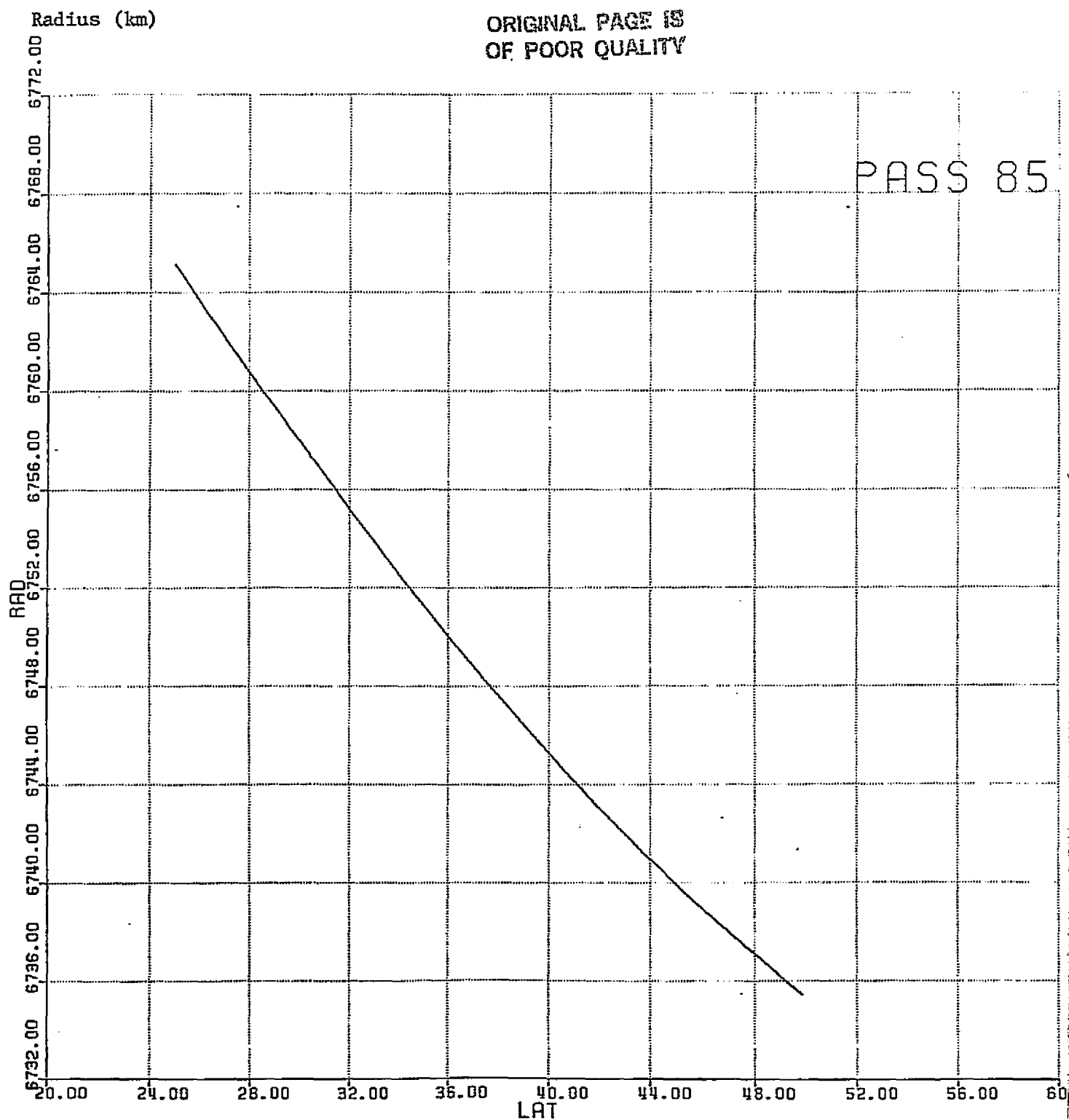
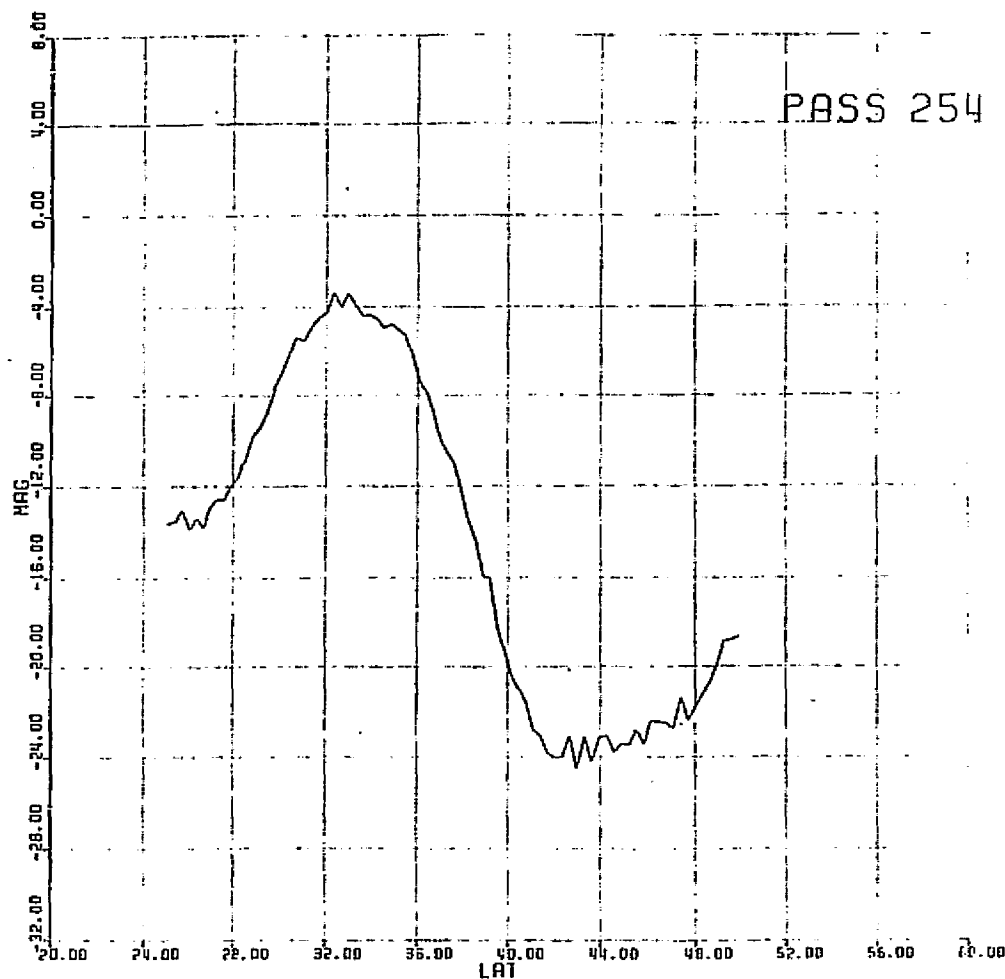
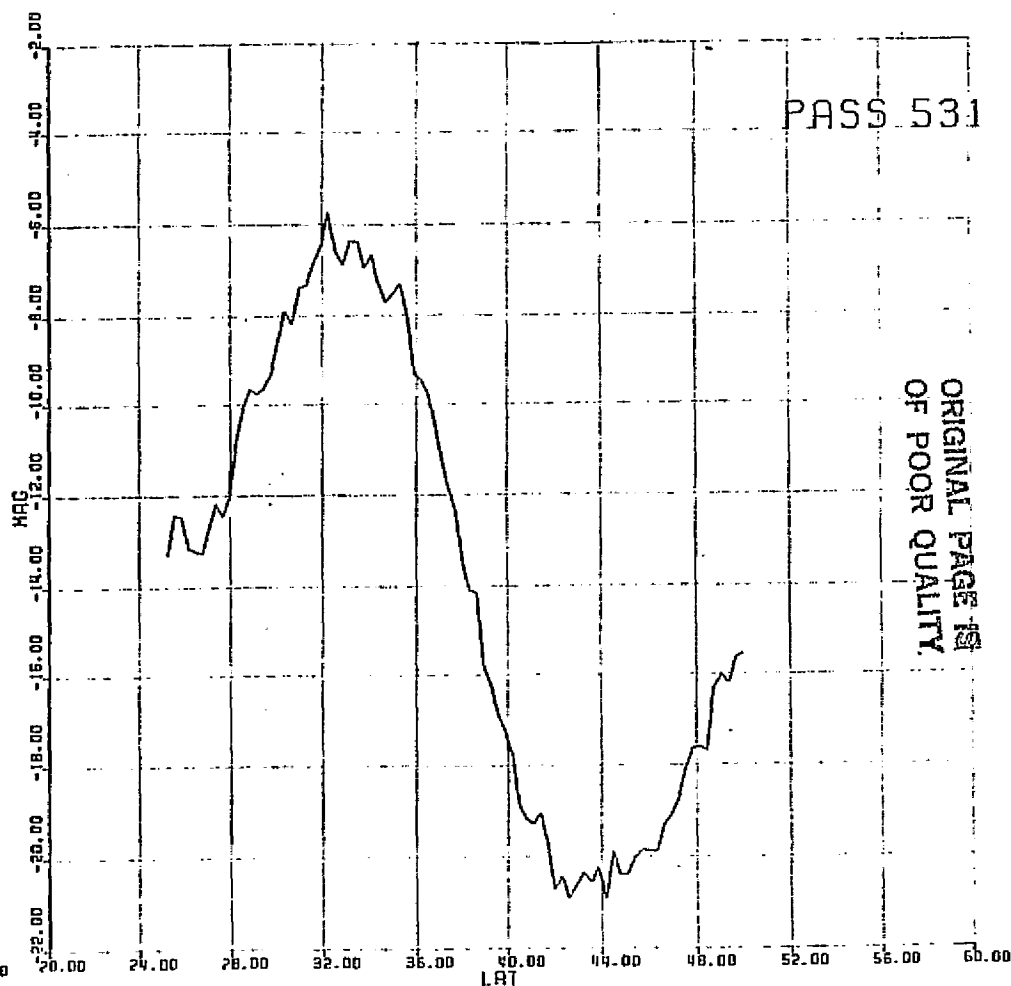


Figure 16. Orbit (radius vs. latitude) for pass 85, along common track of passes 85, 254, and 531. Mean altitude for pass 85 is about 380 km. here.



(a) Pass 254



(b) Pass 531

Figure 17. Comparison of scalar H_T for two passes over same track as pass 85. Field (nT) vs. latitude (degrees North); note that ordinate scales are different. Left end is north-central Mexico, right end is up past North Dakota.

The study area is the U.S. midcontinent--see Figure 18(a)--extending from 80° to 105° W. longitude, and 25° to 50° N. latitude (i.e. about 2800 km). The contour interval is 2 nT.

The H_x and H_y component magnetic-field anomaly data, mapped in Figures 18(b) and (c), are fairly irregular and exhibit apparent striping of the anomalies along the azimuth of track directions. This is due to incomplete equalization of the zero-levels for multiple passes. Simple wavelength filtering* did not improve the appearance significantly. The H_z and (calculated) scalar H_T data are more regular, and are also similar in appearance because of the fairly high magnetic latitudes of the study area. The H_z anomaly map is shown in Figure 18(d), and the H_T map in Figure 19. The geographic latitudes of $35-50^{\circ}$ translate, because of the proximity to the geomagnetic pole (about 79° N. latitude) to about $45-60^{\circ}$ magnetic latitude. For the simple equation for the magnetic-field inclination I at geomagnetic latitude Θ ,

$$\tan I = 2 \tan \Theta$$

the inclination is thus quite high, $64-74^{\circ}$. For a crustal induced magnetization, the vertical-component and total-field anomalies should be similar in appearance.

Wavelength filtering

The H_z and H_T maps were less severely striped along the orbit track direction, and wavelength filtering (two-dimensional) removes the apparent effect of this.**

Figure 20 shows the scalar (H_T , or total-field magnitude) anomaly map, after applying a 4° high-pass wavelength filter (i.e. passing wavelengths greater than 4° , or roughly 400 km). The anomaly values range from highs of 16 nT (over Tennessee/Kentucky) and 10 nT (over north Texas) to a modest high extending from the latter up to the northeast toward Lake Michigan, to lows of -4 nT (over S. Dakota/Nebraska) and -16 nT in the Gulf of Mexico with a diminishing low extending up the Mississippi Embayment. The anomaly values are relative to the arbitrary zero-level chosen

* applying a high-pass wavelength filter (i.e. a low-pass wavenumber filter)

** We should note that for our purposes--interpreting crustal geologic structure and composition--we would like to do as little high-pass filtering as possible. This is so as to retain the short-wavelength anomaly features associated with crustal sources, and achieve the best resolution of these that is possible.

ORIGINAL PAGE IS
OF POOR QUALITY

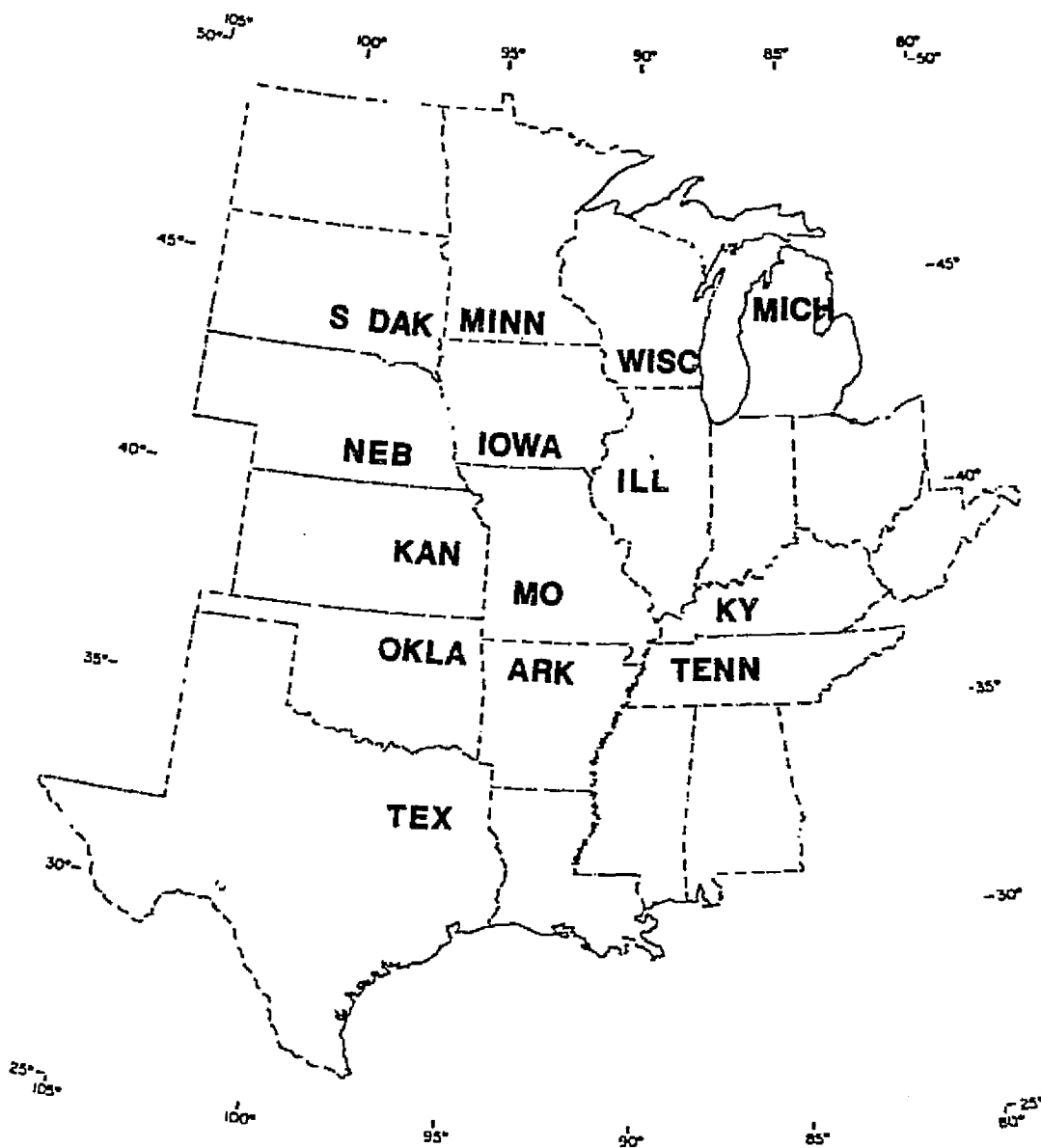


Figure 18. Magsat vector component anomaly maps for U.S. mid-continent. $1^\circ \times 1^\circ$ latitude/longitude grid, data weighted-averaged to altitude of 400 km. Albers projection. (Black, 1981)

(a) Base map. Scale: 5° of latitude is about 550 km.

ORIGINAL PAGE IS
OF POOR QUALITY

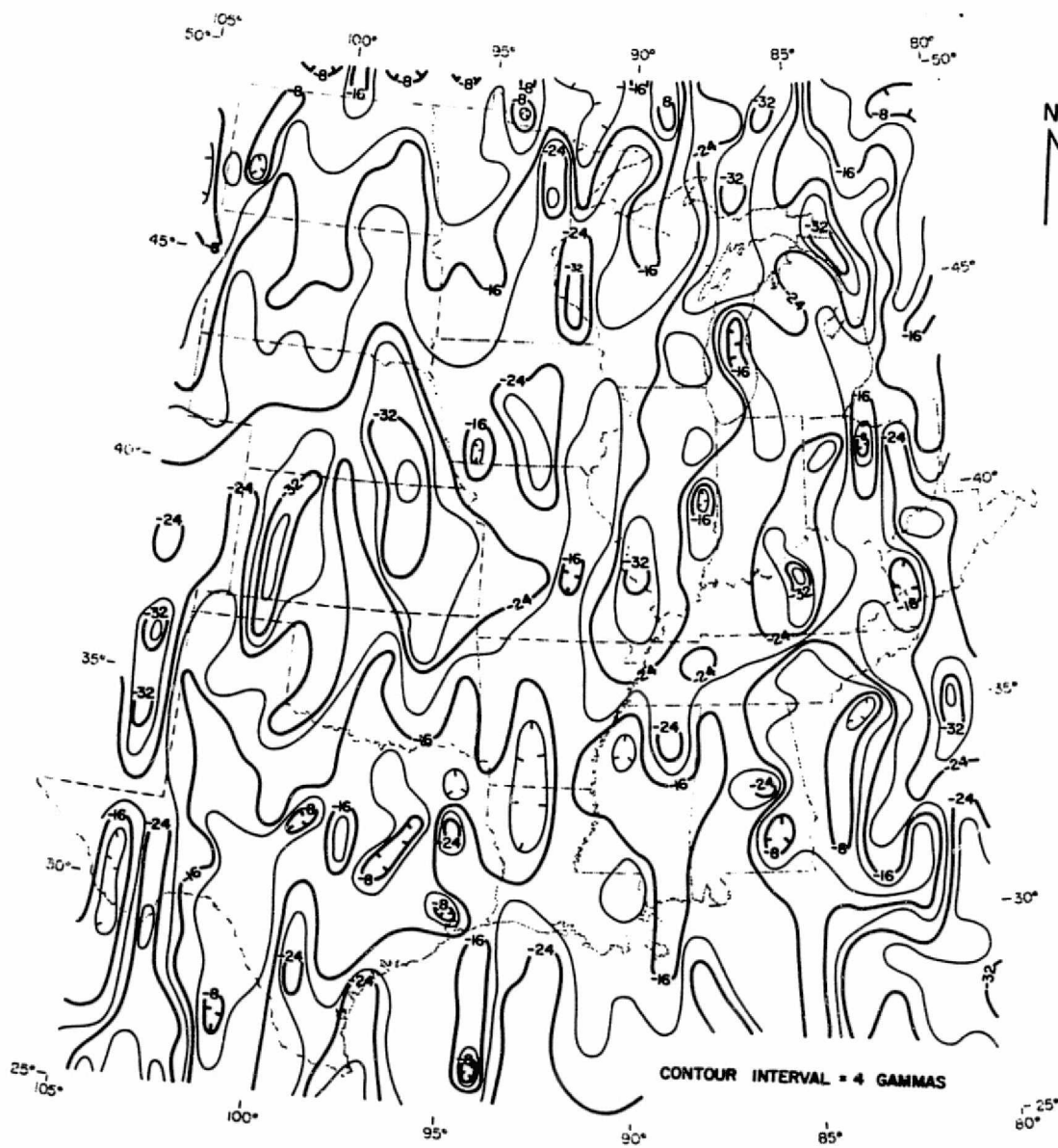


Figure 18. (continued)

(b) delta-X component. Contour interval 4 and 8 nT.

ORIGINAL PAGE IS
OF POOR QUALITY

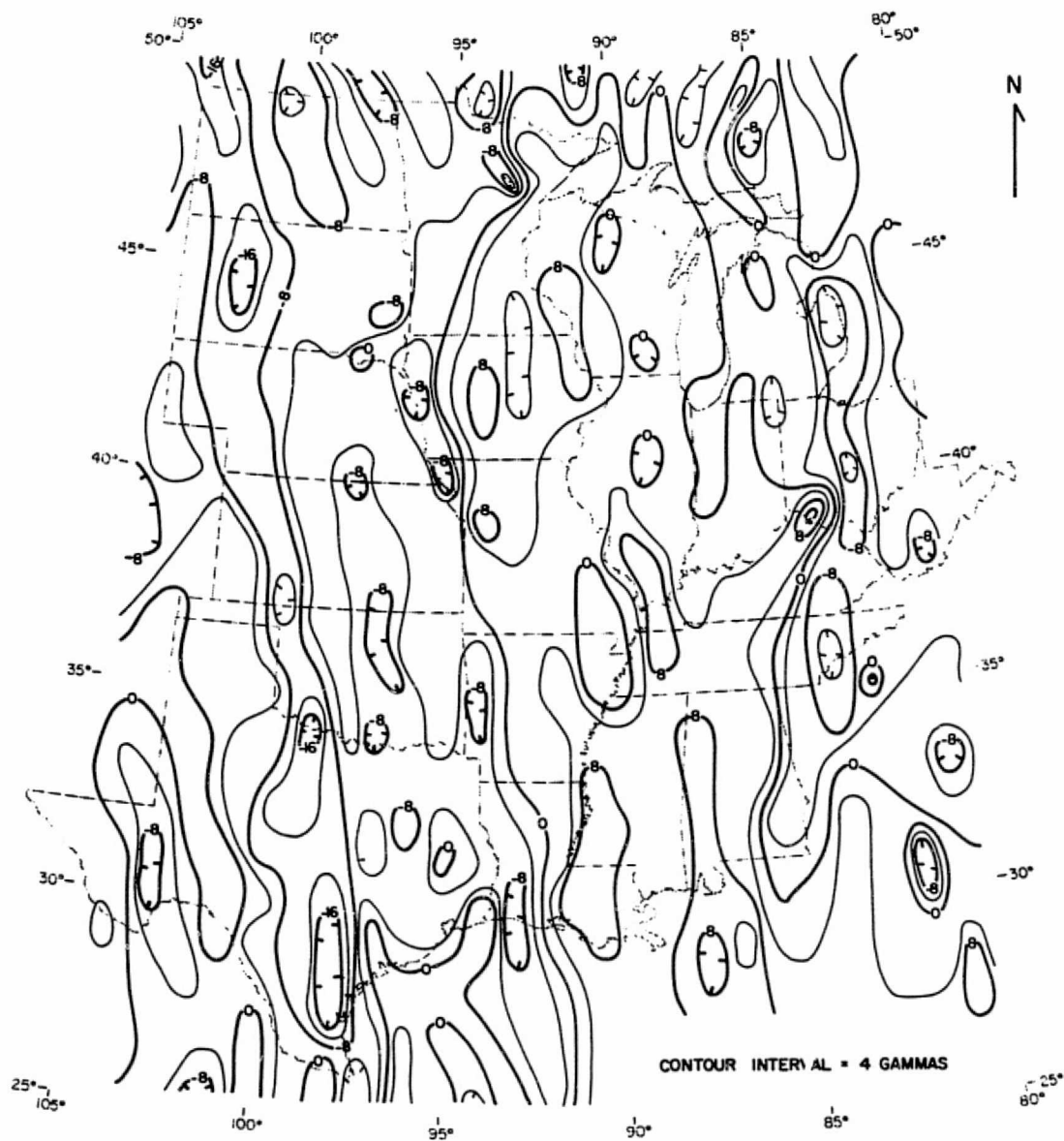


Figure 18. (continued)

(c) δY component. Contour interval 4 nT.

ORIGINAL PAGE IS
OF POOR QUALITY

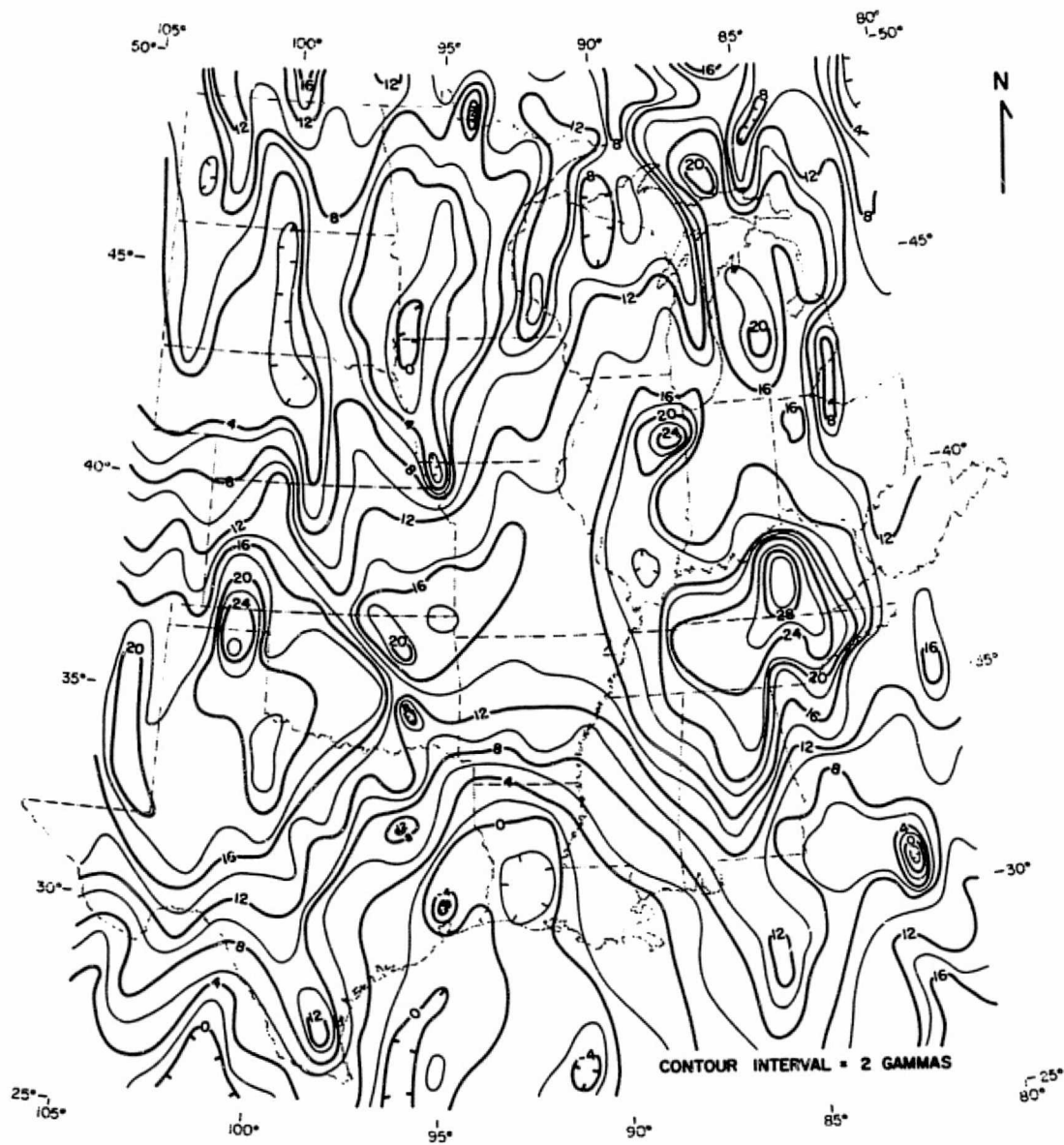


Figure 18. (continued)

(d) delta-Z component. Contour interval 2 nT.

ORIGINAL PAGE 13
OF POOR QUALITY

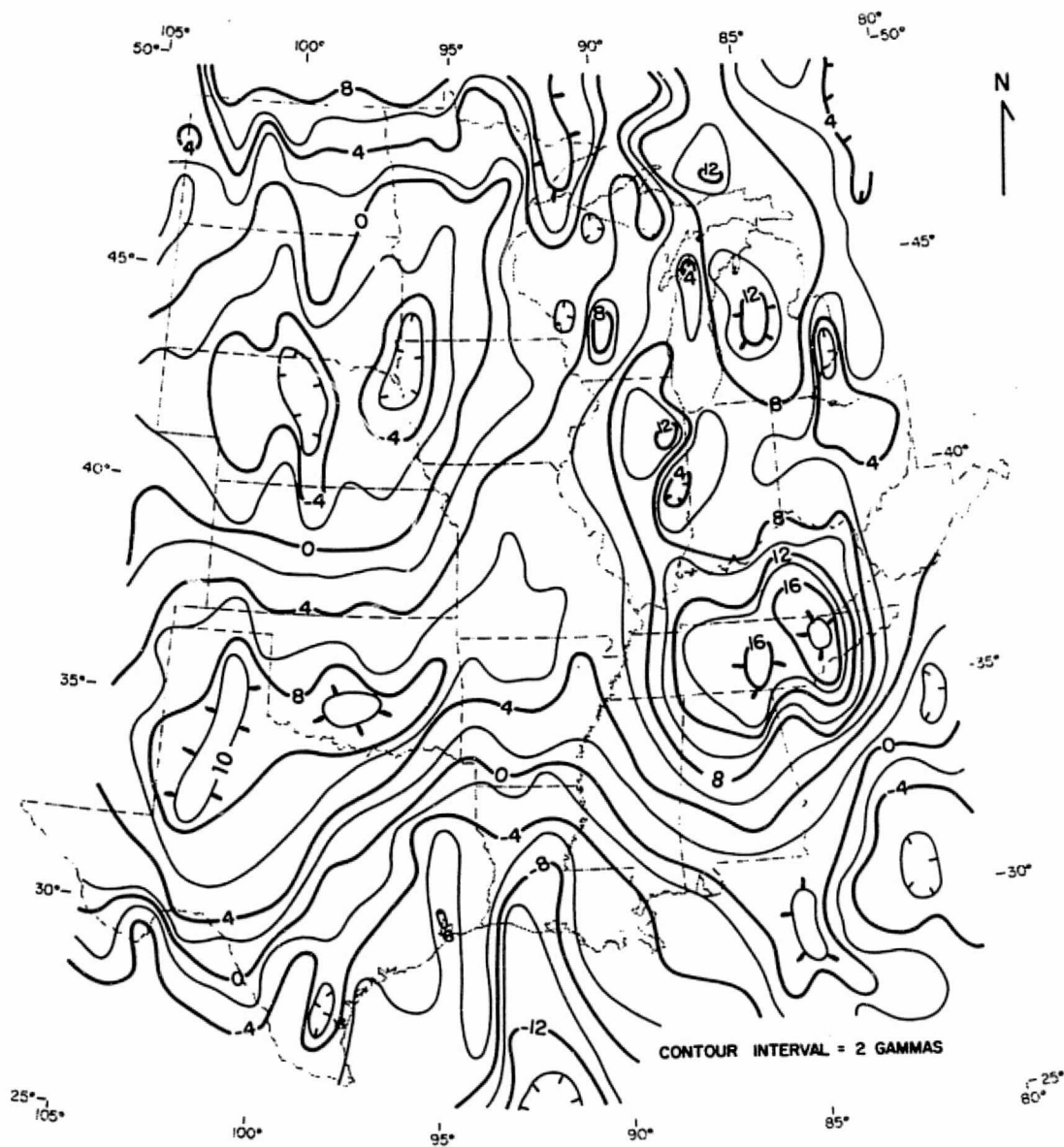


Figure 19. Magsat scalar (total-field) anomaly map, for U.S. midcontinent. $1^{\circ} \times 1^{\circ}$ latitude/longitude grid, data weighted-averaged to altitude of 400 km. Albers projection, contour interval of 2 nT. (Black, 1981)

ORIGINAL PAGE IS
OF POOR QUALITY

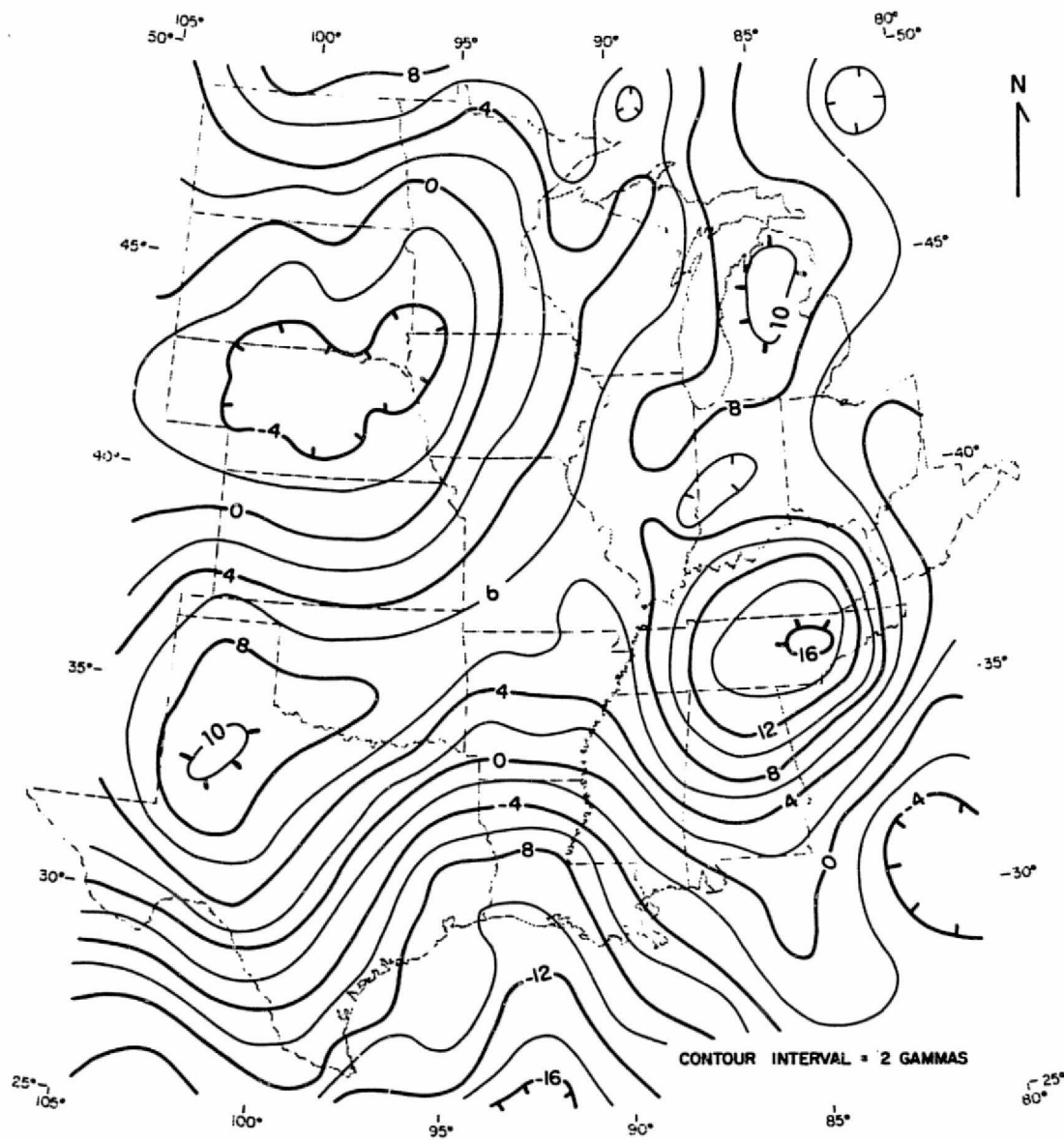


Figure 20. Scalar anomaly map of Figure 19, with (400 km) high-pass wavelength filter applied.

for the area. However, the total anomaly range over the midcontinent (excluding the Gulf of Mexico) is about 24 nT.

Reduction to the magnetic pole

To relate magnetic anomalies (highs and lows, and gradients) to their causative crustal sources, it is helpful to reduce the map "to the pole". This compensates for the variation of magnetic inclination with latitude (from zero at the magnetic equator, to $\pm 90^\circ$ at the magnetic poles), by effectively transposing the area to the north magnetic pole where the magnetic field is vertically downward. There would thus be radial magnetic polarization, and the anomalies are rendered more symmetrical. Implicit in this process is the assumption that the magnetization direction is in the direction of the local Earth's field; that is, that it is all induced magnetization.*

Figure 21 shows the scalar anomaly map of Figure 20, reduced to the pole. This has shifted positive anomaly features to the north by one to two degrees of latitude, and reduced anomaly asymmetry. The alteration of Figure 20 is not dramatic, however, because of the relatively high magnetic latitude of the study area. The major magnetic highs have been shifted northward: the north Texas one up to the Oklahoma border, and the Tennessee one up into Kentucky.

The agreement between the H_T anomaly map and the reduced-to-the-pole map supports the general assumption that, at least on a large (i.e. long-wavelength) scale and as seen at satellite elevations, it is induced crustal magnetization which is responsible for the major anomalies.

It is of interest to consider how data treatment and processing as done here could affect, or improve, the resolution of the satellite magnetic mapping. Figure 22 shows a comparison for the midcontinent of a Magsat scalar anomaly map, as excerpted from a preliminary global data set (NASA, March 1981) with our filtered, reduced to the pole anomaly map.

There is more detail in our anomaly map (Figure 22(b)), and it is useful to try to assess how far the resolution of the satellite data can be "pushed" by processing to reveal crustal structure and properties.

* Or, possibly, induced magnetization plus a viscous remanent magnetization (VRM) acquired in the direction of the present earth's field, under the influence of elevated temperature at depth, and long time.

ORIGINAL PAGE IS
OF POOR QUALITY

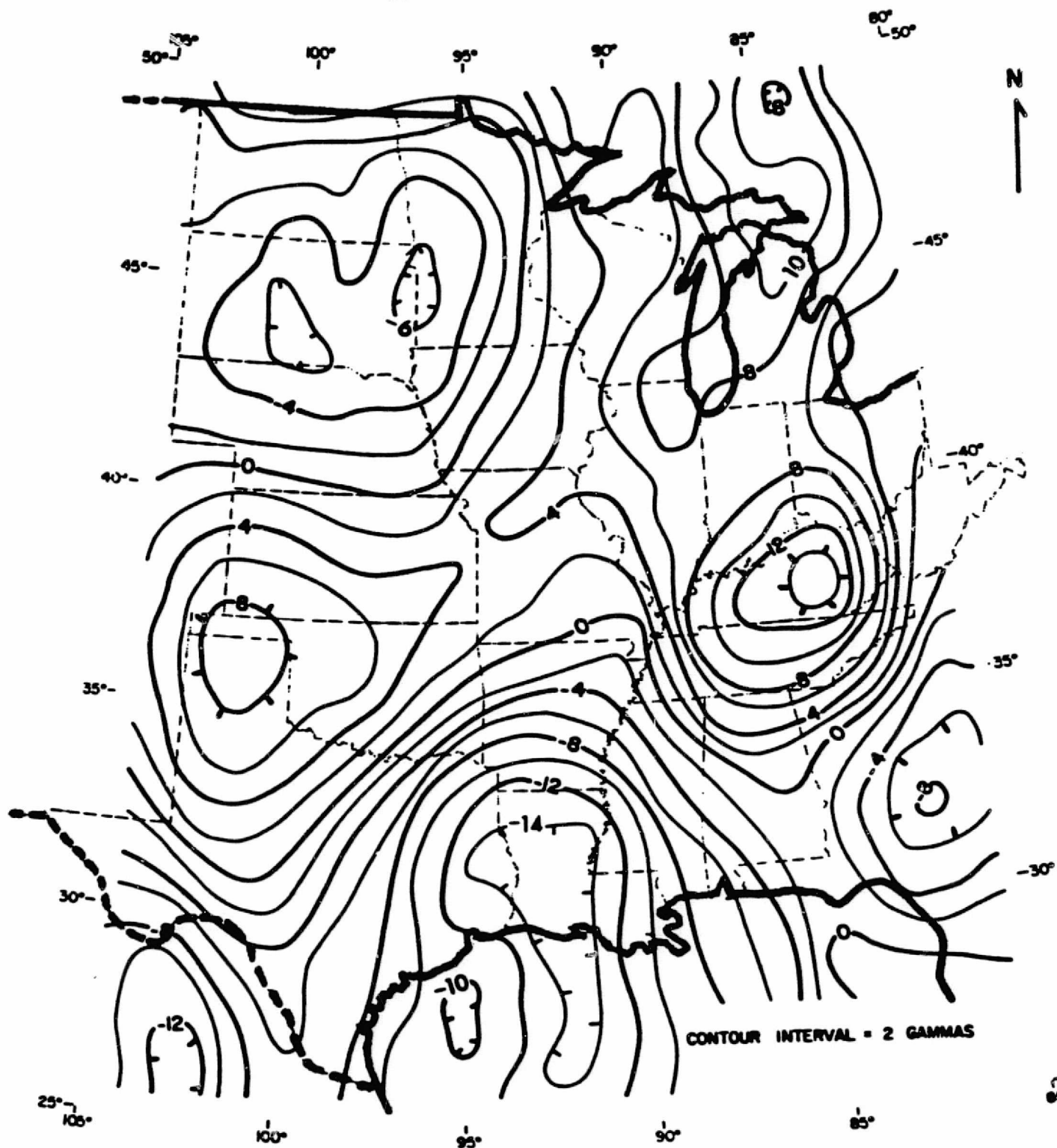
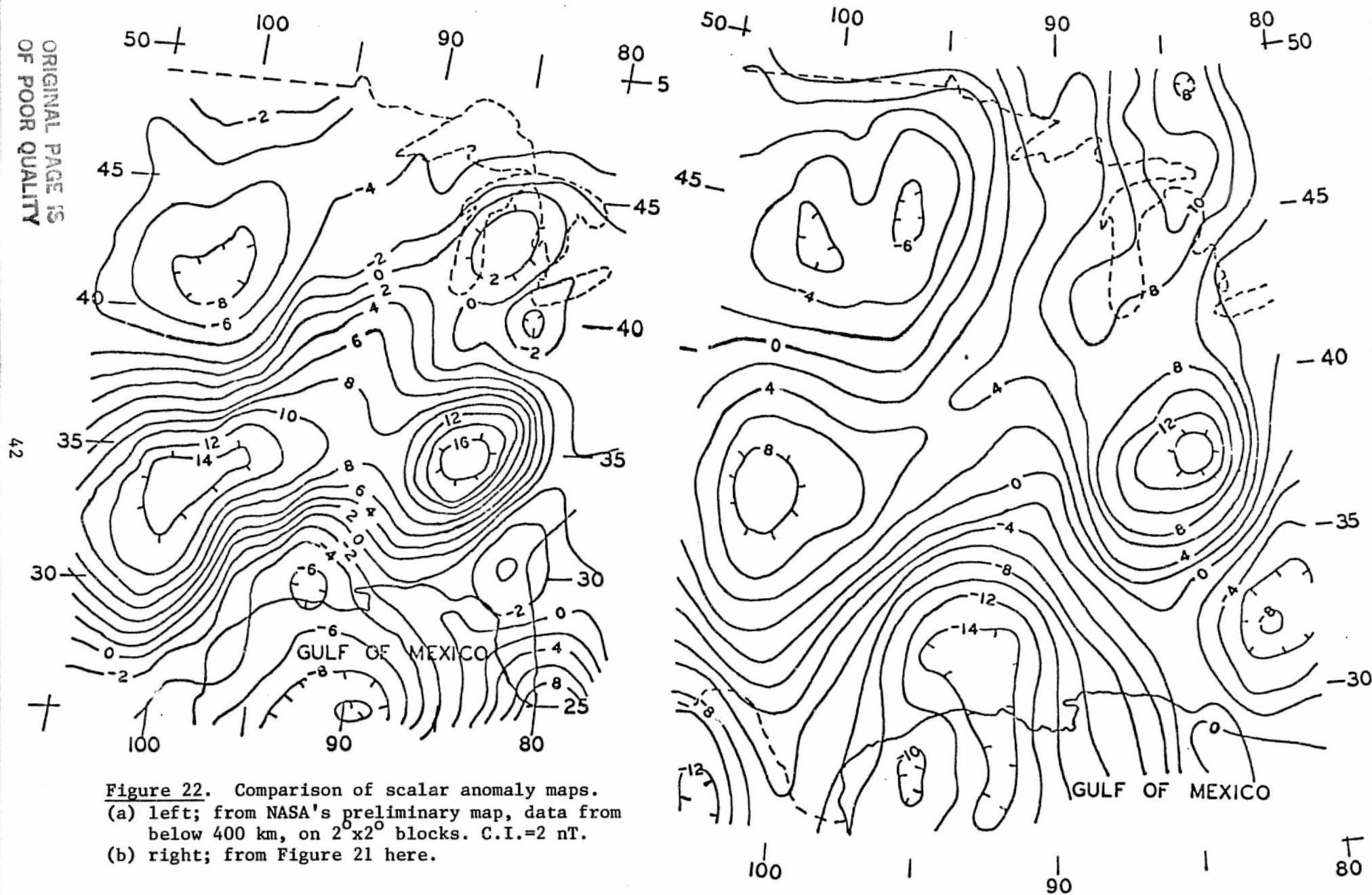


Figure 21. Scalar anomaly map, $1^\circ \times 1^\circ$ data at 400 km altitude, high-pass filtered and reduced to the magnetic pole. Contour interval 2 nT. (Black, 1981)



The greater detail here (see Figure 22 again) is due to

- i) the care taken in removing "bad" data (isolated points, and tracks), and comparing profiles (e.g. of near-neighbor tracks) to optimize the consistency and reliability of the final data set
- ii) treating the data on a finer $1^{\circ} \times 1^{\circ}$ (110 x 110 km) grid, rather than the customary but coarser $2^{\circ} \times 2^{\circ}$ (220 x 220 km) grid spacing used for many global-scale maps
- iii) for a given data prism, doing a weighted-averaging of the data laterally to the central point and vertically to the datum altitude of 400 km. The data closest to the averaged point are thus favored over more extreme values. In contrast, some other compilations of data do a simple averaging of all data in a prism element to arrive at an average value, without regard to the placement of individual points in the prism or the distribution of the whole set of points used.

Figure 23 is a foldout map, repeating Figures 19 (scalar H_T) and 20 (filtered H_T) together for comparison.

ORIGINAL PAGE IS
OF POOR QUALITY

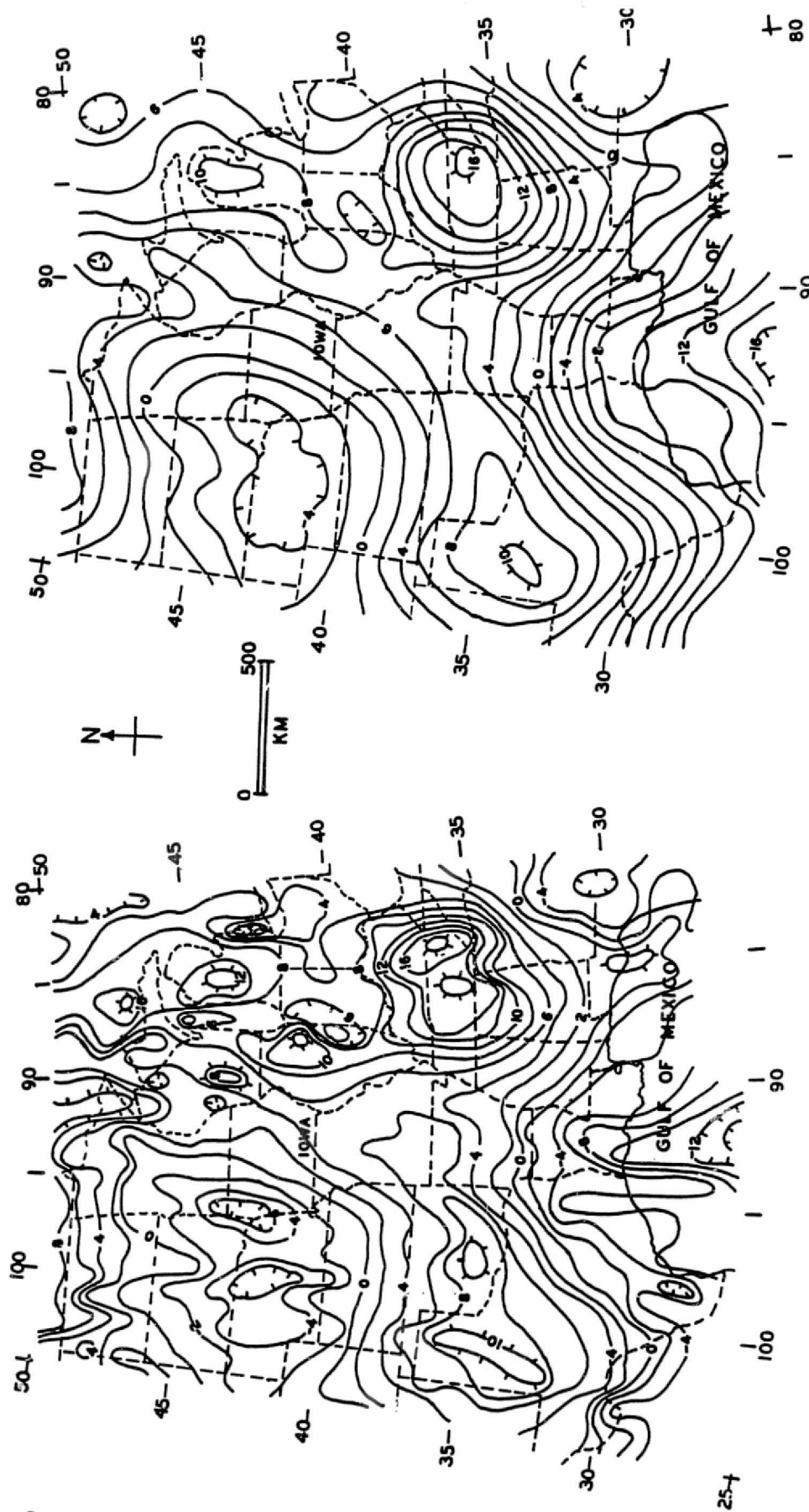


Figure 23a. Comparison of magnetic anomaly map for the midcontinent.
Scalar field, H_T . C.I. = 2 nT.
(left) Anomaly map. (right) Filtered anomaly map.

ORIGINAL PAGE
COLOR PHOTOGRAPH

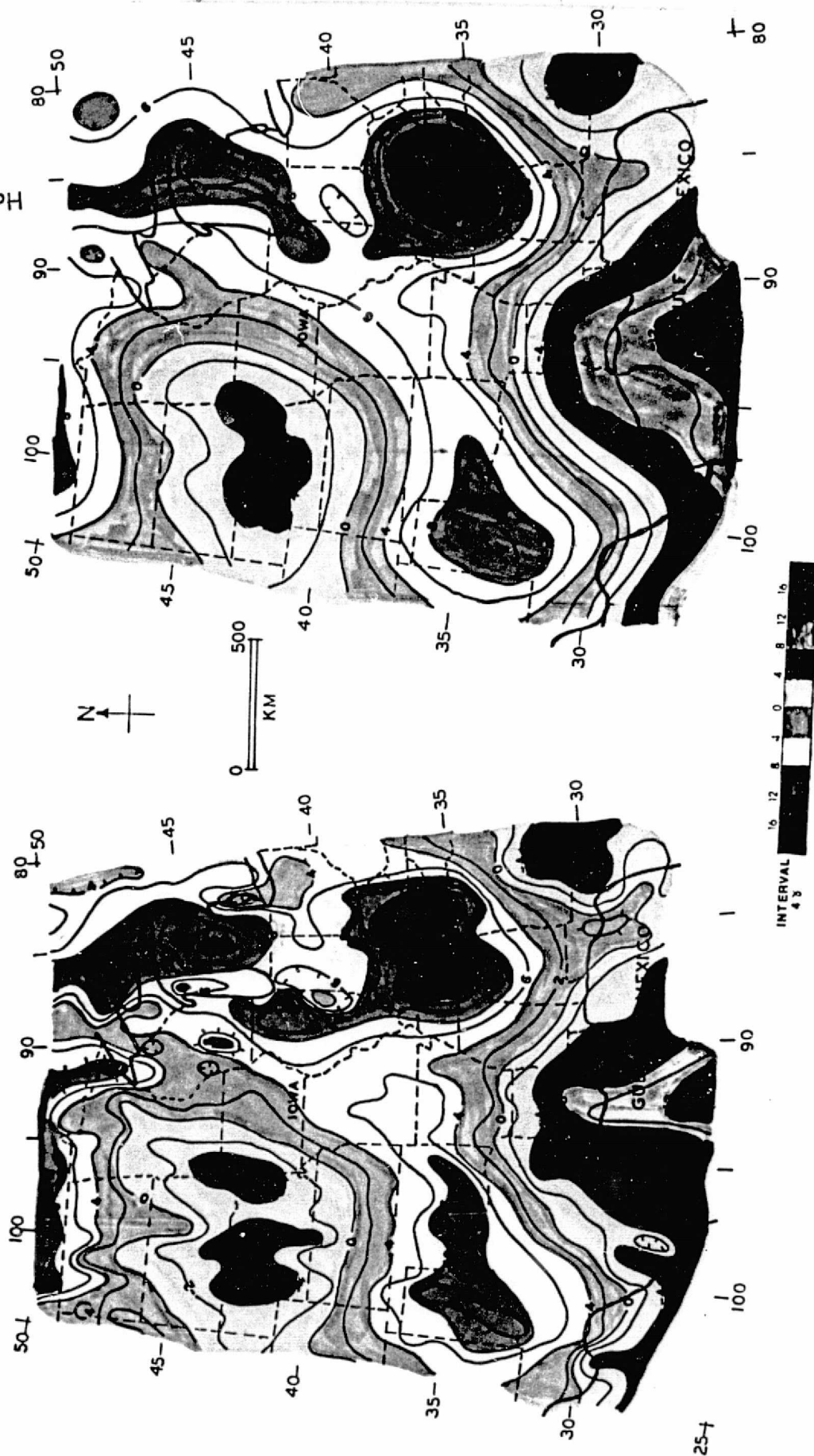


Figure 23b. Colored version of magnetic anomaly map of Figure 23a.

INTERPRETATION OF CENTRAL MIDCONTINENT REGION

Geologic Setting

Figure 24 shows some major tectonic and geophysical features in the larger U.S. midcontinent region. Figure 25 shows our particular study area, the central midcontinent from the Dakotas and Minnesota in the north to Oklahoma and Arkansas in the south. Figure 26 portrays the middle region of the study area, featuring the major arm of the arrested CNARS (Central North American Rift System).

The basement rock of the region consists of a Precambrian craton, exposed in northern Minnesota, northern Wisconsin, and northwestern Michigan and farther north as the Canadian Shield. To the south, it is covered by a veneer of Paleozoic and younger sediments. Major tectonic and geophysical features include the following, several of which are aulacogen (i.e. failed rift arm) structures (e.g. Keller et al, 1983):

i) the Central North American Rift System, which extends from Lake Superior in a major arm over 1000 km southwesterly through Minnesota, Iowa, and eastern Kansas, where it is subparallel to the Nemaha uplift. The CNARS has another arm extending southeasterly from Lake Superior down through Michigan.

ii) the Great Lakes Tectonic Zone, running west-east through Minnesota from South Dakota, and then along the south side of Lake Superior where it is subparallel to the "Great Lakes magnetic lineament"*. It is a boundary between (Superior province) Archean granite and greenstone to the north, of age 2500-3100 million years, and Archean gneiss in central and southern Minnesota to the south, of age 2500-3800 million years.

iii) the Southern Oklahoma aulacogen, to the south. This is represented by the Anadarko basin (western Oklahoma) and Ardmore basin (SE Oklahoma), these being flanked on the southwest by the Amarillo/Wichita

* Presently still an informal term, but used for example in Hildenbrand et al (1983). The term "magnetic (mega)lineament" implies a more-or-less linear alignment of anomalies and gradients, that extends for at least several hundred kilometers, and most likely represents a major structural and lithologic boundary or feature. In the U.S. midcontinent, the magnetic lineaments noted here would be Keweenawan-age (1100 million years) or older, and these zones of crustal weakness would help control the placement and extent of Keweenawan rifting and intrusion.

ORIGINAL PAGE IS
OF POOR QUALITY

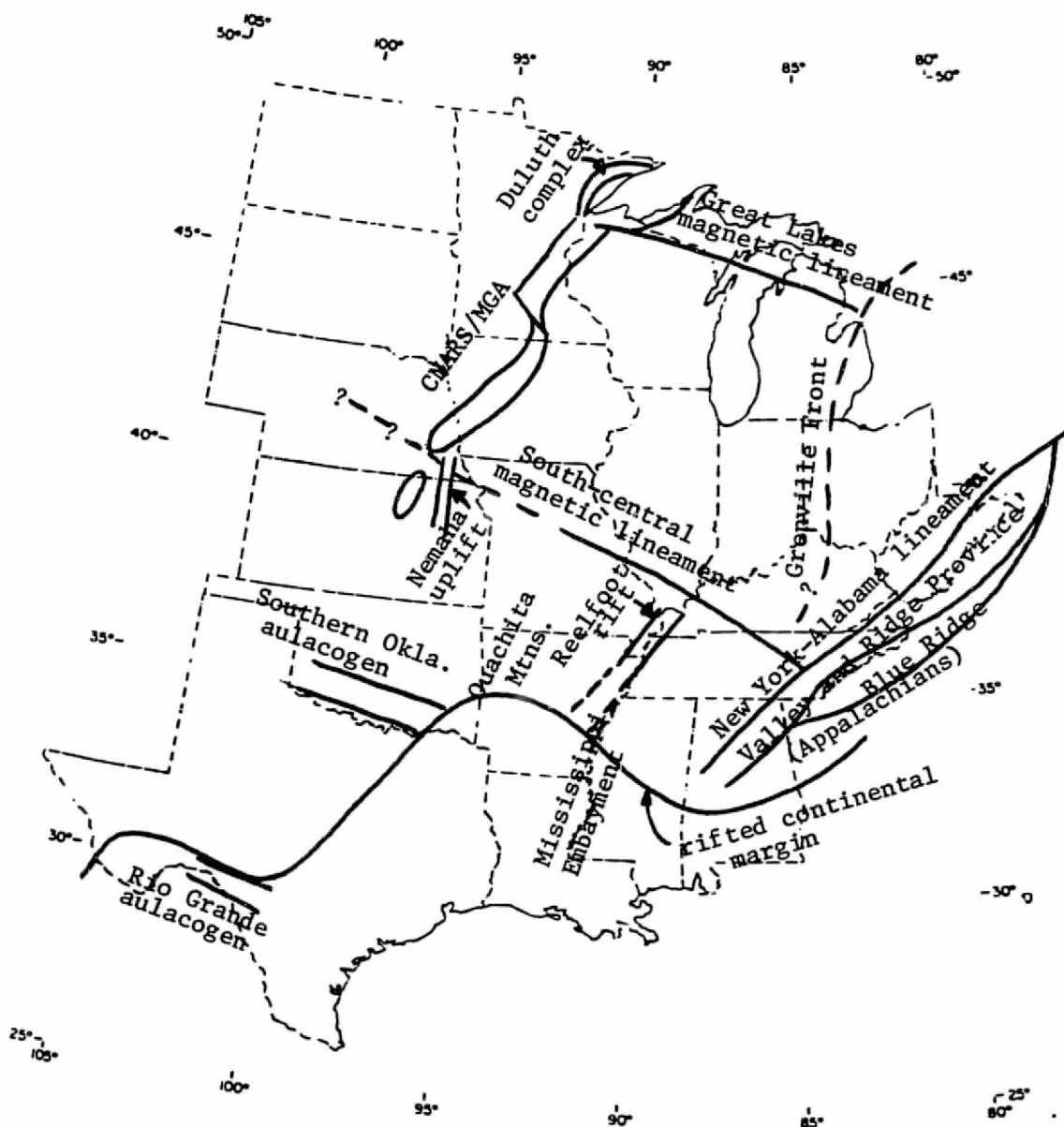


Figure 24. Some major tectonic and geophysical features of the U.S. midcontinent. Albers-projection base map.

ORIGINAL PAGE IS
OF POOR QUALITY

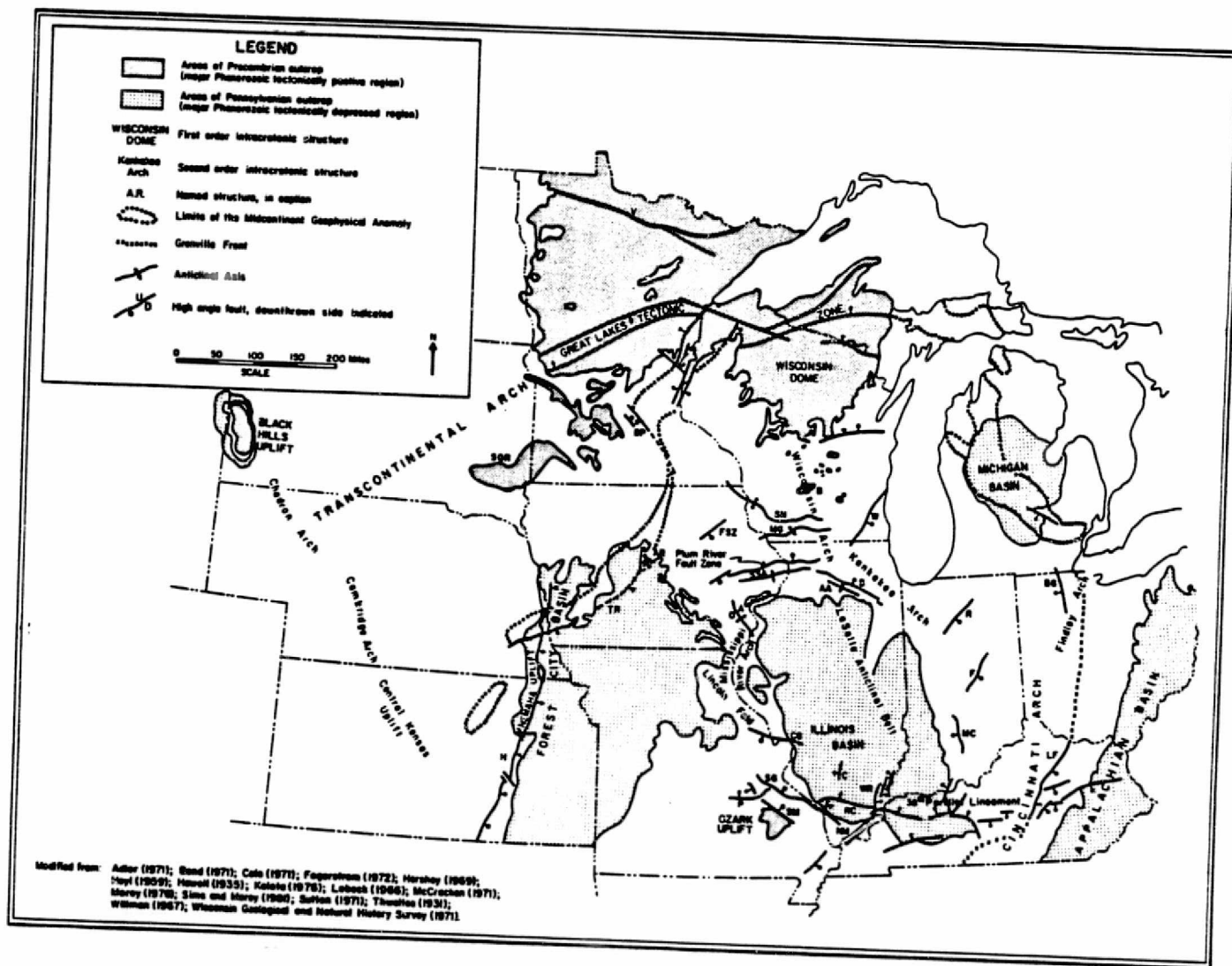


Figure 25. Geologic structures in the central midcontinent.

ORIGINAL PAGE IS
OF POOR QUALITY

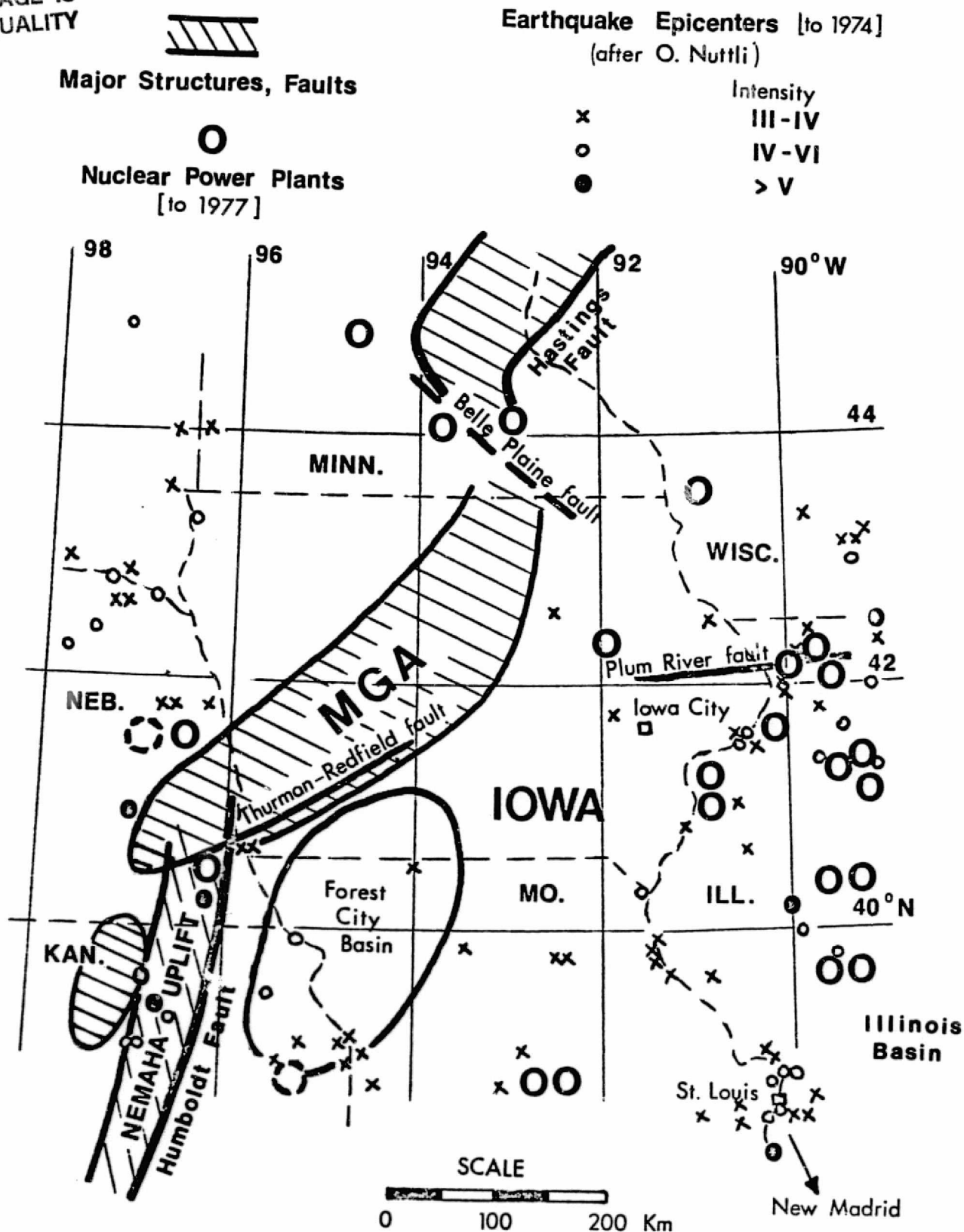


Figure 26. Region of main arm of CNARS, as outlined by MGA (Midcontinent Geophysical Anomaly).

uplift. This aulacogen is attributed to late Precambrian/early Paleozoic rifting that formed the proto-Atlantic, along the "rifted continental margin" noted on Figure 24. It is this margin where the Appalachian and Ouachita mountains, formed in a later continental collision, are now located.

iv) the Mississippi Embayment, with associated aulacogen features such as the Reelfoot rift, which also originated with the late Precambrian/early Paleozoic rifting to its south. The rift was then reactivated in the Mesozoic, forming the Embayment over it as areal subsidence in primarily Cretaceous time. The latter development accompanied the (second) opening of the Atlantic. The Reelfoot rift and associated structures is presently active seismically, especially at the northern end. The rift has a central downdrop (graben) of 1.5 to 3 km.

v) the enigmatic "South-central magnetic lineament" (see footnote on page 45), a belt of magnetic anomalies and trends/alignments, and gravity lows (about -30 milligals), that extends from eastern Tennessee more or less linearly to the northwest. It begins at the "New York-Alabama lineament", that in turn extends SW-NE from Alabama up to central Pennsylvania/New York, and passes through the north end of the Reelfoot rift in the New Madrid region. It continues on to the dislocation of the MGA in southeast Nebraska (see Figure 24 again) (Arvidson et al, 1982; Zietz and Hatcher, 1983). Some suggest it may continue, although as a more obscure anomaly trend, to the northwest as far as Wyoming. There is some speculation that this apparent geophysical trend may be reflective of a transform fault, associated with late-Precambrian plate motions. At the north corner of the intersection of the South-central magnetic lineament and the New York-Alabama lineament, in central Kentucky/Tennessee, there is a region of large magnetic highs. The basement rocks are mafic volcanics and metamorphics. The former are similar to the Keweenawan volcanic rocks of Lake Superior, and may be of the same age (Hildenbrand et al, 1983).

Aulacogens are typically directed into a continental craton from a rifted margin, and these failed (paleo)rift arms represent once-tensional flaws in the crust which can be later reactivated with sufficient tension or compression. The episodes of rifting, either arrested or successful, in the U.S. midcontinent (Keller et al, 1983), are listed on the next page.

<u>Geologic time</u>	<u>Tectonic episode</u>	<u>Associated rift features</u>
Keweenawan (1100 x 10 ⁶ yrs ago)	precursor to opening of proto-Atlantic	CNARS/MGA structure
late-Precambrian/ early Paleozoic (500-800 x 10 ⁶ years ago)	opening of proto-Atlantic	Reelfoot rift; Southern Oklahoma aulacogen
----- then closing of proto-Atlantic -----		
early Mesozoic (150-200 x 10 ⁶ years ago)	opening of Atlantic	Mississippi Embayment; Rio Grande aulacogen*

Rifts are often associated with the formation and development of sedimentary basins. For example, collapse (subsidence) of incipient or failed rift systems may be related to the development of the following basins in the U.S. midcontinent (see Figure 25),

<u>Tectonic development</u>	<u>Sedimentary basins</u>
mid-Michigan (Keweenawan) intrusion (eastern arm of CNARS)	Michigan Basin
Midcontinent Geophysical Anomaly (MGA) intrusion (western main arm of CNARS)	deep narrow basins flanking a central horst, in southern Minnesota and all of Iowa
Southern Oklahoma aulacogen	Anadarko and Ardmore Basins
and possibly	
MGA/Nemaha uplift/granitic plutonism in NE Kansas and NW Missouri	Forest City Basin

Rifting, arrested rifting, reactivation of a paleorift, and deep structural lineaments, can help control subsidence, uplift and erosion, and structural/sedimentary history. This can have important implications for exploration for hydrocarbons. Rifting itself can also have a direct consequence for invasion by hydrothermal fluids, or magmatic intrusion, or other emplacement mechanisms for mineral deposits. It is for understanding of these deep structures and major crustal features, that satellite magnetic data have promise.

The CNARS complex, or Midcontinent Rift System, is buried over most of its length. It was initially identified, and its extent mapped and

* Not to be confused with the Rio Grande Rift farther west in New Mexico.

modelled, using its characteristic gravity and magnetic anomalies extending from Lake Superior down to Kansas. Since its gravity signature was the first known expression of the CNARS, the structure is sometimes referred to as the Midcontinent Gravity (or Geophysical) Anomaly, or MGA.

The MGA arm of the CNARS is a failed paleorift zone of Keweenawan (late Precambrian, 1100 million years ago) age. It formed with attempted rifting of the North American craton, with an elongate seam of mafic intrusives and layered extrusive basaltic rocks, up to 80 km wide. Associated basinal subsidence resulted (in the central portion, in southern Minnesota and Iowa) in deep flanking basinal troughs of downwarped sediments. Reactivation there of the central basaltic seam has left it elevated as a fault-bounded horst with a vertical throw (uplift displacement) of up to 10,000 meters. This is in the major central portion of the MGA, in Iowa.

The MGA's gravity expression of the CNARS is shown in Figure 27, for the Bouguer gravity anomaly, and its aeromagnetic anomaly signature is shown in Figure 28. The anomalous trend, outlining the buried structure (central mafic core and flanking basins), has a length of over 1000 km and total width of up to about 150 km.

The gravity anomaly over the most pronounced portion of the MGA has a central positive zone that exceeds +60 milligals in value, and flanking lows (over the adjacent sedimentary troughs) less than -100 milligals. The maximum difference, of over 160 milligals (on a profile in central Iowa less than 40 km long) is the largest such gravity gradient in North America. This indicates the very long, deep, and pronounced lithologic inhomogeneity in the crust here.

The aeromagnetic expression of the MGA is a belt of anomalies with a well-defined northeasterly trend, but having fairly modest amplitudes.

Early studies of the MGA (e.g. Chase and Gilmer, 1973; Ocola and Meyer, 1973) focussed on the northern fragment of the rift system in northern Minnesota and Wisconsin, where the basement rock outcrops. The central (southern Minnesota, and Iowa) and southwest portions could not be studied in detail because of burial under sediments, and a general lack of comprehensive geophysical information such as seismic surveys or gravity and magnetic mapping and modelling. Further, the structural development (especially as regards fault-bounding of the central basaltic seam,

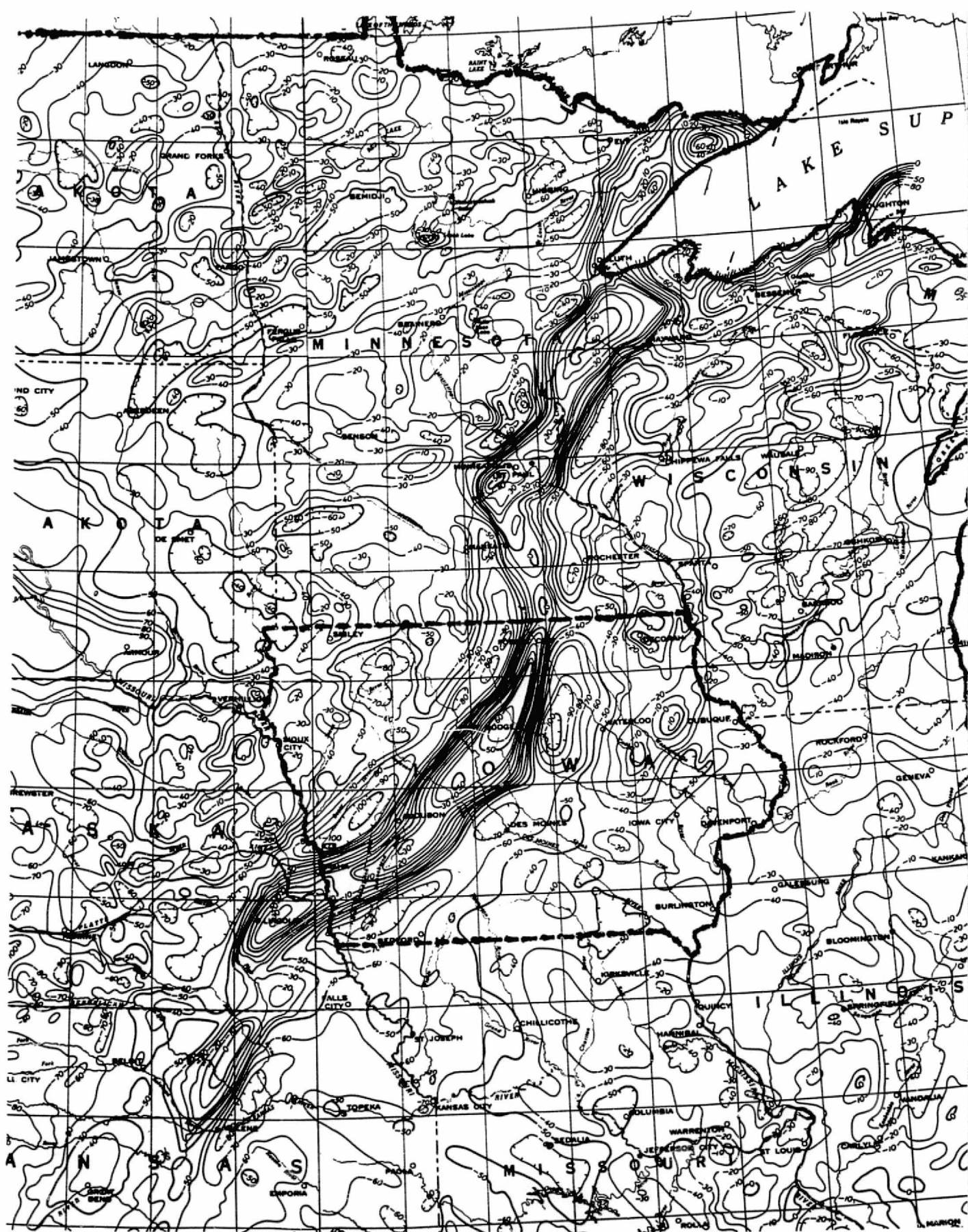


Figure 27. Bouguer gravity anomaly (i.e. MGA) of CNARS paleorift in central midcontinent (map excerpt from Woollard and Joeting, 1964)

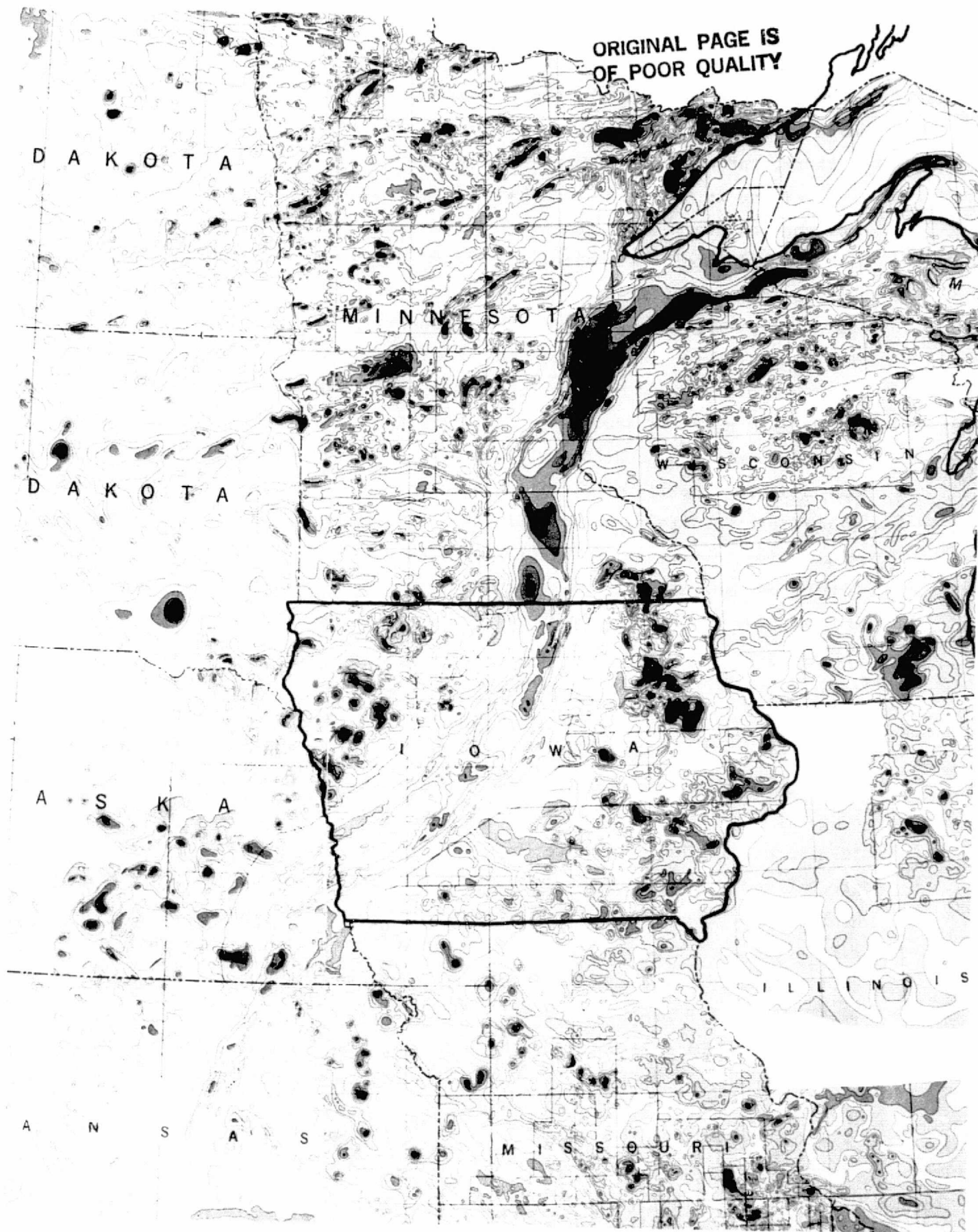


Figure 28. Aeromagnetic anomaly map of MGA and environs in central midcontinent (from USGS/SEG Composite Magnetic Anomaly Map of U.S., USGS Map 954A, 1982)

ORIGINAL PAGE IS
OF POOR QUALITY

and subsequent uplifting to form a great horst) is apparently different north of the Great Lakes Tectonic Zone (see Figure 25) than it is south of there, through central Minnesota and Iowa.

There is now more understanding (e.g. Green, 1983; and here by Anderson and Black, 1981 and 1983) including detailed magnetic and gravity modelling to be described in a later Section. The complete CNARS extends in two long sinuous arms, for a total length of 2200 km from east-central Kansas northward to Lake Superior, then eastward through that basinal lake and down through the Michigan Basin into Ohio. The major western arm, or MGA, has a genesis and structure which most likely varies from north to south. In general, the northerly segment began its attempt to rift the continental craton about 1150-1200 million years ago, with fissure eruption of basaltic lavas onto a broad plain forming a trend of partially-overlapping flood plateaus. Extrusion was accompanied by progressive subsidence in the central region, perhaps because of regional tension or isostatic adjustment to the loading. The successive flows erupted over a period of 20-30 million years (Green, 1983) around 1100 million years ago, producing plateau thicknesses of up to 7000 meters. With crustal subsidence, there was accumulation of thick sediments, which subsequently eroded with uplift of the central mafic core along steep bounding faults. This later reactivation (completed by late-Precambrian time) was not everywhere present in this northern segment, and is attributed to regional crustal compression. While the total volume of flood basalts is estimated to be comparable (over 300,000 km³) to volumes in other great flood basalt provinces (Deccan/India, Parana/Brazil, Columbia River/Washington), there are major differences in character between this paleo-rift event and structure, and the "type" modern rift--the East African rift. This is for the MGA as examined in outcrop in the Lake Superior region. The differences include:

<u>CNARS/MGA failed paleorift</u>	<u>East African rift</u>
plateau basalt rift	plateau basalt rift
----- but -----	
broad subsidence (downwarp) with the extrusion and rift attempt	graben structure with rifting
tholeiitic flood basalts, and basaltic andesites	alkalic basalts, and central volcanoes developing
large positive gravity anomaly	fairly small gravity anomalies

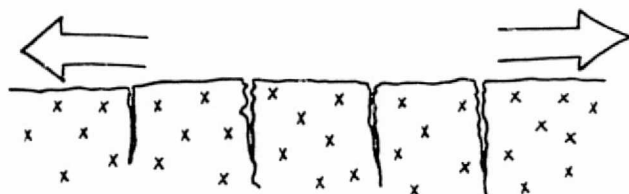
At variance with models for the early stages of much rifting, which include crustal thinning by thermal and tensional influences, the central midcontinent here was apparently not thinned significantly. This is because the crust is now anomalously thick, being 45-50 km thick under much of Lake Superior and at least as thick as the midcontinent average (about 40 km) toward the southwest. Interestingly enough, the region has apparently been in isostatic equilibrium since late Precambrian time, despite having a large gravity anomaly.

The northern portion of the MGA has intrusives accompanying the basaltic lavas. These include diabase sills (e.g. Logan intrusives), and plutons and large cumulate bodies such as the Duluth Complex. This latter set of intrusives, on the Minnesota northwest edge of Lake Superior, is a crescent-shaped system over 200 km long, of layered gabbro. Its basal zone has rich ore mineralization associated with it.

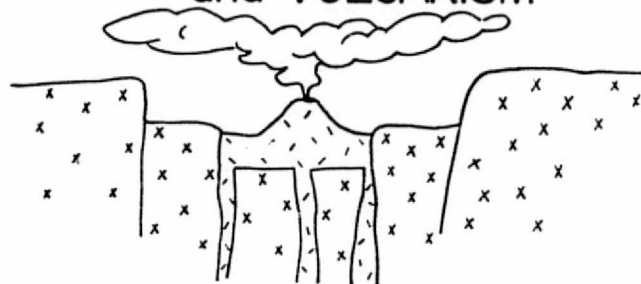
As one proceeds southwards towards the central portion of the MGA, the origin and development of the rift system is associated more with block (graben) normal faulting during crustal extension and emplacement of the basalts as an infilling. Later, there was extensive reverse faulting on steep bounding faults, as the central horst developed (Craddock, 1972; Anderson and Black, 1981 and 1983). In southern Minnesota, the central uplifted block is called the St. Croix horst. The relative vertical displacement of the horst with respect to the deep flanking clastic-filled basins is up to 10,000 meters, and the sediments are thus up to at least this thick in places. A schematic of the hypothetical development of the MGA structure in southwest Iowa, based on geologic analogy and magnetic and gravity modelling (see a later section here) is shown in Figure 29. This was formed largely $1100-1200 \times 10^6$ yrs ago (Keweenaw time), but the central horst and its companion flanking basins continued having relative vertical movements into the Paleozoic era, based on mapping of the post-Precambrian sediments overlying.

There are still some differences of opinion about whether the basaltic and mafic core seam extends from the horst down to the lower crust as a coherent slab, or whether the horst basalt is underlain at intermediate depths by a crustal block of granite (as in Figure 29). Geophysical modelling of the MGA seems to support the latter interpretation.

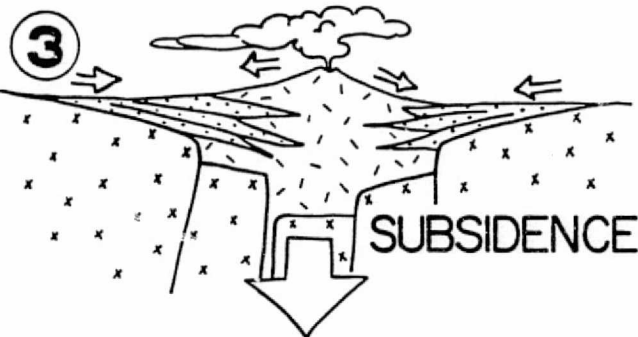
① CRUSTAL EXTENSION
and FRACTURING



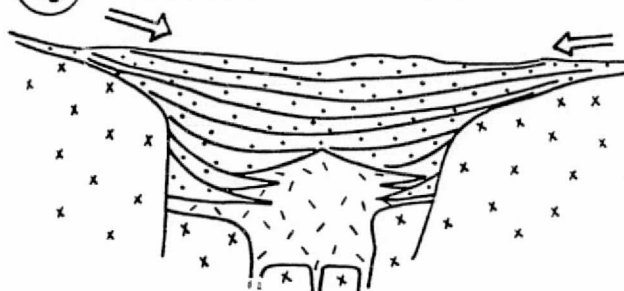
② GRABEN DEVELOPMENT
and VOLCANISM



ORIGINAL PAGE IS
OF POOR QUALITY



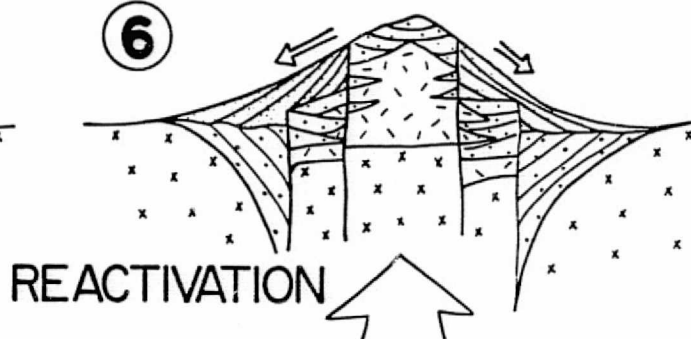
④ SEDIMENTATION



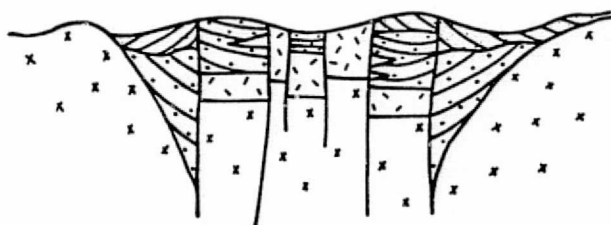
⑤ EROSION



⑥



⑦ EROSION



DEVELOPMENT
OF THE
MGA
IN SOUTHWEST IOWA

by Raymond Anderson
1981

Figure 29. Schematic of development of MGA in southwest Iowa, 1100-1200 million years ago (Anderson, 1981). Granitic rock has x's, basalts have short dashes, sediments have dots.

Farther to the southwest, into Kansas, the CNARS feature is progressively deeper (to its top), and narrower in width, and more modest in structural extent. The sediment troughs are only about 3 km deep. Further, it is intrusive in nature and composition (being gabbroic, from drilling and geophysical modelling) rather than having much mafic (basaltic) extrusives. As a consequence of these characteristics, the MGA gravity and magnetic signature is less pronounced there. To the east of the MGA extension into Kansas is the Nemaha uplift, a subparallel but shallower and later feature. It is an uplift of Precambrian-age (1400 million years) granite, bounded on the east side by the Humboldt fault. This fault had its activation and displacement in Paleozoic time.

The emplacement of the CNARS is a tectonic occurrence which could have consequences for an area which has considerable potential for economic mineral resources. The geologic setting is favorable. Precambrian basement rocks representing abundant time (1100 to 2600 million years ago) underly a sedimentary section of younger rocks. There are major geologic structures--basins, uplifts, faults--which have had basement control and which have affected subsequent depositional environments. For example, there are large deposits of coal in Iowa, Illinois, and other midcontinent states, in the overlying sedimentary section. In the past year or two there has been initiated interest, and exploration efforts, directed at the oil and gas potential of the sediments along (on and adjacent to) the CNARS structure in Minnesota and Iowa, and in the Forest City Basin east of the MGA/Nemaha features. Analysis of the larger tectonic picture--thermal and structural origin, reactivation (neotectonism), and possible effects on structures and stratigraphic conditions in the overlying sedimentary section--could help provide insight into the trapping environments for hydrocarbons.

Further, where the basement rock is exposed at the ground surface or is shallow, as to the north (where, however, it is still often obscured by glacial deposits from the Pleistocene ice age), there are rich and important mineral deposits of iron, lead, zinc, and copper. Since the geology of the basement rock to the south is analogous, in terms of structure and general evolution and the fabric of intrusive activity, the basement there has the potential to be the habitat of major orebodies, mineral provinces, and similar mechanisms for economic mineralization.

Much of the central midcontinent has a basement overlain by several hundred meters of sedimentary rock. It is geophysical methods of prospecting—including magnetic and gravity mapping—that will provide economical, efficient, and revealing means for reconnaissance interpretation of the buried basement's features and bodies, composition (rock type), potential economic resources, structural trends and possible control of subsequent deposition and basin development, and of deeper crustal character and conditions. A regional assessment (including long-wavelength satellite surveying) of deep structures, and their geodynamical significance, geologic evolution and development of an area, and consequences for emplacement of mineral resources, can form the basis for further exploration to help fill the resource needs of the future.

Although the buried basement rock of the central midcontinent is as yet largely unsampled by direct drilling, areal geophysical studies are setting the regional framework of geologic provinces and age relations. This interpretation will be assisted by integration with a large-scale data set such as satellite magnetic anomaly maps.

Figure 30 shows the geologic age provinces of the midcontinent, as determined by radiometric dating.

Correlative Geophysical and Geologic information

The regional (long-wavelength) satellite magnetic data can be combined with more detailed geologic and geophysical information to help interpret the geologic setting of a region and its deeper and broader features. Such comparison can add new information on the structural and tectonic framework of the area, and the relationship of geological provinces.

Figure 31 shows the thickness of the crust in the central midcontinent (Allenby and Schnetzler, 1983). The depth contours are in "kilometers below sea-level"; the total crustal thickness would be that value plus the elevation of the ground surface above sea-level. In the central U.S., the latter is a fairly uniform couple of hundred meters. The crustal thickness here is deduced from seismic refraction profile data. Such seismic coverage is quite sparse in the northern midcontinent, and where particularly doubtful the depth contours are dashed.

ORIGINAL PAGE IS
OF POOR QUALITY

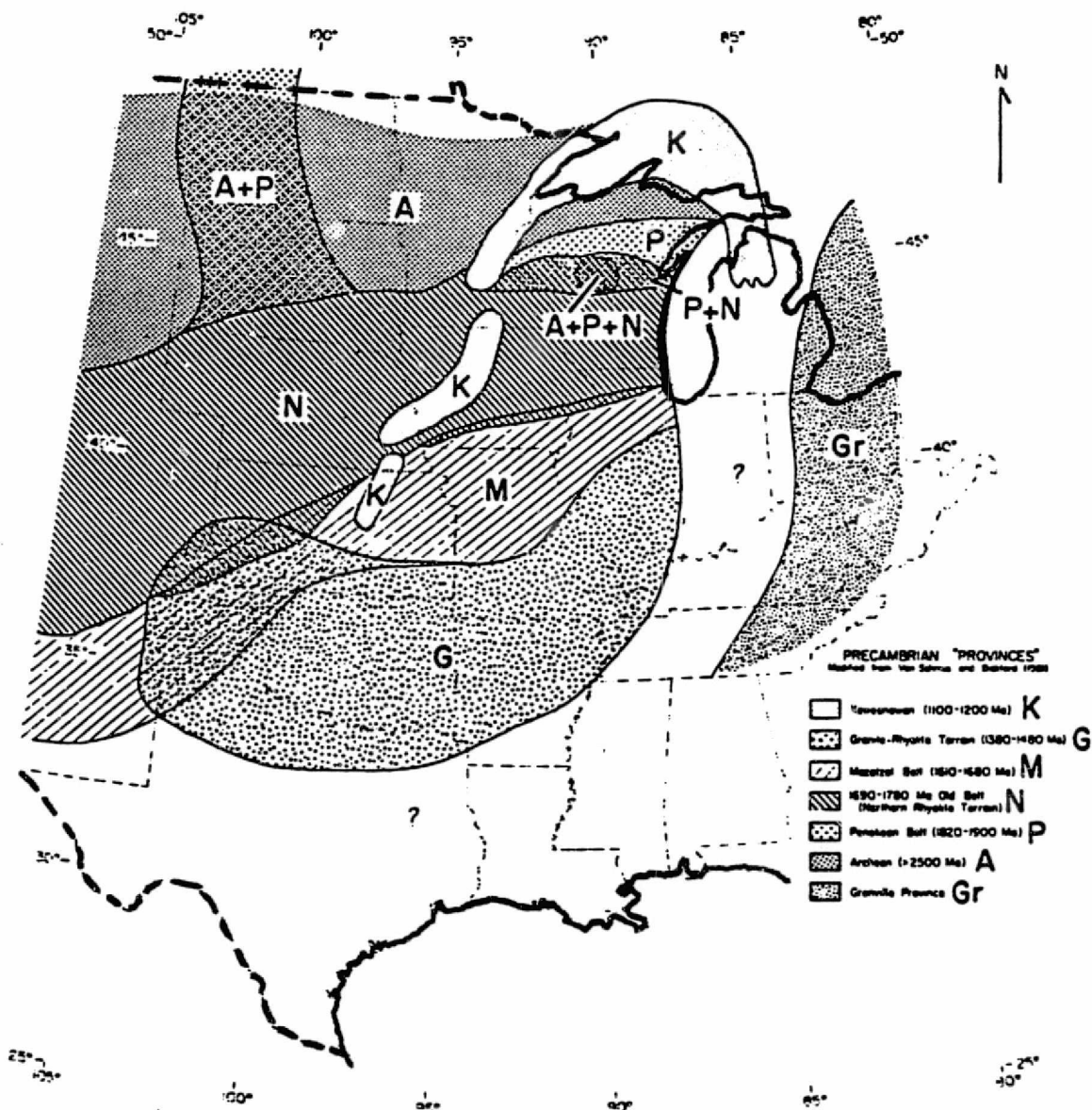
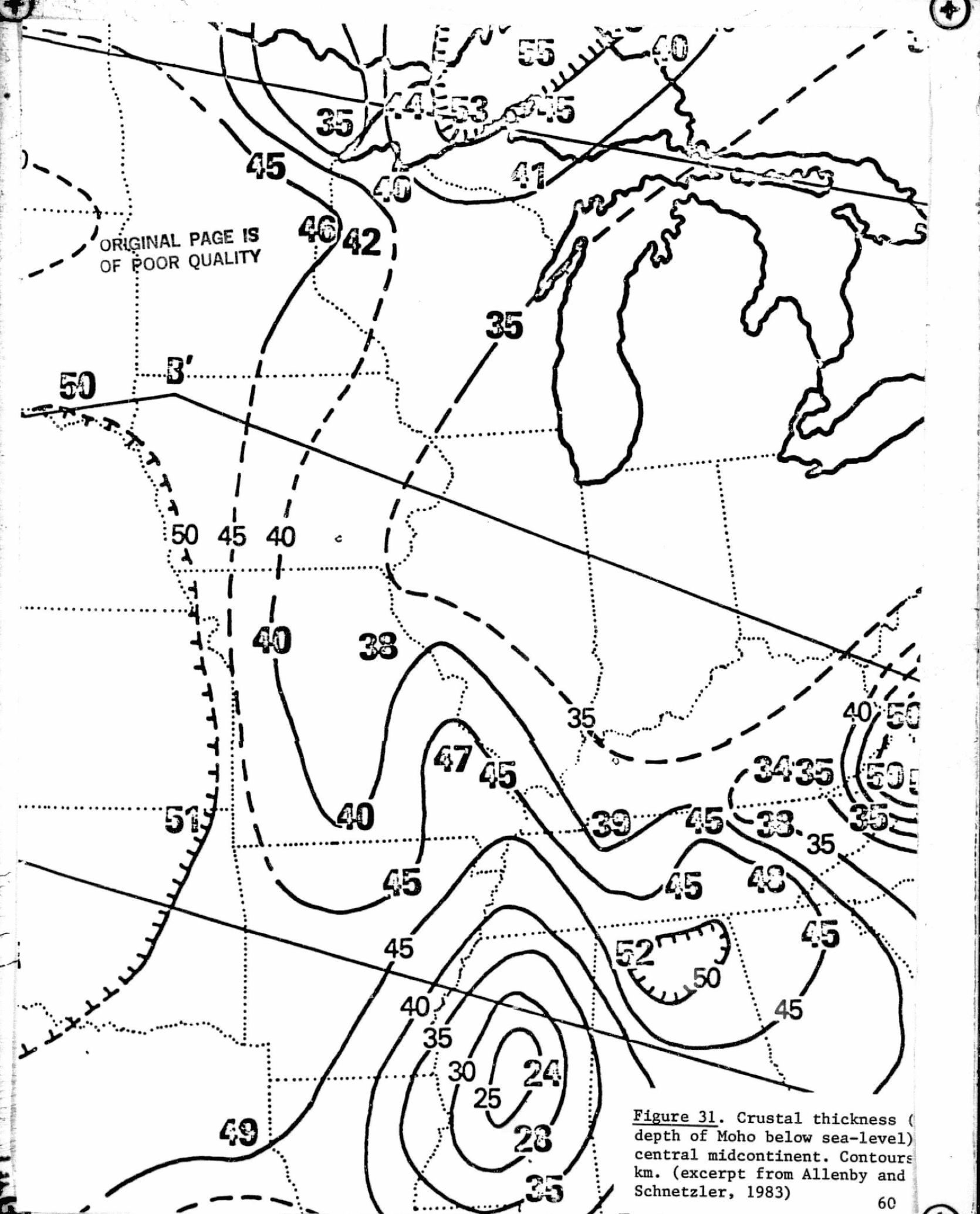


Figure 30. Geologic age provinces of Precambrian basement, U.S. midcontinent (after Van Schmus and Bickford, 1981).



It can be observed (as noted by Allenby and Schnetzler, 1983) that,

- i) the average crustal thickness in the central midcontinent is about 40 km.
- ii) the crust is relatively thicker to the southwest, Oklahoma/north Texas (about 50 km); and to the east, in Tennessee/Kentucky (over 50 km)
- iii) the crust is relatively thinner to the south, in the entrant of the Mississippi Embayment (less than 30 km)
- iv) there is no obvious expression of anomalous crustal thickness for the MGA/CNARS tectonic feature that runs from Kansas up to Lake Superior; it has an apparent crustal thickness of 40-50 km, and lies along a trend that has general gradual thickening towards the west and to the north (above Lake Superior). However, with the scarcity of seismic surveys in the region, there may yet be some more localized ("short-wavelength") variation in crustal thickness to be discovered.

A long-wavelength gravity anomaly map of the region is shown in Figure 32 (from Von Frese et al, 1982b). This is from a gravity map of North America, with data average on a $1^{\circ} \times 1^{\circ}$ grid, and filtered for wavelengths greater than 8° . We can note the gravity lows over Oklahoma/n. Texas, and Kentucky, corresponding in general to the areas of greater crustal thickness (and hence relatively more of the less-dense crustal material) in Figure 31. There is also a gravity low trending from Oklahoma to the north-east, toward Lake Michigan. There is a modest gravity high over the Mississippi Embayment, where the crust is relatively thinner (and where there is relatively more of the denser mantle rock).

An indication of lithospheric properties can be given by study of the propagation of seismic waves. Figure 33 shows the distribution of isoseismal lines for equal observed (Mercalli scale) effects from two earthquakes located in the central midcontinent (data from Docekal, 1970). These earthquakes were of sufficient magnitude to be well reported, so that the pattern of isoseismal contours could be reconstructed. The earthquake events are described on the following page.

ORIGINAL PAGE IS
OF POOR QUALITY

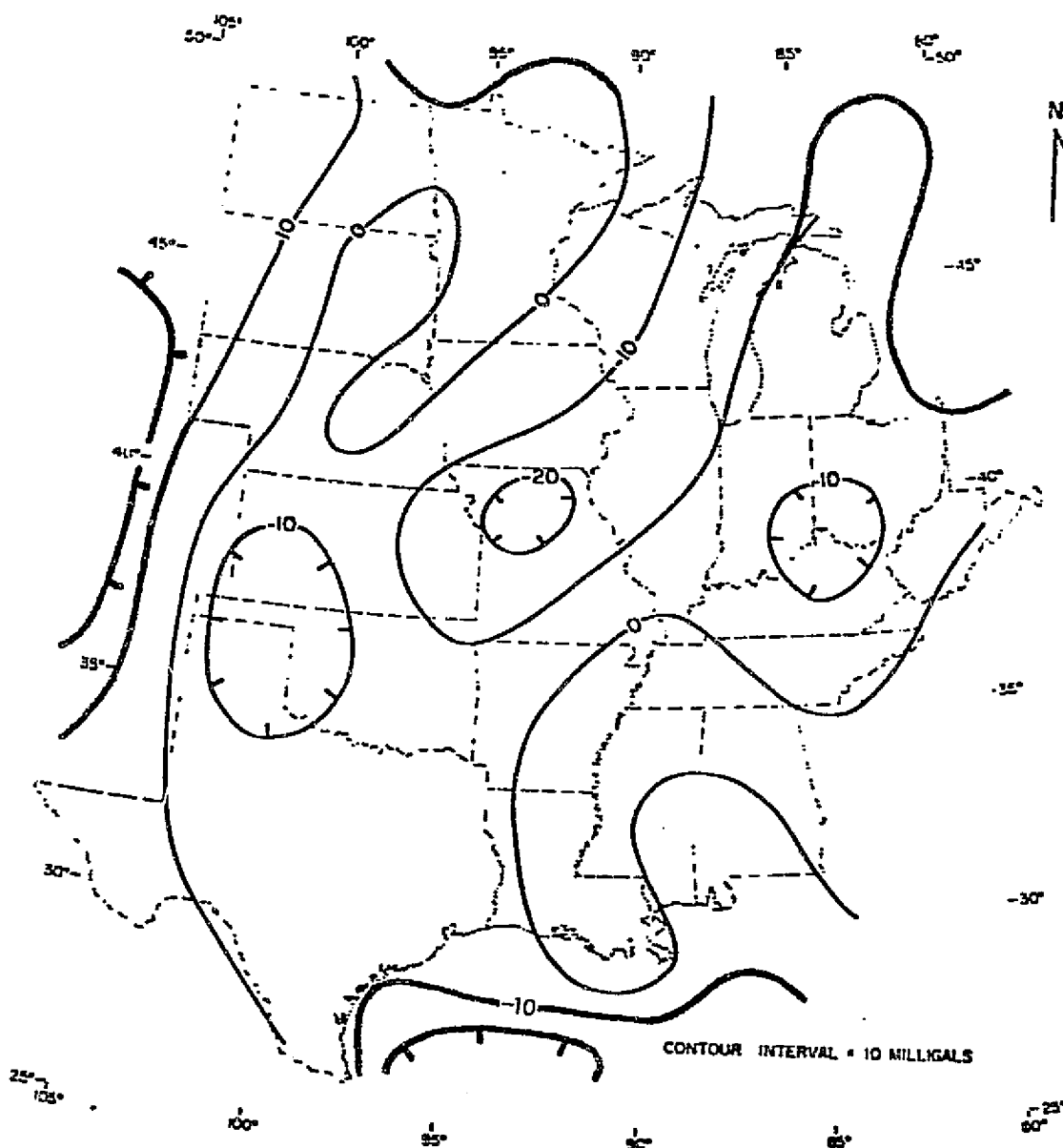

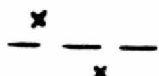


Figure 32. Free-air gravity anomaly map. Data average on $1^\circ \times 1^\circ$, high-pass filtered for wavelengths greater than 8° , and with contour interval of 10 milligals (from Von Frese et al, 1982b).

 1935
 1952

ORIGINAL PAGE IS
OF POOR QUALITY

FROM DOCEKAL, 1970

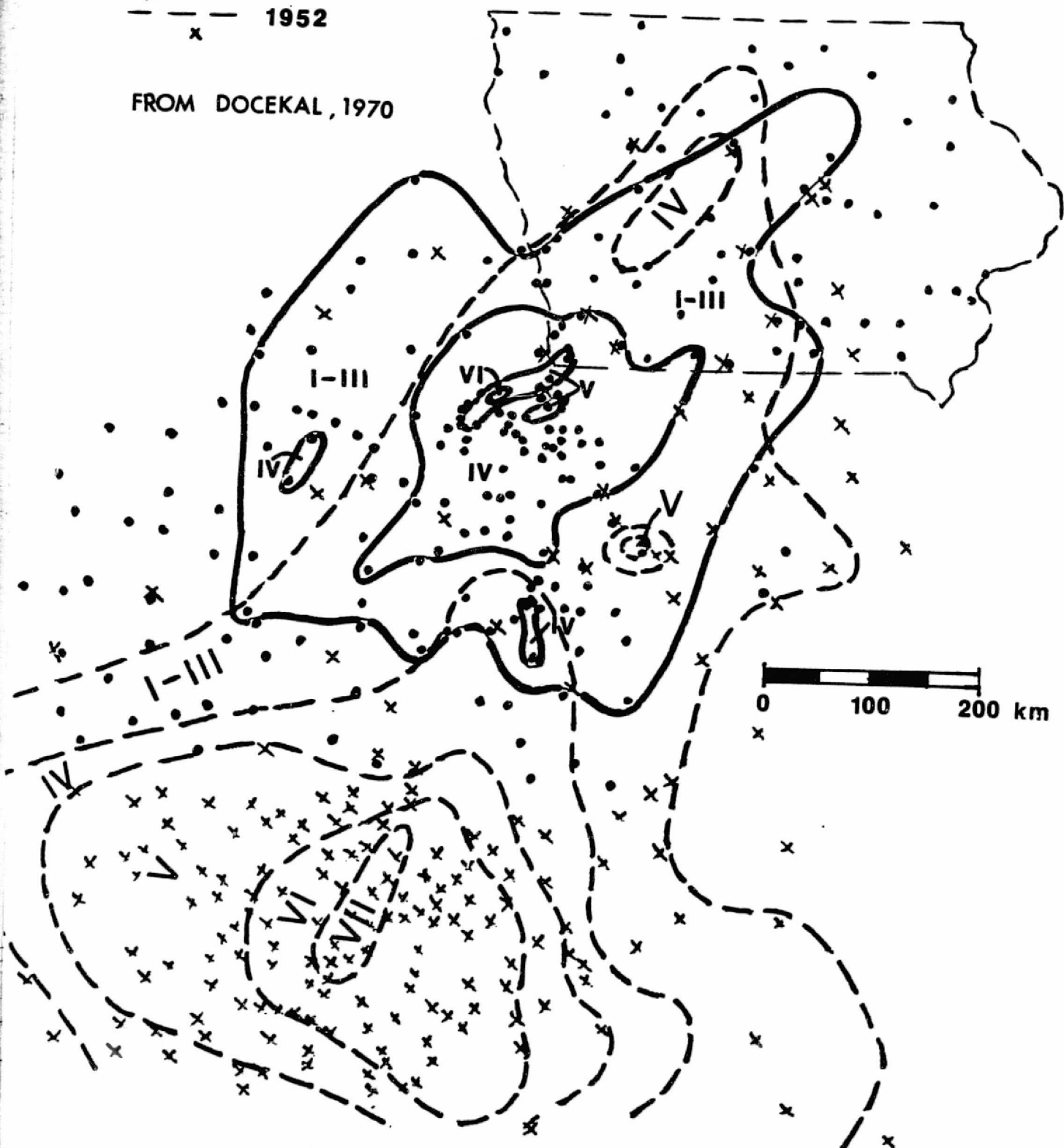


Figure 33. Isoseismal contours for earthquakes in SE
 Nebraska (1935, Mercalli intensity VI) and
 NE Oklahoma (1952, Mercalli intensity VII).
 (data from Docekal, 1970)

The earthquakes are,

- a) 1935; epicenter near Table Rock/Tecumseh, southeast Nebraska; maximum Mercalli intensity $I_m = VI$. The solid dots are the recording (observing) sites, and the solid contours are isoseismal lines of equal Mercalli intensity.
- b) 1952; epicenter near El Reno, northeast Oklahoma; maximum Mercalli intensity $I_m = VII$ (and Richter magnitude about 5.5); focal depth about 4-12 km; was felt in seven states in the vicinity. The crosses are the observing sites, and the dashed contours are the isoseismals.

It can be noted that there is strong azimuthal dependence of the energy propagation. The isoseismal patterns are elongated in the northeast direction, with similar effects being felt twice as far to the northeast as in the orthogonal (NW, or SE) direction. For example, for the 1952 event there were Mercalli intensity IV effects along the axis of the MGA up to 800 km away (to the northeast, in Iowa), but extending only 325 km away in either the northwest or southeast directions from the epicenter. The preferred direction of energy propagation (with less attenuation) is parallel to the major NE-SW structures, the MGA and Nemaha features, and to the general trend of Moho (crustal base) "topography" (see Figure 31). Seismic wave travel depends on rock type (lithology), physical properties, and regional structure. The tendency to travel with reduced attenuation in the northeasterly direction suggests an influence of

- i) reduced absorption of seismic energy, because of denser and more "rigid" mafic rock in the crust and perhaps upper mantle. This could be associated with a geologic province trending to the northeast, or the MGA structure with its major intrusive seam of denser (basaltic) rock of great depth extent.
- or ii) channelling of energy to the northeast, because of intracrustal structure and the Moho-boundary trend.

For prospective analysis and interpretation of any component of remanent magnetization in the crust, contributing to satellite magnetic anomaly fields, we would benefit from paleogeographic reconstruction. That is, rearrangement of crustal blocks (geologic provinces, continental fragments) into their configuration at the time the remanence was acquired by the rocks. This will typically involve both rotation of landmasses, and translation to the appropriate geographic latitude. This can be done by paleomagnetism, using the magnetic inclination and declination (azimuth)

of the remanent magnetization in rocks. This magnetization was acquired in the direction of the earth's field at the time the igneous rock (e.g. basalt, andesite, granite, gabbro) was cooled, or the sedimentary rock (e.g. sandstone) was deposited. The inclination gives ancient magnetic latitude, and the declination gives the amount of rotation of the landmass. The paleomagnetic information can be buttressed by other paleolatitude and paleoclimatic indicators.

The MGA complex of mafic intrusions (e.g. gabbro) and layered mafic (basaltic) volcanic rocks, is the largest upper- to mid-crustal geologic body which could be expected to have major remanent magnetization in the U.S. midcontinent. This is because the central seam of igneous rocks

- i) is very large: length of over 1000 km, from Kansas to Lake Superior; width up to 80 km; large depth extent, from the surface (in Minnesota) or a top at a few hundred meters (in Iowa and Kansas) down to as deep as at least 7 km (from modelling) and some authors would suggest much more than that
- ii) has the potential to be much more anomalously magnetic than the surrounding basement rock, being mafic (ferromagnesian, including higher in magnetite) compared to granite of the surrounding terrain.

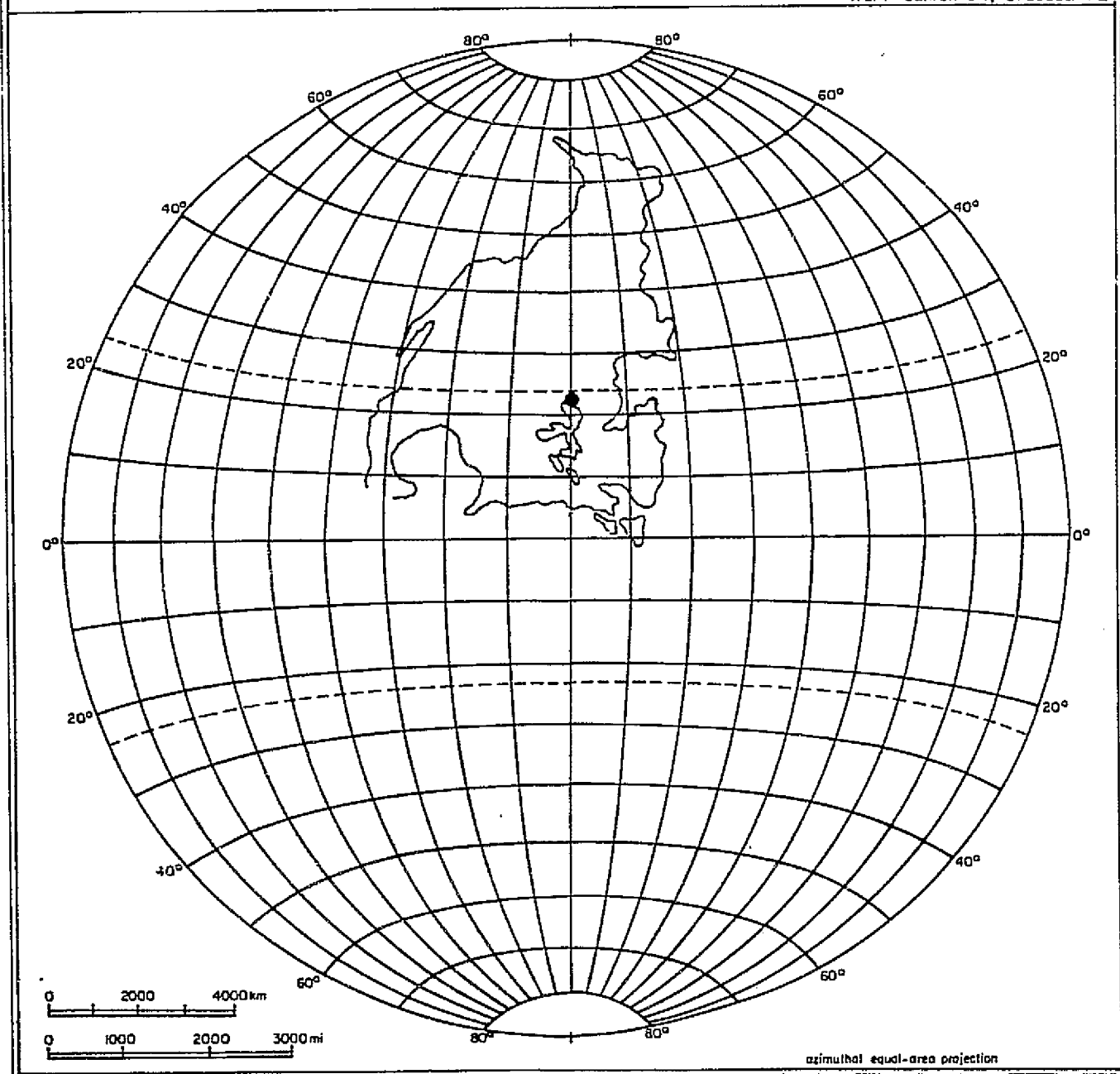
For interpretation of the potential magnetic signature (see later Section), Figure 34 shows the paleogeographic location of the North American (Precambrian) craton in Keweenawan time, 1100 million years ago. This is based (in part) on the paleomagnetic data from the Duluth Complex northwest of Lake Superior. It has a magnetic declination of remanence of 290° , and inclination of 42° . Thus at the time, the central midcontinent was oriented about 70° east of north (with respect to present geographic orientation) and at $15-25^{\circ}$ north latitude.

ORIGINAL PAGE IS
OF POOR QUALITY

DULUTH GABBRO 1100MA

Declination 290° Inclination 42°

from Jahren '64, Craddock '72



ANDERSON 1981

Figure 34. Paleogeographic reconstruction of North American craton in late Precambrian (Keweenawan) time, 1100 million years ago, during formation of CNARS structure. From paleomagnetic data.

Inversion of magnetic anomalies to crustal sources

In order to interpret crustal structure and composition, it is helpful to be able to invert the magnetic anomaly map to the causative magnetic sources. There are some differences to be considered in comparing the inversion process for satellite versus the conventional aeromagnetic data.

<u>Satellite anomaly map</u>	<u>Aeromagnetic map</u>
<ul style="list-style-type: none">- data acquired at altitudes of several hundred km- need to transform data to a common altitude (datum) level- interpretable objective: broad-scale (long-wavelength) sources and features, typically deeper- to invert for large areas: best to use spherical-earth modelling, and use an Earth's field that varies in inclination and magnitude with latitude	<ul style="list-style-type: none">- data acquired at heights of a few hundred to a few thousand meters- objective: localized (short wavelength) sources and features, typically shallower- to invert for local region: can assume flat earth, and an Earth's field constant in inclination and magnitude over the area

As a first approximation for modelling of crustal sources by inversion, it can be assumed that the magnetization is all induced. That is, in the direction of the local Earth's field. One can then compute, by some statistical best-fitting procedure, the "equivalent sources" in the crust that will give the observed magnetic anomaly map. The sources could be a regular grid of dipoles, each oriented in the local direction of the geomagnetic field. The model can be constrained by either

i) assuming a constant thickness of magnetized layer (e.g. the crust), and calculating the different dipole moments (strengths) required. The effective average rock magnetization, in emu/cm^3 *, can be calculated by dividing each dipole moment by its grid element volume. A typical presumed thickness of the "magnetic crust" could be 30-40 km, which could be considered as the effective depth from the surface to the Moho (crust/mantle boundary) or to the Curie-temperature isotherm. At the latter, magnetization is lost due to thermal effects.

* $1 \text{ emu/cm}^3 \text{ (cgs units)} = 10^3 \text{ amp/m (SI units)}$

or

ii) assuming a constant magnetization intensity for the crust, so that different calculated dipole strengths relate to different thicknesses of magnetized layer

or

iii) some combination of the above.

The "crustal magnetization" as deduced, would be the net bulk magnetization. This could be the (vector) sum of the following,

i) induced magnetization, because rock of magnetic susceptibility "k" is sitting in the Earth's magnetic field H_E , i.e.

$$J_i = k H_E$$

ii) viscous remanent magnetization (VRM), acquired slowly in the direction of the present Earth's field, because of thermal activation. This is particularly the case at temperatures above, say, 300°C , in the mid- to lower-crust; i.e.

$$J_{\text{VRM}}$$

iii) paleomagnetic remanence, such as a thermo-remanent magnetization (TRM) or chemical remanent magnetization (CRM) in basement rock bodies. This would be in the direction of the Earth's field at the time the rock as formed, and where the rock mass was then located geographically. Because of plate tectonic rotations and lateral translations of continental blocks, the paleoremanence direction could be in a direction very different from that of the present Earth's inducing field locally. Call this remanence,

$$J_{\text{rem.}}$$

Efforts to invert satellite magnetic anomaly data to crustal sources have suggested that, for the long-wavelength fields being modelled, paleomagnetic remanence can be neglected. That is, one can reproduce the observed satellite fields satisfactorily well by assuming only "induced" magnetization (i.e. crustal dipoles in the direction of the present local Earth's field) (Gallagher and Mayhew, 1982).

The net magnetization is thus

$$\begin{aligned} J_{\text{net}} &= J_i + J_{\text{VRM}} \\ &= k H_E + Q_{\text{VRM}} k H_E \\ &= k (1 + Q_{\text{VRM}}) H_E \\ &= k_{\text{app}} H_E \end{aligned}$$

where k = true average magnetic susceptibility of the crustal rock being modelled

k_{app} = effective, or apparent, susceptibility, combining the effects of induced magnetization and viscous remanence

$$= k(1 + Q_{VRM})$$

Q_{VRM} = Koenigsberger ratio for the VRM,

$$\text{i.e. } Q_{VRM} = \frac{J_{VRM}}{kH_E}$$

where H_E = magnitude of local Earth's field.

The viscous remanence contribution could, for lower-crustal rocks having resided at elevated temperatures for a long period of time in the present Earth's field*, exceed the induced magnetization in magnitude. That is, Q_{VRM} could be greater than unity in magnitude. This makes it difficult to make definitive petrologic (rock type, composition) identifications of major crustal source bodies based on interpreted "effective" susceptibilities. It is the "true" susceptibility which would be more diagnostic, but this is included within the modelled "apparent" susceptibility. One is thus limited to differentiating rock types by general gross category of

- i) mafic character (relative proportion of ferromagnesian---iron-rich minerals, including magnetite, the most magnetic of the rock-forming minerals),

	<u>petrologic category</u>	<u>typical crystalline rocks</u>
more mafic, and typically higher suscep- tibility ↓	acidic, or sialic	granite, rhyolite
	intermediate	diorite
	basic, or simatic	gabbro, basalt

in combination with

- ii) degree of metamorphism, for continental Precambrian cratons and lower-crustal rock provinces. Intermediate-pressure granulite-grade metamorphic rocks, especially if mafic, typically have the strongest-intensity magnetization.

* The last major polarity reversal of the geomagnetic field was about 700,000 years ago.

In the inverse magnetic modelling, it should also be recalled that it is the "anomalous" magnetization that is deduced. This is based on the contrast in properties between the source body and the surrounding rock. A uniformly-thick layer of constant susceptibility gives no anomalous field. In the foregoing, therefore, it is the lateral susceptibility contrast, Δk or Δk_{app} , which is calculated.

After the anomaly map has been inverted to give an equivalent-source array of dipoles, one can then reduce the data to-the-magnetic-pole by reorienting the "crustal" dipoles vertically (i.e. to simulate radial polarization) and computing the new magnetic anomaly field.

Experience has indicated (e.g. Mayhew, 1982; Mayhew and Galliher, 1982) that the POGO satellite data can be reliably inverted to a grid of dipoles down to about 300 km apart, whereas the higher resolution Magsat satellite data can be inverted to a set of dipoles 220-240 (i.e. $2^\circ \times 2^\circ$ grid) km apart. That is, the inversion technique has an associated resolution of about half the data altitude.

A refinement of the "constant-thickness, varying magnetization layer" or the "constant-magnetization, varying thickness layer" inverse modelling, is constraining the crustal magnetization to originate from some plausibly-defined source layer. Based on considerations of susceptibility magnitude, magnetic mineralogy, Curie-temperature depth, and magnetic modelling (see later Section), this is best taken as the mafic lower-crustal region or layer defined by higher seismic velocities. This layer is generally found, and conventionally taken as, lying between the Conrad and Moho discontinuities.

A map of the crustal thickness of the continental U.S., based on seismic refraction data, is given in Figure 35 (Allenby and Schnetzler, 1983). An excerpt of this, for the central U.S., was given here in Figure 31. The map shows contours of depth-to-Moho below sea level, in kilometers. The seismic coverage is sparse in the midcontinent region. The Moho is deeper (i.e. the crust has a root, more than 50 km below sea level) under the main belt of the Rocky Mountain (continuing down to Oklahoma/n. Texas), the Sierra Nevada range to the west, the Appalachian mountains, and in central Kentucky/Tennessee. The Moho is shallower (less than 30 km deep) under the Mississippi Embayment/aulacogen, the Rio Grande rift in New Mexico, and the intermontane region in the northwest between the Cascade and Rocky mountains.

ORIGINAL PAGE IS
OF POOR QUALITY

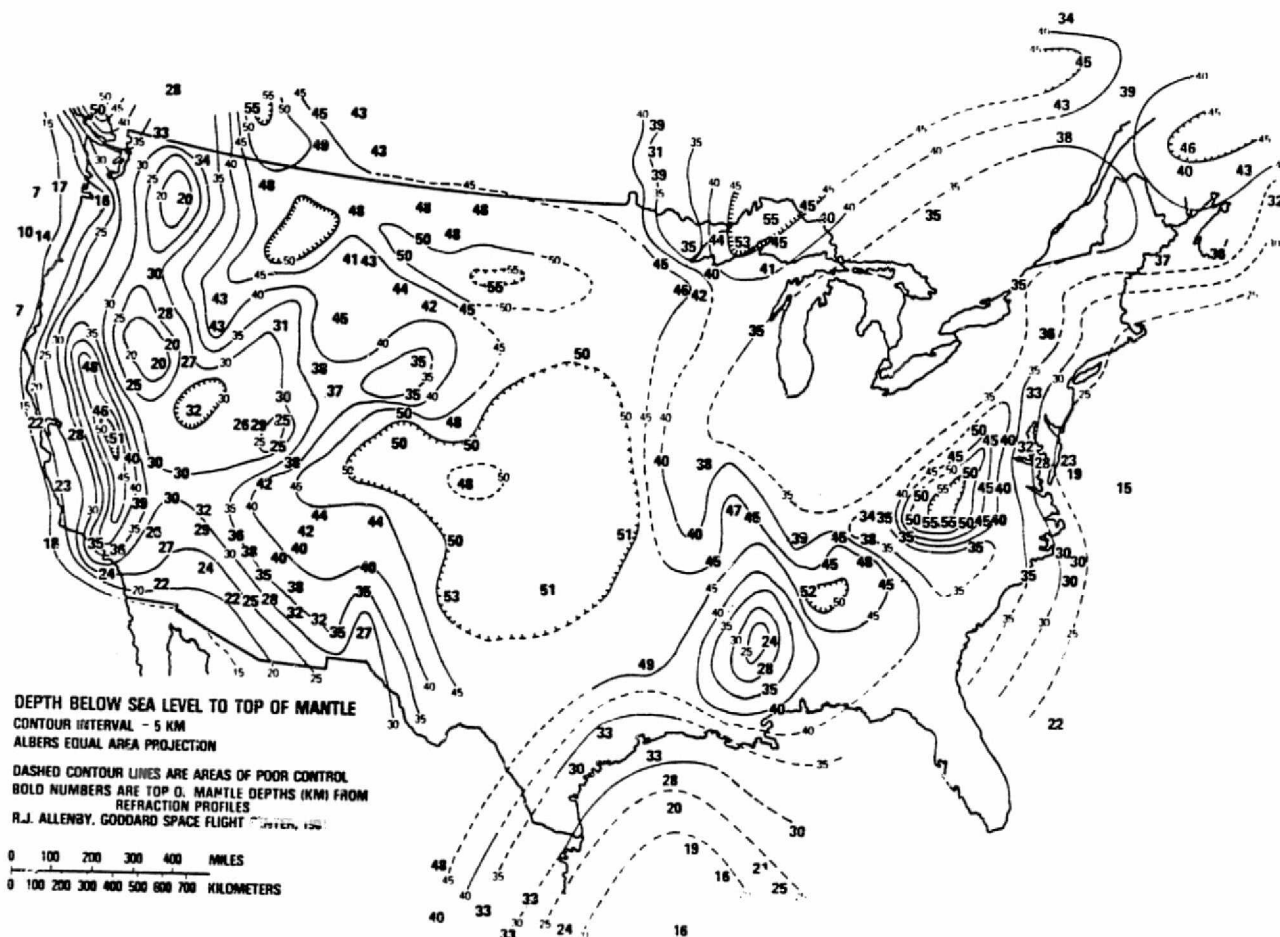


Figure 35. Crustal thickness (as depth of Moho boundary below sea level) for continental U.S. Contours in km. (Allenby and Schnetzler, 1983)

The thickness of the lower-crustal layer, again as identified from seismic refraction data, is typically about 18 km for the continental U.S. It is about 20 km in the midcontinent (see Figure 36). The basal layer is anomalously thick (over 30 km) under Kentucky/Tennessee, and under western Lake Superior. Combining the thickness of the magnetic lower-crustal layer, with a map of dipole moment strength (see Figure 37, from equivalent-source inversion of satellite anomaly data), one can estimate the effective magnetization intensity of the lower-crustal rocks (Schnetzler and Allenby, 1983).

The variation in intensity of magnetization, as deduced, is shown in Figure 38. This is a map of magnetization calculated from the modelled dipole moment strength divided by the grid volume (surface grid area times the seismologically-determined basal "magnetic layer" thickness). The average net magnetization of the lower crust for the continental U.S. is determined to be 3.5 ± 1.1 amp/m (i.e. $3.5 \pm 1.1 \times 10^{-3}$ emu/cm³) by Schnetzler and Allenby (1983).

Although the seismic data coverage is not sufficiently complete in the midcontinent region, there are indications for the lower crust there of,

- more highly magnetized rock under central Kentucky/Tennessee, where both the total crust (Figure 35) and lower-crust (Figure 36) are also thicker, and where there is a large magnetic high on the satellite anomaly map (Figure 21).
- average magnetized rock under Oklahoma/north Texas, where the total crust is thicker in general (but not anomalously-so locally), and where there is a moderately large magnetic anomaly high
- more highly magnetized rock under central Missouri, where the crust is of average or less-than-average thickness, and where there is a satellite anomaly high that is part of a trend high to the north-east
- less magnetized rock under the southern Mississippi Embayment, where the crust is thinner and the satellite anomaly map shows a large magnetic low
- progressively less-magnetized rock as one proceeds from the central midcontinent (Nebraska/Iowa) towards the north (the Dakotas, and Minnesota). This is accompanied by a relatively thicker total crust, and a satellite magnetic low.

ORIGINAL PAGE IS
OF POOR QUALITY

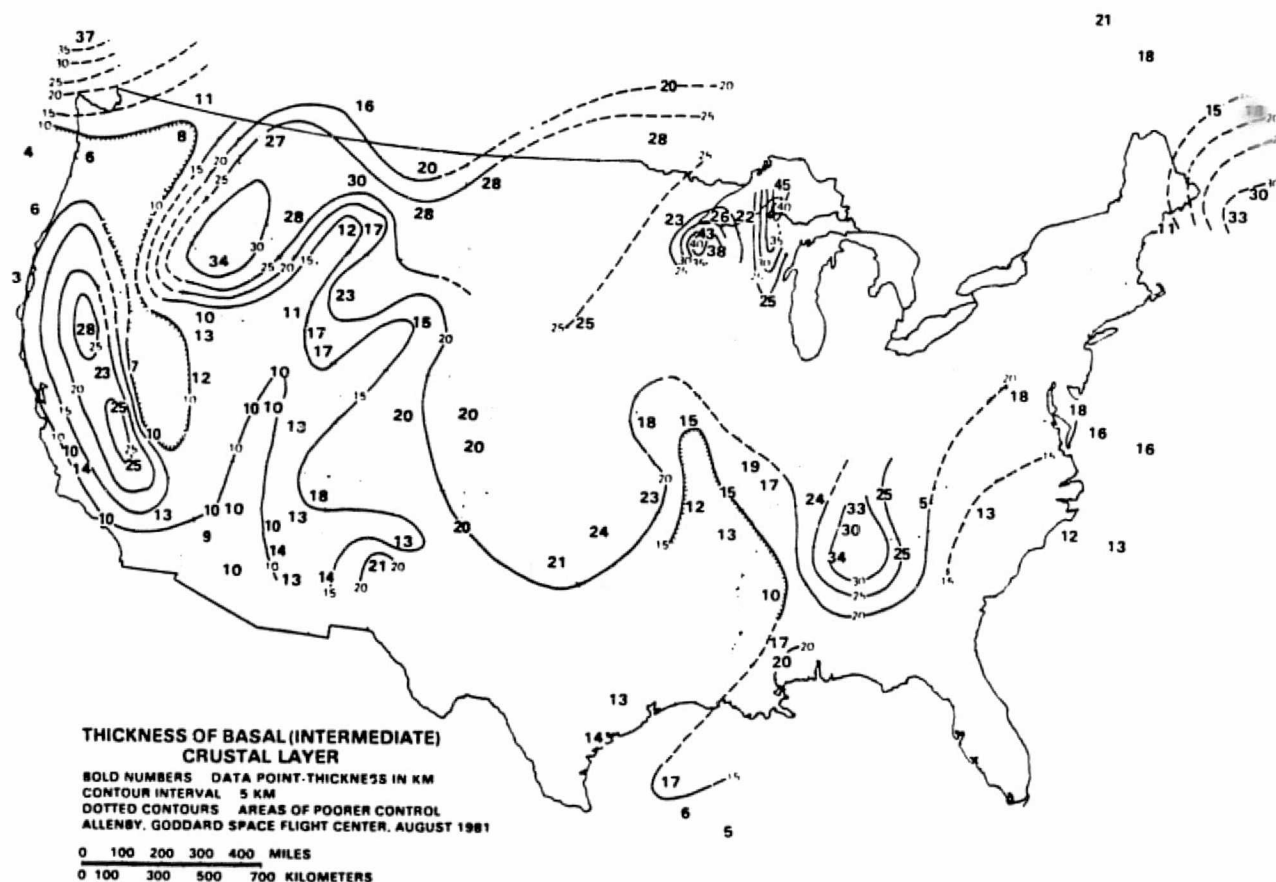


Figure 36. Thickness of the lower-crustal (mafic) layer, for continental U.S., in km. (Allenby and Schnetzler, 1983)

ORIGINAL PAGE IS
OF POOR QUALITY

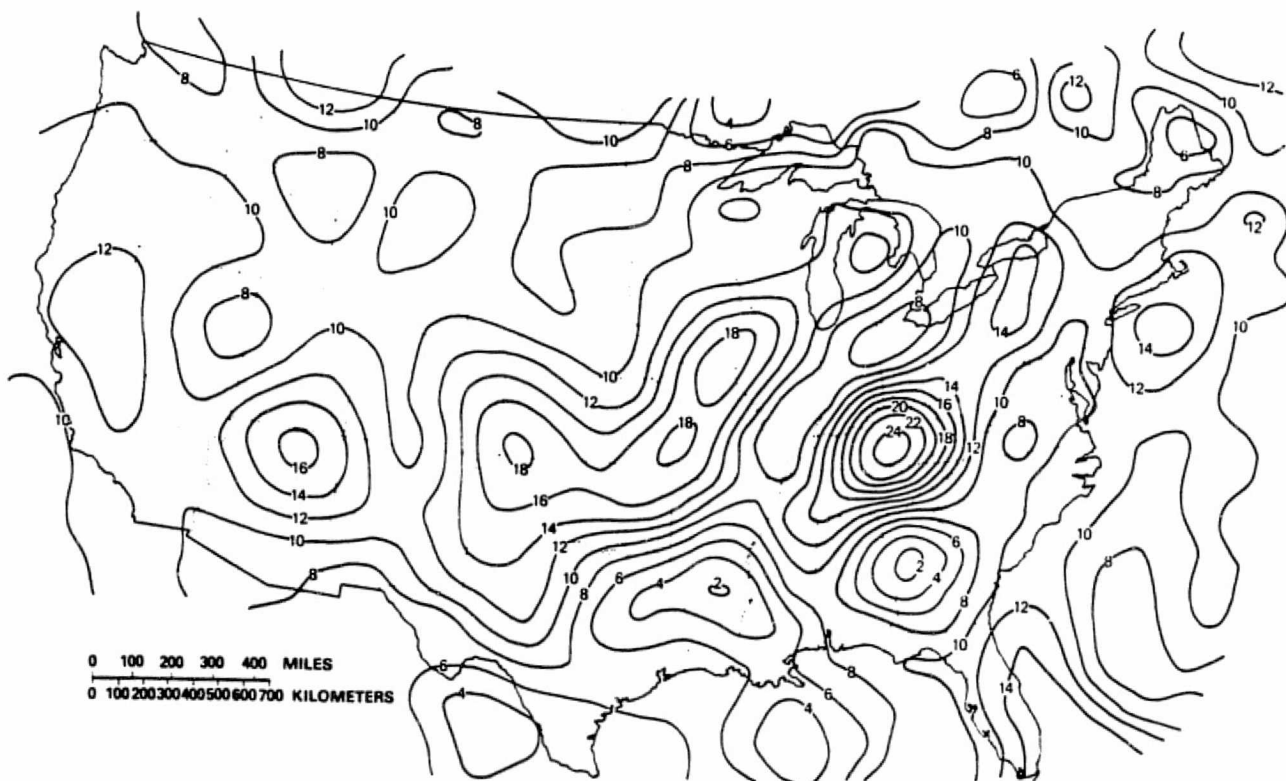


Figure 37. Equivalent-source dipole moment strength, for continental U.S. Derived from inversion of POGO satellite magnetic anomaly field. Dipoles are on a grid 150 x 150 km; contour values in 10^{17} amp-m² (from Allenby and Schnetzler, 1983, as modified from Mayhew, 1982).

ORIGINAL PAGE IS
OF POOR QUALITY

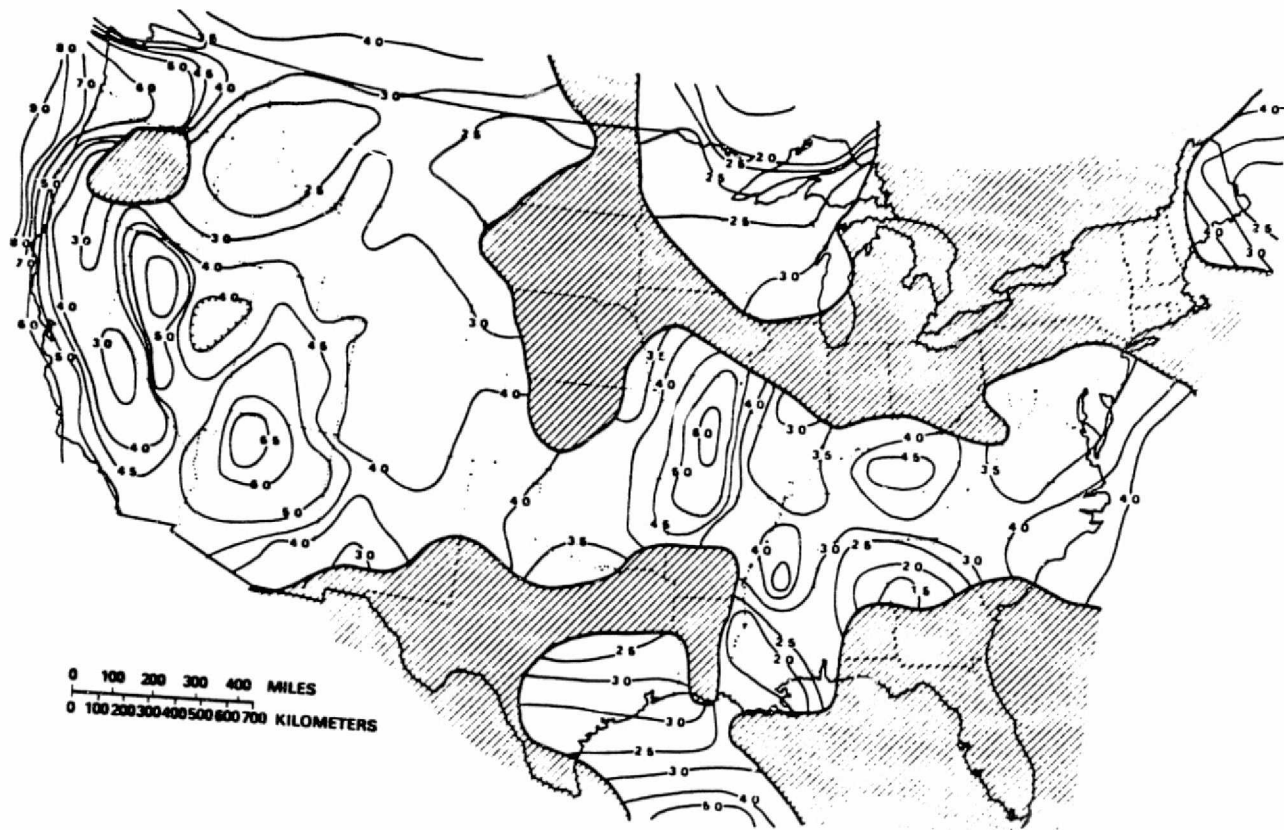


Figure 38. Rock magnetization intensity in the interpreted lower-crustal layer, for continental U.S. (Schnetzler and Allenby, 1983). Shaded area has insufficient data control. Units are amps/m (10^3 emu/cm³).

Based on the assumptions, which seem reasonable in light of current studies, that

- i) the satellite (POGO, and Magsat) magnetics present anomalies having wavelengths greater than 250 km
- ii) the crustal magnetization source is primarily the mafic lower crust
- and iii) the magnetization is all "induced" (or at least is in the direction of the local Earth's field),

Schnetzler and Allenby suggest that satellite magnetic anomalies owe their presence, on a continental average, more or less equally to the effects

of -- differences in lower-crustal layer thickness

and

-- lateral variations in rock magnetization intensity.

Resolution of satellite magnetics

With the characteristic magnetic-field wavelengths "seen" by Magsat at satellite elevations of 350-550 km, it will be of interest to estimate the resolution of the resulting satellite anomaly maps. The best data set would include magnetic "quiet-time" data, in sufficient quantity to give reliable and consistent results for a given data point, and from the lowest altitude possible. Figure 3 shows how the resolution (i.e. ability to distinguish between different sources) increases for a theoretical model field as one decreases in altitude.

For the Magsat anomaly-field data set, as pre-processed by NASA and distributed to investigators, Sailer et al (1982) estimate that one can resolve crustal-source anomalies down to 250 km. This was based on spectral analysis of magnetic signal and noise for the Indian Ocean region, but the analysis was of general utility. By equivalent-source inversion of anomaly data, Mayhew and Galliher (1982) suggest that a regular grid of dipoles spaced down to 220-240 km apart can be used to represent the observed satellite anomaly field.

The resolution of individual actual crustal sources will depend on factors such as

- i) relative magnetization of the source with respect to neighboring anomalous sources, and of the surrounding crustal rock
- ii) size and shape of the source, including the length-to-width ratio of the body or feature
- iii) orientation of an elongated source with respect to the azimuth of the satellite track (here, roughly north-south)
- iv) orientation of an elongated source with respect to the direction of the local earth's field, in both
 - inclination: anomaly shapes and relative magnitudes will vary as a function of magnetic latitude, unless the data are "reduced-to-the-pole"
 - declination: for example, east-west borders or edges of features give H_z and H_T anomalies predominantly; north-south borders or edges give expression as H_y anomalies.

Analysis and interpretation of satellite anomalies in the study area

This Section will summarize interpretation of our processed magnetic anomaly map for the central midcontinent (Figure 21), aided by the information and figures in the Sections on "Geologic Setting" and "Correlative geophysical and geologic data".

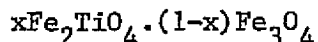
(a) General factors for magnetic interpretation of crustal character

Let us first consider some general considerations for interpreting the causative crustal sources of the long-wavelength anomalies mapped at satellite elevations. The magnitude and character of the magnetic anomalies will depend in principle on:

1) the thickness of the "magnetic lithosphere" that is magnetizable. This will be the outer layer of the Earth that has as its lower bound the Curie temperature (T_c) isotherm of magnetic minerals. Below this level, the temperature is too high for minerals to retain magnetization, and they have negligible susceptibility and no magnetic remanence. This depth will depend on the local geothermal gradient. A higher gradient, as beneath regions of volcanic and geothermal activity such as hot spots (mantle plumes) or active rifts, will result in a thinner crustal magnetic layer. The depth will also depend on the Curie temperature of the dominant magnetic mineral species. This is titanomagnetite, which is almost ubiquitous in crystalline crustal rocks and has a relatively strong magnetization. Pure magnetite, Fe_3O_4 , has a Curie temperature of $575^{\circ}C$., and as the amount of impurity titanium increases this T_c temperature is lowered. From petrologic considerations and analysis of typical (lower) crustal rocks, a representative Curie temperature of $555-575^{\circ}C$. is often accepted (e.g. Schlinger et al, 1983). More will be said on the variation of Curie temperature with magnetic mineralogy, in a later Section.

Theoretical work, considering typical geothermal gradients and the magnetic mineral series titanomagnetite,

ulvospinel - magnetite



suggests a depth to the T_c -isotherm of the following (Carmichael, 1977):

for mineral titanomagnetite:	$T_c (^{\circ}C)$	T_c depth (km)	
		oceanic crust	ancient shields
Fe_3O_4 (i.e. $x = 0$)	575	33	60
$x = 0.1$	510	29	51
$x = 0.3$	410	23	40

Depths for the effective "bottom" of magnetic sources, calculated and interpreted from magnetic modelling of localized anomalies on continents, are summarized by Green (1976) as:

	<u>magnetic "bottom" (km)</u>
5 studies, North America	20 - 48
3 studies, USSR	15 - 35
1 study, Britain	15 - 26

Depending on the geothermal gradient, the T_c could be above the Moho boundary between crust and mantle, or even above the "Conrad discontinuity" locally. The latter is a seismic/petrologic boundary or gradational zone in the mid- to lower-crust, but not everywhere identifiable. It divides the crust into an upper ("sialic"*) layer and a more mafic lower ("simatic"*) layer. The Curie-temperature could be shallower than this, for example, in the Yellowstone (NW Wyoming) region, or the Basin and Range in southern Nevada. By contrast, a typical T_c of 560°C. would be below the Moho in the "eastern U.S." generally (geologically, east of the Rocky Mountains).

It has been suggested that the Moho physicochemical boundary is also a lower bound of the magnetic layer (a.g. Wasilewski et al, 1979). That is, where the Curie-temperature isotherm depth is below the Moho, as for some regions of oceanic crust and thin continental crust, the magnetic "bottom" is up at the shallower Moho. The evidence for this derives from analysis of rocks formerly resident in the lower crust and upper mantle. The inference is that the upper mantle is characterized by non-magnetic, complex-composition spinels of "normal" structure, rather than by the ferrimagnetic "inverse" spinel titanomagnetite of the crust.**

ii) the relative partitioning of the crust into a sialic upper-crustal portion, or "layer", and a more mafic lower-crustal layer. As mentioned, these layers or zones can be differentiated by their seismic expression (e.g. velocity, from seismic refraction), or petrologic composition if the samples are available. The latter can occur if the lower

* characterized by rocks of sialic (Si + Al) composition (lower density; less mafic; less magnetic) such as granite, as contrasted to simatic (Si + Mg) composition (higher density; more mafic--i.e. more magnesium and iron; more magnetic) such as gabbro or basalt.

** A contrary view, suggesting that non-oxide phases may contribute to magnetization of the lower crust and upper mantle, is expressed by Haggerty (1979)

crust is lifted, thrust, or extruded upward by major tectonic activity.

It is being recognized that, for modelling and interpretation of long-wavelength (e.g. satellite) magnetic anomalies, the distinction between these two crust zones--and in particular, the contribution of the mafic lower-crustal layer--may be very important and often dominating. The large scale magnetic anomalies may be more dependent on this lower crustal layer than on the thickness of the crust as a whole. In one of the earlier such studies, Hall (1974) analysed intermediate-wave-length aeromagnetic anomalies over south-central Canada, to interpret the effect of major crustal structure. He excluded wavelengths less than 60 km, attributable to localized structures and bodies in the upper crust, and greater than 4000 km, presumably arising from geomagnetic (core) fields. The intermediate wavelengths correlated with the thickness of the lower crustal layer (having a magnetization of 5.3 amp/m), rather than to lateral (compositional) inhomogeneity in the crust or to the crustal thickness as a whole.

Typical properties of the crustal layers are given below (and see other data assemblies in Wasilewski and Mayhew, 1982; and Schnetzler

approx. Magnetic Properties of major crustal zones

Magnetization J is "net" (total) magnetization
 $1 \text{ emu/cm}^3 \text{ (cgs)} = 10^3 \text{ amp/m (SI)}$

	<u>Upper-crust</u> J (amp/m)	<u>Lower-crust</u> J (amp/m)
continental U.S. (Schnetzler and Allenby, 1983)		3.5 ± 1.1
continental crust, in general (various authors: Hinze, Hall, Shuey et al, Elming & Torne, Hahn)		2 - 5
(Hinze)	0.2	
(Schnetzler)	0.1 - 0.5	
(Krutikhovskaya & Pashkevich, 1977)	0.1 - 0.6	typically 4, locally up to 6
localized intrusive (mafic) bodies (various authors: Mayhew et al, Hinze, Coles, Riddihough)	3 - 5	
oceanic crust (Hinze)	5	

and Allenby, 1983 for a map of the continental U.S. shown here as Figure 38). The values in the foregoing table are derived and interpreted from magnetic modelling, e.g. by inversion of long-wavelength aeromagnetic or satellite anomalies, and measured in lab study of rock properties.

In general, then, it is interpreted that the lower-crustal layer has an effective magnetization, and thus an apparent magnetic susceptibility, an order of magnitude larger than for the upper crust. The mafic (ultrabasic) lower crust is more magnetic, and is also more magnetizable in the Earth's field because it probably has relatively lower magnetic coercivity. The latter would be due to coarser grain sizes, and the elevated temperatures.

iii) contribution of different components of magnetization. These will include (and see p. 68-69 here),

- induced magnetization, due to rock with magnetic susceptibility being in the ambient Earth's magnetic field
- viscous remanence, acquired with time and particularly at elevated temperature. This would be in the direction of the present Earth's field, and could be expected to be most prevalent for the lower crust (deeply buried, higher temperature, more magnetizable mafic rock). The higher temperatures, say 300-400°C, would result in thermally-activated acquisition of the viscous remanence. The elevated temperature could also result in enhancement of magnetic susceptibility (the "Hopkinson effect") near the Curie temperature, although the relative importance of this in the lower crust is not yet known.
- other remanence, e.g. thermal (acquired at the time the crystalline rock cooled below its Curie temperature) or chemical (acquired with later physicochemical changes, as during metamorphism). This could be in any direction, reflecting the ancient direction of the paleo-field. This would depend on the orientation (azimuth) and paleo-latitude of the local crustal segment at the time the remanence was acquired. It appears that this remanence is not significant in the lower crust, presumably not being stable against the higher temperatures and for the long residence time there.

iv) relative metamorphic grade of the crustal (basement) rocks. Metamorphism is the change of rock type, and their constituent minerals, under the influence of higher temperature, pressure, fluid solutions, and long time. This can occur for localized bodies in the crust, or regionally over large areas as for lower-crustal rocks which reside in an elevated-temperature, higher-pressure environment. The physical and magnetic properties of the rocks change along with the physicochemical metamorphic changes to the minerals. Long-wavelength magnetic anomalies can thus depend in part on the metamorphic character (grade) of

- geologic terranes of polymetamorphic character, due to experiencing different geologic histories and changes, as in the large ancient cratons (continental shields). It is possible that over ancient cratons, such as the Precambrian (Canadian) Shield in north-central North America, the magnetic anomalies associated with the upper crust may be determined more by metamorphic grade and structure than by the inherent rock type (lithology). This would apply for geologic provinces of some lateral and depth extent, and which contribute to the "long-wavelength" anomalies as mapped aeromagnetically (or correspondingly, the "shorter-wavelength" ones of those mapped by satellite).
- mid- to lower-crustal rocks, as in the basal more mafic layer.

Since analysis and interpretation of long-wavelength satellite anomalies generally suggests that much of the causative magnetization originates in the lower crust, the degree of regional metamorphism there can be important. Schlinger et al (1983) suggest that different metamorphic grades are characterized by:

<u>Metamorphic grade</u>	<u>Typical rock type</u>	<u>Magnetization</u>
low-pressure	greenschist	less magnetic, and less stable magnetically
intermediate-pressure	granulites	most magnetic (especially if mafic), most stable magnetically
high-pressure	eclogites	less magnetic, and less stable magnetically

One of the reasons that granulite-grade metamorphism in the lower crust results in higher magnetization may be that there is exsolution of the titanomagnetite/ilmenite to produce fairly pure magnetite as one component.

v) lateral inhomogeneity and differences in crustal character.

Localized intrusions of rock having anomalous magnetization (for example, a mafic pluton or dike swarm) produce magnetic anomalies. Larger blocks of crust also produce anomalies, and these are more representative of the wavelength distribution "seen" at satellite elevations. Such blocks could be brought in conjunction by the ongoing process of continental rifting, translation and rotation of continental (plate) fragments, and then collision and suturing together, that is associated with plate tectonics. The lateral conditions, geologically and thus magnetically, that result in anomalies include variations in:

- crustal "thickness" (of the total crust, or crustal zone down to the T_c isotherm, or lower-crustal mafic layer)
- geologic processes, with rocks of different petrology (composition), age, structural texture (e.g. intrusions, faults), magnetic properties (e.g. susceptibility), or depth to T_c -isotherm (because of the crustal blocks' different ages and thermal histories).

In general, one expects regional-scale magnetic "highs" (allowing for variations of anomaly appearance with magnetic latitude) to be associated with one or more of:

- thicker crust
- thicker lower-crustal layer (since is more mafic, and resides at moderately elevated temperatures)
- deeper Curie-temperature isotherm (and lower geothermal gradient)
- higher magnetite content of rocks
- intermediate-grade (granulite) metamorphism
- borders or boundaries between crustal terranes of different thickness, rock type (composition, age), structural style.

The characteristics of a magnetic anomaly map, that can be used for magnetic interpretation of crustal character, are:

- magnetic highs and lows (or positives and negatives, if the zero-level is arbitrarily set at a median level)
- magnetic gradients; these can indicate geologic and structural trends, and boundaries. Gradients can be accentuated by second-derivative analysis.
- areas of different magnetic character and pattern. Different textures and "morphologies" of magnetic pattern could indicate different tectonic blocks (now sutured together), different lithologies, or different regional metamorphic grades.

Satellite magnetic anomaly maps provide broad-scale (continental-wide) coverage with observed wavelengths characteristic of geologic provinces and features of crustal dimensions. That is, one can hope to "see" anomalous crustal sources of regional lateral extent, and of great depth extent. The latter would extend down to the Curie-temperature isotherm, or Moho boundary, whichever is shallower. These crustal sources would include continental fragments (or blocks, or microplates). Thus if the good-resolution Magsat data can resolve and distinguish these blocks, and their extensional or collisional boundaries, then satellite surveying can help interpret the patterns of plate tectonics. This would apply for both:

- modern plate tectonics. Magnetic anomaly mapping might help interpret the thermal regime (geothermal gradient, variation in depth to T_c -isotherm) and any associated crustal or lithospheric thinning, at active rifts at extensional plate boundaries, or at localized hot spots. Sample study areas would include the midocean spreading rifts, and Iceland, Hawaii, Yellowstone, and the Red Sea.

and

- ancient plate tectonics. This would involve old paleorifts where continental rifting failed (i.e. aulacogens), or collisional zones where continental blocks have been welded together.

The expected relationship between magnetic anomalies and the depth to T_c -isotherm in volcanic/geothermal/rifting areas is that the

elevated Curie temperature isotherm will give a thinner "magnetic crust" and thus a more subdued magnetic anomaly. That is, a magnetic "low" compared to the surrounding crust of normal, or average, thermal character. This relation may not apply, however, for:

- very old thermal tectonism. After the original thermal perturbation and associated effects, the crust would have equilibrated thermally and the T_c -isotherm returned to its normal lower level. There would thus now be no anomalous thermal signature to contribute to a magnetic anomaly. Any anomaly would be due to the residual differences in crustal composition, or magnetic properties, or thickness of crustal layers.

or

- very young thermal tectonism. With recent volcanic or plutonic activity, the intrusion upward of molten or semi-molten rock and geothermal fluids would be accompanied by an elevated T_c -isotherm. This would be a local phenomenon, however, since rock is a poor thermal conductor. It would take some time for the T_c isotherm to become established and equilibrated shallow over a broad-enough region and result in changes in the long-wavelength anomalies seen by satellite.

(b) Related interpretations

Now let us consider general interpretations that can be made relating satellite magnetic anomalies to causative crustal sources. A number of major crustal geologic features are expressed on NASA's global Magsat anomaly map, as interpreted by Frey (1982a and b). The spatial relationship of anomalies to crustal sources is even better defined if one uses a reduced-to-the-pole version of the magnetic map, as done for POGO data by Langel and Frey (1983). In general, with respect to the observed magnetic anomalies*,

i) ancient (i.e. Precambrian-age) continental shields are generally magnetic highs (positive). Some are not, however (e.g. southern Superior province in North America, and southern India), and there can be variations in the magnetic texture and signature due to differences in regional metamorphic grade of the crustal rocks. In general, a greater degree of metamorphism produces a higher (more positive) anomaly expression.

* The largest magnetic anomalies measured by Magsat, after "normalizing" for local geomagnetic field intensity (i.e. induced-magnetization anomalies are greater at higher latitudes, because the earth's field intensity is stronger there) are, in order, Bangui (west Africa), Kursk (USSR), Kentucky/Tennessee, and Tibet.

ii) ancient structures seem to have anomalies arising mainly from intracrustal lithologic variation. An example of this might be the large Bangui anomaly in the Central African Republic. Here (Regan and Marsh, 1982; Hastings, 1982), magnetic modelling suggests a central Precambrian shield (with depth of about 40 km) flanked by younger and less-magnetic sedimentary basins. To the north is an arm of the Chad basin, with depth about 13 km, and to the south is the Congo basin, with depth about 10 km. A possible alternative model is a paleorift. However, modelling of the observed anomaly apparently requires effects of more than a single body having a near-horizontal magnetization (with such inclination, because the feature is near the magnetic equator).

as compared with

younger structures and tectonic features (typically, of Cenozoic age--i.e. younger than 70 million years), which seem to have anomalies resulting from variations in Curie-temperature-isotherm depths.

iii) rifts should have a magnetic expression, depending on the age and maturity of the tectonic development. Although the process could be variable, one could perhaps make a tectonic distinction between

-- "aulacogen-style" rifting, to yield failed paleorifts. This would have doming and arching of the lithospheric plate, due to the thermal upwelling in the upper mantle, but leaving the lithosphere largely unfractured.

and

-- true rifting, with extension. This would have thinning and fracturing of the lithosphere, leading to lateral movement apart of the plates (i.e. continental drift).

For an early stage of rifting of continental crust accompanied by crustal thinning and elevation of the T_c -isotherm, both effects would produce a magnetic anomaly low. This characteristic should endure with time, except that the thermal regime would equilibrate back to normal and the T_c -isotherm contribution would diminish. There are (on reduced-to-the-pole anomaly maps) magnetic lows over the Rio Grande rift (New Mexico; an active "rift" feature but with little associated volcanism), East African rift, and over such (failed) paleorifts as the Mississippi Embayment/aulacogen, the Benue trough (an aulacogen rift, north of the Bangui anomaly, presumably from a triple junction associated with the

opening of the present Atlantic), Amazon River valley, and several in the Siberian continental platform (Frey, 1982a and b). With tectonic evolution of a rift, there may be injection of mafic rock in the axial crustal zone, and emplacement of a rift "pillow" below the rift's central thinned crust. The latter rock, a mafic differentiate of the upper mantle, would be ultrabasic and highly magnetic (high susceptibility). Such material, because it offsets the crustal thinning and contributes more-magnetic rock, results in a thicker "magnetic lithosphere" locally. This would yield a magnetic anomaly high, or at least partially negate the pre-existing magnetic low. There can thus be a combination of effects. For example, the magnetic low over the Mississippi embayment has been attributed to crustal thinning, elevated isotherms, and if it does have an axial lower-crustal or sub-crustal rift pillow (the crust locally is 35-40 km thick) then this is anomalously less magnetic. This may be (Thomas, 1983) because of the presence of higher-titanium titanomagnetite in the lower crustal rock, which may be gabbroic in composition. Titanium reduces both the magnetization and Curie-temperature of magnetite; this also raises the T_c -isotherm depth without an increase in geothermal gradient.

A related aspect of rifting would be the thermal (and possibly physical) thinning of the lithosphere as a tectonic plate moves over a relatively fixed thermal disturbance, such as a mantle plume (hot spot). An example would be the Hawaiian islands, where the Pacific oceanic plate moves west-northwest over a plume. Depending on the plume's areal extent, temperature, and magmatic activity, as well as the initial thickness of the lithosphere, the rate of plate movement, and the thermal conductivity of the lithospheric rock, there would be a lag in the recovery of the thermal thinning back to normal. For a fast-moving plate, there could be a small magnetic anomaly low displaced a little "downstream" from the source plume.

iv) most submarine platforms and rises are magnetic highs, as contrasted to many oceanic abyssal plains and basins which are lows.

v) several subducting lithospheric slabs are magnetic highs (Langel and Frey, 1983). This would be due to the cooler slab penetrating down into the upper mantle, carrying the isotherms (including the

T_c -isotherm) with it*. The magnetic anomaly would be expected to be greater for more rapid subduction, and would reduce with time as the subducted lithosphere becomes thermally equilibrated to the higher temperatures.

vi) continental crust has larger-amplitude anomalies than oceanic crust. This is because the latter is thinner, and has a shallow T_c -isotherm, even though oceanic crustal rock is more magnetic (per unit volume) than typical continental crust.

(c) Interpretation of study area

The processed Magsat magnetic anomaly map (scalar H_T , reduced-to-the-pole) for the central U.S. midcontinent was shown in Figure 21, and is repeated here as Figure 39. Some of the related geologic and geophysical features are given in Figure 24 (major tectonic structures) which is included here as a transparent overlay on Figure 39, and also Figure 30 (basement age provinces), Figure 31 (crustal thickness), and Figure 36 (thickness of lower-crustal layer).

Several major anomalous features are observed on the anomaly map of Figure 39. They are:

i) a bullseye magnetic high over east-central Kentucky/Tennessee (centered at $37\frac{1}{2}^{\circ}$ N. Lat., $84\frac{1}{2}^{\circ}$ W. long.). This is one of the most prominent anomalies on the Magsat anomaly map of the world, and was identified also on the earlier POGO satellite data.

On the reduced-to-the-pole map here, the anomaly has a central maximum of about 15 nT with respect to the general regional field value. It is generally attributed to a mafic basement rock complex in the upper crust, and a lower crust intrusion which is also anomalously ultrabasic. This occurs at the intersection of the southeast-trending "south-central magnetic lineament" and the southwest-northeast-trending "New York-Alabama lineament" (see Fig. 39). It may also be along the southward extension of the Grenville front, which comes down from Lake Huron and separates older rock on the west from younger rock (approximately Keweenawan age, about 1100 million years old) on the east.

* Subduction rates are typically several cm per year. By modelling of the thermal regime and rock properties, it is deduced that for very small subduction rates (well under 1 cm/yr), temperature isotherms are "dragged down" in the lithosphere slab faster than heat can be conducted upward to maintain lateral equilibrium. This is for the case of heat transport by conduction alone.

ORIGINAL PAGE IS
OF POOR QUALITY

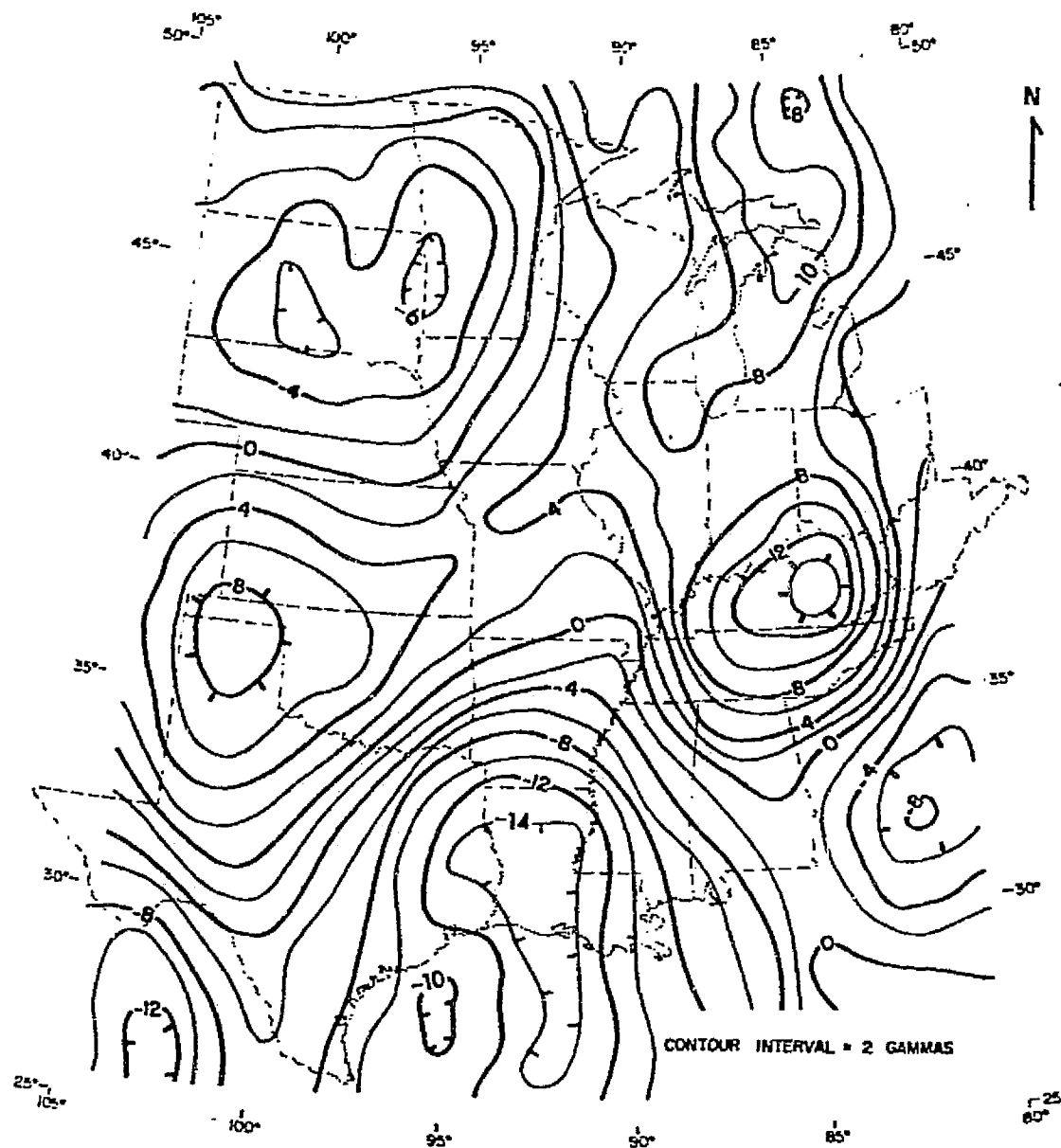


Figure 39. Magsat scalar anomaly map, reduced to the magnetic pole. Repeated from Figure 21.

The basement rocks here are mafic volcanics and metamorphics. The former are similar to the Keweenaw (late-Precambrian) volcanic rocks of the western Lake Superior region, and may also be of the same age (Hildenbrand et al, 1983). The high-resolution aeromagnetic map for the region is a jumble of high-amplitude anomalies, in contrast to the satellite expression (in effect a high-pass wavelength-filtered version) of a large, single high.

Geophysical modelling of the anomaly (Mayhew, Thomas, and Wasilewski, 1980; J. Phillips/U.S.G.S.) suggests a feature such as portrayed in Figure 40. A mafic intrusion such as gabbro in the crust would give the increased density (3.0 gm/cm^3 , versus crustal value of 2.8 gm/cm^3) and magnetization (anomalously greater by 4 amp/m, or 0.004 emu/cm^3) to yield the positive gravity and aeromagnetic anomalies. The intrusive body is interpreted as extending from 5 to 25 km down (with the Moho at about 30 km), and has a width extent of about 40 km. This modelling is thus based on an effectively thicker localized lower crustal "layer", for an otherwise constant-thickness (i.e. as gauged by depth-to-Moho) crust. This is consistent with seismically-determined crustal thickness in the region (see Fig. 31, Allenby and Schnetzler, 1983) of 35 km in east-central Kentucky/Tennessee, although the crust thickens to the southwest and to the east to 50 km. There is a thickening of the lower-crustal layer from a regional value of about 20 km to a thicker 30 km, in an area extending from central Kentucky through central Tennessee to northern Alabama (see Fig. 36). There is in fact a corresponding elongation of the magnetic anomaly high in this direction (Figure 39, again). In the interpreted/calculated map of lower-crustal magnetization (Fig. 38), an anomalous value of 4.5 amp/m is assigned for the localized region of east-central Kentucky/Tennessee. This is close to the value of 4.0 amp/m deduced for the simple modelling of the aeromagnetic data.

ii) a magnetic high over NW Texas/Oklahoma (centered at 36°N . lat., $101\frac{1}{2}^\circ\text{W}$. long.), then extending in an arcuate moderate high up to the northeast through Missouri to Lake Michigan. While this anomaly could also be noted on POGO data, its continuation up to the northeast is better evidenced in this data here.

ORIGINAL PAGE IS
OF POOR QUALITY.

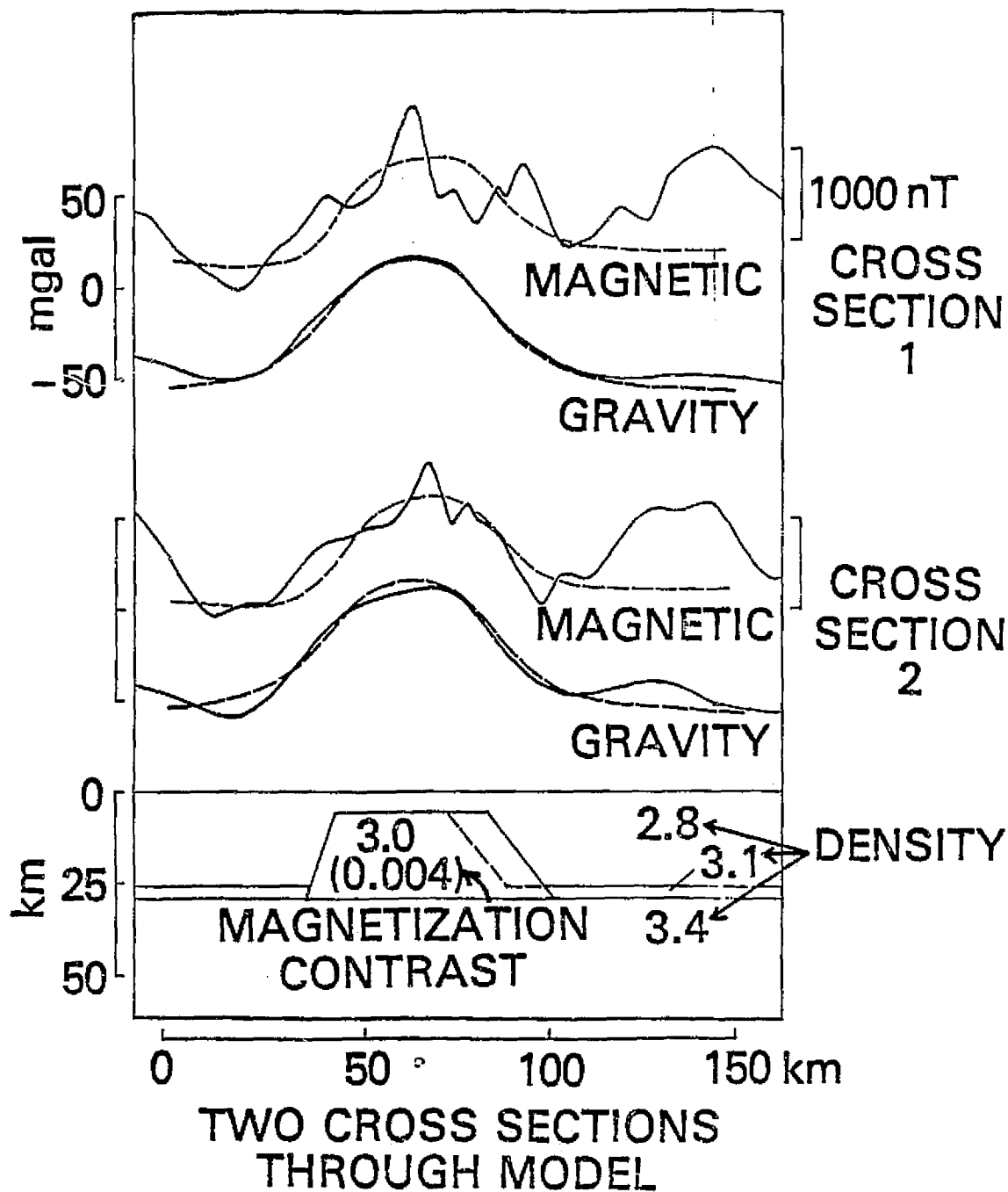


Figure 40. Two-dimensional magnetic and gravity modelling of . Kentucky/Tennessee magnetic high. Profiles are west-east; solid lines are measured anomalies, dashed lines are modelled. Densities in gm/cm³, magnetization contrast is 4 amp/m (0.004 emu/cm³). (Mayhew, Thomas, and Wasilewski, 1980)

The magnitude of the anomaly over NW Texas/Oklahoma is about 9 mT. The origin of this anomaly is not well known. There is a gravity anomaly low centered over the area (Fig. 32), implying a thicker crust, and the crustal thickness map (Fig. 35) shows anomalously thick crust (50 km) in the larger region. There is insufficient seismic coverage to define the local crustal thickness there in detail. If one attributes the localized magnetic high to crustal thickening (i.e. a thicker magnetizable crust), there is less need to invoke anomalously more-magnetic crustal rock. In fact the lower-crustal magnetization map (Fig. 38) interprets little if any such anomalously magnetic rock in the area.

The source of the anomaly high trend towards the northeast is also uncertain. There are a couple of possibilities:

1) the origin is a zone of greater crustal thickness, perhaps developed in late Precambrian time (Black, 1981) either during the Mazatzal orogeny, or where the subsequent and subparallel Granite-rhyolite terrane of the upper crust now is emplaced. The Mazatzal was a tectonic/deformation episode, possibly at a convergent plate boundary, of 1600-1700 million years ago, and the Granite-rhyolite terrane has an age of 1400-1500 million years. These geologic provinces of the Precambrian basement are shown in Figure 30, as developed from radiometric age-dating and basement petrology (rock types). The Mazatzal belt ("M") runs from NW Texas/Oklahoma up through Missouri to Lake Michigan, and the Granite-rhyolite terrane ("G") sweeps up on the southern and eastern margin. Additional and more recent borehole and age-date information suggests that the northern boundary of this latter terrane should be placed farther north into NE Missouri, SE Iowa, and northern Illinois.* Thus either geologic trend (Mazatzal, or Granite-rhyolite), or both, could contribute to the elongate magnetic anomaly high.

The gravity anomaly map (Fig. 32) does show a low along the trend of the magnetic high and the Mazatzal belt, implying a thicker crust. However, the crustal thickness map of Fig. 35 shows no anomalous thickening in a fairway up to the northeast, but rather a general thickening in the northern midcontinent from east to west. Unfortunately, the seismic coverage is incomplete. On the other hand, there is also the fairly remarkable tendency for seismic energy in the crust to be propagated preferentially in the northeast direction from Oklahoma, as seen in Fig. 33 for earthquake isoseismal contours.

* although there is a possibility that the rock bodies sampled, and whose younger ages would extend the Granite-rhyolite terrane farther north, represent later events or intrusions in the older Mazatzal terrane.

or

2) the origin of the anomaly high trend toward the northeast is due to a zone in the lower crust which is more magnetic.* For example, in central Missouri the crust is of average thickness (about 40 km), but the interpreted lower-crustal magnetization is higher than average (5 to 6 amp/m; see Fig. 38).

iii) a magnetic low over the Mississippi Embayment/aulacogen, over the Gulf Coast and extending from about 91-94° W. longitude. The anomaly has a minimum (low) of about -15 nT over the Gulf of Mexico coast of Louisiana, and extends north-northeast up the Mississippi River (and the Reelfoot rift) to the New Madrid seismically-active zone in southeast Missouri.

Gravity and magnetic modelling of the region, in addition to what is known of the subsurface geologic structure from seismic, drilling, and other information, suggests the probable origin of the regional magnetic low (Von Frese et al, 1980 and 1982b; Keller et al, 1983). The Embayment is a broad reentrant of Mesozoic and Cenozoic-age sedimentary rocks extending into the Precambrian craton. It originated with the late Precambrian/early Paleozoic rifting of the proto-Atlantic at the "rifted continental margin" (see Figure 39) to the south. Associated with this were aulacogen features such as the Reelfoot rift. With the (second) opening of the Atlantic in Mesozoic time, the Embayment formed with areal subsidence. The central rift and associated structure, particularly at the northern end, are presently still active seismically.

There are major and broad anomalies--a gravity high, and a (POGO, and Magsat) magnetic low--over the Embayment. This negative correlation between long-wavelength magnetic and gravity anomalies for large crustal sources, and the positive correlation generally observed between satellite magnetics and continental crustal thickness, suggests that the anomalies here are due to crustal thinning. This would presumably have resulted from the paleorift development. The thinning would give the gravity high, due to upwarped denser mantle, and the magnetic low due to a thinner magnetizable crust.

The crustal thickness map (Fig. 35) shows that there is some localized thinning of the crust, to 25 km, compared to the general

* An ultramafic and more magnetic lower crust here might have originated, or been associated, with a continental collision/subduction which helped form the midcontinent craton in Precambrian time.

vicinity which has a thickness of about 40 km. However, the thinning does not appear to reflect the elongated nature and length-extent of the observed magnetic low. Another contributing factor could be a shallower T_c -isotherm depth (to produce, for example, the localized magnetic anomaly low over Yellowstone), but there is no substantial evidence for a higher regional geothermal gradient in the Mississippi embayment.

Another possibility for the magnetic low, and suggested by the geophysical anomaly modelling, is that the local lower-crustal layer has the usual higher density (to contribute to the gravity high)* but an anomalously low magnetization. To explain this, one could invoke mineralogic/petrologic conditions, such as more titanium impurity in the magnetite, to reduce the magnetization. The interpreted lower-crustal rock magnetization (Fig. 38) shows a value under Louisiana of about 2-3 amp/m, which is below the regional (and continent's average) value of 3.5 amp/m.

iv) a magnetic low over South Dakota, with magnitude of about -6 nT. This could be due to some combination of:

- elevated Curie-temperature isotherm; however, regional geothermal gradients are not well known in the area. Preliminary recent heat flow data suggest that northern Nebraska (and perhaps southern S. Dakota) may have higher heat flow (at least in the upper crust) than the U.S. midcontinent in general (Goswold, 1980).
- crustal thinning; however, the crust is about 45-50 km thick under South Dakota itself, which is at or a little thicker than the average for the northern midcontinent. On the other hand, the crust is even thicker, over 50 km thick, to the north and south of S. Dakota where the magnetic low is centered.
- anomalous magnetization deficiency in the lower-crustal layer. There is a hint of this in Fig. 38, suggesting a local magnetization of 2.4-2.8 amp/m, which would indeed be below the U.S. continental average of 3.5 amp/m. Such a magnetization deficiency could be due to less-mafic rock having less magnetite (e.g. being diorite, rather than gabbro), or rock with a lower degree of regional metamorphism than granulite-grade, or magnetite with more titanium as an impurity (and thus lower magnetization and lowered Curie temperature).

* and the lower crust here may also have an anomalously higher density for this basal layer, as a relic of the aulacogen rifting

v) a magnetic low over west-central Georgia (south-southeast of the Kentucky/Tennessee anomaly), with magnitude about -8 nT. This is probably attributable to a localized region of anomalously less-magnetic lower crust, as interpreted in Figure 38. The value assigned from analysis is 1.5-2.0 amp/m, again well below the continental average of 3.5 amp/m.

vi) a general tendency for the magnetic pattern to follow and reflect the southern "rifted continental margin" of the North American craton (see Fig. 39) in this area. This margin was formed in late Precambrian/early Paleozoic time, with the opening of the proto-Atlantic, and had associated with that rifting event a number of failed rift arms (aulacogens) directed into the craton. These include the Reelfoot rift, and the southern Oklahoma aulacogen (Keller et al, 1983). The margin was then the site for the Appalachian and Ouachita mountains, formed in the later collision closing the proto-Atlantic.

Referring to Fig. 39, it is seen that the ancient continental margin approaches from the east, wraps concave-northward around the contour lines of the large Kentucky/Tennessee magnetic anomaly high (and also the south end of the Appalachians), then wraps concave-southward around the contour lines of the magnetic low associated with the Mississippi embayment, and then wraps concave-northward around the south side of the large NW Texas/Oklahoma anomaly high.

vii) a lack of apparent magnetic expression for the Central North American Rift system/Midcontinent Geophysical Anomaly (CNARS/MCA). This long, deep, and major paleorift--an immense seam of mafic rock in the upper crust--would be expected to have a magnetic anomaly, even if due only to induced magnetization. That it does not--there is no satellite anomaly, and even the aeromagnetic signature is modest in amplitude--may be due to a combination of factors:

-- there is a combination of normal and reversed remanence, the latter being of opposite polarity and acquired during a time period when the Earth's geomagnetic field was reversed. The adding of opposing magnetic effects serves to reduce the net total magnetization of the anomalous mafic (largely basaltic) seam, in terms of the external anomalous field produced. Geophysical modelling, to be presented in the next Section, supports this interpretation.

-- the CNARS main arm, from Kansas over 1000 km up to western Lake Superior, is oriented along the north-south azimuth of the satellite orbit track. It is thus less likely to show an anomaly than an east-west trending structure or boundary. This is because a narrow, along-track anomaly may be degraded in the data processing, by corrections for geomagnetic field removal, for base level adjustment due to external-field transient effects (i.e. taking out long-period transient variations, which can "look" like crustal anomalies on a track profile), or for adjustment to observed fields made for altitude differences of the orbit along a track or between different passes.

-- the feature is aligned with its long axis roughly along the azimuth of the present Earth's field. Thus the anomaly is less well defined (e.g. in terms of distribution of "free poles" on the causative source body) than if it were oriented east-west.

Geophysical modelling of CNARS/Midcontinent Geophysical Anomaly
-- magnetics and gravity

As described previously ("Geologic Setting", page 50-57), the major arm of the Central North American (paleo)Rift system has its greatest tectonic development, and largest gravity anomaly expression, in the central portion. This is in the state of Iowa, between the MGA extremities in Kansas to the southwest and northern Minnesota/Lake Superior to the north-northeast (see Fig. 24-26, and Fig. 39 and overlay). The basement rocks for this late-Precambrian aulacogen are covered by younger sediments, and have been penetrated by drilling only infrequently and not in a geologically-systematic way. The best evidence for the nature, extent, and properties of this huge crustal structure--a seam of intrusive and extrusive mafic rock in an otherwise granitoid upper crust--remains the interpretation of gravity and magnetic anomalies. Deep probing by reflection and refraction seismology is rare in the northern midcontinent, although detailed reflection work

- has been done in the past couple of years by the COCORP university consortium, on profiles in northern Minnesota (because of interest in the tectonic westward extension of the "Great Lakes Tectonic Zone") and northeast Kansas (for interest in the southern extension of the CNARS and the subparallel Namaha uplift)
- is being done commercially at present (for the first time) in Iowa, as "frontier" reconnaissance exploration for oil and gas potential associated with the MGA structure and related basin development.

The MGA's gravity anomaly map is shown in Fig. 27, the Iowa-region aeromagnetic (total-field) anomaly map in Fig. 28, and a schematic of its hypothesized development in the area in Fig. 29. The anomalous expression for the MGA arm, a deep-seated failed paleorift, is over 1000 km long and up to 150 km wide. The maximum gravity difference between the central uplifted basalt-dominated horst, and the flanking deep sedimentary basins, exceeds 160 milligals. The aeromagnetic expression for this major crustal inhomogeneity with highly anomalous magnetic properties compared to the adjacent "country rock", is a belt of elongate and linear anomalies with a well-defined trend but very modest amplitudes. Anomaly variations over the MGA, in the central portion in Iowa,

are generally less than several hundred nanoTeslas, whereas anomalies due to localized basement intrusions nearby can exceed a couple of thousand nanoTeslas.

Researchers here and at the Iowa Geological Survey have been doing gravity and magnetic modelling of the MGA feature, in order to understand the dimensions of the source structure, the composition and physical rock properties of it and its crustal environment, and its evolution as a paleorift (Anderson and Black, 1981). This work will also help interpret a magnetic expression seen (or not seen) at Magsat satellite altitude. A model for the feature's crustal evolution may also provide clues to the potential emplacement and distribution of mineral deposits or other resources.

The above authors modelled for over a dozen profiles, across the MGA feature in southwest Iowa (see Figure 41). Typical profiles are shown in Figures 42, 43, and 44. In this region, the maximum gravity anomaly difference is about 140 milligals, and the variation of aeromagnetic anomaly (scalar) field is about 600 nT. For a given profile, first a rough density model was created to approximate the observed gravity anomaly. This was then modified to give a calculated magnetic anomaly matching the observed magnetic anomaly. The model was then adjusted to have its gravity anomaly more closely fit the observed anomaly, and finally refined to match the magnetic anomaly even more closely. Using plausible lithologies and rock properties to fit the observed gravity and aeromagnetic fields, they suggest a central uplifted block of mafics (primarily basalt), about 45-60 km wide, extending from a top (i.e. of the crystalline basement) at a few hundred meters, down to a bottom that in places exceeds a depth of 7,000 meters. This horst is floored by normal-crustal granitic rock, and bounded laterally by high-angle faults. It is flanked by sedimentary troughs of Precambrian clastic rocks, which can have depths as great as 10,000 m. The central basaltic seam should have physical property contrasts to the adjacent sediments and granite. Typical ones used for modelling are listed on page 103.

ORIGINAL PAGE IS
OF POOR QUALITY

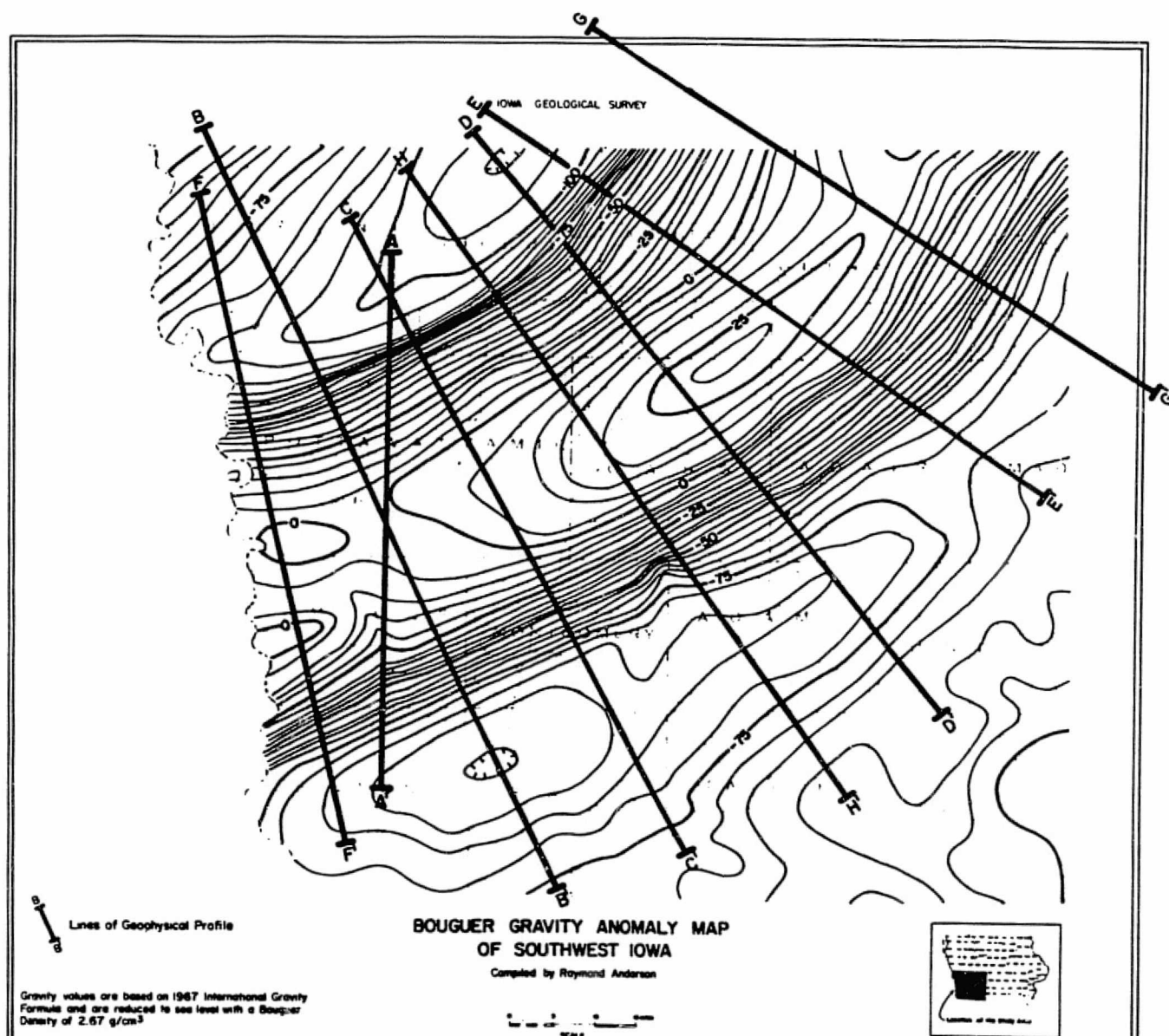


Figure 41. Location of profiles for geophysical modelling of CNARS/MGA paleorift structure, in southwest Iowa. On Bouguer gravity anomaly map; C.I. = 5 milligals.

ORIGINAL PAGE IS
OF POOR QUALITY

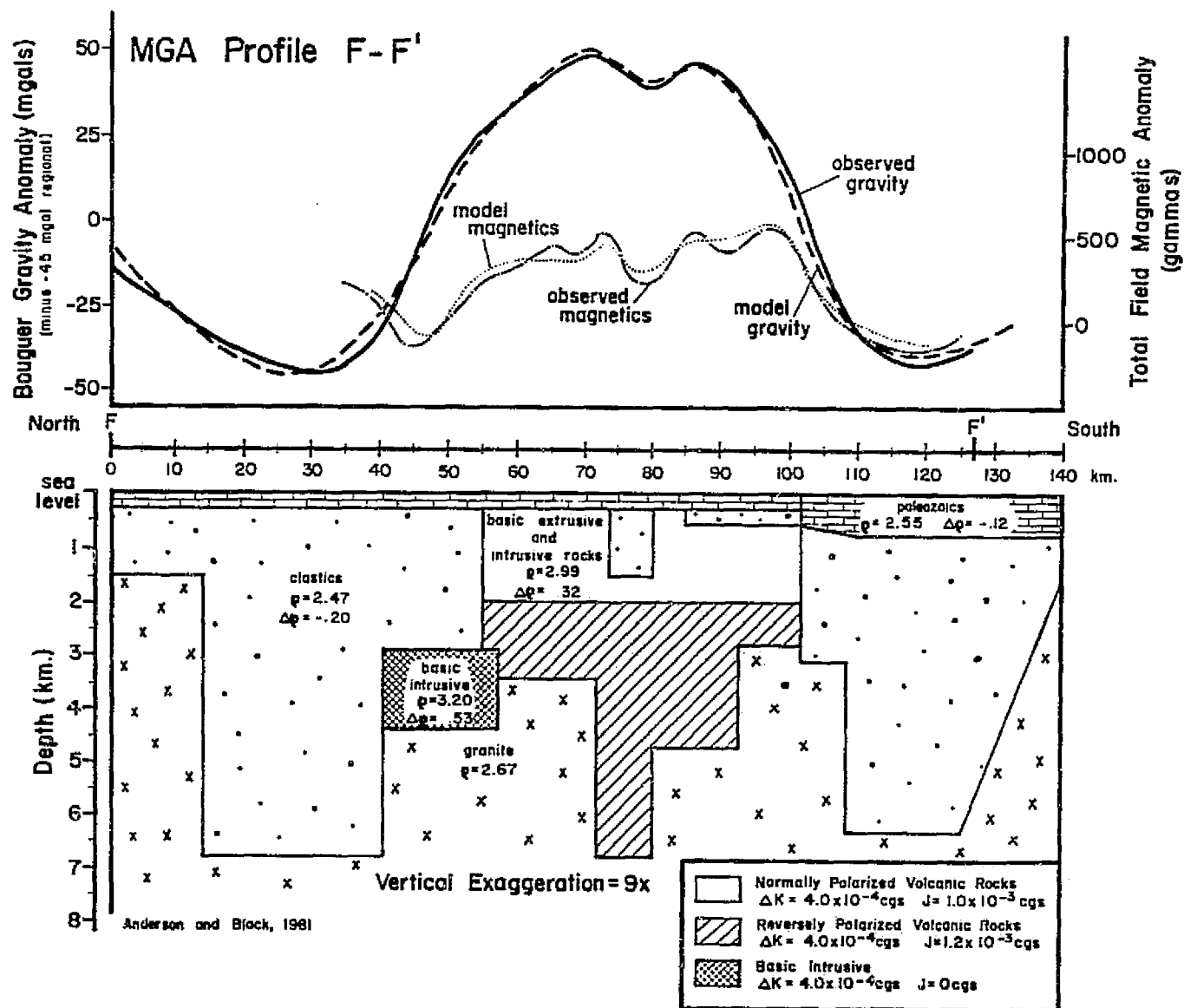


Figure 42. Gravity and magnetic modelling on profile F-F' across MGA structure (Anderson and Black, 1981). Note there is a vertical exaggeration of 9X.

ORIGINAL PAGE 18
OF POOR QUALITY

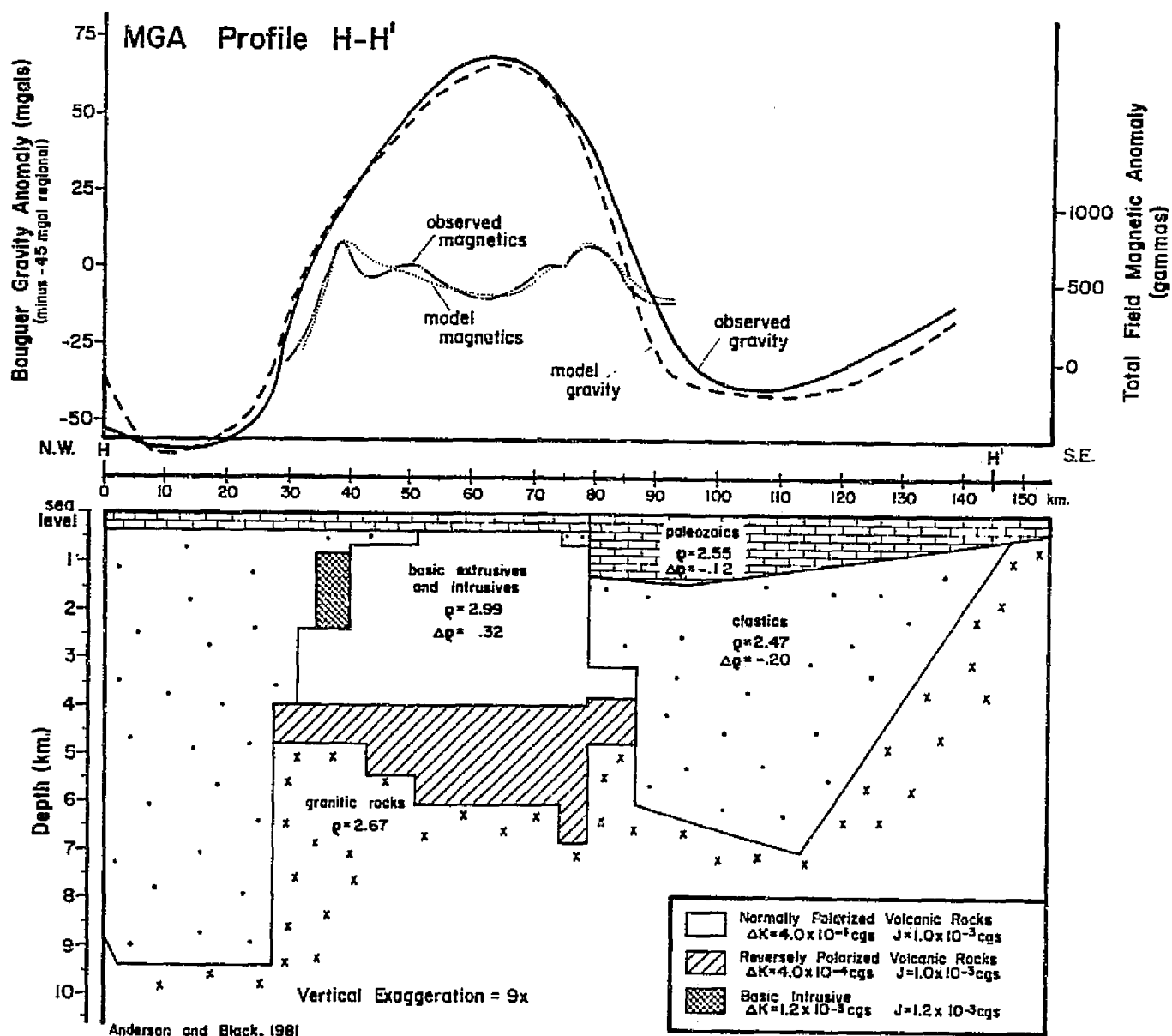


Figure 43. Gravity and magnetic modelling on profile H-H' across MGA structure (Anderson and Black, 1981).

ORIGINAL PAGE IS
OF POOR QUALITY

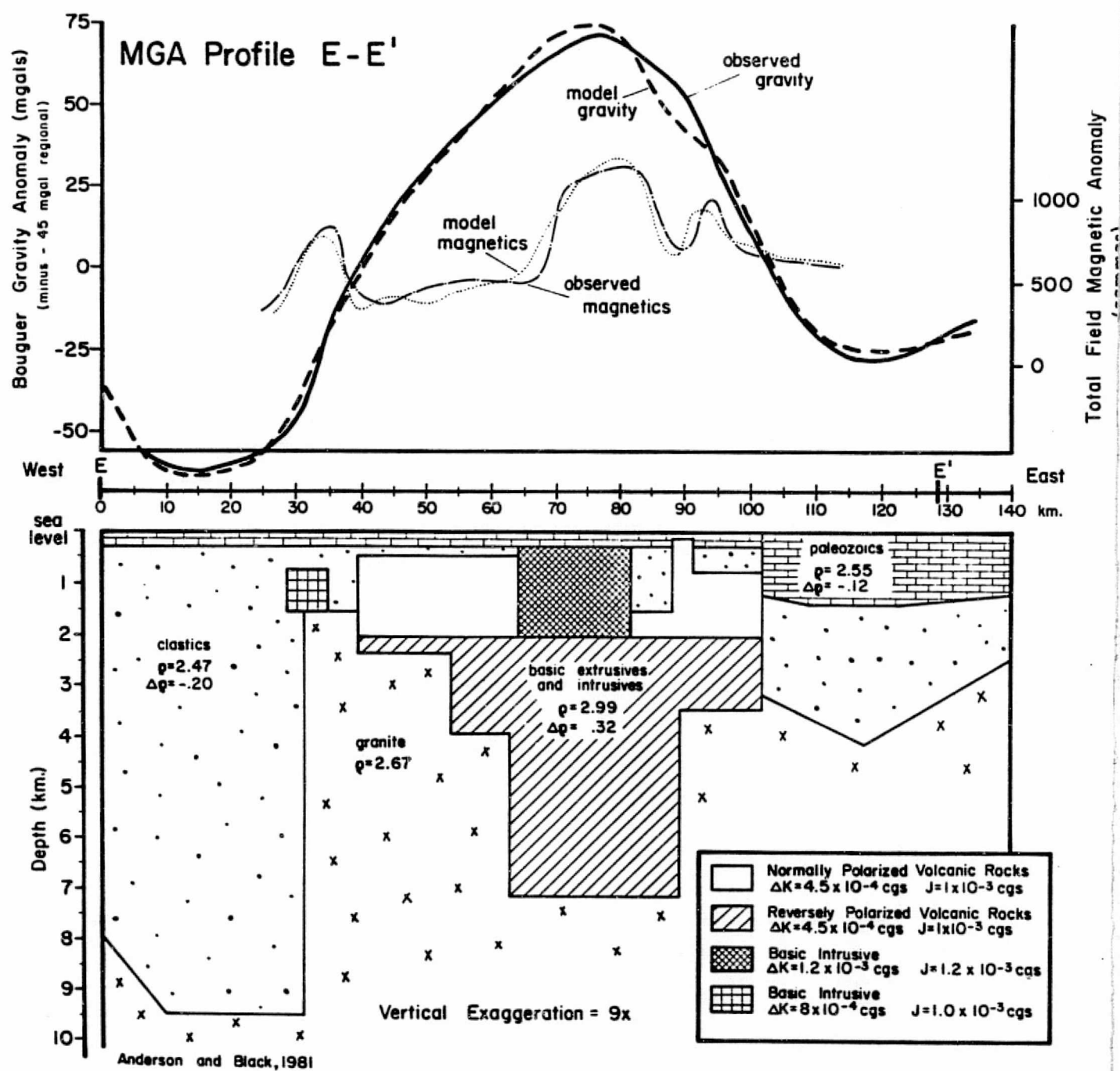


Figure 44. Gravity and magnetic modelling on profile E-E' across MGA structure (Anderson and Black, 1981).

Parameters for Modelling of CNARS/MGA in Iowa

	Structure component		
	<u>Central horst</u>	<u>Flanking Sediments</u>	<u>Surrounding Basement</u>
Rock type:	basalt-dominated	clastics	granite
Property:			
density (gm/cm ³)	2.99	2.47	2.67
susceptibility contrast (emu/cm ³)	4-4.5 x 10 ⁻⁴	--	--
remanence contrast (emu/cm ³)	1-1.2 x 10 ⁻³	--	--

The magnetic susceptibility alone of typical basaltic rock should result in a large magnetic anomaly for a body of this size. Since it does not, the implication is that either,

-- the mafic block is anomalously non-magnetic. This is an unlikely prospect for basalts here, especially since where analogous rocks are accessible or exposed at the surface (to the north), they have typical mafic magnetic properties

or

-- the rock "pile" has both normal* and reversed magnetic remanence, which combine to give a net reduced magnetization (induced, plus the normal and reversed remanence) for the crust as a whole.

The latter possibility is very plausible. This is because there is a major geomagnetic field transition from (older) reversed to (younger) normal in Keweenaw time and dated at about 1100 million years ago, as measured for rocks of the same age and geologic/tectonic origin exposed around western Lake Superior. Since the central block of mafic rocks is largely layered, with the oldest rock layers on the bottom, the presumption that it is the bottom portion of the block that has reversed-polarity remanence is a reasonable one. The emplacement of the MGA intrusives and extrusive lavas thus apparently "caught" a magnetic polarity

* "normal" polarity remanence does not imply greater normalcy, but rather that it represents and reflects the configuration of the geomagnetic field as present, i.e. with the "north" magnetic pole near the north geographic pole.

transition of the Earth's field.

The direction of remanence in the rock is introduced as appropriate for Keweenawan time. This is a declination (azimuth of the paleo-field) of 290° * (i.e. west-northwest presently), and paleoinclination of 40° . This information is obtained from lab study of CNARS rocks where exposed farther north, and the paleomagnetism thus says that in Keweenawan time, the U.S. northern midcontinent was located geographically closer to the equator, and was rotated (70°) clockwise, compared to now.

The rock fractions with normal and reversed remanence are assigned the identical value for susceptibility, since there is no reason to think that petrologic composition varies with changes in the terrestrial magnetic field. The relative contributions of the normally and reversely magnetized zones can be adjusted to give the net observed magnetic anomaly. This is done by changing the relative volumes of them in the central mafic horst. A further refinement to modelling that could be considered is that the remanent magnetization acquired when the field was reversed may be greater (of stronger intensity) than the remanence acquired when the field was of normal polarity. This is because paleointensity determinations for Keweenawan-age rocks from the western Lake Superior region (Pesonen and Halls, 1982) indicate that the Earth's field (there, at that time) was about 40% stronger when it was of reversed polarity, than when it was "normal". Because of the stronger remanence that would result, the relative volume fraction required of reversely-magnetized rocks would be reduced somewhat. The authors further note that, based on experimental study, in late Precambrian (Keweenawan) time the earth's field in general was about 40% stronger than it is at the present time.

A schematic diagram for the development of the MGA in the region of southwest Iowa was shown in Figure 29. The geologic setting has also already been described. It is important to understand the evolution of continental rifts, and ancient aulacogens, so that we can better understand tectonic regimes on continental cratons, plate tectonic processes in the past and any subsequent resurgent activation (such as seismic activity, and uplift or subsidence which has consequences for basin development), and relation to emplacement of mineral deposits or

* i.e. $N.70^{\circ}W.$

other resources.

The detailed modelling by Anderson and Black here clarifies several matters:

i) while the CNARS/Midcontinent Geophysical Anomaly in the northern Minnesota/Lake Superior region may have a central seam of fissure-fed successive flood basalts deposited along a subsiding trend (Green, 1983), the structure farther south (as in Iowa) was characterized during formation by major graben development with steep bounding faults. The axial rift valley progressively filled with successive volcanics and intrusions, perhaps brought up along the fault zones bounding the central graben block.

ii) the central block, now uplifted with reactivation to form a horst, is floored (at a depth of 3-7 km, in the model profiles of Figs. 42-44) by crustal granite. This is the crustal block that subsided with the rift-initiated graben development. This is in contrast to speculation that the central mafic seam extends all the way down to the middle or lower crust. If the latter were the case, the mass anomaly (due to the density contrast of the mafics/basalt compared to the upper-crustal granitoid rock) would give a gravity anomaly over the MGA much greater even than it is now.

iii) retaining reasonable petrologies (analogous to CNARS rocks where they are exposed farther north) and corresponding density and magnetic properties, one can explain the observed gravity anomaly by the structure proposed, and the observed modest magnetic anomaly by partitioning the central mafic block into zones of opposite remanence. This involves a lower, older zone of reversed remanent magnetization, and an upper younger zone of normal remanent magnetization. In support of this, there is a known polarity transition from reversed to normal paleofield (as reflected in remanent magnetizations) in rocks of Keweenaw age, 1100 million years old, in the region.

Resources potential

The U.S. midcontinent has some important economic resources, from the major oil and gas provinces of the Texas/Louisiana/Mississippi Gulf coast (both onshore and offshore) in the south, and substantial reserves in sedimentary basins farther north in Oklahoma and Kansas, to the mineral deposits of copper, zinc, lead, and iron ranging northwards from Missouri through Wisconsin to northern Minnesota and upper Michigan. The region has considerable potential for discovery of new resources, particularly of mineral deposits associated with the buried basement* rock. This is because much of the northern Midcontinent is covered by a veneer of glacial deposits from the most recent (Pleistocene) period of glaciation and, except for the craton exposed in northern Minnesota, Wisconsin, northern Michigan and farther north, the region's basement is overlain by a sequence of sedimentary rocks deposited on ancient marine platforms and in subsiding basins. This "overburden" hampers exploration and development of mineral deposits in, or immediately overlying, the crystalline basement rock.

The region, particularly the northern half where the basement is not too deeply buried, holds much promise for discovery of new resources for the future. This is because the basement rock is often analogous in age, geologic setting, tectonic evolution, and geophysical "texture" (aeromagnetic and gravity anomaly patterns of intrusives and structures), to terrane which is exposed or accessible and which is economically mineralized. For example, the Precambrian basement rock of Iowa, generally buried beneath a few hundred meters of sedimentary rock and which has seldom been drilled to any appreciable penetration, should be similar in many ways to the basement rocks of northern Minnesota and Wisconsin, or southern Missouri, which have exploitable mineral deposits.

Major factors hampering exploration programs have been,

-- the economics of deep mining of ores from buried basement rock. Hence the characterization of many of the potential natural resources here as being "resources for the future".

* The basement rock is the crystalline complex of igneous and metamorphic rocks that underlies sediments and sedimentary rock, and extends down to the crustal base (Moho). It is typically, and in the U.S. midcontinent, of Precambrian age, and represents part of an ancient continental craton (shield).

-- the past absence of sufficient encouragement from remote methods-- gravity, magnetics, seismic, satellite remote sensing--to pursue prospects in otherwise unprobed terrain. In the past decade there has been much new data gathered and areally compiled, by state geological surveys, federal agencies, and others, so that a regional picture of subsurface geology can be developed in considerable detail. It is the regional geophysical surveying that allows "mapping", or at least interpretation, of the buried geology. Examples of this would be the U.S. gravity and magnetic anomaly maps (U.S. Geological Survey/Soc. of Explor. Geophysicists, 1982), and the magnetic anomaly map for the central U.S. (Hildenbrand et al, 1983).

Interpretation of the long-wavelength Magsat anomaly map, in conjunction with the other more detailed geophysical and geological data sets, may aid in encouraging future exploration for resources. This might be particularly the case in reconnaissance exploration in frontier regions, that is where there has been little study to date or at depths that had not previously been considered. It is for such work that the satellite magnetic data could contribute in establishing the crustal framework for exploration strategy: the gross crustal structure and tectonic evolution, boundaries between terranes of different geologic character, possibly the thermal regime in the crust, and anomalous zones in the lower crust which may have consequences for mineralization in the upper crust or overlying sediments.

Two crustal tectonic features, and which can have major geophysical expression, are of special importance:

-- basins, formed by subsidence of crust locally and accompanying deposition of sedimentary rock. These can provide the source rocks, reservoir rocks, and traps for the accumulation of hydrocarbons (oil and gas).

-- major boundaries between crustal blocks. These could represent either compressional suture zones, where continental fragments (plates, or microplates) have collided and been welded together, or transverse/shear faults where crustal blocks have moved sideways against one another, or tensional (failed) rift zones where continental blocks have tried to separate. These boundaries are zones of major crustal weakness, can be identified as deep structural lineaments, and can be the locus of much

geologic "action". The latter can involve enrichment and emplacement processes that can in turn lead to economic mineralization. This geologic activity would include deformation (folding, faulting, mountain-building), intrusion and plutons at depth with upward injection of dikes and sills, perhaps extrusion of magma at the Earth's surface, circulation and invasion of hydrothermal fluids and minerals from depth up through the network of fractures, and reactivation later along the pre-existing zone of crustal weakness.

For example, the paleorifting that resulted in the development of the Mississippi Embayment might be causally related, thermally and structurally (via uplift and subsidence) to the lead-zinc deposits in the "Mississippi Valley" region (Arkansas, Missouri, up to Illinois). Also, there are many faults in the Duluth complex, a crescent-shaped intrusive system 200 km long on the northwest shore of Lake Superior, and which developed as part of the CNARS/MGA paleorifting. These may have helped control the later intrusion by hydrothermal fluids to deposit the copper/nickel sulphide orebodies at the base of the complex.

Continental rifts--with their tendency for tensional and thermal thinning of the crust, and doming or graben development--can be associated with the development of some sedimentary basins. This is because early rifting, failed rifting, and later reactivation can all affect the formation of basins by controlling subsidence, uplift, and the depositional/sedimentary/structural character of the sediment package being deposited. For example, regional subsidence or uplift can affect deposition versus erosion, affect cycles of marine transgression and regression, and introduce facies changes. Such changes in depositional environment are very important for developing hydrocarbon accumulations. Faults can also propagate up through younger sediments, and affect basinal structures, from reactivated faults in the older underlying Precambrian basement.

Thus for many aspects of upper-crustal geology,

"...the Precambrian basement calls the shots."

Anonymous
4th Internat. Conf. on Tectonics
Aug. 1981

It is in the interpretation of major structure, composition, and tectonic development of this crustal basement rock, that satellite magnetic anomaly data can hope to provide an assist.

Let us consider now in more detail the resource prospects for the study area--the central Midcontinent.

(a) Oil and gas

To date, the potential for hydrocarbon resources in the northern midcontinent has not been considered to be high. Significant, but still fairly modest, exceptions are the oil and gas found in localized basins in Kansas and around the periphery of the Michigan Basin in lower Michigan (see Figure 25). There have been, for example, no oil finds or producing wells in Iowa.

Although it is not widely known, due to the proprietary nature of oil exploration, there has arisen in the past year or two a serious interest in the oil and gas potential of the Iowa region of the midcontinent. This activity comes to the surprise of some, and to the disbelief of others. The interest is in the form of geophysical (seismic) reflection work, leasing of land, and plans for test drilling in the near future. While we are not involved in any of this exploration in what could be considered, geologically, to be a "frontier" area as regards prospects, the state Geological Survey does monitor the activity. Such exploration probably has its impetus from a combination of:

- thoughts, or hopes, that improved economics of oil and gas production will in the future allow exploitation of what might now be marginal reserves
- the desire for domestic and more secure sources of oil and gas
- interest in the geologic nature and development of the CNARS/Midcontinent Geophysical Anomaly and its associated structures. The latter would be particularly the sedimentary basin development along the flanks of the central horst, and on top of the horst block, and in the vicinity (e.g. the Forest City Basin, in southwest Iowa and northwest Missouri). The location of the MGA in the Iowa region is shown in Figure 26, and geophysically interpreted cross-sections showing the CNARS structure (horst and basins) are given in Figures 42-44. Note that the latter models have a vertical exaggeration of 9X.

The basins of greatest interest, but as of yet unknown prospects, are thus,

i) the Forest City Basin (Figure 26). This has over 1500 meters of Paleozoic sedimentary rocks. It is not clear if these sediments have been buried deeply enough to mature organic material to oil, or even if there was sufficient organic source material, or if the rocks (and oil) might be too old to have retained hydrocarbons to the present. If the organic material was present at depths not generally great enough to encounter temperatures suitable for maturing it to oil, a thermal pulse could have helped. Such a change in the thermal regime, perhaps associated with major deep intrusion or a paleorifting attempt, would raise the geothermal gradient and elevate isotherms for a period of time. Apart from the thermal rift tectonism of late-Precambrian time here, there is some speculation that there may have been Cretaceous-age intrusion of some older basement rock upward, and injection of kimberlites, at least into eastern Kansas. Such a thermal event, with associated hydrothermal fluids, might have provided sufficient localized heating to mature hydrocarbons.

ii) basins, structural or erosional in origin, on the top of the mafic central horst of the MGA. These would be relatively more accessible to drilling. Such basins are shown schematically in the hypothetical "model" of Figure 29, and the gravity- and magnetics-calculated cross-sections of Figures 42-44. The latter suggest that basins (on these three profiles) could have widths up to 15 km, and depth extents up to 1500 meters or so. These basins contain Precambrian clastic sediments. The rationale for the potential for "Precambrian" oil or gas would be that there is hydrocarbon-rich oil shale in Precambrian sediments in northern Michigan (e.g. in the White Pine copper mine, on the Keweenaw peninsula), and there may be the prospect for gas in these old rocks. The source for hydrocarbons along the central portion of the MGA might have been from algae and bacteria, in sediments in ponded depressions along the subsided rift zone in Precambrian time. A modern analogy might be the algae similarly located in lakes and ponds along the East Africa rift system today. Other factors to consider would be the thermal regime of the CNARS paleorift in late-Precambrian time, and subsequent geothermal history, to assist maturation of the shallower organic material to oil, and also whether appropriate trapping structures exist to retain oil or gas.

iii) basins, flanking the central horst. As modelled (as in Figs. 42-44) and by analogy to geologic sections exposed to the north in

Minnesota, these long downwarped troughs have widths up to 50 km, and depths from 5 to as much as 10 km. The sedimentary rocks are Precambrian clastics. These basins have been virtually unsurveyed seismically, and are untested by deep drilling. Speculations on their hydrocarbon content must again consider whether they are too old to have retained oil and gas, and whether their greater depth (especially for depths over 5000 m.) would result in the higher temperatures having "cooked" oil to gas completely.

(b) Mineral deposits and provinces

Figure 45 shows the location of known copper, zinc, and lead deposits and provinces in the central midcontinent (from Tooker et al, 1980). "Provinces" are areas where there are groups of economic deposits, and subeconomic occurrences, and are thus favorable search areas. If mineral provinces can be causally related to major structural or tectonic features, and the latter can be identified using remote geophysical methods (including satellite magnetic mapping as an aid), then the initial exploration process can be improved. For example, from observation of the distribution of mineral occurrences in the continental U.S., Tooker et al (1980) suggest that,

- "copper provinces seem to be closely identified with characteristic geologic environments and host rocks in the two main types of crustal plates on the (U.S.) map--accreted oceanic and island arc, and old continent."
- zinc provinces seem to be identified with old continental crustal rocks, especially uplifted regions where Precambrian rocks are exposed. The deposits are often localized in the sedimentary or other younger rocks covering or adjacent to the ancient crystalline basement rocks. "Stratabound zinc provinces, mostly of the Mississippi Valley type*", are spaced at intervals along two broad northeast-trending zones that seem to parallel axes of uplifted and locally exposed basement rocks." The most prominent zone lies in a band from Oklahoma/Arkansas to northern Illinois/Indiana; it

* i.e. in carbonate sedimentary rocks along the basin platform margins adjoining areas of uplift

ORIGINAL PAGE IS
OF POOR QUALITY

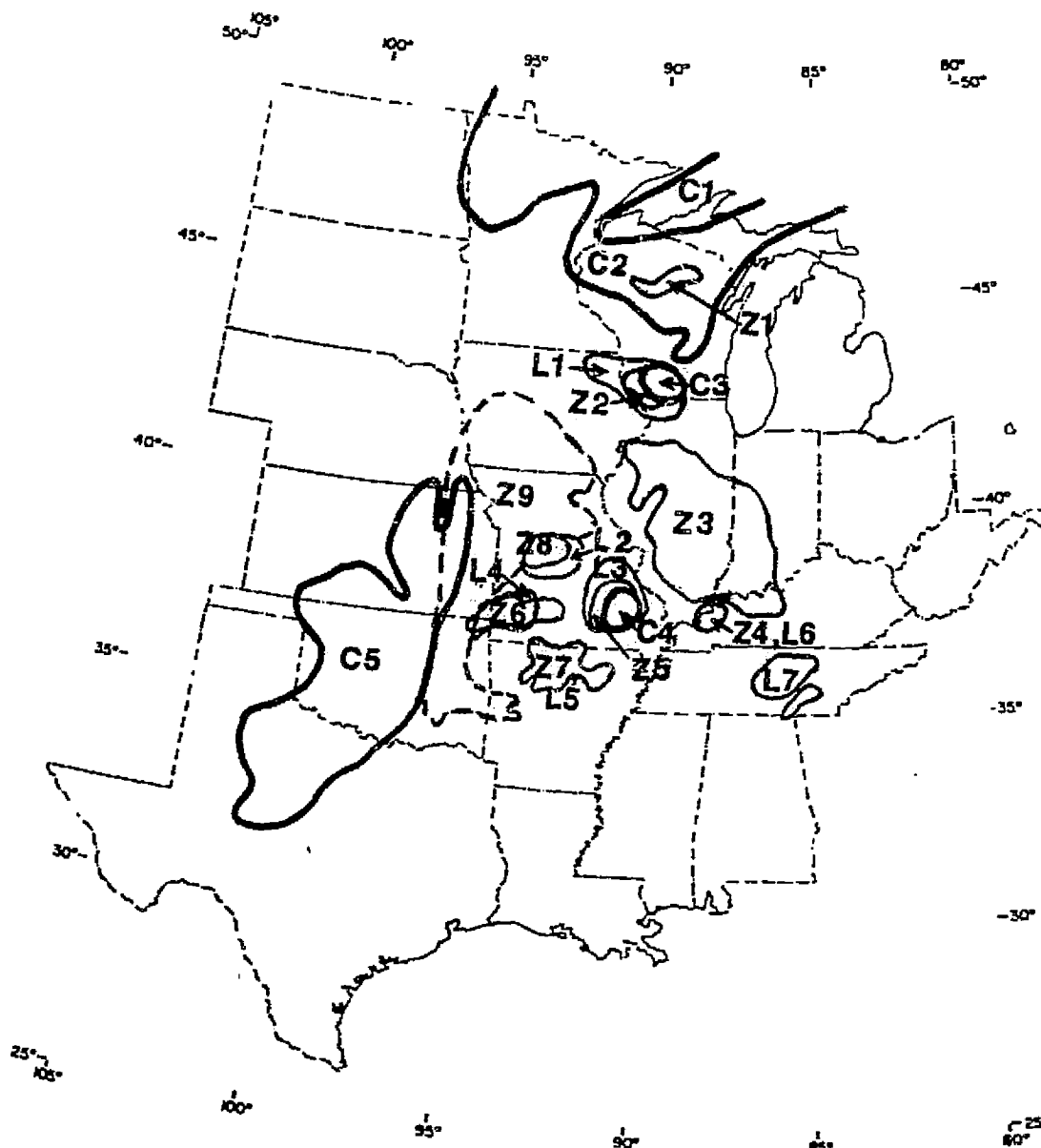


Figure 45. Location of known metallic-mineral deposits and provinces in the central midcontinent, for copper ("C"), zinc ("Z"), and lead ("L"). Numbers are keyed to listing in text here. Scale: 5° of latitude is about 550 km. (adapted from Tooker et al, 1980)

lies roughly between provinces Z3 and Z9 on Figure 45, and is closely associated with faulted uplifted basement rocks.

-- lead provinces are found mostly in old continental crust (rather than accreted oceanic and island-arc terranes), typically in Phanerozoic sedimentary rocks over Precambrian basement rocks and especially if the latter have been uplifted.

The mineral resource localities shown in Figure 45 are listed below:

Description of mineral deposits and provinces
in the U. S. Midcontinent

<u>Number</u>	<u>Location</u>	<u>Type of deposit</u>
..... Copper		
C1	northern Michigan (in late-Precambrian terrane)	stratabound in (volcanogenic or metasedimentary) sedimentary rock; disseminated deposits in conglomerate & basaltic rocks - has one active copper mine, plus other mines presently inactive, plus occurrences of unproven value
C2	Minnesota, Wisconsin, n. Michigan (in mostly Precambrian terrane)	stratiform in volcanogenic sediments, and maybe greenstones; massive sulphide deposits - southeast lobe has occurrences of unproven value (there are disseminations of copper and nickel in mafic rocks at the base of the Duluth Complex); region may have "large but unevaluated" resources of copper (Tooker et al, 1980)
C3	s. Wisconsin, n. Illinois ("Upper Mississippi Valley lead district")	hydrothermal, in sedimentary rock; vein or replacement deposits - occurrences of unproven value
C4	southeast Missouri ("Lead district")	hydrothermal, in sedimentary rock; includes deposits in early-Paleozoic carbonate reef rocks which are peripheral to exposed late-Precambrian basement rock - has one active deposit (copper is a byproduct) plus other occurrences of unproven value
C5	Kansas, Oklahoma, Texas (in Permian sedimentary basins)	stratabound in sedimentary rock; disseminated deposits - occurrences of unproven value

<u>Number</u>	<u>Location</u>	<u>Type of deposit</u>
---------------	-----------------	------------------------

.....Zinc.....

Most economic concentrations are as zinc sulphide or oxide, from ores of zinc, zinc/lead, or copper/zinc/lead. The zinc is believed to be concentrated by residual solutions from magmatic processes at depth, or by brines from basin sediments. "The (zinc) provinces in the Central Plains already have provided large production, and retain a high potential for extensive future production...A potentially large but as yet unevaluated future resource (here) may be the zinc sulphides that fill fractures in coal beds in the Illinois and Iowa/Kansas/Missouri (e.g. Forest City Basin) coal basins." The prominent zinc province that trends northeast, mentioned previously, lies between coal basins (localities Z3 and Z9 in Figure 45).

- | | | |
|----|--|---|
| Z1 | northern Wisconsin | stratabound; massive sulphides in volcano-genic rocks |
| Z2 | Wisconsin/Illinois/Iowa ("Upper Mississippi Valley district") | stratabound replacement and pore filling in platform carbonates and breccia |
| | - includes an active zinc mine | |
| Z3 | Illinois (in coal basin) | stratabound or stratiform; in sedimentary rocks |
| | - no known occurrences | |
| Z4 | Illinois/Kentucky ("Hicks dome" district) | vein or pore filling, from hydrothermal solutions |
| | - at uplifted domal structure at the north end of the Mississippi embayment | |
| Z5 | Missouri (southeast lead district/Viburnum trend) | same as for Z2 |
| | - a major producing area; has several active mines with zinc as the primary or coproduct metal | |
| Z6 | Kansas/Okla./Missouri ("Tri-State district") | stratabound replacement in carbonates, or supergene (oxidized) enrichment, or residual deposits |
| | - has formerly-active zinc mines | |
| Z7 | northern Arkansas | same as for Z2 |
| Z8 | Missouri ("central lead district") | same as for Z2 |
| Z9 | Iowa/Missouri/Kansas/Oklahoma | stratabound, disseminated in sedimentary basin rocks |
| | - in coal basin; unassessed localities | |

<u>Number</u>	<u>Location</u>	<u>Type of deposit</u>
---------------	-----------------	------------------------

.....Lead.....

Most of the U.S. production of lead comes from Mississippi Valley-type deposits in the Central Plains region (the Ozark uplift in southeast Missouri, see Fig. 25; and through Missouri). These are stratiform deposits in vein fillings and pores in breccia, and as bedded replacement in Paleozoic platform carbonates that lie along the margins of uplifted regions.

- | | | |
|----|--|--|
| L1 | Wisconsin/Iowa/Illinois
(upper Mississippi
Valley) | fissure veins and replacement in sedimentary rocks, generally related to intrusive bodies; or stratiform or stratabound disseminations and pore fillings formed diagenetically in carbonates |
| | - includes an active mine with lead as a byproduct | |
| L2 | Missouri
(central district) | fissure veins and replacements in sedimentary rocks |
| L3 | southeast Missouri
(Viburnum trend) | stratiform or stratabound disseminations and pore fillings in carbonates |
| | - includes several active mines and inactive ones; is the largest lead-mining producing district in the U.S. | |
| L4 | SE Kansas/SW Missouri/
NE Oklahoma
(Tri-State district) | same as for L1 |
| | - includes an inactive mine | |
| L5 | northern Arkansas | same as for L2 |
| L6 | s. Illinois/Kentucky
(Hicks dome) | same as for L2 |
| L7 | central Tennessee
(Nashville dome) | same as for L1 |

It might be noted that the most magnetically-anomalous region of the mafic lower-crustal layer in the central U.S. is a north-south elongate zone that underlies much of the state of Missouri (see Figure 46 here, an excerpt from Figure 38). It has an interpreted magnetization intensity of 5-6 amp/m, compared to the U.S. continent lower-crustal average of 3.5 amp/m and a typical range of values of 2.5-4.0 amp/m in the central U.S. as a whole. These magnetization values are calculated (Schnetzler and Allenby, 1983) by considering the magnetic moment strength

ORIGINAL PAGE IS
OF POOR QUALITY

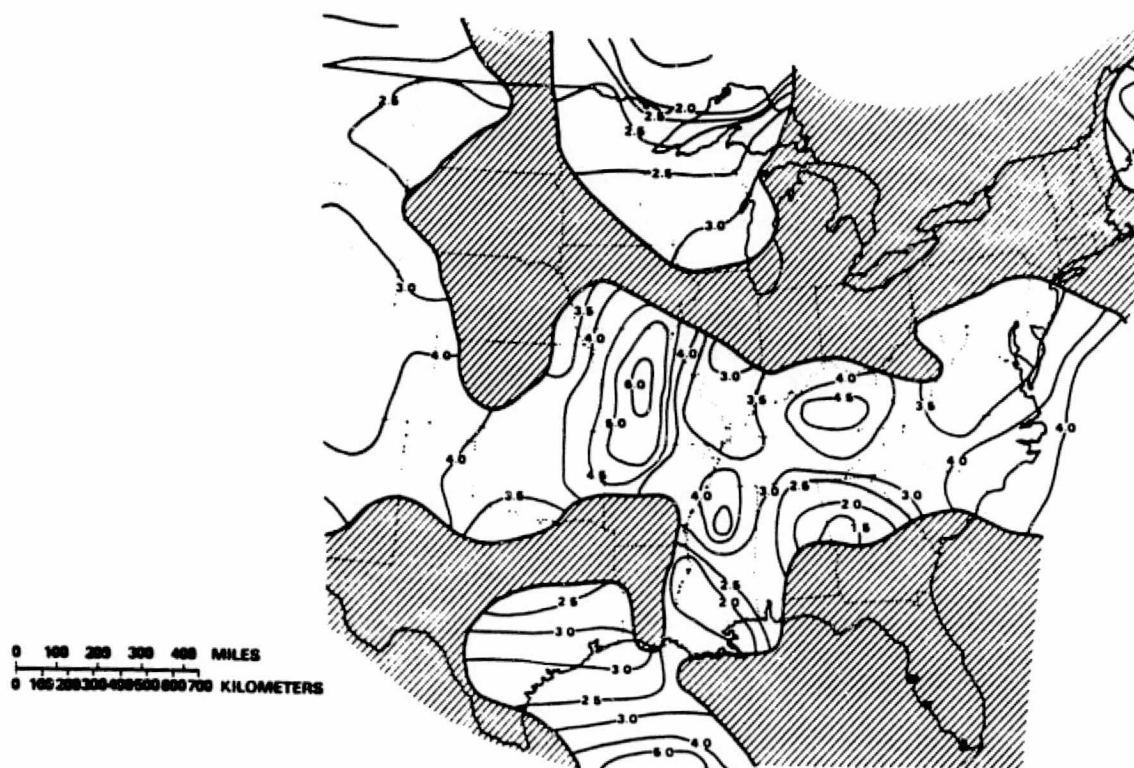


Figure 46. Magnetization intensity in the lower-crustal mafic layer, for central midcontinent (excerpt from Figure 38; Schnetzler and Allenby, 1983). Units are amp/m.

of the source crust (as obtained by inversion of satellite magnetic anomaly data) and the thickness of the lower-crustal layer. The latter is assumed to be the source of the long-wavelength satellite anomalies. The resulting map shows the lateral variation in magnetization of the lower crust. The central-Missouri value in excess of 6 amp/m is about as high (i.e. as magnetically intense) as any lower-crustal rock that has yet been modelled for the earth (see Table of values, page 80 here). This major anomalously-magnetic zone is perhaps related to an ultrabasic intrusive complex or to a continental fragment of particularly favorable composition or metamorphic grade. In any event, it apparently underlies the region of the central midcontinent which has the greatest number,

variety, and richness of metallic mineral deposits (see Figure 45). This is central and southern Missouri, and extending slightly south into Arkansas. This area includes the following economic mineral deposits and provinces:

- Zinc Z5-Z8: includes the "Lead district/Viburnum trend", a major zinc-producing area, in the southeast, and the "Tri-State district" in the southwest, and the "Central district"
- Lead L2-L4: includes the Viburnum trend (the largest lead-producing district in the U.S.), and Tri-State district, and Central district
- Copper C4: in the Lead district, and has one of the two copper deposits being mined in the midcontinent at present

One can, at this stage, only speculate on a possible genetic relationship between the deep-seated highly-magnetic mafic rock, as identified by inversion of satellite magnetic data, and the relative abundance of metallic ore deposit localities and occurrences found in the overlying crustal rocks in this region.

In addition to the above metallic mineral deposits, there are also economic iron-ore resources in the region (Hutchison, 1983). These include the sedimentary iron formations (e.g. Biwabik-Gunflint) in northern Minnesota and upper Michigan, and the Kiruna-type massive iron ore in southeast Missouri. The latter is at Pea Ridge, about 40 km north of the Viburnum trend's lead deposits. The iron ore, primarily magnetite and of Precambrian age, is believed to be intrusive and genetically related to magmatic activity from below. The rhyolitic St. Francois Mountain area at Pea Ridge has ten known iron occurrences and three major ore deposits.

MAGNETIC PROPERTIES FOR MAGNETIC MODELLING

Magnetic modelling of crustal bodies to match observed anomalies, or inversion of anomalies to their causative sources, will be aided by knowledge of what plausible physical properties of rock types would be.

The influence of crustal structural and petrologic factors has been discussed (pages 78-85). These include:

- i) the thickness of the "magnetic lithosphere" that is magnetizable
- ii) the relative proportions of the crust that are (sialic) upper-crust, and (more mafic) lower-crust
- iii) relative contributions of induced and remanent components of magnetization
- iv) relative metamorphic grade of the crystalline basement rocks
- v) lateral geologic inhomogeneity of crustal blocks or terranes (having, for example, different thicknesses, composition, age, structural texture, physical and magnetic properties).

In addition to these "bulk" characteristics, however, we should consider the magnetic mineralogy and associated magnetic properties of the rock types in the crust and upper mantle. This is because it is the magnetic minerals--and their relative abundance, composition of impurities, chemical conditions (e.g. oxidizing, reducing, hydrating) during initial crystallization or later metamorphism, thermal history and current temperature, grain size--that determine the magnetization. For example, it is the Curie temperature (dependent on chemical composition of the magnetic mineral grains) which determines, in combination with the local geothermal gradient, the magnetic "bottom" of crustal sources.

Magnetic mineralogy

The most important minerals for rock magnetism are in the compositional range bounded by the solid-solution series, ulvospinel-magnetite (titanomagnetite series), Fe_2TiO_4 - Fe_3O_4 , and ilmenite-hematite (ilmeno-hematite series), FeTiO_3 - Fe_2O_3 . This is shown in Figure 47. By far the dominant magnetic mineral in importance for magnetization is magnetite, Fe_3O_4 . The magnetic mineralogy, and associated magnetic and physical properties, are given on the pages to follow (excerpt from Carmichael, 1982; pages 246-255).

ORIGINAL PAGE IS
OF POOR QUALITY

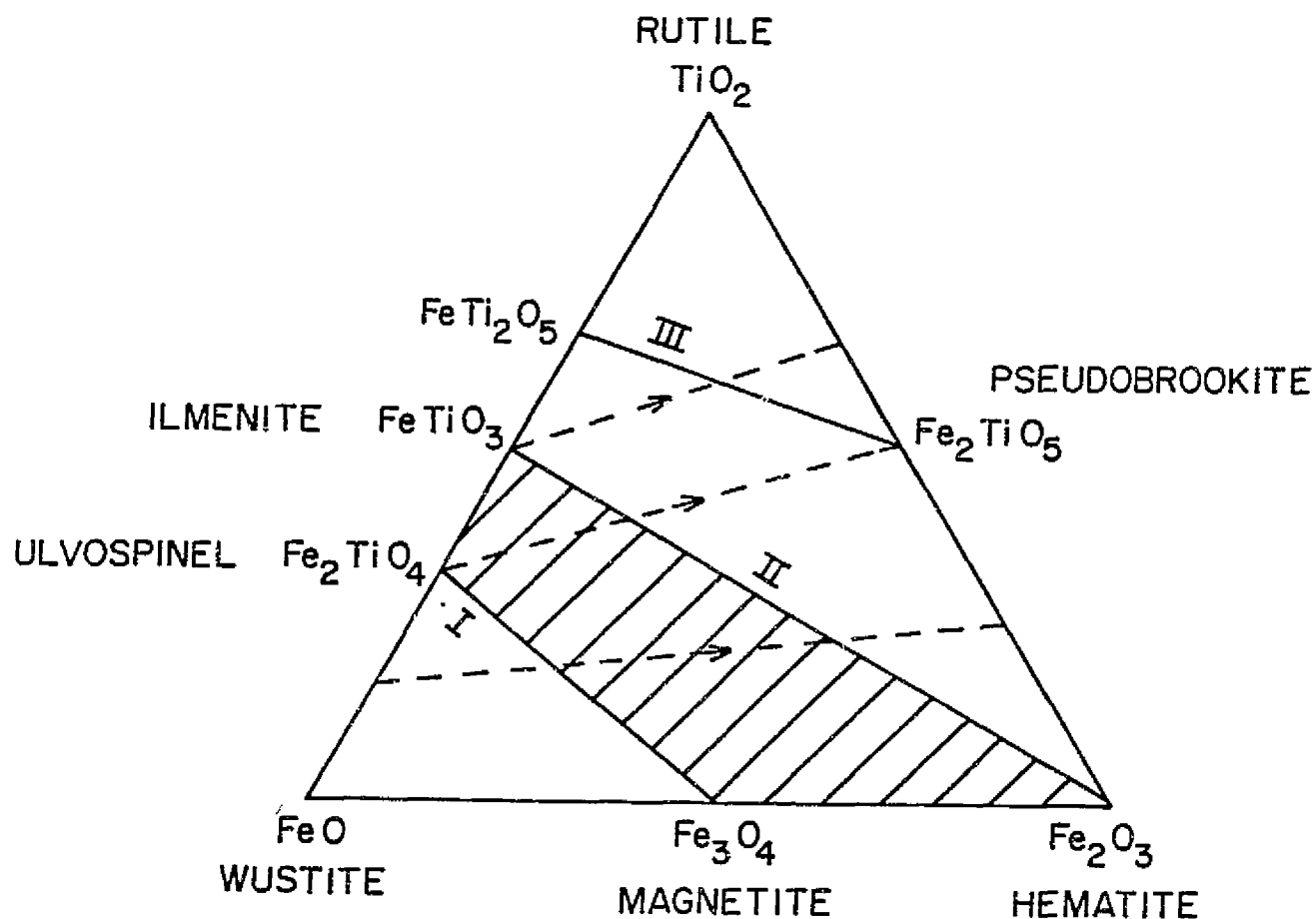


Figure 47. Magnetic mineral compositions in ternary diagram $\text{FeO-TiO}_2\text{-Fe}_2\text{O}_3$. Solid-solution series "I" is titanomagnetite, "II" is ilmeno-hematite. (from Carmichael, 1982)

Chapter 2

MAGNETIC PROPERTIES OF MINERALS AND ROCKS

Robert S. Carmichael

TABLE OF CONTENTS

Introduction	230
Notation and Units (Table 1)	231
Magnetization: Types and Parameters	231
Types of Intrinsic Magnetism	231
Types of Remanent Magnetization	233
Terms and Parameters (Hysteresis, Shape Effect) (Table 2)	234
Magnetic Domains (Table 3)	237
Effect of Grain Size (Tables 4 to 5)	240
Magnetocrystalline Anisotropy (Table 6)	240
Magnetostriction Anisotropy	244
Magnetic Mineralogy, Crystalline and Magnetic Properties	246
Important Minerals in Rock Magnetism (Iron Oxides, Iron Oxyhydroxides, Sulfides, Others)	246
Magnetic Properties	256
Saturation Magnetization, Curie/Néel Temperatures, Cell Dimensions (Tables 7 to 8)	256
Coercive Force (Tables 9 to 10)	262
Magnetic Susceptibility (Tables 11 to 18)	262
Permeability (Table 19)	281
Effects of Depth, Temperature, and Pressure (Tables 20 to 22)	281
References	285

119 A

MAGNETIC MINERALOGY, CRYSTALLINE AND MAGNETIC PROPERTIES

The magnetization of rocks is retained in certain magnetic minerals. These minerals and their physicochemical state control the intensity and stability over time of the remanent and induced magnetization. Proper geological interpretation, as for magnetic prospecting or paleomagnetism, of the magnetic character of rock samples depends on knowledge of the mineralogic, structural, magnetic, and mechanical properties of the minerals present.

Representative values for important properties are given here. The values are "typical". There is sometimes considerable discrepancy between published values; this is often due to the differing conditions and composition of the "natural" minerals and rocks studied.

Important Minerals in Rock Magnetism

The major minerals having magnetization, or being of interest in studies of magnetic mineralogy are

Iron oxides

titanomagnetite series:	ulvospinel-magnetite $x\text{Fe}_2\text{TiO}_4 \cdot (1-x)\text{Fe}_3\text{O}_4$
ilmenohematite series:	ilmenite-hematite $y\text{FeTiO}_3 \cdot (1-y)\text{Fe}_2\text{O}_3$
maghemite	$\gamma\text{Fe}_2\text{O}_3$
martite	$\alpha\text{Fe}_2\text{O}_3$
goethite	αFeOOH (the most common of the natural hydrous ferric oxides, i.e., "limonite", $\text{Fe}_2\text{O}_3 \cdot \text{H}_2\text{O}$)
lepidocrocite	γFeOOH
akaganeite	βFeOOH

Sulfides

pyrrhotite series:	troilite-pyrrhotite $y\text{FeS} \cdot (1-y)\text{Fe}_{1-x}\text{S}$
pyrite	FeS_2
marcasite	FeS_2
mackinawite	FeS

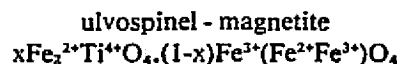
Carbonates

siderite	FeCO_3
magnesite	MgCO_3

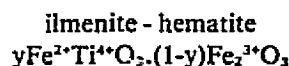
Iron Oxides

The most important and common rock-forming magnetic minerals for the study of rock magnetism and paleomagnetism are the iron oxides. They can be represented in the ternary diagram $\text{FeO}-\text{TiO}_2-\text{Fe}_2\text{O}_3$ shown in Figure 9. There are three main solid solution series:

1. Titanomagnetite series — cubic structure (inverse spinel)



2. Ilmenohematite series — hexagonal/rhombohedral structure



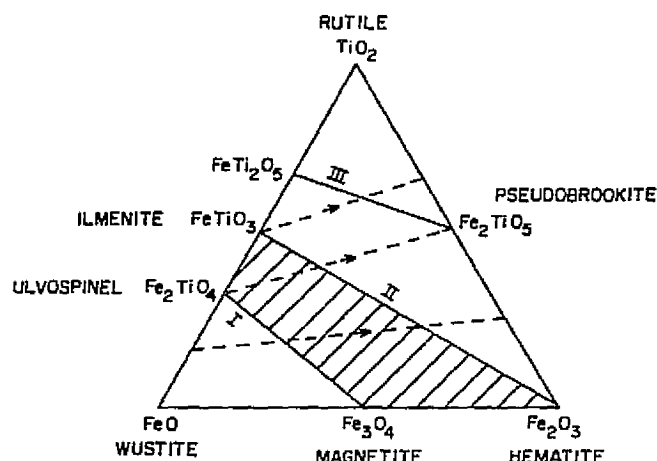
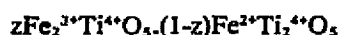


FIGURE 9. Compositions in ternary diagram FeO-TiO₂-Fe₂O₃. Solid-solution series are I — titanomagnetite, II — ilmenohematite, III — pseudobrookite. Dotted lines represent direction of oxidation.

3. Pseudobrookite series — orthorhombic structure



Possible impurity phases are MnO, MgO, Al₂O₃, and V₂O₃. The solid solution region of greatest interest in nature is shaded in Figure 9. The dotted lines are lines of constant Fe:Ti ratio and represent trend of oxidation/reduction. The oxidation increases to the right.

TiO₂ has three polymorphs. It is called rutile with a tetragonal structure (*c* axis = 0.6 Å) or anatase if tetragonal (*c* axis = 1.8 Å), and brookite if orthorhombic.

The diagram is drawn on the basis of molecular ratios. Thus,

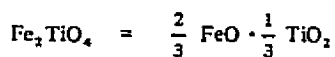
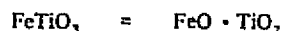


Figure 10 shows crystallographic structure and type of magnetism in the ternary diagram. In the ilmenohematite series, the magnetism varies with the composition as

$y \approx 1$	antiferromagnetic	(Fe and Ti both occupying all cation layers equally)
0.45 y 0.95	Ferrimagnetic	(ordered state of Fe and Ti, with Ti ions occupying every second cation layer perpendicular to the "c" axis)
0 y 0.45	Antiferromagnetic	(parasitic (spin-canted) antiferromagnetism; Fe and Ti occupying all cation layers, i.e., disordered state)

For $0.45 < y < 0.60$, synthetic specimens show self-reversal of magnetization.

Summarized in Figure 11 are some magnetic properties of the minerals. The Curie temperatures for the end-members of the series are shown in degrees centigrade. They vary uniformly from one end-member to the other. The increase in lattice parameter "a" is shown by arrows, likewise for saturation magnetization J_s , and the constants K for magnetocrystalline anisotropy and λ for magnetostriction. An auxiliary series is magnetite — hausmannite, $(1-x)\text{Fe}_3\text{O}_4 \cdot x\text{Mn}_3\text{O}_4$. For $0 \leq x < 0.6$, it is cubic structure. For $0.6 < x \leq 1$ it is tetragonal.

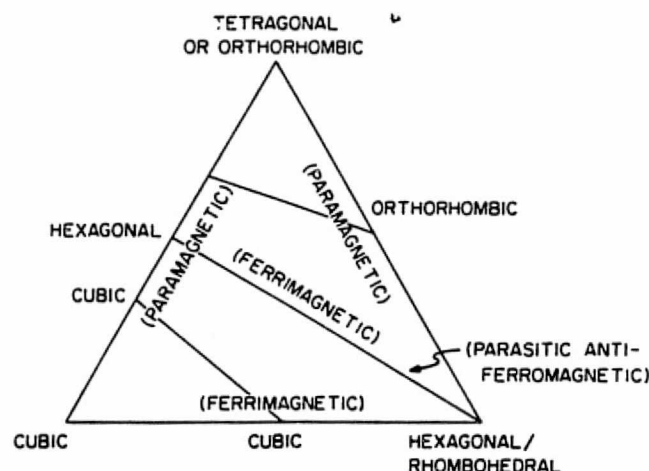


FIGURE 10. Structure and magnetism (at room temperature) in ternary diagram.

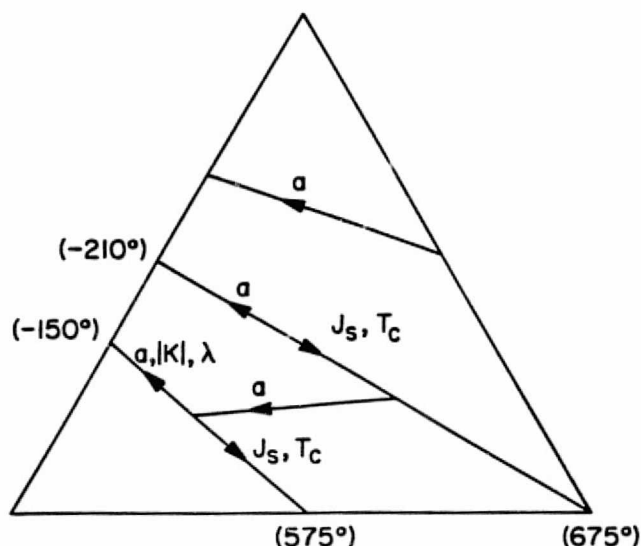


FIGURE 11. Magnetic properties in the ternary diagram. Curie temperatures in °C, "a" is cell dimension. Arrows indicate direction of increasing parameters.

The relationships between the main iron oxides are shown in Figure 12. The temperatures given are approximate. Values vary widely in the literature, depending on the sample condition and experimental conditions such as ambient atmosphere (air, vacuum, etc.). The structural conversion from maghemite to hematite is pressure-dependent. The goethite to hematite conversion could occur during consolidation of sediments, as $2\text{FeOOH} \rightarrow \text{Fe}_2\text{O}_3 + \text{H}_2\text{O}$. The magnetite to hematite oxidation could occur during initial cooling of igneous rock, at temperatures of about 600 to 1000°C. The magnetite to maghemite conversion could occur as low-temperature oxidation, as in late cooling or weathering.

The conditions for precipitation of different iron minerals are shown in Figure 13. The stability fields are outlined by the parameters Eh (volts) representing oxidizing

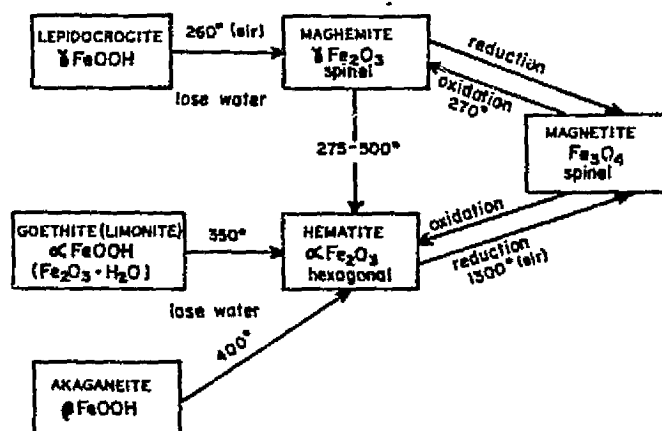


FIGURE 12. Conversion of iron-oxide magnetic minerals. Temperatures are approximate.

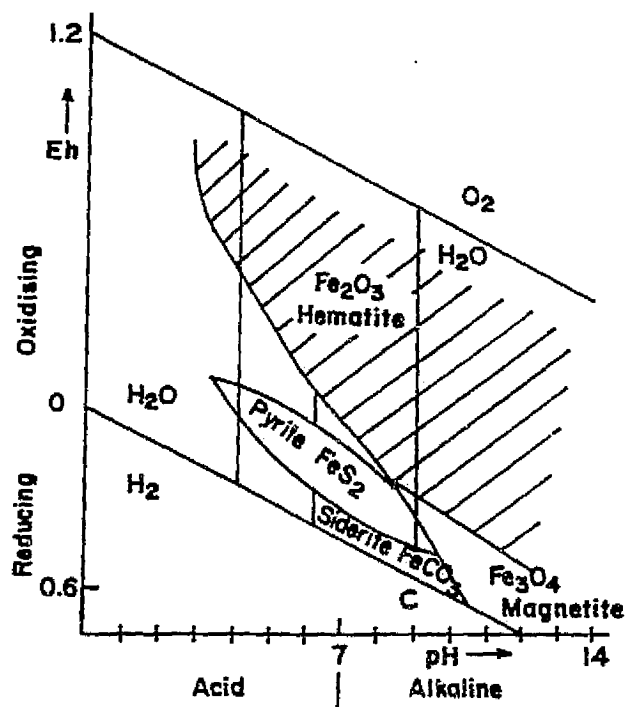


FIGURE 13. Conditions for precipitation of different iron minerals. (From Gass, I., et al., *Understanding the Earth*, MIT Press, Cambridge, MA, 1971, 179. Article by Watson, E. K.)

potential, and pH (concentration of H ions) representing acidity/alkalinity. The stability fields also depend on the concentration of components (e.g., Fe) in solution. ABCD is the range of naturally occurring solutions. The upper hatched area is the stability field of $\alpha\text{-Fe}_2\text{O}_3$.

The main minerals will now be described briefly. These oxides and oxyhydrates can be described in terms of stacked "almost-close-packed" layers of oxygen atoms with iron atoms behaving as interstitials. These irons have an atomic radius such that they

will not quite fit into the available sites of the oxygen lattice without distorting it. The distances between the oxygen planes in all the structures are about the same, ranging from 2.3 to 2.5 Å. The stacking sequences are characteristic of close-packed lattices, i.e., either the -ab-ab-ab- (hexagonal close packed) type, or the -abc-abc- (face centered cubic) type.

In the following, Z = number of formula units per unit cell, T_k = temperature of magnetocrystalline transition, T_c = Curie temperature, T_N = Neel temperature, E = Young's modulus of elasticity, and G = shear modulus of elasticity (modulus of rigidity).

Values are at room temperature unless otherwise noted.

Magnetite

1. Chemical formula: Fe_3O_4 ; $Z = 8$; percent by weight: Fe^{2+} (24.1), Fe^{3+} (48.3), O^{2-} (27.6).
2. Structure: cubic, spinel of inverse type (see Figure 14). Stacking of hexagonal close packed oxygen planes with an -abc-abc- sequence along the $\langle 111 \rangle$ direction. The general spinel structure is $\text{A}^2\text{B}_2\text{O}_4$, where A occupies a tetrahedral site and B octahedral sites. In the unit cell, there are 32 oxygens, 64 available A sites, and 32 available B sites. The "normal" spinel has 8 A's in tetrahedral sites and 16 B's in octahedral sites. The "inverse" spinel has 8 B's in tetrahedral sites, and 8 A's and 8 B's in octahedral sites. Cations occupy layers between two adjacent oxygen planes; successive layers have cations either in the octahedral (B) sites between individual oxygens, or one third in the octahedral and two thirds in the tetrahedral sites. The inverse spinel arrangement for magnetite is $\text{Fe}^{3+}(\text{Fe}^{2+}\text{Fe}^{3+})\text{O}_4$. The occupied tetrahedral sites form a diamond-type lattice. The octahedral sites have sixfold coordination, and the tetrahedral fourfold. The oxygen atoms form a face-centered-cubic lattice. The structure converts from inverse spinel to orthorhombic below about -155°C . The transition is abrupt for synthetic magnetite crystals, but can be spread over about 10° for natural crystals. The presence of impurities lowers the transition temperature. At high pressures (about 225 to 240 kbar), Fe_3O_4 undergoes a phase transition to a monoclinic phase with density about 6.4 gm/cm^3 . Cell dimensions (cubic phase): $a = 8.394 \text{ Å}$; distance between $\{111\}$ oxygen planes $\sim 2.9 \text{ Å}$; distance between Fe and O, octahedral site — 2.06 Å , tetrahedral site — 1.87 Å ; angle between O-Fe-O, octahedral site — $88.1^\circ, 90^\circ, 91.9^\circ$, tetrahedral site — 109.5° .
3. Mineral characteristics: crystals are generally octahedral form $\{111\}$, but may occur as cubic $\{100\}$ or dodecahedral $\{110\}$; twinning and parting on $\{111\}$; hardness about 6 on Moh's scale; density = 5.18 gm/cm^3 .
4. Magnetic properties: ferrimagnetic at room temperature; saturation magnetization $J_s \sim 98 \text{ emu/gm}$ (at 0°K); $\sim 92 \text{ emu/gm}$ (at room temperature) = 480 emu/cm^3 ; critical single-domain size about $0.1\text{--}1 \text{ }\mu\text{m}$; magnetic anisotropy — magnetocrystalline transition at $T_k = -140^\circ\text{C}$;

$$\begin{array}{ll}
 T_k < T < T_c & \text{-- easy axis } \langle 111 \rangle \left. \begin{array}{l} \text{hard axis } \langle 100 \rangle \\ \text{hard axis } \langle 111 \rangle \end{array} \right\} K_1 \text{ negative} \\
 -155^\circ < T < T_k & \text{-- easy axis } \langle 100 \rangle \left. \begin{array}{l} \text{hard axis } \langle 100 \rangle \\ \text{hard axis } \langle 111 \rangle \end{array} \right\} K_1 \text{ positive} \\
 T < -155^\circ & \text{-- easy axis orthorhombic "c" axis} \\
 K_1 & \sim -1.35 \times 10^6 \text{ ergs/cm}^3 \\
 K_2 & \sim -0.48 \times 10^6 \text{ ergs/cm}^3
 \end{array}$$

T_k transition suppressed if grain size too small (less than about $0.1 \text{ }\mu\text{m}$); $\lambda_{100} \sim -20 \times 10^{-6} \text{ cm/cm}$; $\lambda_{110} \sim 60 \times 10^{-6}$; $\lambda_{111} \sim 78 \times 10^{-6}$; $\lambda_s \sim 40 \times 10^{-6}$; $T_c = 575^\circ\text{C}$; domain (Bloch) walls thickness about 500 to 1500 Å and energy about 1 erg/cm^3 .

ORIGINAL PAGE IS
OF POOR QUALITY

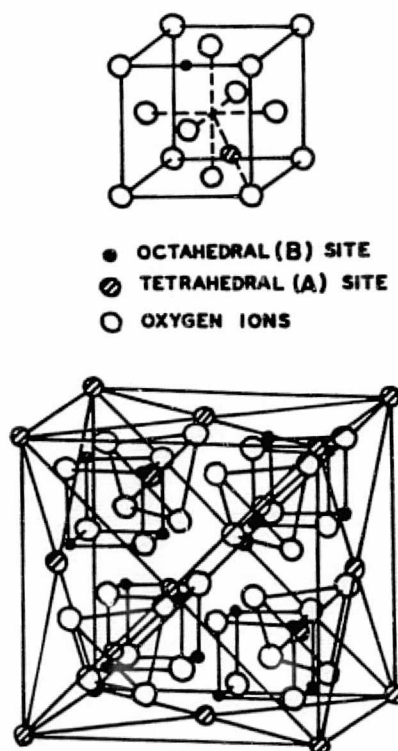


FIGURE 14. Spinel structure of magnetite. Top cube is 1/8 of unit cell.

5. Mechanical and other properties: $E \sim 1.6 \times 10^6 \text{ kg/cm}^2$; $G \sim 0.5 \times 10^6 \text{ kg/cm}^2$; Poisson's ratio $\sigma \sim 0.3$; slip plane $\{111\}$, slip direction $\langle 110 \rangle$ for dislocations; ultimate compressive strength (crystal) $\sim 1000 \text{ kg/cm}^2$; electrical resistivity $\rho \sim 10^{-3} - 10^2 \text{ ohm-meter}$ (places it in the range of semiconductors, 10^{-5} to 10^8 ohm-meters . Other ferrites are generally much less conductive.)

Ulvospinel

1. Chemical formula: Fe_2TiO_4 ;
percent by weight: $\text{Fe}^{2+}(50)$, $\text{Ti}^{4+}(21.4)$, $\text{O}^{2-}(28.6)$
2. Structure: cubic, spinel of inverse type (see Figure 14). Fe^{2+} and Ti^{4+} replace 2Fe^{3+} in magnetite. Cell dimension: $a \sim 8.5 \text{ \AA}$
3. Mineral characteristics: occurs as intergrowth on $\{100\}$ faces of magnetite; density about 4.8 g/cm^3 .
4. Magnetic properties: paramagnetic at room temperature: $T_c \sim -150^\circ\text{C}$; weakly ferrimagnetic below T_c (should be antiferromagnetic, in theory).

Maghemite

1. Chemical formula: $\gamma\text{Fe}_2\text{O}_3$
2. Structure: a polymorph of hematite ($\alpha\text{Fe}_2\text{O}_3$); cubic, defect spinel of inverse type (see Figure 14). Isostructural with magnetite except 1/9 of cations missing. These vacancies are distributed either randomly throughout octahedral and tetrahedral sites, or in octahedral sites alone, as in $4\text{Fe}^{3+}\text{O}_3 \rightarrow 3[\text{Fe}^{3+}\text{O}.\text{Fe}_{2/3}^{3+}.\square_{1/3}\text{O}_3]$ where \square represents a vacancy. Cell dimension: $a \sim 8.35 \text{ \AA}$; transition to $\alpha\text{Fe}_2\text{O}_3$ at $T \sim 250$ to 500°C ; distance between Fe and O, octahedral site — 2.05 \AA , tetrahedral site — 1.86 \AA

3. Mineral characteristics: may form as oxidation product of magnetite ($3\text{Fe}^{2+} \rightarrow 2\text{Fe}^{3+}$), or converted from lepidocrocite (see Figure 12). The tetrahedral sites are less available for oxidation than the octahedral sites, since the former are covalently bonded and the latter ionically bonded; Density = 4.88 g/cm^3 .
4. Magnetic properties: ferrimagnetic; $J_s = 83.5 \text{ emu/g}$ (407 emu/cm^3); $T_c \sim 675$ to 750°C . (depends on structural state).

Wustite

1. Chemical formula: FeO
2. Structure: cubic, NaCl type; stacking of hexagonal close-packed oxygen planes with -abc-abc- sequence along the $\langle 111 \rangle$ direction. Lattice is like two interpenetrating f.c.c. lattices, one of oxygen and the other of irons. Defect structure, deficient in Fe, i.e., $x \sim 0.83\text{--}0.95$; cell dimension: $a \sim 4.30 \text{ \AA}$; distance between Fe and O — 2.15 \AA ; angle between O-Fe-O — 90° .

Hematite

1. Chemical formula: $\alpha\text{Fe}_2\text{O}_3$; percent by weight: $\text{Fe}^{2+}(70)$, $\text{O}^{2-}(30)$; $Z = 6$ for hexagonal unit cell; $Z = 2$ for rhombohedral unit cell.
2. Structure: hexagonal system, trigonal subsystem, rhombohedral class (see Figure 15). Stacking of slightly distorted hexagonal close-packed oxygen planes with -ab-ab-ab- sequence, along the $[0001]$ direction, corundum-type structure. Groups of three oxygen atoms form a common face of two neighboring octahedra with a face parallel to $\{0001\}$. The stoichiometric number of iron atoms occupy octahedral interstices (sixfold coordination) between oxygen planes. They form Fe_2O_3 groups in the form of a trigonal dipyrmaid. Two thirds of the available cation positions are filled, with each Fe being surrounded by six oxygen in a near-octahedron. Cell dimensions (refer to Figure 15): hexagonal unit cell — $a = 5.035 \text{ \AA}$; $b = 13.75 \text{ \AA}$; rhombohedral unit cell — $a_r = 5.426 \text{ \AA}$; $\alpha = 55^\circ 16'$; distance between oxygen planes about 2.16 \AA ; distance between Fe and O — $r_1 = r_2 = r_3 = 2.08 \text{ \AA}$, $d_1 = d_2 = d_3 = 1.95 \text{ \AA}$; angle between O-Fe-O (angle defined by bonds listed) — $r_1r_2 = r_2r_3 = r_1r_3 = 77^\circ$; $r_1d_2 = r_2d_3 = r_3d_1 = 86.1^\circ$; $r_3d_2 = r_2d_1 = r_1d_3 = 90.8^\circ$; $d_1d_2 = d_2d_3 = d_1d_3 = 102.5^\circ$.
3. Mineral characteristics: crystals have form of positive rhombohedron $\{10\bar{1}1\}$, negative rhombohedron $\{01\bar{1}2\}$, or pinacoid $\{0001\}$; parting on $\{0001\}$ or rhombohedral plane $\{01\bar{1}2\}$ due to twinning. Twinning on $\{0001\}$ as penetration twins and on $\{01\bar{1}2\}$ usually lamellar. Hardness 5-6; density = 5.27 gm/cm^3 .
4. Magnetic properties: each sheet of Fe is ferromagnetic, but sheets are coupled antiferromagnetically, i.e., two antiferromagnetic sublattices. There is a systematic deviation from oppositely-directed spin configuration, resulting in weak spin-canted (anti)ferromagnetism. Magnetic anisotropy: magnetocrystalline transition T_A at about -23°C (-13°C for synthetic material); $-23^\circ < T < T_c$ — atomic moments in $\{0001\}$ plane. Weak ferromagnetism. Fe atoms on trigonal axis of rhombohedral unit cell have spins parallel in groups of two, pointing in direction of "a" axis of hexagonal unit cell. Easy axis is $\langle 10\bar{1}0 \rangle$, hard axis is $[0001]$. $T < -23^\circ$ — atomic moments point along trigonal axis. Perfectly antiferromagnetic (no net magnetization). Successive spins directed oppositely. Easy axis is $\{0001\}$. Transition suppressed for grain size sufficiently small. $T_c < T < 725^\circ\text{C}$ (T_N) — antiferromagnetic. Has a hard isotropic stable magnetization which endures until T_N (Néel temperature). Probably associated with unbalanced spins due to lattice defects or impurities, and is found in natural, not synthetic, material. $J_s \sim 0.45 \text{ emu/gm}$ (2.4 emu/cm^3); decreases with grain size; T_c (weak ferromagnetism disappears) = 675°C ; T_N (antiferromagnetism disappears) = 725°C . Criti-

cal single domain size, about 10 to 100 μm ; $\lambda_{111} \sim 1.3 \times 10^{-6}$ cm/cm (i.e., normal to (0001)); $\lambda_{112} \sim 8 \times 10^{-6}$ cm/cm (i.e., in (0001) plane). Both λ 's become negative below region of magnetocrystalline transition.

5. Mechanical properties: $E \sim 2 \times 10^6$ kg/cm²; $G \sim 0.8 \times 10^6$ kg/cm²; Poisson's ratio $\sigma \sim 0.27$.

Ilmenite

1. Chemical formula: FeTiO_3 ; percent by weight: Fe^{2+} (36.8), Ti^{4+} (31.6), O^{2-} (31.6); $Z = 6$.
2. Structure: hexagonal system, trigonal subsystem, rhombohedral class. Layers of Ti separated by Fe layers of alternating magnetic polarity. Cell dimensions: hexagonal unit cell — $a = 5.08 \text{ \AA}$; $c = 14.13 \text{ \AA}$; rhombohedral unit cell — $a_r = 5.52 \text{ \AA}$; $\alpha = 54^\circ 51'$.
3. Mineral characteristics: twinning on {0001}, parting on {0001}, {01 $\bar{1}$ 2}; hardness 5-6; density = 4.78 gm/cm³; may occur as lamellae on octahedral {111} of Fe_3O_4 .
4. Magnetic properties: paramagnetic at room temperature; $T_N \sim -210^\circ\text{C}$; $T < T_N$, antiferromagnetic.

Martite

1. Chemical formula: $\alpha\text{Fe}_2\text{O}_3$.
2. Structure: polymorphous after magnetite. Has cubic spinel outer form but rhombohedral internal structure.

Iron Oxyhydroxides

(Minerals of the family of hydrous ferric oxides, generally designated as Limonite)

Goethite

1. Chemical formula: αFeOOH , or 2HFeO_2 ; $Z = 4$.
2. Structure: orthorhombic, corresponds to hematite. Stacking of hexagonal close-packed oxygen planes with -ab-ab-ab- sequence along [001]. Iron atoms occupy only the octahedral positions. Converts to hematite (see Figure 15). Cell dimensions: $a = 4.60 \text{ \AA}$; $b = 9.95 \text{ \AA}$; $c = 3.02 \text{ \AA}$.
4. Magnetic properties: antiferromagnetic at room temperature, but may have some stable remanence due to spin-canting or unbalanced spins. Fe atoms alternate direction of spin along axis of magnetization, [001]. $T_N \sim 120^\circ\text{C}$.

Lepidocrocite

1. Chemical formula: γFeOOH , or $2(\text{FeO}.\text{OH})$; $Z = 4$.
2. Structure: orthorhombic. Stacking of oxygen-hydrogen planes with an -abc-abc- sequence along <051> direction of the orthorhombic unit cell (corresponds to <111> direction of a distorted cubic arrangement). Hexagonal packing of oxygen atoms in a sheet is not regular. Iron atoms occupy only octahedral sites. Each H atom is associated with an O atom, forming a discrete hydroxyl group. Cell dimensions: $a = 3.06 \text{ \AA}$; $b = 12.4 \text{ \AA}$; $c = 3.87 \text{ \AA}$.
3. Mineral characteristics: {010} cleavage.

Akaganeite

1. Chemical formula: βFeOOH ; $Z = 8$.
2. Structure: tetragonal.
4. Magnetic properties: T_N from -160°C to 20°C .

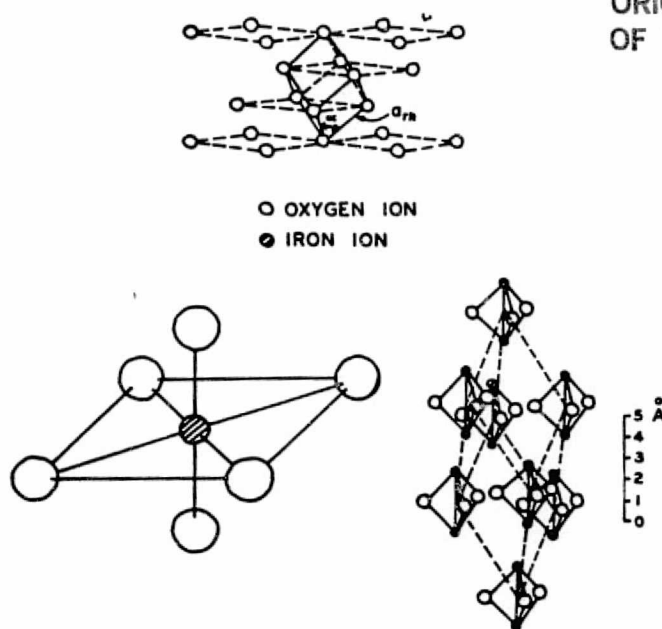
ORIGINAL PAGE IS
OF POOR QUALITY

FIGURE 15. Hematite structure. Top — rhombohedron in hexagonal system; Left — schematic of Fe-O configuration; Right — rhombohedron of Fe_2O_3 units.

Sulfides

The main magnetic sulfides of interest to rock magnetism are in the troilite-pyrrhotite series, troilite-pyrrhotite, $y\text{FeS} \cdot (1-y)\text{Fe}_{1-x}\text{S}$. Troilite is hexagonal in structure, with Fe and S atom layers alternating. It has a niccolite (NiAs) structure (see Figure 16). It is antiferromagnetic, with a Neel temperature of 320°C . The tetragonal form of FeS is termed mackinawite. For $x = \frac{1}{2}$, or pyrite (FeS_2), the structure is cubic and the crystal is paramagnetic at room temperature.

Pyrrhotite

1. Chemical formula: Fe_{1-x}S , where $0 < x < 0.125$.
 $Z = 2$
2. Structure: hexagonal system, rhombohedral class. In Fe_{1-x}S , $x = 0$ - hexagonal; $0 < x < 0.07$ - mixed structure; $0.07 < x < 0.1$ - hexagonal; $0.1 < x < 0.125$ - monoclinic. When hexagonal, it has a defect NiAs structure (see Figure 16). It is related to FeS in that Fe^{3+} replaced Fe^{2+} , leaving some cation vacancies. Cell dimensions (for $x = 0.115$); $a = 3.446 \text{ \AA}$; $c = 5.848 \text{ \AA}$.
3. Mineral characteristics: crystals usually tabular on {0001}; hardness 3.5 to 4.5; density $\sim 4.6 \text{ gm/cm}^3$.
4. Magnetic properties: $0 < x < 0.09$ - antiferromagnetic; $0.09 < x < 0.14$ - ferrimagnetic; J , $\sim 18 \text{ emu/gm}$ (83 emu/cm^3) for monoclinic phase; this maximum J , occurs for Fe_7S_8 , or $\text{Fe}_{0.875}\text{S}$ (i.e., $x = 0.125$); $T_c \sim 320^\circ\text{C}$; hard axis of magnetization [0001].

Carbonates

Siderite

1. Chemical formula: FeCO_3 ;
 $Z = 6$.

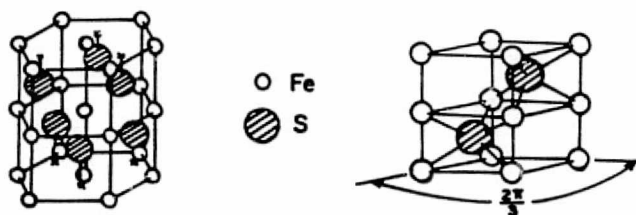


FIGURE 16. Hexagonal (NiAs, niccolite) structure for pyrrhotite.

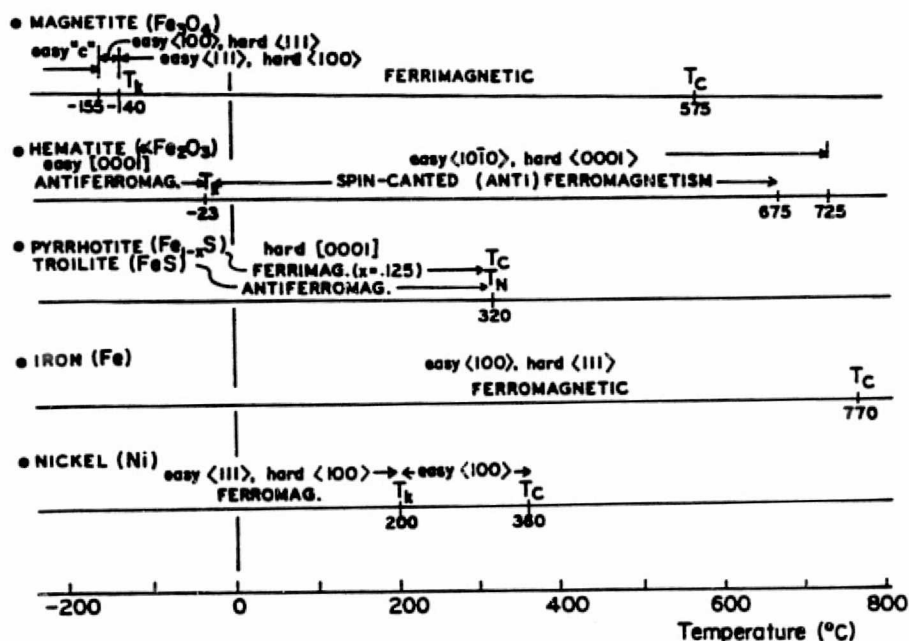


FIGURE 17. Variation of magnetism with temperature, for magnetic minerals and ferromagnetics.

2. Structure: hexagonal system, trigonal subsystem, rhombohedral class. Fe atoms are at points of a face-centered rhombohedron, CO₃ groups midway between Fe's. CO₃ groups are trigonal, planar parallel to [0001]. Cell dimensions: $a = 4.72 \text{ \AA}$; $c = 15.46 \text{ \AA}$.
3. Magnetic properties: antiferromagnetic; $T_N \sim -230^\circ\text{C}$; magnetization along [0001].
4. Mineral characteristics: crystals commonly rhombohedral {1011}, sometimes {0112}, {0221}, {4041}, or tabular on {0001}; cleavage {1011}; hardness 4; density = 3.96 gm/cm^3 .

Figure 17 shows the variation of magnetic properties with temperature for magnetic minerals and ferromagnetics.

Values of Curie temperatures and magnetization, and their variation with mineral composition, follow (as "Table 7" and "Figures 18, 19, and 20", on excerpt pages 256-260). This is then followed by magnetic properties of rocks--remanent magnetization, susceptibility, and Koenigsberger ratios--in "Table 16" (pages 272-279, Carmichael 1982).

Experimental study of the variation of magnetic susceptibility, with pressures of upper-crustal significance (up to 2.7 kbars) on magnetite and rocks, is given in Nulman, Shapiro, Maksimovskikh, Ivanov, Kim and Carmichael (1978). Additional information on the more chemical aspects of magnetic mineralogy is given in Haggerty (1979).

An uncertainty with regard to magnetic properties in situ at depth, as in the lower crust, is the likely Curie-temperature there. This will depend on the compositional state of the titanomagnetite. For example, titanium-rich titanomagnetite has a low T_c ("Fig. 11", p. 122). However, if there are oxidizing conditions (high oxygen fugacity) and high temperatures, as in the lower crust or in regional thermal metamorphism at depth, then there could be exsolution within the titanomagnetite grains to form ulvospinel and magnetite, and oxidation toward ilmenite. The ulvospinel would be non-magnetic, the ilmenite (of, say, intermediate composition) would have a low T_c and small magnetization, but the magnetite would have a high T_c (575°C.) and strong magnetization.

An additional possibility for a contributor to the magnetization of the lower crust, and perhaps even the upper mantle, could arise from the serpentinization of deep mafic rocks (Haggerty, 1979). The suggestion is that the olivines and sulphides would undergo reduction, yielding alloys of iron/nickel/cobalt/copper. These would be appreciably magnetic, and would also have much higher Curie-temperatures (600-1100°C.) than the usual iron oxide minerals. Their ability to retain magnetization would thus extend to greater depths.

MAGNETIC PROPERTIES

Saturation Magnetization, Curie/Néel Temperatures, and Cell Dimensions

Table 7
 J_s AND T_c/T_N OF MAGNETIC MINERALS, ROCKS, AND METALS

Material	Composition	Notes a	Density (gm/cm ³) b	T _c , T _N (°C) c	J _s		Ref.
					(emu/cm ³)	(emu/gm)	
<u>Minerals</u>							
Magnetite	Fe ₃ O ₄	Ferrimagnetic (pure) 5.18 (natural) 5-5.4		578	480 ^d 510 ^d 471	92.3(24°C) 98.2(0°K)	10 10 10
				580			63
				575	480		
		0.6% Ti			410-430		16
		0.06% Ti			480-500		16
	Titanomagnetite, x = 0.55			210			37
Ulvospinel	Fe ₂ TiO ₄	antiferro- magnetic	4.8	-153			63
Maghemite	γFe ₂ O ₃	Ferrimagnetic	4.88	675 ^e	407 ^d 417 545-675 ^e 750	83.5(24°C)	10 10 63 73
Hematite	αFe ₂ O ₃	Spin-canted (anti) ferromagnetic or ferrimagnetic	5.26	675	2.6	0.5(24°C)	10
		(Synthetic)		670	2.1	0.39(24°C)	10
				680	2.6	0.5	63
				680	2.2	0.42	8
		"T defect" parasitic antiferromagnetic ^f		725			
	Ilmenohematite, y = 0.75	max. ferrimagnetism in series		~10		19.5	34
Ilmenite	FeTiO ₃	Antiferro- magnetic	4.72	-205 -216		~0	74 63
Wustite	FeO	Antiferro- magnetic		-87 -83			74 10
Goethite	αFeOOH	Antiferro- magnetic	4.27	120			63
Akaganeite	βFeOOH	Antiferro- magnetic		-196 to 23			63
Magnesian- ferrite	MgFe ₂ O ₄	Ferrimagnetic ^g	4.18			24.5	63
				310	110		10
					110	23	74
				440	110	25	4
					140	29(0°K)	4

Table 7 (continued)
 J_s AND T_c/T_N OF MAGNETIC MINERALS, ROCKS, AND METALS

Material	Composition	Notes a	Density (gm/cm ³) b	T _c , T _N (°C) c	J _s		Ref.
					(emu/cm ³)	(emu/gm)	
Jacobsonite	MnFe ₂ O ₄	Ferrimagnetic ^g	4.95	300	416	84	63
					400	81	4
					408		10
					560	112(0°K)	4
Chromite	FeCr ₂ O ₄	Ferrimagnetic ^g	4.5-5.1	-185			10, 63
Trevorite	NiFe ₂ O ₄	Ferrimagnetic ^g	5.35	585	270	51	63, 74
					300	56(0°K)	4
					267		10
Franklinite	ZnFe ₂ O ₄	Ferrimagnetic ^g	5.1-5.3	-258			74
				-264			10
Fayalite	Fe ₂ SiO ₄	Antiferromagnetic		-147			63
Pyroxene	FeSiO ₃	Antiferromagnetic		-233			63
Pyrrhotite	Fe _{1-x} S	Ferrimagnetic	4.6	300-325	62	13.5 ^d	10
				320	90 ^d	19.5 max. at Fe ₇ S ₈	63
				300			8
Troilite	FeS	Antiferromagnetic	4.83	320			74
				340			10
Pyrolusite	MnO ₂	Antiferromagnetic	5.06	-189			10, 63
Chromium dioxide	CrO ₂	Ferrimagnetic		119	515		74
Siderite	FeCO ₃	Antiferromagnetic	3.96	-233			63
Rhodochrosite	MnCo ₃	Antiferromagnetic	3.70	-243			63
<u>Metals</u>							
Iron	Fe	Ferromagnetic	7.87	770	1714	218	2
					1760	224(0°K)	2
Nickel	Ni	Ferromagnetic	8.9	358	485	54	38
					510	57(0°K)	2, 38
					360		4
					370		82
Cobalt	Co	Ferromagnetic	8.85	1120	1420	160	2
					1445	163(0°K)	2
High permeability metals:							
4% Si-Fe				690			74
45 Permalloy				440			74
Mumetal				400			74
Supermalloy				400			74

Table 7 (continued)
 J_s AND T_c/T_N OF MAGNETIC MINERALS, ROCKS, AND METALS

Material	Composition	Notes a	Density (gm/cm ³) b	T_c, T_N (°C) c	J_s		Ref.
					(emu/cm ³)	(emu/gm)	
2V Permendure				980			74
Rocks							
Sandstones	Red; Britain; 12 sites, Triassic and Devonian				(0.2–1.2) $\times 10^{-2}$		75, 20
Basalt	Titanomagnetite $x = 0.6$			200–400			37
Magnetite ore	Lodestone (Fe_3O_4)					50–80	66
Lunar rocks							
Soils	8 samples					0.9–1.5	28
Breccia	16 samples					0.05–2	28
	Anorthosite breccia			765		0.145	44
Anorthosite	2 samples					0.7–2.6	28
Basalt				760		0.2–2.2	44
	10 samples					0.1–2	28
	3 samples					0.1–3(0°K)	28
Gabbro	2 samples					0.2–0.7	28
Igneous rocks				760–790			28
Breccia and fines				745–790			28
Meteorites							
4 Iron meteorites (ie., Ni–Fe)				600–780			32

a Magnetic state is at temperatures below T_c or T_N ; would be paramagnetic above.

b Used to convert emu/cm³ to emu/gm or vice versa; density values from *Handbook of Materials Science*, Vol. I, Lynch, C. T., Ed., CRC Press, Boca Raton, Fla., 1974, p. 235, and Vol. III, p. 184.

c T_c is Curie temperature, for ferrimagnetic or ferromagnetic materials; T_N is Néel temperature for antiferromagnetics.

d Calculated, from other J_s units.

e May have been converted to hematite.

f Present in natural specimens, due to effect of lattice imperfections.

g Spinel structure, i.e., $A^{+2}B^{+3}_2O_4$

Variation of J_s , T_c , and Cell Dimension With Chemical Composition

The titanomagnetite series is ulvospinel-magnetite, $xFe_2TiO_4 \cdot (1-x)Fe_3O_4$. Figure 18 shows the variation of Curie temperature (T_c) and cell dimension (cubic lattice parameter, i.e., unit cell size, "a") with "x" in the above series.

The relationships for titanomagnetite can be represented by

$$\text{cell parameter, } a = 8.395 + 0.135x \text{ \AA}$$

$$\text{i.e., } a = 8.395 \text{ \AA for magnetite (} x = 0 \text{)}$$

$$a = 8.53 \text{ \AA for ulvospinel (} x = 1 \text{)}$$

$$\text{Curie temperature, } T_c = 575 - 725x + 600x \left(\frac{1}{2} - x \right) (1 - x) ^\circ\text{C.}$$

$$\text{i.e., } T_c = 575 ^\circ\text{C for magnetite}$$

$$= -150 \text{ for ulvospinel}$$

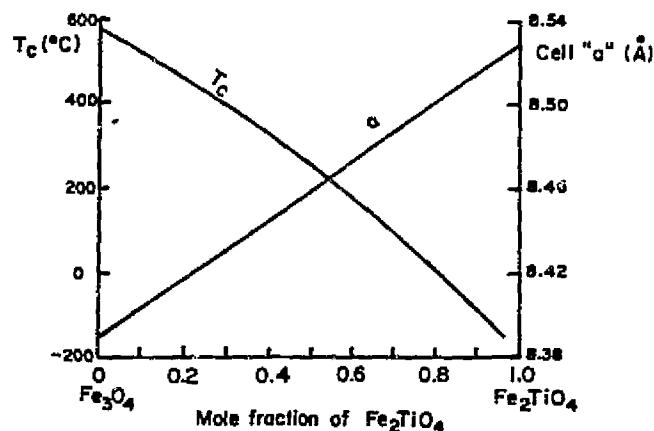


FIGURE 18. Variation of T_c and cell parameter "a" in titanomagnetite series.*

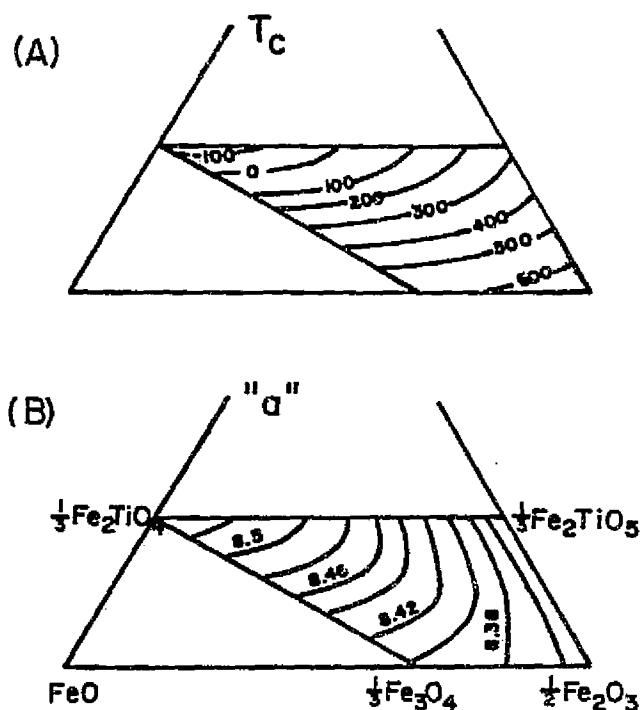


FIGURE 19. Variation of Curie temperature (T_c) and cell parameter "a" in $\text{FeO-TiO}_2\text{-Fe}_2\text{O}_3$ ternary diagram. (A) for T_c , in $^{\circ}\text{C}$, (B) for "a", in \AA .

Figure 19 shows the variation of T_c and "a" in the compositional range of interest in the $\text{FeO-TiO}_2\text{-Fe}_2\text{O}_3$ ternary diagram.

The variation of saturation magnetization, J_s , for the titanomagnetite series at room temperature is given by $J_s = 92(1 - x) - 42x(1 - x)$ emu/gm, i.e., $J_s = 92$ emu/gm for magnetite, $J_s = 0$ for ulvöspinel.

Table 8 shows a typical experimental determination of the variation of J_s with composition in the titanomagnetite series.

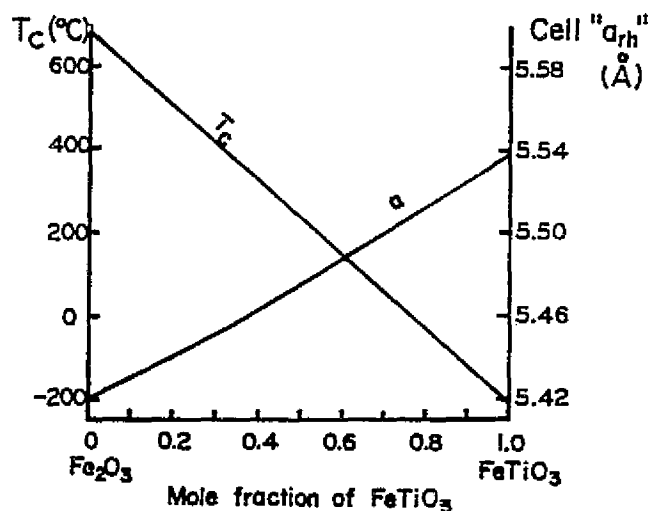


FIGURE 20. Variation of T_c and rhombohedral cell parameter " a_{rh} " in ilmenohematite series.⁶

Table 8
VARIATION OF J_s WITH
COMPOSITION IN THE
TITANOMAGNETITE AND
ILMENOHEMATITE SERIES^{12,34}

Titanomagnetite $x\text{Fe}_2\text{TiO}_4 \cdot (1-x)\text{Fe}_2\text{O}_3$		Ilmenohematite $y\text{FeTiO}_3 \cdot (1-y)\text{Fe}_2\text{O}_3$	
x	J_s (emu/gm)	y	J_s (emu/gm)
0	93	0	0.5 ^a
0.04	90	0.25	0.6 ^a
0.10	82	0.45	0.6 ^a
0.18	73	0.5	2.9 ^b
0.31	59	0.6	9.2 ^b
0.56	29	0.7	17.4 ^b
0.68	15	0.75	19.5 ^b
		0.8	18.2 ^{b,d}
		0.9	5.3 ^{b,d}
		0.95	1.6 ^{b,d}
		1.0	0 ^{a,d}

- ^a Spin-canted (anti)ferromagnetic.
- ^b Ferrimagnetic.
- ^c Antiferromagnetic.
- ^d For $x \geq 0.75$, T_c is below room temperature, so the material is paramagnetic at room temperature.

The ilmenohematite series is ilmenite-hematite, $y\text{FeTiO}_3 \cdot (1-y)\text{Fe}_2\text{O}_3$.

Figure 20 shows the variation of T_c and cell parameter a_{rh} with " y " in the series.

Relationships can be represented by Curie temperature $T_c = 680 - 890y$ °C, i.e., $T_c = 680$ °C for hematite ($y = 0$), $T_c = -210$ for ilmenite ($y = 1$); volume of unit cell, $V = 100.4 + 3.8y$ Å³, i.e., $V = 100.4$ Å³ for hematite, $V = 104.2$ for ilmenite. The variation of J_s with composition " y " is shown in Table 8.

Table 16
MAGNETIC PROPERTIES (J_n , K , Q) OF ROCKS

Material	Notes	J_n (in 10^{-6} emu/cm ³) a	K (in 10^{-6} emu/cm ³)	Q_n b	Ref.
Sedimentary rocks					
Soils	Typical Texas Coast		1-100 5		29
Marine sediments	Sandy clay, Texas continental slope	10-150	15-35	~5	
Silty shale	Ventura basin, Calif.	5-40	20-120	~5	
Siltstone	Precambrian, Britain; 4 samples			0.02-2	6
Clays			20		65
Shale	137 samples		5-1478 ave. 52		25
Sandstone	230 samples		0-1665 ave. 20-30		25
	Redbeds, Precam- brian, 9 samples		100	1.6-6	6 26
	Redbeds, U.S., 82 sites	2-20	0.4-40 3-76	1-3	45 87
	Redbeds, Wyoming, Triassic	4-29	2-13	ave. 4.4	21, 22
	Britain, 12 sites	0.2-3.3	10-28		75, 20
	Redbeds, typical	0.5-50			21, 22
Limestone	66 samples		2-280 ave. 23		25
			0-5		26
Dolomite	66 samples		8		25
Coal			2		65
Typical sedimentary rocks, average		1-100	3-300	0.02-10	
Igneous rocks					
Typical igneous rocks, average		100-40,000	50-5000	1-40	
Granite	Pluton, Yosemite Calif.	100-800	1000-4000	0.3-1	58, 62, 24
			10		26
	97 samples, Okla. 41 samples	1000-180,000	280-2000 30-2700	28	62, 24
	Minnesota, 31 samples		0-4000		25
	<1.4% Fe ₃ O ₄		ave. 470		42
	Without Fe ₃ O ₄		1-5		58
	Intrusives, Japan			0.1-0.5	58
Acidic intrusives	58 samples		3-6527 ave. 647 30-60		76

Table 16 (continued)
MAGNETIC PROPERTIES (J_n , K , Q) OF ROCKS

Material	Notes	J_n (in 10^{-6} emu/cm ³) a	K (in 10^{-6} emu/cm ³)	Q_n b	Ref.
Granodiorite	Minnesota, 17 samples		350		42
	Nevada			0.1-0.2	13, 58
Diorite			200		26
Dolerite (diabase/dikes)					
	sills, England, 5 samples			2-3.5	6
	dikes, India, 28 samples		55-1100 ave. 337		53
Diabase	Typical	1900-4000	1500-2300 80-1000	2-3.5	25
	Minnesota, 19 samples <3.4% Fe_3O_4		800-12000 ave. 2600		42
	dikes, Precambrian		100-20000	0.2-4	62
Gabbro	Minnesota, 37 samples, <0.9% Fe_3O_4		80-6100 ave. 1000		42
	Minnesota			1-8	26
	Sweden		2000	9.5	58
			70-2400		25
Intrusives	Sudbury basin, Ontario	1000-60,000	20-5000	0.1-20	62
	Precambrian, basic		2000-9000	1-2	76
Basic	78 samples		44-9711 ave. 2596		53
	Precambrian, India, 5 samples		3675-4300		53
Basalt/diabase	Minn., 64 samples		2500		42
Volcanics	Montana, Eocene, 455 samples	11,000	700	~30	62
	rapidly-cooled			30-50	
Basalt	Australia, Cenozoic, 127 samples	2100	900	~5	58, 62
	Minn., 37 samples <2.5% Fe_3O_4		20-8400 ave. 2950 3000-8000 40-9600		42
	Iceland, Tertiary, 70 samples			6	6
	NSW Australia, Tertiary, 7 sites	2000-30,000			6
	India, Deccan traps, 60 samples		1000-6000 ave. 2300		53
	W. Greenland, Tertiary			1-39	58
			2000		26
	Seamounts, N. Pacific			8-57	71
	Seafloor, EM-7 Mo- hole, NE Pacific			15-105 ave. 40	71
	Seafloor, mid-Atlantic ridge		24-2900	1-160 ave. 48	71

Table 16 (continued)
MAGNETIC PROPERTIES (J_n , K , Q) OF ROCKS

Material	Notes	J_n (in 10^{-6} emu/cm ³) a	K (in 10^{-6} emu/cm ³)	Q_n b	Ref.
	Seafloor, depth 1-6 meters	5000-8000	300-600	25-45	
(and for comparison:)					
	Titanomagnetite grains, $x = 0.6$, size 1-2 μm			Q_T^c	
	10 μm			35	37
	20 μm			17	
				10	
	Magnetite powder, 2% by wt dispersion in epoxy, grain size 1-2 μm			20	37
	4-8 μm			5.4	
	37-75 μm			1.5	
	75-150 μm			1.3	
	Titanomagnetite powder, $x = 0.55$, 2% by wt dispersion in epoxy, grain size				
	1-2 μm			39	37
	5-15 μm			23	
	75-150 μm			1	
	Magnetite powder dispersed, grain size:	J_T^d (emu/cm ³ of magnetite)	(per cm ³ of magnetite)	Q_T	
	1.5 μm	0.55	0.19	7.2	11, 51
	6	0.15	0.19	2.0	
	19	0.041	0.19	0.54	
	21	0.032	0.21	0.38	
	58	0.046	0.22	0.52	
	88	0.041	0.21	0.49	
	120	0.044	0.24	0.46	
Metamorphic rocks		J_n		Q_n	
Metasediments	Precambrian		20-200		76
Granite/gneiss	Precambrian, India, 12 samples		30-100 ave. 59		53
Gneiss			0-240		25
Slate	Minn., 26 samples, <.2% Fe ₃ O ₄		0-100 ave. 50		42
Greenstone	Precambrian, 8 samples Minn., 15 samples, <.2% Fe ₃ O ₄		10-60 40-880 ave. 100		76 42
Basic metaigneous	Precambrian		200-4000	0.5-2	76
Serpentinite			250-6000		87
	61 samples		0-5824 ave. 349		25
Peridotite			12,500 5000		25 26

Table 16 (continued)
MAGNETIC PROPERTIES (J_n , K , Q) OF ROCKS

Material	Notes	J_n (in 10^{-6} emu/cm ³) a	K (in 10^{-6} emu/cm ³)	Q_n b	Ref.
Ores					
Magnetite ore	Sweden			1-10	70
	Sweden, 31-63% Fe ₃ O ₄		240,000- 490,000		67
	Sweden, 86-95% Fe ₃ O ₄		1,000,000- 1,120,000		67
	76% by wt Fe ₃ O ₄		350,000		47
	90% Fe ₃ O ₄ , grainsize 0.2 x .2 mm		400,000		47
	Lodestone iron ore, 5,000,000- 7 samples	35,000,000			66
	Lodestone ore, 13,100,000		323,000	94	10
	Arkansas				
	Lodestone ore, 11,100,000		311,000	80	10
	Japan				
	Biwabik & Soudan, U.S.; 15-26% Fe ₃ O ₄		50,000- 120,000		42
	6 samples	200,000- 800,000			66
Hematite ore	Sweden		330-800		10
	Precambrian		60-750		76
Chromite ore	FeCr ₂ O ₄ ; 27- 58% Fe		600-100,000		50
Hausmannite ore	Mn ₂ O ₄ ; Sweden		130		67
Pyrite ore	Sweden		420		50
	Sweden		8-400		50
Pyrrhotite ore	Sweden		60		50
Lunar rocks					
	typical	(in 10^{-6} emu/gm) 0.1-1000	(in 10^{-6} emu/gm) 500-2000	0.001-1 ^e	
Soils	7 samples		1100-3500		28
Breccia	15 samples		50-3300		28
Anorthosite	2 samples		200-900		28
	Breccia		400 x 10^{-6} emu/cm ³		44
Gabbro			50 x 10^{-6} emu/gm		28
Basalt	8 samples		50-700 x 10^{-6} emu/gm 100-300 x 10^{-6} emu/cm ³		28 44
Meteorites					
		(in cgs)	(in cgs)		
Meteorites	60 samples (48 irons, i.e., Ni-Fe; 12 stony-irons)	0.05-.3	0.2-4		32

^a J_n is natural remanent magnetization (NRM).

^b Q_n is Koenigsberger ratio for NRM, i.e., $Q_n = J_{NRM}/KH_E$ where H_E is earth's field (about 0.5 oe).

^c Q_T is Koenigsberger ratio for TRM, i.e., $Q_T = J_{TRM}/KH_E$ where J_{TRM} is TRM acquired in Earth's field.

^d Lab TRM, in $H = 0.4$ oe.

^e In $H = 0.5$ oe.

Table 17
SUSCEPTIBILITIES OF ROCK TYPES, CALCULATED FROM THEIR
MAGNETITE AND ILMENITE CONTENT^{25,49}

Material	Magnetite Content and Susceptibility,* cgs units							
	Minimum		Maximum		Average		Ilmenite, average	
	%	$k \times 10^4$	%	$k \times 10^4$	%	$k \times 10^4$	%	$k \times 10^4$
Quartz porphyries	0.0	0	1.4	4,200	0.82	2,500	0.3	410
Rhyolites	0.2	600	1.9	5,700	1.00	3,000	0.45	610
Granites	0.2	600	1.9	5,700	0.90	2,700	0.7	1000
Trachyte-syenites	0.0	0	4.6	14,000	2.04	6,100	0.7	1000
Eruptive nephelites	0.0	0	4.9	15,000	1.51	4,530	1.24	1700
Abyssal nephelites	0.0	0	6.6	20,000	2.71	8,100	0.85	1100
Pyroxenites	0.9	3000	8.4	25,000	3.51	10,500	0.40	5400
Gabbros	0.9	3000	3.9	12,000	2.40	7,200	1.76	2400
Monzonite-latites	1.4	4200	5.6	17,000	3.58	10,700	1.60	2200
Leucite rocks	0.0	0	7.4	22,000	3.27	9,800	1.94	2600
Dacite-quartz-diorite	1.6	4800	8.0	24,000	3.48	10,400	1.94	2600
Andesites	2.6	7800	5.8	17,000	4.50	13,500	1.16	1600
Diorites	1.2	3600	7.4	22,000	3.45	10,400	2.44	4200
Peridotites	1.6	4800	7.2	22,000	4.60	13,800	1.31	1800
Basalts	2.3	6900	8.6	26,000	4.76	14,300	1.91	2600
Diabases	2.3	6900	6.3	19,000	4.35	13,100	2.70	3600

* Using $k_{\text{magnetite}} = 0.30 \text{ emu/cm}^3$; $k_{\text{ilmenite}} = 0.137 \text{ emu/cm}^3$.

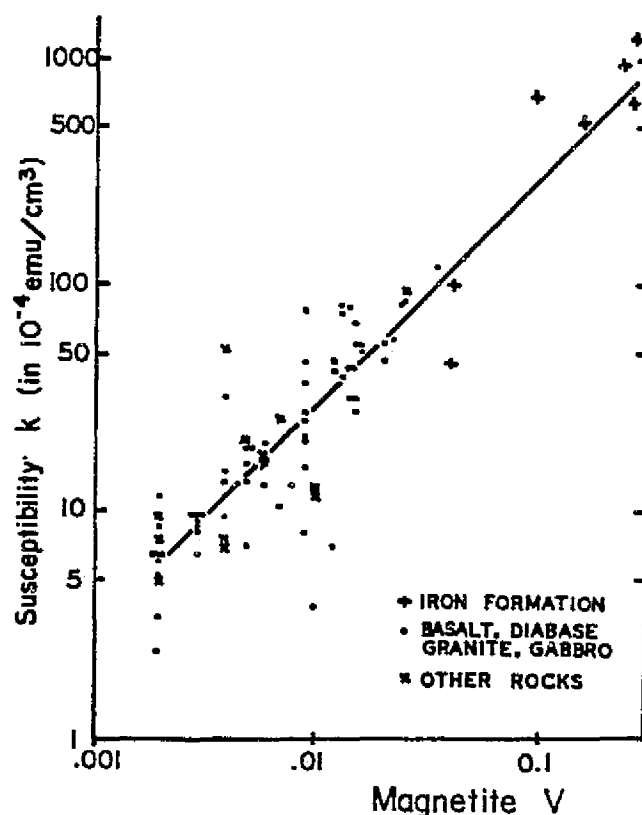


FIGURE 23. Relation of susceptibility to magnetite content for some igneous and ore rocks (Precambrian, of Minnesota).⁴⁴

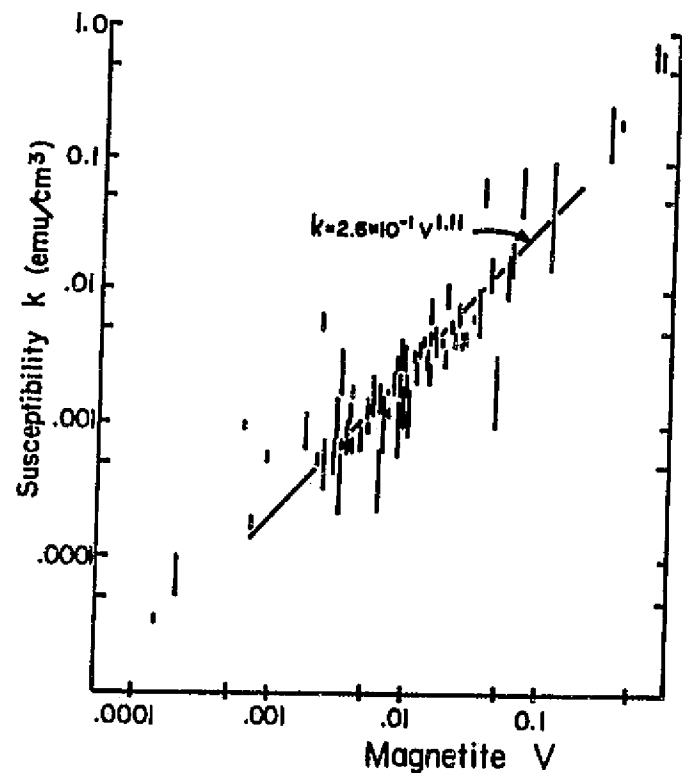


FIGURE 24. Relation of susceptibility to magnetite content for some metamorphic rocks (Adirondacks.) (Reference 29, from data of Reference 15).

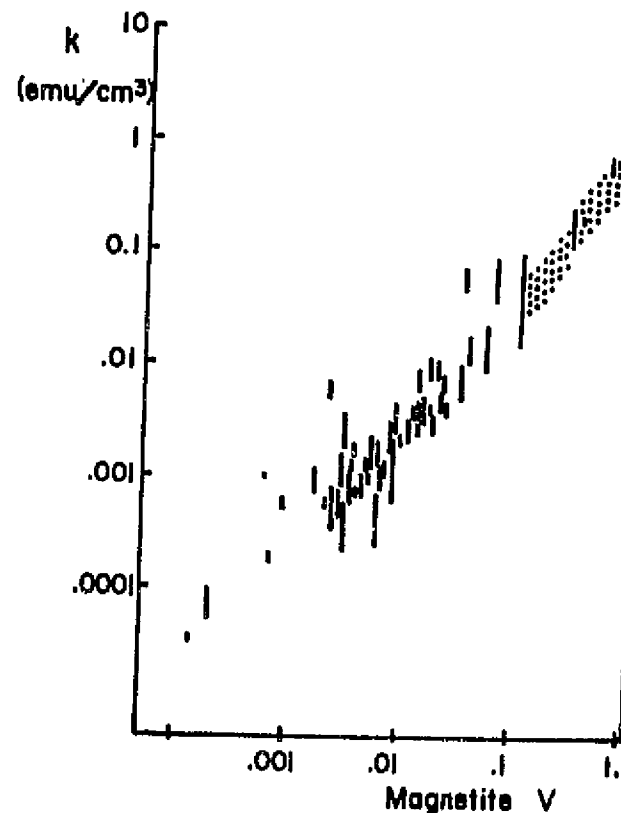


FIGURE 25. Susceptibility and magnetite content of rocks and ores. (Reference 7; data from Reference 15 for lines, Reference 67 for stippled area.)

ORIGINAL PAGE IS
OF POOR QUALITY

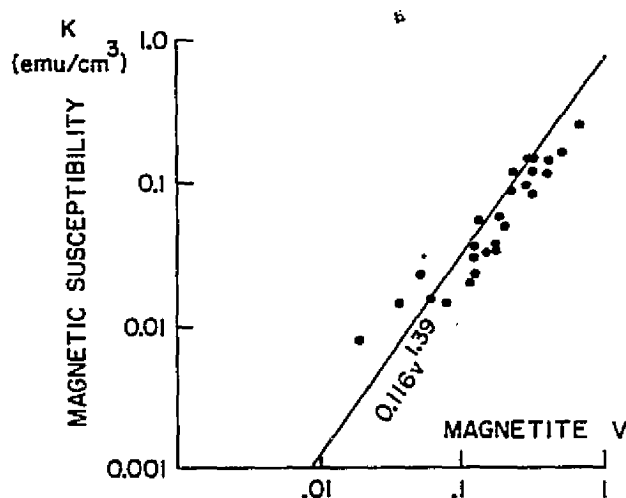


FIGURE 26. Susceptibility and magnetite content for iron formation ore (Reference 50, from data of Reference 36).

Table 18
DISTRIBUTION OF MEASURED SUSCEPTIBILITIES FOR
MAJOR ROCK TYPES^{7,49}

Rock type	Number of samples	Percent of samples with k (in 10^{-6} emu/cm ³)			
		<100	100—1000	1000—4000	>4000
Basic extrusive	97	5	29	47	19
Basic intrusive	53	24	27	28	21
Granite etc. (i.e., acidic igneous)	74	60	23	16	1
Metamorphic (gneiss, schist, slate)	45	71	22	7	0
Sedimentary	48	73	19	4	4

Note: Where the terms indicate: basic = mafic; high in iron/magnesium silicates, i.e., the denser and darker-colored ferromagnesian minerals; acidic = siliceous; high in quartz; extrusive = formed by cooling after extruding onto the land surface, or seafloor; typically finer-grained; intrusive = plutonic; formed by cooling at depth; typically coarser-grained.

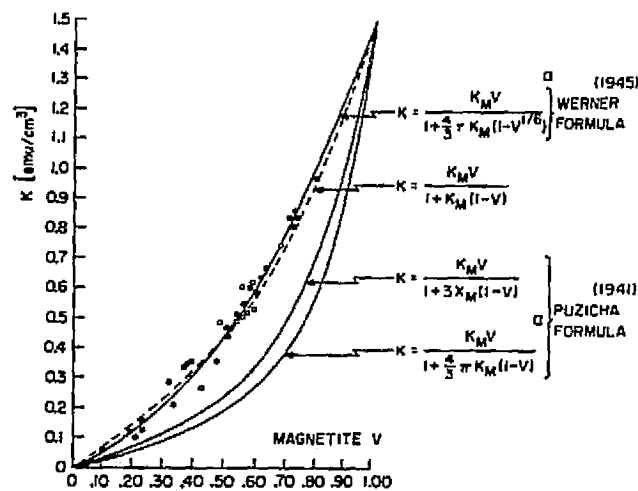


FIGURE 27. Variation of susceptibility with magnetite content for magnetite-rich ores (Sweden) with various formulas. Using $K_M = 1.5$ emu/cm^3 .^{42,47} a— with $N = 4\pi/3$.

Table 19
RELATIVE PERMEABILITY OF MINERALS AND
ROCKS**

Material	μ_r (relative permeability)
Minerals	
Quartz (diamagnetic)	0.999985
Calcite (diamagnetic)	0.999987
Rutile (paramagnetic)	1.0000035
Pyrite	1.0015
Hematite	1.053
Ilmenite	1.55
Pyrrhotite	2.55
Magnetite (ferrimagnetic)	5.0
Rocks	
% magnetite	
	0 ~1.0
Granites	0.2 1.006
	0.5 1.017
	1.0 1.04
Basalts	2.0 1.08
	3.0 1.12
	5.0 1.18
Iron ore	10.0 1.34
	20.0 1.56

Depth to Curie-temperature isotherm

Depths to the Curie temperature (T_c) isotherm, below which remanent and induced magnetization is lost, were given here (pages 78-79) for typical continental (ancient shields) and oceanic crustal terranes.* These calculations, consistent with interpreted magnetic bottoms from modelling, assumed the dominant magnetic mineral was titanomagnetite and typical geothermal gradients are as given in Figure 48. The T_c gradients (A, B, and C) are given for titanomagnetite of composition $x = 0$ (i.e. pure magnetite), 0.1, and 0.3, respectively. The variation of Curie temperature with composition in the titanomagnetite series is shown in "Figure 18" of the preceding excerpt pages. The T_c increases slightly with hydrostatic pressure and therefore with depth, at the rate of 1.9-2.0 °C/kbar for magnetite (Carmichael, 1982). The geothermal gradients in Figure 48 are based on data from Blackwell, Wyllie, and Roy (Carmichael, 1977).

Magnetite ($x = 0$) has a T_c of 575°C. For titanomagnetite, values are 510°C. for $x = 0.1$, 450°C. for $x = 0.2$, and 410°C. for $x = 0.3$. Typical geothermal gradients are 25-30°C/km for a global average near the Earth's surface; and averaged over the upper 40 km of the Earth, representative ones are about 17°C/km for oceanic crust and about 10°C/km for continental shields.

* If the Moho physicochemical boundary between crust and mantle is also a lower bound on magnetization (because of the minerals in the upper mantle being non-magnetic), then the magnetic bottom of sources could be shallower than the T_c -isotherm where there is an appropriate condition of thinner crust or lower geothermal gradient. Interpretation of an essentially non-magnetic upper mantle comes from petrologic and geochemical study (Wasilewski et al, 1979), but there is work supporting a contrary view (Haggerty, 1979).

ORIGINAL PAGE IS
OF POOR QUALITY

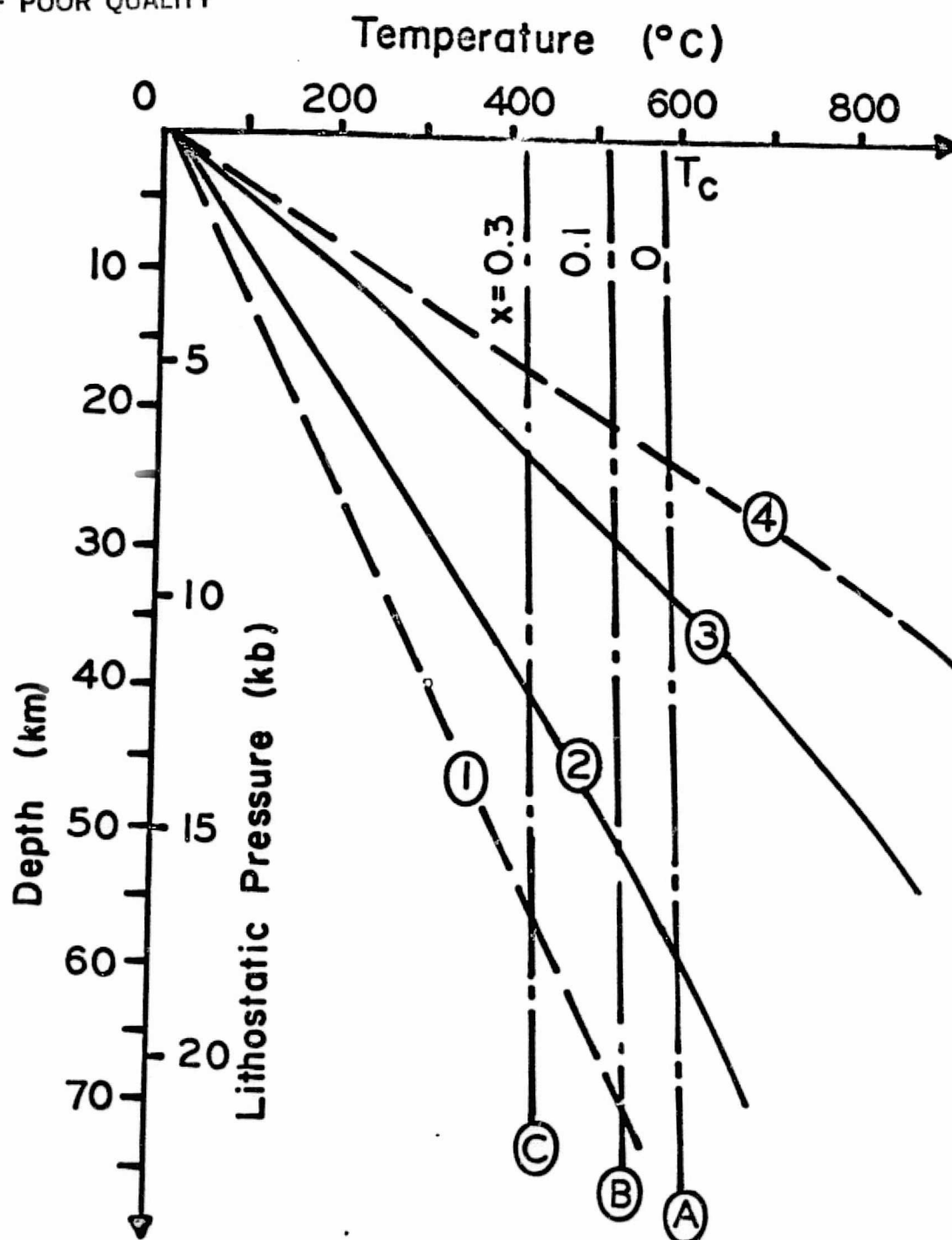


Figure 48. Typical geothermal gradients in geologic areas, as a basis for calculating Curie-temperature isotherm depths. 1--low gradient (e.g. Sierra Nevada, southwest USA); 2--ancient shield; 3--oceanic crust; 4--high gradient (e.g. Basin and Range, western USA). A, B, and C are T_c -gradients for titanomagnetites. (Carmichael, 1977)

SUMMARY

Our objective has been to use the satellite magnetic anomaly field observed by Magsat, with its characteristically long-wavelength information, to help interpret gross crustal structure, composition, properties of the upper and lower crust, major geologic terranes (e.g. accreted continental fragments), tectonic development, and any relation to economic resource provinces such as mineral deposits and oil and gas basins. This was to assess the utility of such large-scale geophysical surveying for geological studies in "stable interior"-type geological areas. Analysis and interpretation was done for the study area of the central midcontinent of the U.S. The satellite data set was examined in conjunction with other geophysical and geological data.

The anomaly data set has been derived by processing the original NASA satellite data, by cleaning, correcting, and correlation, and then reducing to a $1^{\circ} \times 1^{\circ}$ latitude/longitude grid at a common altitude of 400 km, applying wavelength filtering, and then reducing the data "to the magnetic pole" to aid in interpretation.

Satellite anomalies are expressions, primarily, of broad and deep-seated magnetic properties and gross geologic crustal structure. The magnitude (amplitude) and pattern of anomalies depend on such considerations as:

i) the thickness of the "magnetic lithosphere" that is magnetizable. That is, the crustal zone that has as its lower bound (and magnetic "bottom") the Curie-temperature of the magnetic minerals, below which the rock is non-magnetizable. An additional lower bound may be the Moho physicochemical boundary, below which the rock-forming minerals may be nonmagnetic because of compositional factors.

ii) the relative partitioning of the earth's crust into a sialic upper-crustal "layer", and a more mafic (more ferromagnetian/iron-rich minerals) lower-crustal "layer". The latter layer is believed to be much more magnetic (due to higher susceptibility, and thermally-activated viscous remanent magnetization), and may play a dominant role in producing the long-wavelength crustal anomalies. Of consequences are both differences in lower-crustal layer thickness, and lateral varia-

tions in the rock magnetization intensity.

iii) magnetic mineral content of rocks. It is the amount of magnetite (in the titanomagnetite mineral series) with properties determined by its chemical origin and thermal history, which is most important in producing magnetization.

iv) relative metamorphic grade of large terranes of crustal rock, particularly for deeper basement rock. Granulite-grade metamorphism seems to provide the most favorable condition for larger magnetization.

v) boundaries between, or major intrusions in, crustal "blocks" of different thickness, rock type (composition, age), physical properties, and structural style. These borders can yield distinguishable anomaly patterns, such as magnetic lineaments.

vi) the orientation of the local Earth's magnetic field. This determines the direction of the induced (and deep-seated viscous) magnetization, and the resulting anomaly pattern will vary in appearance with latitude unless the data are "reduced-to-the-pole".

vii) satellite magnetic mapping presents anomalies which have characteristic wavelengths greater than 250 km.

The major anomalous features in the central Midcontinent are:

i) a large magnetic high over east-central Kentucky/Tennessee, at the intersection of major magnetic/geologic lineaments. The anomaly is attributed to a mafic basement rock complex in the mid- and lower-crust, which is anomalously ultrabasic and magnetic, and possibly also to some localized crustal thickening.

ii) a magnetic anomaly high over NW Texas/Oklahoma, and then extending in an arcuate moderate high up to the northwest through Missouri to Lake Michigan. The former may be due to crustal thickening, with the latter trend to the northeast being due also to a different geologic terrane (the Precambrian Mazatzal/Granite-rhyolite belts) and which has an anomalously more-magnetic lower crust (especially under Missouri).

iii) a magnetic low over the Mississippi Embayment/aulacogen, which extends from the Gulf Coast up to the New Madrid (southeast Missouri) seismic zone. This is believed due to crustal thinning, associated with the rift attempt in late Precambrian/early Paleozoic time, com-

bined with anomalously less-magnetic lower crust.

iv) a magnetic anomaly low over South Dakota, for which there is some evidence for contributions from localized crustal thinning, an elevated Curie-temperature isotherm, and a magnetization deficiency in the lower crust.

v) a magnetic low over west-central Georgia, probably due also to an anomalously less-magnetic lower crust.

vi) a tendency for the satellite magnetic anomaly pattern to follow and reflect the southern "rifted continental margin" formed in late Precambrian/early Paleozoic time with the opening of the proto-Atlantic.

vii) a lack of distinguishable magnetic expression for the Central North American Rift system/Midcontinent Geophysical Anomaly, a long, deep, and major crustal structure and intrusion developed in late-Precambrian (Keweenawan) time. This is apparently due to the opposing contributions of reversed and normal polarity remanence in the upper-crustal mafic rock seam, resulting in a reduced net magnetization, and to the north-south alignment of this relatively narrow structural feature. This seam, a basalt-dominated sequence of extrusives and intrusives, is interpreted as having its lower portion with reversed remanence, and its (younger) upper portion with normal remanence. In support of this, there is known to be a reverse-to-normal transition of the geomagnetic field in Keweenawan time.

We have also compiled data on magnetic properties of minerals responsible for magnetization in the Earth's crust. Such information will help in subsequent modelling and interpreting crustal sources for anomalies mapped by satellite or other long-wavelength surveys. It will provide guidance for selecting properties to deduce crustal composition, structure, and thermal regime (as depth to the Curie-temperature isotherm).

Magsat anomaly data is a promising new aid for reconnaissance exploration of major geologic and tectonic features of the Earth's crust. It may be helpful in identifying and interpreting plate tectonic boundaries, now and in the past as at ancient collisional zones where continental blocks have been sutured together. If there is a causal relationship between such tectonism and the processes of con-

centration and emplacement of ore deposits, then there is the prospect for assistance with exploration for economic mineral resources. It might be noted that the (interpreted) most highly-magnetically-anomalous region of the mafic lower-crustal layer in the central U.S., an elongate zone underlying Missouri, underlies the region of the central Midcontinent which has the greatest number, variety, and richness of metallic mineral deposits (lead, copper, zinc, iron).

BIBLIOGRAPHY OF EXTERNAL REFERENCES CITED

(Bibliography of project-related publications
by our group is given in following listing)

- Allenby, R. J. and C. C. Schnetzler, United States crustal thickness, Tectonophysics, v. 93, p. 13, 1983; and based in part on earlier report of R. J. Allenby, U.S. crustal structure and satellite magnetic anomalies, NASA Techn. Memo. 81990, Aug. 1980
- Arvidson, R.E., E. Guinness and J. Strebeck, Linear basement structure in the midcontinent USA--gravity, topography, remote sensing, and seismicity data (abstract), EOS trans. A.G.U., v. 63, May 1982
- Bhattacharyya, B.K., Reduction and treatment of magnetic anomalies of crustal origin in satellite data, J. Geophys. Res., v. 82, p. 3379, 1977
- Carmichael, R.S., Depth calculation of piezomagnetic effect for earthquake prediction, Earth and Plan. Sci. Lett., v. 36, p. 309-316, 1977
- Carmichael, R.S., Magnetic properties of minerals and rocks, Chapter (p. 229-287) in Volume II of Handbook of Physical Properties of Rocks, CRC Press Inc., edited by Robert S. Carmichael, 1982
- Chase, C. and T. Gilmer, Precambrian plate tectonics: the Midcontinent gravity high, Earth and Plan. Sci. Lett., v. 21, p. 70, 1973
- Craddock, C., Keweenawan geology of east-central and southeastern Minnesota, in Geology of Minnesota: a Centennial Volume, Minnesota Geological Survey, p. 416-424
- Docekal, J., Earthquakes of the stable interior with emphasis on the midcontinent, Ph.D. Thesis, Univ. of Nebraska/Lincoln, 1970
- Frey, H., Magsat scalar anomaly distribution: the global perspective, Geophys. Res. Lett., v. 9, p. 277, 1982a
- Frey, H., Magsat scalar anomalies and major tectonic boundaries in Asia, Geophys. Res. Lett., v. 9, p. 299, 1982b
- Gallagher, S.C. and M.A. Mayhew, On the possibility of detecting large-scale crustal remanent magnetization with Magsat vector magnetic anomaly data, Geophys. Res. Lett., v. 9, p. 325, 1982
- Goswold, W.D., Preliminary heat flow data from Nebraska (abstract), EOS Trans. A.G.U., v. 61, p. 1193, 1980; and W.D. Goswold and D. Ever-
soll, Usefulness of heat flow data in regional assessment of low-

- temperature geothermal resources with special reference to Nebraska, Geothermal Resources Council Trans., v. 5, p. 1, Oct. 1981
- Green, A.G., Interpretation of Project MAGNET aeromagnetic profiles across Africa, Geophys. J. Roy. Astron. Soc., v. 44, p. 203-228, 1976
- Green, J.C., Geologic and geochemical evidence for the nature and development of the Middle Proterozoic (Keweenaw) midcontinent rift of North America, Tectonophysics, v. 94, p. 413, 1983
- Haggerty, S.E., The aeromagnetic mineralogy of igneous rocks, Can J. Earth Science, v. 16, p. 1281-1293, 1979
- Hall, D.H., Long-wavelength aeromagnetic anomalies and deep crustal magnetization in Manitoba and northwestern Ontario Canada, J. Geophys., v. 40, p. 403-430, 1974
- Hastings, D.A., Preliminary correlations of Magsat anomalies with tectonic features of Africa, Geophys. Res. Lett., v. 9, p. 303, 1982
- Hildenbrand, T.G., R. Kucks and R. Sweeney, Digital magnetic anomaly map of the central U.S.: description of major features, U.S. Geol. Survey Map GP-955, 1983
- Hutchison, C.S., Economic Deposits and their Tectonic Setting, J. Wiley and Sons, 1983, e.g. p. 214-222
- Keller, G.R., E. Lidiak, W. Hinze and L. Braille, The role of rifting in the tectonic development of the midcontinent USA, Tectonophysics, v. 94, p. 391, 1983
- Krutikhovskaya, Z.A. and I.K. Pashkevich, Magnetic model for the Earth's crust under the Ukrainian shield, Can. J. Earth Sci., v. 14, p. 2718-2728, 1977
- Langel, R.A., Near-earth satellite magnetic field measurements: a prelude to Magsat, EOS Trans. A.G.U., v. 60, p. 667, Sept. 1979
- Langel, R.A., Magsat scientific investigations, Johns Hopkins APL Technical Digest, v. 1, p. 214, 1980
- Langel, R.A. and H. Frey, A reduced-to-pole satellite anomaly map of the world and its relationship to global tectonics (abstract), EOS Trans. A.G.U., v. 64, p. 214, May 1983
- Langel, R.A., G. Ousley, J. Berbert, J. Murphy and M. Settle, The Magsat mission, Geophys. Res. Lett., v. 9, p. 243, 1982a
- Langel, R.A., J.D. Phillips and R.J. Horner, Initial scalar magnetic anomaly map from Magsat, p. 269; and Initial vector magnetic anomaly map from Magsat, p. 273; both in Geophys. Res. Lett., v. 9, 1982b

- Mayhew, M.A., An equivalent layer magnetization model for the U.S. derived from satellite-altitude magnetic anomalies, *J. Geophys. Res.*, v. 87, p. 4837, 1982
- Mayhew, M.A. and S. Galliher, An equivalent layer magnetization model for the U.S. derived from Magsat data, *Geophys. Res. Lett.*, v. 9, p. 311, 1982
- Mayhew, M.A., H. Thomas and P. Wasilewski, Regional modeling--the Kentucky anomaly, in *NASA Techn. Memo 80642*, ed. by L. Carpenter, p. 2-37 to 2-43, Jan. 1980; and Satellite and surface geophysical expression of anomalous crustal structure in Kentucky and Tennessee, *Earth and Plan. Sci. Lett.*, v. 58, p. 395, 1982
- Nulman, A., V. Shapiro, S. Maksimovskikh, N. Ivanov, J. Kim and R.S. Carmichael, Magnetic susceptibility of magnetite under hydrostatic pressure and implications for tectonomagnetism, *J. Geomag. and Geoelect.*, v. 30, p. 585-592, 1978
- Ocola, L.C. and R.P. Meyer, Central North American Rift system--1. Structure of the axial zone from seismic and gravimetric data, *J. Geophys. Res.*, v. 78, p. 5173, 1973
- Pesonen, L.J. and H.C. Halls, Thellier paleointensity determinations of late Precambrian Keweenawan rocks (abstract), *Proc. Europ. Geophys. Soc./Europ. Seismol. Comm. Assembly*, Leeds U.K., 1982
- Regan, R.D. and B.D. Marsh, The Bangui magnetic anomaly, *J. Geophys. Res.*, v. 87, p. 1107, 1982
- Regan, R.D., J.C. Cain and W.M. Davis, A global magnetic anomaly map, *J. Geophys. Res.*, v. 80, p. 794, 1975
- Sailer, R.V., A. Lazarewicz and R.F. Brammer, Spatial resolution and repeatability of Magsat crustal anomaly data over the Indian Ocean, *Geophys. Res. Lett.*, v. 9, p. 289, 1982
- Schlenger, C.M., B.D. Marsh and P. Wasilewski, The magnetic petrology of the deep crust and the interpretation of regional magnetic anomalies (abstract), *EOS Trans. A.G.U.*, v. 64, p. 213, May 1983
- Schnetzler, C.C. and R.J. Allenby, Estimation of lower crust magnetization from satellite-derived anomaly field, *Tectonophysics*, v. 93, p. 33, 1983
- Thomas, H., *NASA Techn. Memo. 85075*, Goddard Space Flight Center, July 1983
- Tooker, E.W., Preliminary map of copper provinces in the conterminous U.S., Report 79-576D, U.S. Geol. Survey, 1980; E.W. Tooker and

- H. Wedow, Preliminary map of zinc provinces in the conterminous U.S., Report 79-576Q, U.S. Geol. Survey, 1980; E.W. Tooker and H. Morris, Preliminary map of lead provinces in the conterminous U.S., Report 79-576P, U.S. Geol. Survey, 1980
- Van Schmus, W.R. and M.E. Bickford, Proterozoic chronology and evolution of the midcontinent region North America, ch. 11 (p. 261-296) in Precambrian Plate Tectonics, A. Kroner ed., Elsevier Publ. Co., 1981
- Von Frese, R.R., W.J. Hinze and L. Braile, Spherical Earth analysis and modeling of lithospheric gravity and magnetic anomalies, NASA Techn. Memo. 80709, Goddard Space Flight Center, May 1980
- Von Frese, R., W. Hinze, J. Sexton and L. Braile, Verification of the crustal component in satellite magnetic data, *Geophys. Res. Lett.*, v. 9, p. 293, 1982a
- Von Frese, R., W. Hinze and L. Braile, Regional North American gravity and magnetic anomaly correlations, *Geophys. J. Roy. Astron. Soc.*, v. 69, p. 745-761, 1982b
- Wasilewski, P.J., H. Thomas and M. Mayhew, The Moho as a magnetic boundary, *Geophys. Res. Lett.*, v. 6, p. 541, 1979
- Wasilewski, P.J. and M. Mayhew, Crustal xenolith magnetic properties and long-wavelength anomaly source requirements, *Geophys. Res. Lett.*, v. 9, p. 329, 1982
- Woollard, G.P. and H. Joesting, Bouguer gravity map of the U.S., U.S. Geol. Survey, 1964
- Zietz, I., F. Gilbert and J. Kirby, Aeromagnetic map of Iowa, Map GP-910 and 911, U.S. Geol. Survey, 1976
- Zietz, I. and R. Hatcher, The first magnetic map of the U.S.: a crustal interpretation (abstract), *EOS Trans. A.G.U.*, v. 64, p. 320, May 1983

PROJECT-RELATED PUBLICATIONS

The availability of Magsat data and anomaly maps provides opportunities for research and publications that will continue for some time to come. Some communicated and published results to date are included below. They relate to analysis and use of Magsat anomaly data, and interpretation of U.S. midcontinent geology and geophysics. They are by staff and students, in collaborative efforts of the University's Department of Geology and the State Geological Survey.

- Anderson, R. R. and R. Black, Geophysical interpretation of the geology of the central segment of the Midcontinent Geophysical Anomaly (abstract), Ann. Midwest Meeting of American Geophysical Union, Minneapolis Minn., Sept. 1981; and see abstract in EOS Trans. AGU, p. 615, Aug. 1982
- Anderson, R. R. and R. Black, Early Proterozoic development of the southern Archean boundary of the Superior province in the Lake Superior region (abstract), Ann. Meeting of Geological Society of America, Indianapolis Indiana, Oct. 1983
- Black, R. A. and R. S. Carmichael, Analysis and use of Magsat satellite magnetic data to help interpret crustal character of U.S. central Midcontinent (abstract), Fourth Scientific Assembly. of Internat. Assoc. of Geomagnetism and Aeronomy (and NASA Magsat meeting), Edinburgh, Aug. 1981
- Black, R. A., Geophysical processing and interpretation of Magsat satellite magnetic anomaly data over the U.S. Midcontinent, M.S. Thesis, University of Iowa, Nov. 1981
- Carmichael, R. S., Magnetic properties of minerals and rocks, chapter (p. 229-287) in Volume II of Handbook of Physical Properties of Rocks, CRC Press Inc., edited by Robert S. Carmichael, Vol. I and II published in 1982, Vol. III in press
- Carmichael, R. S., R. A. Black, and R. A. Hoppin, Use of Magsat satellite data to interpret crustal geology, structure, and geophysical properties of the U.S. central Midcontinent, Fourth Internat. Conference on Tectonics, Oslo Norway, Aug. 1981
- Carmichael, R. S. and R. Black, Use of Magsat satellite magnetic anomaly data to interpret crustal character and resource potential of the U.S. midcontinent (abstract), Ann. Meeting of Soc. of Exploration Geophysicists (special Magsat session), Dallas, Oct. 1982
- Carmichael, R. S. and R. A. Black, Analysis and use of Magsat satellite magnetic data for interpretation of crustal character in the U.S. midcontinent, in preparation, for Magsat compilation in special issue of J. of Geophysical Research, 1984
- Mohan, M., Crustal studies using satellite magnetic data over the Indian subcontinent region, M.S. Thesis in progress, University of Iowa

APPENDIX A: Abstracts of Project-related Publications

(chronological)

- paper, 4th Scientific Assembly of Internat. Assoc. of Geomagnetism and Aeronomy, Aug. 1981
- paper, 4th Internat. Conference on Tectonics, Aug. 1981
- paper, Ann. Midwest Meeting of American Geophysical Union, Sept. 1981
- paper, Ann. Meeting of Soc. of Exploration Geophysicists, Oct. 1982
- chapter in "Handbook of Physical Properties of Rocks", CRC Press, 1982
- paper, Ann. Meeting of Geological Soc. of America, Oct. 1983

February 10, 1981

Department of Geology
Trowbridge Hall



1847

Abstract for: 4th Scientific Assembly of Internat. Assoc. of
Geomagnetism and Aeronomy
August 3-15, Edinburgh Scotland
To: Dr. N. Fukushima, Geophysics Research Lab,
University of Tokyo, Tokyo 113, Japan
From: Robert S. Carmichael, Department of Geology
University of Iowa, Iowa City, Iowa USA 52242
Session: I-1 (Scientific Results from the MAGSAT Mission), Aug. 4-5
Convenor (and copy of abstract sent to):
Dr. R. A. Langel, Code 922, Goddard Space Flight Center,
Greenbelt, Maryland USA 20771
Presentation: Oral or Poster
Special request: prefer session indicated (I-1), since speaker may not
be at meeting during 2nd week of IAGA

ANALYSIS AND USE OF "MAGSAT" SATELLITE MAGNETIC DATA TO
HELP INTERPRET CRUSTAL CHARACTER OF U.S. CENTRAL MIDCONTINENT

R. A. BLACK (Iowa Geological Survey, Iowa City, Iowa USA)

R. S. CARMICHAEL (Department of Geology, University of Iowa,
Iowa City, Iowa USA 52242)

NASA's MAGSAT satellite measured magnetic fields from October 1979 until June 1980. The processed magnetic data yield long-wavelength anomalies that arise from crustal and upper-mantle sources. Interpretation of the anomalies, done in conjunction with correlative data such as gravity and aeromagnetism, heat flow and geothermal gradients, and known nearsurface geology, can lead to better understanding of major deep-seated geologic structures and crustal composition. Such work has application to resource exploration, as well as to geotectonics. As part of the NASA project to investigate and use the MAGSAT data, we are developing analysis techniques to help interpret the structure and character of the lithosphere in central North America. The region includes the "Midcontinent Gravity Anomaly" paleorift zone (1200 km long, 80 km wide, intruding 1.1 billion years ago) and the New Madrid rift/seismic zone, both of which are of paleotectonic and neotectonic interest. Our preliminary analysis of the initial MAGSAT data, combined with correlative geological and geophysical data, shows the utility of the satellite data for regional crustal and basement study. Work in progress supported in large part by NASA contract NAS5-26425.

The University of Iowa

Iowa City, Iowa 52242

U.S.A.

ORIGINAL PAGE IS
OF POOR QUALITY



Department of Geology
Trowbridge Hall

January 25, 1981

Abstract for: 4th International Conference on Basement Tectonics
August 10-14, Oslo Norway

To: Roy Gabrielsen, Dept. of Geology, University of Oslo
P. O. Box 1047, Blindern, Oslo 3, Norway

For: Poster or oral presentation

From: Robert S. Carmichael, Department of Geology, University of Iowa
Iowa City, Iowa U.S.A. 52242

Suggested session: S5 (Regional Studies I), August 13th

Use of MAGSAT satellite data to interpret crustal geology, structure,
and geophysical properties of the U.S. central Midcontinent

R. S. Carmichael, R. A. Black, and R. A. Hoppin

Department of Geology, University of Iowa
Iowa City, Iowa U.S.A.

NASA's MAGSAT satellite measured magnetic fields from Oct. 1979 until June 1980. The processed magnetic data yield long-wavelength anomalies that arise from crustal and upper mantle sources. Interpretation of the anomalies, done in conjunction with correlative data such as gravity and aeromagnetics, heat flow and geothermal gradients, and known nearsurface geology, can lead to better understanding of major deep-seated geologic structures and crustal composition. Such work has application to resource exploration, as well as geotectonics. As part of the NASA project to investigate and use the MAGSAT data, we are developing analysis techniques to help interpret the structure and character of the lithosphere in central North America. The region includes the "Midcontinent Gravity Anomaly" paleorift zone (1200 km long, 80 km wide, intruding 1.1 billion years ago) and the New Madrid rift/seismic zone, both of which are of paleotectonic and neotectonic interest. Our preliminary analysis of the initial MAGSAT data, combined with correlative geological and geophysical data, shows the utility of the satellite data for regional crustal and basement study.

Abstract for Ann. Midwest Meeting of American Geophysical Union,
Minneapolis Minn., Sept. 1981 (from EOS Trans. A.G.U., p. 615,
August 1982)

GEOPHYSICAL INTERPRETATION OF THE GEOLOGY OF THE
CENTRAL SEGMENT OF THE MIDCONTINENT GEOPHYSICAL
ANOMALY

R. R. Anderson

R. A. Black (both at: Iowa Geological Survey,
Iowa City Iowa 52242)

The midcontinent Geophysical Anomaly (MGA) is a pronounced linear gravity high with flanking gravity lows stretching from northern Lake Superior to central Kansas. The anomaly is created by a central basalt-dominated horst, bounded on the east and west by deep, clastic-filled basins. It is divided into three distinct sections, separated by apparent transform faults into northern, central and southern segments. The central segment, the majority of which lies in Iowa, displays measured Bouguer gravity anomaly values ranging from greater than +67 mgals to less than -113 mgals. In this study the Bouguer gravity anomaly and aeromagnetic field of 19 profiles across the central segment of the MGA have been modeled. These models provide estimates of the thickness of the basalt-dominated volcanics of the central horst (locally greater than 12,000 m), location of the high-angle faults which bound the horst, and determination of the geometry of the clastic-filled marginal basins which reach maximum depths in excess of 10,000 m. This is the most detailed examination of this portion of the MGA yet undertaken.

Abstracts of papers presented at the 52nd Annual International SEG Meeting, October 17-21, 1982 in Dallas.

Magsat Session

Magsat Mission: Crustal Studies

Results of the Magsat Mission

M. Settle, NASA, and R. Langel,
Goddard Space Flight Center

MAG1

The Magsat satellite mission obtained worldwide measurements of magnetic field strength with an accuracy and spatial resolution that surpassed all previous global surveys. In addition, Magsat was the first satellite to measure directional characteristics of the earth's magnetic field on a global basis. Magsat carried a scalar magnetometer capable of measuring total field strength to an accuracy of ± 3 gammas, and a vector magnetometer capable of measuring component field strength in three orthogonal directions to an accuracy of ± 6 gammas. Total altitudes of 350-560 km over a $7\frac{1}{2}$ products are improved spherical main (core) field, and crustal an wavelength variations in the crust are available through the National Goddard Space Flight Center, G

Data Selection Techniques of Magsat Data Over Australia

B. David Johnson and C. N. G. Macquarie Univ., Australia

The Magsat data require critical self-consistent data set suitable for interpretation. The interactive procedures described in this paper, involve the oriented data base and a color graphics employed to select profiles that lie at minimum altitude, and satisfy various criteria. The initial scan selects profiles which have their perigee (lowest altitude of orbit) within the survey region. Subsequent scans through the data are made to select profiles that contain data below a given altitude. Each profile selected by these automatic search criteria is displayed for visual validation. Various interactive procedures are available to remove data spikes, trim the ends of the profile, and detrend the data values. This corrected profile data may then be compared with other profiles already in the data base and then finally stored in the data base if selected. The large degree of redundancy in the Magsat data enables the rejection of noisy or bad profiles and the detection of time-varying effects in the data.

Large-Scale Crustal Magnetization Models Derived from Satellite Magnetic Anomaly Data

MAG3

M. A. Mayhew, BTS, Inc.

An equivalent layer magnetization model for the U.S. and environs derived from Magsat total field anomaly data is presented. Information contained in such a model is essentially lateral variation, to a certain limit of resolution, in the vertical integral of magnetization from the earth's surface to the Curie isotherm. Resolution for the described technique and Magsat data is about 200 km dipole spacing. Apparent magnetization variations are due to Curie isotherm depth variations, regional variations in crustal magnetic properties, or to discrete mafic plutonic complexes. In the western U.S., the first effect appears to dominate. Excellent correlations between apparent magnetization and large-scale tectonic provinces, including the Colorado plateau, the Rio Grande rift, the Wichita uplift, the south end of the Midcontinent rift, the achita belt, and the

Use of Magsat Satellite Magnetic Anomaly Data to Interpret Crustal Character and Resource Potential of the U.S. Midcontinent

MAG5

Robert S. Carmichael and Ross Black, Univ. of Iowa

The assessment of future resources of petroleum, minerals, and geothermal energy, is best served by an exploration strategy that

467

combines geophysical exploration with geologic interpretation of the structure, composition, and thermal and tectonic development of the earth's upper crust. A promising tool for reconnaissance exploration of the crust and its energy and resource potential is the use of satellite sensing and measurements. NASA's Magsat satellite measured in 1980 the earth's long-wavelength magnetic field anomalies arising from major crustal sources. Acquired at altitudes of 350-560 km, the data provide global coverage with resolution not previously achieved by satellite sensing. Magsat anomalies have a magnitude range up to 26 gammas, and a magnetic-source resolution of about 150-200 km.

ita MAG4

at State Univ. elements as long wavelength in the residual total field. orbital drift while retaining a best-fit first-order effect of the altitude road scale anomalies, we common altitude by using a station. To interpret these terms, we devise a model of magnetization in additional matrix of rectangular

is used to represent the variation of the magnetic susceptibility, which eventually vanishes at the Curie depth. Both of these new methods are verified to be effective for the simulated anomalies. The results from the actual data must be compatible with such surface data as Magnet U.S. aeromagnetic data or a crustal model based on the seismic profiles.

ORIGINAL PAGE IS
OF POOR QUALITY

the field at
the series
the size of
tion of the
y to sets of
crustal appli-
this paper.
terly done.
agnet U.S.
igure 2. On
initially the

assumed a
magnetized
ization in a
assumed to

ie depth in
a method to
ually van-
3-D matrix
a magnetic
ck the size
each side
ne can be

(2)

e between
ceptibility

oximately
rs to tens
ation (2)
he blocks
te data to
This fact
ta at least
etermine
ch block.
region to
previous
nd vector
suscepti-
erified to

be effective up to the number of blocks 351 using a simulated data set for a simple theoretical anomaly.

References

- Bhattacharyya, B. K., 1964, Magnetic anomalies due to prism-shaped bodies with arbitrary polarization: *Geophysics*, v. 29, p. 517-531.
———, 1977, Reduction and treatment of magnetic anomalies of crustal origin in satellite data: *J. Geophys. Res.*, v. 82, p. 3379-3390.
Henderson, R. G., and Cordell, L., 1971, Reduction of unevenly spaced potential field data to a horizontal plane by means of finite harmonic series: *Geophysics*, v. 36, p. 856-866.
Langel, R., Berbert, J., Jennings, T., and Homer, R., 1981, Magsat data processing: A report for investigators, NASA tech. memo. 82160, November.
Mayhew, M. A., 1979, Inversion of satellite magnetic anomaly data: *J. Geophys.*, v. 45, p. 119-128.
Won, I. J., and Son, K. H., 1982, A preliminary comparison of the MAGSAT data and aeromagnetic data in the continental U.S.: *Geoph. Res. Letter* (in press).

Use of Magsat Satellite Magnetic Anomaly Data to Interpret Crustal Character and Resource Potential of the U.S. Midcontinent

MAG5

Robert S. Carmichael and Ross Black, Univ. of Iowa Summary

The assessment of future resources of petroleum, minerals, and geothermal energy, is best served by an exploration strategy that combines geophysical exploration with geologic interpretation of the structure, composition, and thermal and tectonic development of the earth's upper crust. A promising tool for reconnaissance exploration of the crust and its energy and resource potential is the use of satellite sensing and measurements. NASA's Magsat satellite measured in 1980 the earth's long-wavelength magnetic field anomalies arising from major crustal sources. Acquired at altitudes of 350-560 km, the data provide global coverage with resolution not previously achieved by satellite sensing. Magsat anomalies have a magnitude range up to 26 gammas, and a magnetic-source resolution of about 150-200 km.

The satellite data, used in conjunction with correlative geophysical and geological data such as aeromagnetics, gravity, Landsat imagery, and near-surface geology can lead to better understanding of major deep-seated geologic structure and conditions and the associated potential for the localization of energy and mineral resources. With the central U.S. as a study area, we have been investigating the use and applicability of the satellite magnetic data in interpreting the midcontinent's crustal structure and composition. The anomaly data set has been derived by processing the original satellite data, reducing to a $1^\circ \times 1^\circ$ latitude/longitude grid at a common altitude datum of 400 km, applying wavelength filtering, and then reducing the data "to the pole" to aid in interpretation. The major anomalous features are a magnetic high over Kentucky, a high over northern Texas and extending to the northeast towards Lake Michigan, and magnetic lows over the Mississippi embayment, and South Dakota. These features are interpreted in terms of variation in crustal thickness, depth of Curie-temperature isotherm, and petrologic variation between different geologic provinces. Supporting information is provided by gravity anomalies, and crustal thickness as determined from regional seismic data.

Abstract

Exploration for future supplies of energy fuels (oil, gas), mineral resources, and geothermal energy, will be best pursued by combining geophysical prospecting with geologic interpretation of the structure, petrologic character, tectonic history, and thermal and chemical condition of the earth's crust. A promising tool for aiding in reconnaissance exploration of energy and resource pro-

inces, and potential localization of economic objectives, is the use of satellite sensing and measurements.

NASA's Magsat satellite measured in 1980 the earth's magnetic field anomalies arising from major crustal sources. This was the first satellite to measure component-field (i.e., X, Y, Z) data to yield relatively low-altitude global magnetic anomaly maps. These maps have a resolution not previously achieved by satellite magnetic-field surveying. The satellite operated at altitudes of 350-560 km, mapped anomalies having a magnitude range up to 26 gammas (nanoteslas), and yielded a magnetic source resolution of about 150-200 km.

The satellite magnetic data, and resulting maps, constitute a new aid for interpreting the crust of the earth and as a reconnaissance component in a geophysical exploration strategy. They can be integrated with correlative geophysical and geologic data sets such as aeromagnetics, gravity coverage, Landsat remote sensing imagery, and near-surface geology. This can lead to a better understanding of crustal geologic structure and composition, and the associated energy and mineral resource potential. The long-wavelength magnetic anomalies measured at satellite elevations are expected to reflect differences in crustal thickness, the petrologic character and properties of major geologic provinces, and variations in geothermal gradient and thus the depth of the Curie-temperature isotherm.

With the central U.S. as a study area, we have been investigating the applicability of satellite magnetic data in interpreting the midcontinent's crustal geologic structure and composition. NASA/Goddard Space Flight Center has provided Magsat data as measured along the satellite tracks, with some preliminary corrections applied. We then did computer processing and analysis of the data set, with steps including: (1) removal of spurious data points, arising from the data acquisition process rather than from terres-

trial sources; (2) statistical smoothing, comparison, and correlation of individual data tracks, to reduce the effect of geomagnetic temporal and transient disturbances; (3) reduction of data by weighted averaging to a grid with $1^\circ \times 1^\circ$ latitude/longitude spacing, with altitudes interpolated and weighted to a common datum elevation of 400 km (from the orbit range of 350-560 km); (4) wavelength filtering, to remove (or retain) anomaly features of desired wavelengths; and (5) reduction of the anomaly map "to the magnetic pole" to compensate for variation of magnetic inclination with latitude and aid in interpreting the anomalies with respect to causative crustal features.

Figure 1 shows the Magsat anomaly map we extracted from the data for the central U.S. Here, as for subsequent figures, it is for magnitude (i.e., scalar) data, as calculated from the X, Y, and Z-component vector data as measured by the satellite. The actual area of processed data is about 50 percent larger than shown, and this belt-way around the study area was used to prevent "edge effects" in the processing to follow.

Figure 2 shows the previous map, now filtered with a low-cut wavelength filter which removes wavelengths less than about 400 km. This map has similarities to maps of some previous satellite studies over the U.S., but is more detailed and revealing because of (1) the care taken in removing bad data points and tracks, and comparing profiles to optimize data reliability, and (2) treating the data on a finer $1^\circ \times 1^\circ$ grid rather than the customary but coarser $2^\circ \times 2^\circ$ grid spacing often used for global-scale maps. For comparison, Figure 3 shows the Magsat anomaly map as derived by NASA (March 1981) from a preliminary global data set. There is less detail in the latter, and it is a prime purpose of our study to assess, for prospective resource exploration and crustal interpretation, how far the satellite magnetics resolution can be extended by data processing and analysis.

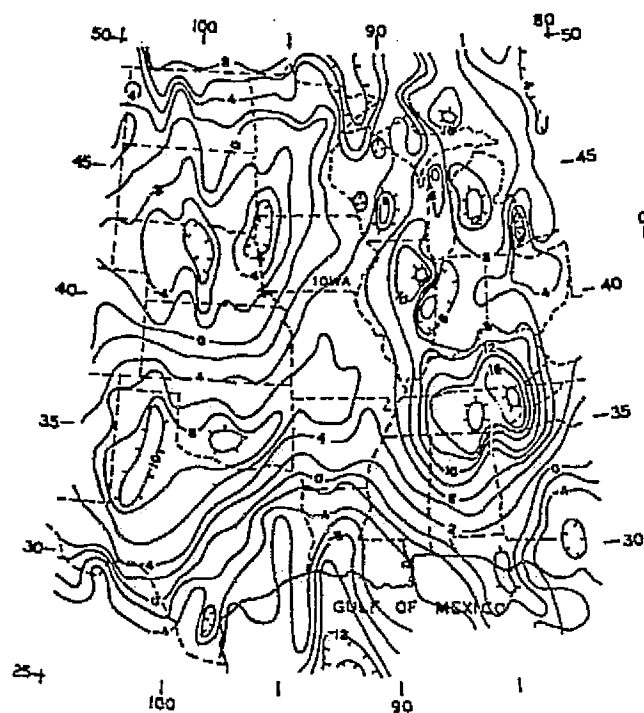


Fig 1. $1^\circ \times 1^\circ$ weighted-averaged Magsat scalar (magnitude) data, for the U.S. midcontinent. Albers equal-area projection; contour interval of 2 gammas. Plot by Black (1981).

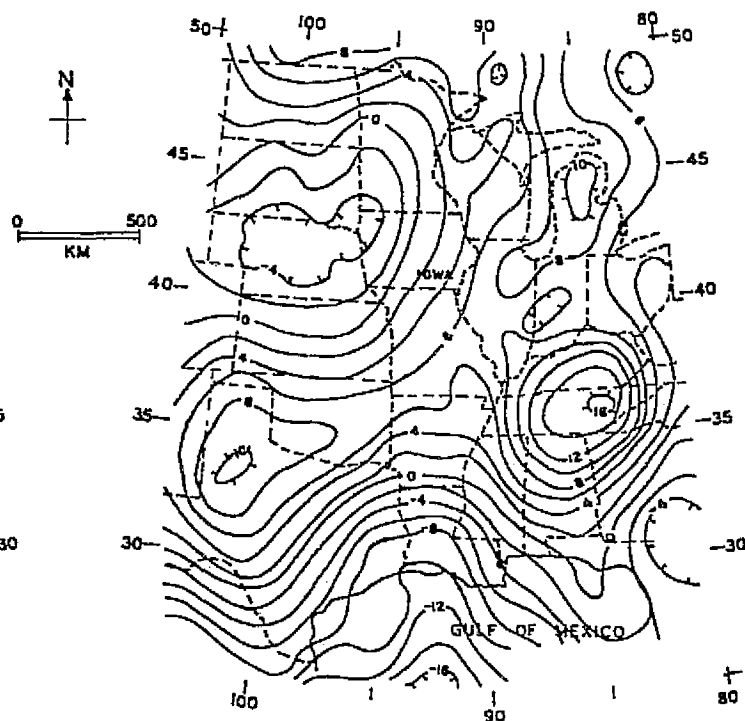


Fig 2. Low-cut (400 km) wavelength-filtered scalar data of Figure 1. Contour interval of 2 gammas.

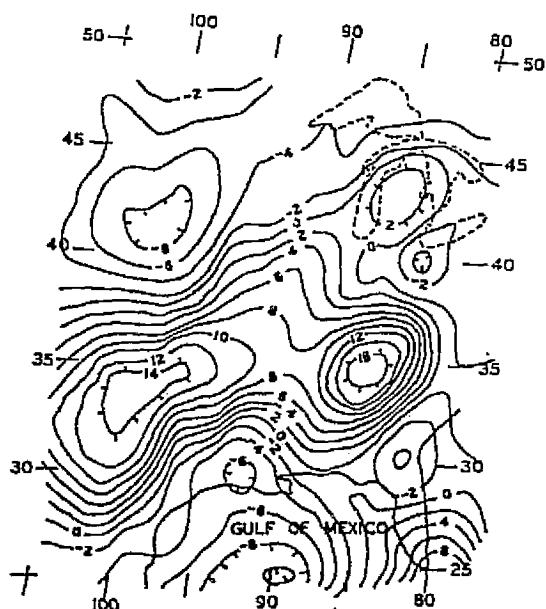


Fig. 3. NASA's preliminary Magsat scalar anomaly map. Data from below 400 km altitude, on $2^\circ \times 2^\circ$ blocks. Contour interval of 2 gammas. Zero-level is arbitrary.

Figure 4 shows the data of Figure 2, now reduced to the magnetic pole. The alteration is not dramatic, because of the relatively high magnetic latitude (about $45\text{--}65^\circ$ N.) of the study area with respect to the north magnetic pole. The major magnetic highs have been shifted north—the north Texas one up to the Oklahoma border, and the Tennessee one up into Kentucky.

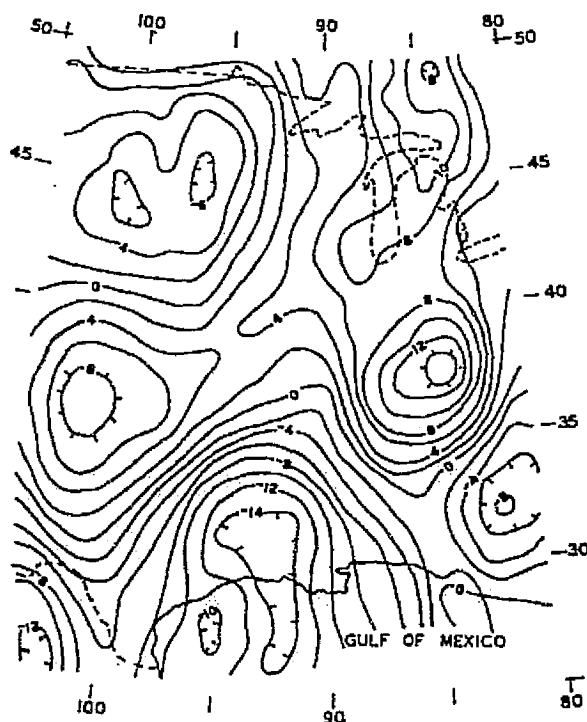


Fig. 4. $1^\circ \times 1^\circ$ scalar data at 400 km altitude, high-pass filtered and reduced to the magnetic pole. Contour interval of 2 gammas. Zero-level is arbitrary. Plot by Black (1981).

Several major anomalous features are observed on the processed scalar magnitude map (Black, 1981) of Figure 4. They are: (1) a bulls eye magnetic high over Kentucky, as noted on previous POGO satellite data and interpreted by others as due to a mafic basement rock complex and intrusion in the lower crust; (2) an arcuate magnetic high extending from its maximum over northern Texas up to the northeast and the Lake Michigan area, probably originating from a zone of greater crustal thickness developed in late Precambrian time; (3) a magnetic low over the Mississippi embayment/rift, as noted by others and having an origin associated with a combination of crustal thinning accompanying failed (paleo)rifting, petrologic character of the lower crust, and elevated Curie-temperature isotherm; and (4) a magnetic low over South Dakota.

Supporting correlative information for this study of satellite magnetic anomaly data includes the distribution of basement rock provinces, gravity anomaly data, and crustal thickness as determined from regional seismic data. For example, in the midcontinent region the areas of thicker crust (i.e., thickness over 45 km) are those with the magnetic highs on the satellite map—north Texas/Oklahoma, and Kentucky/Tennessee.

This work is supported in large part by a NASA/Goddard Space Flight Center contract.

ORIGINAL PAGE IS
OF POOR QUALITY

ORIGINAL PAGE IS
OF POOR QUALITY

Handbook of Physical Properties of Rocks Volume II

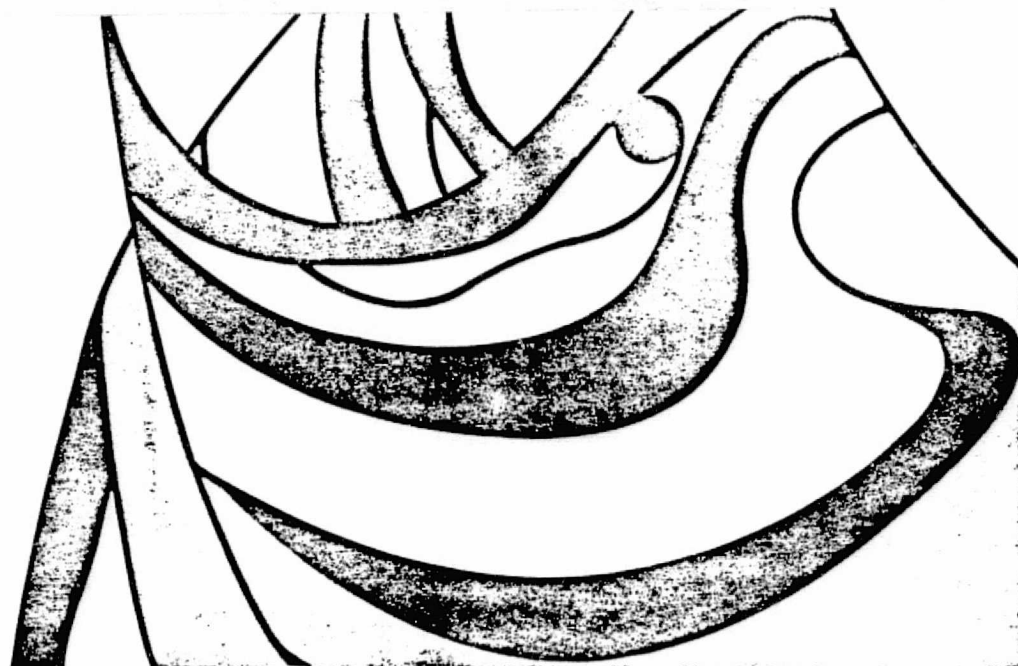
Editor

Robert S. Carmichael, Ph.D.
Head, Geophysics Program
Department of Geology
University of Iowa
Iowa City, Iowa



CRC Press, Inc.
Boca Raton, Florida

New Titles in SPACE SCIENCE and METEOROLOGY



CRC PRESS, INC.
2000 Corporate Blvd., N.W.
Boca Raton, Florida 33431

CRC Handbook of CHEMISTRY and PHYSICS 63rd Edition

Edited by ROBERT C. WEAST, Ph.D., Vice President, Research, (Retired).
Consolidated

CRC Handbook of For access MATERIALS SCIENCE fingertip Handbo

The CRC Handbook of Materials Science is a current, readily accessible guide to the physical properties of solid state and structural materials. Interdisciplinary in approach and content, it covers a broad variety of types of materials, including materials of present commercial importance plus new biomedical, composite, and laser materials. In view of the importance of having critically evaluated property data available on materials in order to solve modern problems, this handbook is published to fill the gap between single material class and general reference works, with only limited property and classification data on materials. Updated Selected 7 x 10, 1982, utilizing a largely tabular format for easy reference and comparability of various properties, this reference is of use to those seeking information on materials outside their specialized field of competence as well as for experts in the field seeking detailed property data.

Volumes I, II, and III Edited by CHARLES T. LYNCH, Ph.D., Senior Scientist, U.S.A.F., Air Force Materials Laboratory, Wright-Patterson AFB.

Volume I GENERAL PROPERTIES

400 pp., 7 x 10, 1974, ISBN-0-87819-231-X.

SECTION 1 — THE ELEMENTS.

SECTION 2 — ELEMENTAL PROPERTIES.

SECTION 3 — MISCELLANEOUS TABLES OF PHYSICAL PROPERTIES.

SECTION 4 — CONVERSION TABLES, MISCELLANEOUS MATERIALS PROPERTIES AND BINARY PHASE INFORMATION.

SECTION 5 — MATERIALS STANDARDS: Analytical Standards, General Standards, Tables of Specific Compositional Standards.

WALL CHART* — Large 3 1/2' x 2 1/4' multi-colored chart, "Summary of Binary Phase Diagrams."

Additional charts available at \$5.00 each catalog 0200ZN.

Catalog no. 0231ZN, \$76.50
Outside U.S. \$88.00

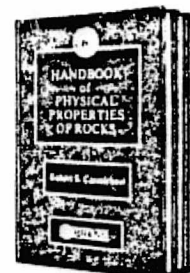
Volume II METALS COMPOSITES

CRC PRESS, INC.
2000 Corporate Blvd., N.W.
Boca Raton, Florida 33431

BULK RATE
U.S. POSTAGE

1983

ORIGINAL PAGE IS
OF POOR QUALITY



CRC Handbook of PHYSICAL PROPERTIES of ROCKS

Edited by ROBERT S. CARMICHAEL, Ph.D., Professor of Geophysics, Department of Geology, University of Iowa, Iowa City.

- Current Data
- Tabular Format

Reliable, comprehensive data on various properties of rocks, minerals, and other related materials is compiled in an organized manner. Format is largely tabular for easy use in comparison and referencing. Chapters are written by recognized experts working in education, industry, and government. The information is of particular value to those in geology, geophysics, materials engineering, and allied fields.

VOLUME I: Mineral Composition: Chemical composition and properties of rocks, minerals, and crystals, pore fluids, ores, coal, petroleum, Earth's crust, meteorites. **Electrical Properties:** Resistivity and dielectric constants of minerals, dry and wet rocks, sedimentary rock sequences, Earth's interior. **Spectroscopic Properties:** Absorption/transmission, reflectance and emission, and spectral characteristics of minerals and rocks in the visible and infrared range. 416 pp., 7 x 10, 1982, ISBN-0-8493-0226-9.

Catalog no. 0226ZN, \$69.50
Outside U.S., \$80.00

VOLUME II: Seismic Velocities: Compressional and shear wave velocities for rocks, minerals, marine sediments, Earth's crust, ice; variation with fluid saturation, pressure and temperature. **Magnetic Properties:** Properties of magnetic minerals and rocks, and their variation with different parameters. **Engineering Properties:** Factors, tests, and properties relating to rock appraisal, characterization, and assessment of hardness, strength, and deformation. 360 pp., 7 x 10, 1982 ISBN-0-8493-0227-7.

Catalog no. 0227ZN, \$64.00
Outside U.S., \$74.00

ORIGINAL PAGE IS
OF POOR QUALITY.

CRC PRESS

HANDBOOK OF PHYSICAL PROPERTIES OF ROCKS

Editor: Robert S. Carmichael

Table of Contents

<u>Volume I</u>	(published 1982)	<u>416 pages</u>
Mineral Composition of rocks		
-- Kenneth F. Clark, Geology, University of Texas/El Paso		
Electrical Properties of rocks and minerals		
-- George V. Keller, Geophysics, Colorado School of Mines		
Spectroscopic Properties of rocks and minerals		
-- Graham R. Hunt, Petrophysics & Remote Sensing, U.S.G.S.		
<u>Volume II</u>	(published 1982)	<u>360 pages</u>
Seismic Velocities		
-- Nikolas I. Christensen, Geological Sciences, Univ. of Washington		
Magnetic Properties of minerals and rocks		
-- Robert S. Carmichael, Geology, University of Iowa		
Engineering Properties of rocks		
-- Allen W. Hatheway, Mining Petrol. & Geol. Engineering, Univ. of Missouri		
-- George A. Kiersch, Cornell University (emeritus)		
<u>Volume III</u>	(in press)	<u>380 pages</u>
Density of rocks and minerals		
-- Gordon R. Johnson and Gary R. Olhoeft, Petrophysics and Remote Sensing, U.S.G.S./Denver		
Elastic Constants of minerals		
-- Orson L. Anderson, Geophysics & Planetary Physics, U.C.L.A.		
-- Yoshio Sumino, Earth Sciences, Nagoya University		
Mechanical Properties (Inelastic)		
-- Stephen H. Kirby, Earthquake Office, U.S.G.S./Menlo Park		
-- John W. McCormick, State University of N.Y./Plattsburgh		
Radioactivity Properties of minerals and rocks		
-- W. Randall Van Schmus, Geology, University of Kansas		
Seismic Attenuation		
-- Mario S. Vassiliou, Seismological Lab, California Institute of Technology		
-- Carlos A. Salvado and Bernard R. Tittmann, Earth and Planetary Sciences, Rockwell International Science Center, California		

ORIGINAL PAGE IS
OF POOR QUALITY

Abstract for Ann. Meeting of Geological Society of
America, Indianapolis Indiana, Oct. 1983

EARLY PROTEROZOIC DEVELOPMENT OF THE SOUTHERN
ARCHEAN BOUNDARY OF THE SUPERIOR PROVINCE IN THE
LAKE SUPERIOR REGION.

ANDERSON, Raymond R., and BLACK, Ross A., Iowa Geological Survey,
123 N. Capitol St., Iowa City, IA 52242.

The earliest Proterozoic rocks in the western Great Lakes area represent two major regimes. The oldest regime (2100-1900 Ma) is characterized by sequences of supracrustal rocks, dominantly conglomerates, quartzites, arkoses, iron formations, and carbonates, and coeval mafic and intermediate volcanics. The second regime (1840-1800 Ma) includes deformation and metamorphism of these earlier rocks and emplacement of a suite of dominantly calc-alkaline volcanic rocks and plutons and deposition and metamorphism of a variety of sediments including conglomerates, pelites, graywackes, tuffs, and carbonates.

These early rock suites are described by most authors as the product of a single orogenic event, the Penokean Orogeny. In this study, it is proposed that these events represent two unrelated tectonic events. The first, here called the Lake Superior Taphrogen, is characterized by extensional tectonics, graben development, platformal and basinal sedimentation, and mafic-dominated vulcanism culminating in rifting and ocean development on the southern margin of the Superior Province. The second, the Penokean Orogeny, included the closing of the ocean, subsequent collisional tectonics, and the development of a calc-alkaline volcanic suite.

The rifted continental margin and subsequent suture zone is represented by the Niagara Fault Zone in Michigan and northern Wisconsin and its southwest-trending geophysical extension, the Storm Lake Trend, which crosses Minnesota, Iowa, and extends into Nebraska. This paper will address the evidence for the location of this zone and propose a scenario for the chronology, stratigraphy, and structural development of the area in Early Proterozoic time.

---PLEASE DETACH FOR MAILING---